Mapping the intracellular molecular mechanisms of chemokine signalling within cancer

---

Gerald Roman Sion Keil

A thesis presented for the degree of Doctor of Philosophy at the University of East Anglia, School of Pharmacy

March 2019

Abstract

Chemokines are extracellular signalling molecules which function as chemoattractants for leukocytes by directing their migration towards sites of inflammation as part of the immune response. On epithelial cells chemokine receptor expression is normally low or absent. However during cancer progression, chemokine receptors can become overexpressed on cancer cells, whilst chemokines are frequently present at sites of metastasis. Consequently aberrant chemokine signalling is associated with both metastasis and a poor prognosis in cancer patients. The chemokine signalling network is therefore consider a potential therapeutic target for cancer treatment. The aim of the research undertaken in this thesis was to identify novel therapeutic targets involved in chemokine downstream signalling in cancer cells.

To investigate the chemokine downstream signalling pathway, a number of different chemokines and small molecules were used with their effects on cellular intracellular calcium signalling and migration of different leukemic and carcinoma cells assessed.

The findings from the screen identified a role for CCL2 and CCL3 signalling in the migration of PC-3 and MCF-7 cells respectively. In MCF-7 cells, CXCL12 intracellular calcium signalling was shown to be dependent on $G\alpha_i$, Syk/Src, c-Raf, DOCK1/2/5 and Arp2/3. With DOCK1/2/5 also shown to be essential for CCL3 and CXCL12 intracellular calcium signalling in both MCF-7 and THP-1 cells, as well as for CXCL12 chemotaxis of Jurkat cells. For Arp2/3 its importance in chemokine signalling was specific to MCF-7 cells, whilst the roles of the microtubules and FAK were dependent on both the chemokine and cell type.

In this thesis DOCK1/2/5 was identified as a novel target for blocking leukemic T-cell migration (Jurkats) in response to CXCL12. In addition, Arp2/3 and the microtubules were implicated in chemokine signalling and therefore would warrant further investigation to establish their importance in cancer cell migration.

Contents

List of Figures

Chapter 1.0

Chapter 2.0

Chapter 3.0

Chapter 5.0

List of Tables

Chapter 1.0

Chapter 2.0

Chapter 3.0

Acknowledgements

I would like to firstly thank my PhD supervisor Dr Anja Mueller for all her support throughout my PhD, as well as, for the proof reading of this PhD thesis. I would also like to acknowledge my second supervisor Dr Leanne Stokes for her input and help during my PhD.

In addition I would like to mention both past and present members of my lab group: Dr Shirley Mills, Dr Poh Hui Goh, Isabel Hamshaw and Enana Al Assaf, for all their help during my time at the UEA. Especially Dr Shirley Mills and Dr Poh Hui Goh both of whom helped me to settle into life at the UEA and in the lab when I first started.

I have made many friends during my time at the UEA however I would particularly like to acknowledge Greg Hughes, Ross Goodyear, Tom Leggo-Bridge, Gareth Hughes, Tom Storr and Michael (Celestial Wong Chi Kin), all of who kept me company every Friday evening at the Scholars bar.

Finally I would like to thank my parents, brother and sister in law, as well as, my extended family and friends for their support both before and during my PhD.

1.0 Introduction

1.1 Cellular Signalling

Cells are considered the most basic unit of life and as such perform fundamental biological processes including growth, migration and respiration. Within the cell, proteins interact with one another and other molecules giving rise to biochemical pathways which regulate these biological processes [1].

For these biological functions to be possible a cell must respond to the chemical, physical and biological composition of its external environment [2]. To achieve this cells have evolved the ability to communicate with their surroundings through a mechanism known as cellular signalling allowing the cell to not only detect changes in their surroundings but also influence them [3, 4].

In principle cellular signalling is when an external molecule (ligand) binds and activates a protein (receptor) on or within the cell [4, 5]. Signals at the cellular membrane can be relayed inside the cell by non-protein molecules such as nucleotides or ions and are commonly referred to as secondary messengers. These secondary messengers can activate various intracellular proteins to initiate signal transduction [6]. Alternatively the cytosolic side of the receptor can also interact with intracellular proteins to activate signal transduction. These activated proteins act as effectors to either reduce or increase enzymatic activity and/or gene transcription. The end result of the signalling pathway is a cellular response which often involves a physiological change, such as migration, division or death (apoptosis) [3-5] (figure 1.1).

Due to the importance of cellular signalling, many of the molecular mechanisms involved have been conserved through evolution [7-10]. Nonetheless, a variety of different signalling pathways present in cells has arisen, with each pathway encompassing its own distinct set of proteins, molecules and function [11, 12]. These differences can also depend on the organism type, such as between prokaryotes and eukaryotes [13] or plants and animals [14], and most likely reflects their diverging needs.

Within the animal kingdom, cells have four main types of signalling pathways according to the receptor type: ion channels, enzyme linked receptors, guanine nucleotide-binding protein (G-protein) coupled receptors and intracellular receptors [3, 4].

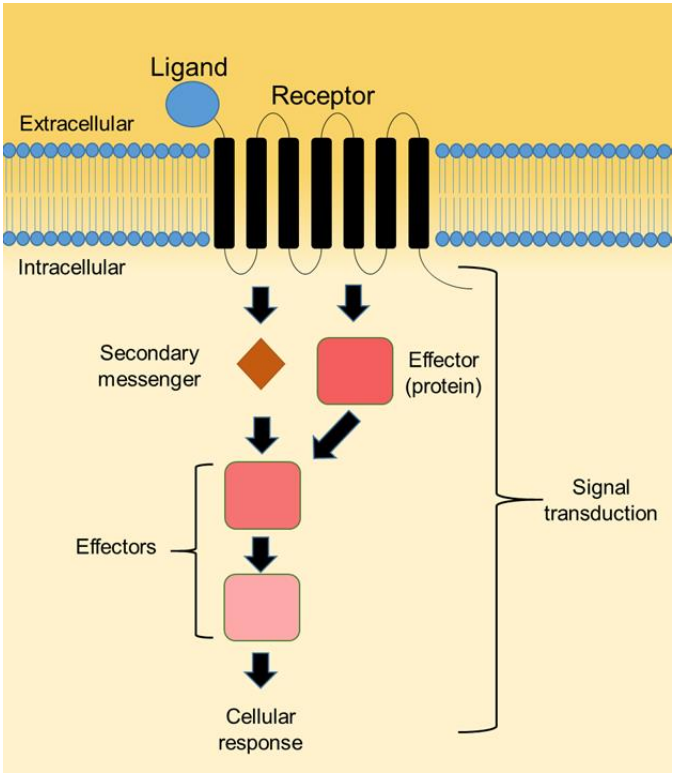

Figure 1.1. Overview of a general transmembrane cellular signalling pathway.

1.2 G-protein Coupled Receptors

1.2.1 Structure

The G-protein-coupled receptor family (GPCRs) are the largest group of receptors in mammalian cells numbering above 800 [15]. GPCRs are characterised by their distinct seven transmembrane α-helical domains (7TM), which are connected by three extracellular and three intracellular loops. On the extracellular face is the N-terminal tail which varies in length depending on the receptor. Whilst the C-terminal tail resides on the cytosolic side of the receptor [16] (figure 1.2).

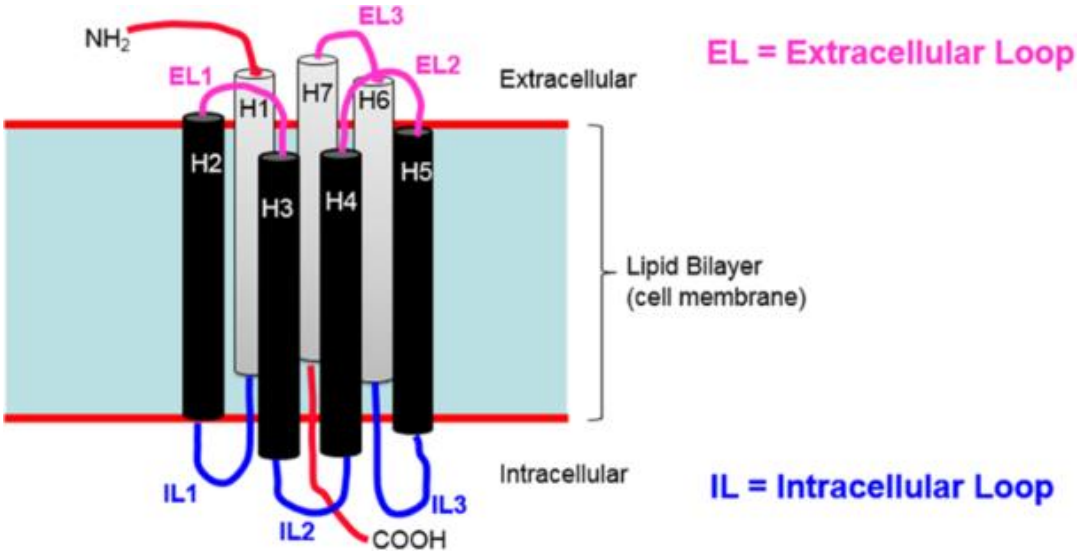

Figure 1.2. The general structure of GPCRs (image taken from [17]).

The extracellular residues of the GPCR are important for ligand-receptor interactions, with the N-terminal tail a common site for ligand binding. The extracellular loops are also key for ligand binding, as well as receptor activation [18, 19]. Receptor activation induces a conformational change in the 7TM, which recruits the G-protein to the intracellular loops for downstream signalling [18]. One particularly important G-protein binding site is the highly conserved Asp-Arg-Tyr motif on the second intracellular loop (IL2), known as the DRY motif. The arginine in the DRY motif forms an ionic salt-bridge with the glutamate on the third intracellular loop (IL3), to stabilise the receptor's inactive conformation [20]. Upon receptor activation, the conformational change allows the DRY motif to become a main binding site for the G-protein [21]. Following receptor activation, the serine/threonine residues on the C-terminal tail become phosphorylated by the G-protein-coupled receptor kinase (GRK), which desensitises the receptor to ligand stimulation. These phosphorylated serine/threonine residues recruit β-arrestin to promote receptor internalisation and thereby regulate receptor signalling [22].

1.2.2 Classification

Despite the universal 7TM, GPCRs display considerable variability in both their amino acid sequences, as well as, the N-terminal tail structures, and therefore can be further categorised into six discreet classes: A, B, C, D, E and F.

The vast majority of GPCRs are class A receptors (80%), known as rhodopsin-like receptors, and have an 8th α-helix and a palmitoylated cysteine on the C-terminal tail [23]. In the receptors inactive state, the Phe residue of the 8th α-helix, forms a hydrophobic bond with the Tyr in the NPxxY motif on the 7th α-helix. This 8th α-helix has shown to be important for receptor signalling [24]. Examples of class A GPCRs include chemokine receptors, opoid receptors and β-adrenergic receptors. Class B GPCRs, known as the Secretin receptor family, feature a 120 amino acid long N-terminal tail, which is stabilised by disulphide bonds. Class C receptors, have a long 600 amino acid, distinctive clam shaped, N-terminal tail and are commonly referred to as metabotropic glutamate receptors. The other remaining GPCR classes, are the class D: fungal mating pheromone receptors, class E: cyclic adenosine monophosphate (cAMP) receptors and class F: frizzled/smoothened [23].

1.2.3 Heterotrimeric G-protein Signalling

GPCRs are coupled to the heterotrimeric G-protein, which consist of the Gα, Gβ and Gγ subunits. In its inactive state the Gα subunit of the G-protein is bound to guanosine diphosphate (GDP) [25]. Upon GPCR activation, the G-protein is recruited to the intracellular loops, which catalyses the exchange of GDP for guanosine triphosphate (GTP), to activate the G-protein. GTP binding reduces Gα affinity for the Gβγ subunits, causing the G-protein to dissociate into the Gα and Gβγ subunits, which are then free to bind and activate various effectors [26] (figure 1.3). The Gα subunit is divided into four main classes: $G\alpha_s$ (stimulatory), $G\alpha_q$, $G\alpha_i$ (inhibitory) and G_{12}: each of which has its own distinct mode of signalling (figure 1.3) [26].

$G\alpha_s$ activates adenylate cyclase (AC) to generate the secondary messenger: cyclic adenosine monophosphate (cAMP) from adenosine triphosphate (ATP), whilst $G\alpha_i$ has the oppositie effect to $G\alpha_s$ and inhibits AC activity. Hence, $G\alpha_s$

is referred to as stimulatory, whilst $G\alpha_i$ as inhibitory [25]. For $G\alpha_q$ and G_{12} their known downstream effectors are phospholipase C (PLC)-β and Rho guanine exchange factor (RhoGEF) respectively [27]. $G\alpha_q$ activation of PLC leads to the mobilisation of calcium ions (Ca^{2+}) from the intracellular stores through the cleaving of phosphatidylinositol 4,5-biphosphate (PIP_2): to produce inositol 1,4,5-triphosphate (IP_3). IP_3 opens the IP_3 channels present on the intracellular calcium stores [28].

Receptor coupling of different Gα classes is not mutually exclusive and GPCRs can activate more than one type of Gα subunit [27]. This allows GPCRs to activate multiple different signalling pathways, thereby producing a variety of cellular physiological changes in response to the stimuli. Besides the Gα subunit, the Gβγ heterodimer is also able to mediate its own separate signalling pathways by directly interacting with a variety of different effectors including phospholipase Cβ2 (PLC2), phosphoinositide 3-kinase (PI3K)γ, GRK, AC and Ca^{2+} ion channels [26, 29] (figure 1.3).

The Gα subunit has an intrinsic GTPase activity and eventually hydrolyses GTP to GDP, allowing the Gα and Gβγ subunits to reassociate into their inactive state, as a means of self-regulation. This process is facilitated by GTPase activating proteins (GAPs) [26, 30].

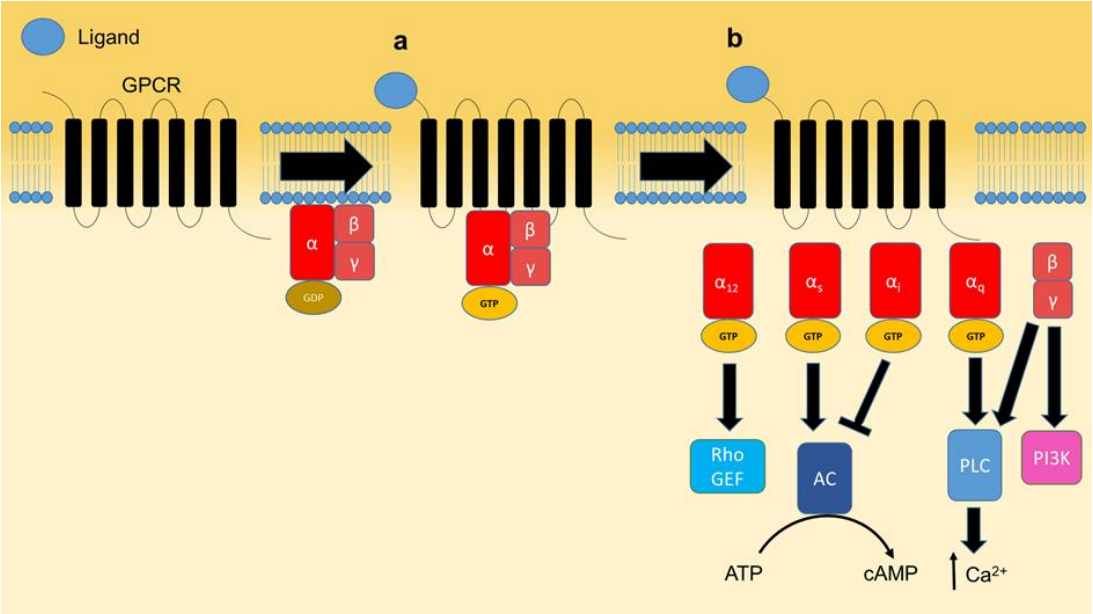

Figure 1.3. Overview of heterotrimeric G-protein signalling (Image adapted from [31, 32]). (a) Ligand binds to the GPCR which recruits the G-protein to the intracellular loops to facilitate the exchange of GDP for GTP on the Gα subunit of the G-protein [25]. (b) The activated G-protein then dissociates into the Gα and Gβγ subunits. The four different Gα subunit classes: $G\alpha_s$, $G\alpha_q$, $G\alpha_i$ and G_{12}, each activate their own separate intracellular signalling pathway. The Gβγ is also able to directly activate several effectors, such as PLC and PI3K [26].

1.3 Chemokine Receptors

Chemokine receptors are members of the class A, rhodopsin-like family of GPCRs [33], of which 23 have been discovered in humans [34]. Amongst the 23 chemokine receptors, 4 are classified as atypical chemokine receptors (ACKR) and cannot signal via the heterotrimeric G-protein due to an absent or altered DRY motif [35]. For “typical” chemokines receptors, they are primarily coupled to the $G\alpha_i/\beta\gamma$ heterotrimeric G protein and thus are sensitive to pertussis toxin (PTX) [36-39] which specifically blocks $G\alpha_i/\beta\gamma$ signalling through the attachment of an ADP-ribose onto the cysteine residue of the $G\alpha_i$ subunit [40]. Nonetheless, despite this sensitivity to PTX, incidences of chemokine receptors signalling via $G\alpha_q$ have also been observed [41, 42].

1.4 Chemokines

Chemokines are small extracellular cytokines (8-11 kDa in size), which are synthesised and secreted by cells [43]. Chemokines were first discovered in 1987 [44, 45], with at least 50 identified in humans since [46]. As there are 50 chemokines and only 20 chemokine receptors, many chemokine receptors can be activated by several different chemokines. In addition, a large number of chemokines also display similar levels of promiscuity for receptor binding (figure 1.4). This overlapping of ligand-receptor binding originally led many researchers to postulate that there was a high level of functional redundancy involved in chemokine signalling [47].

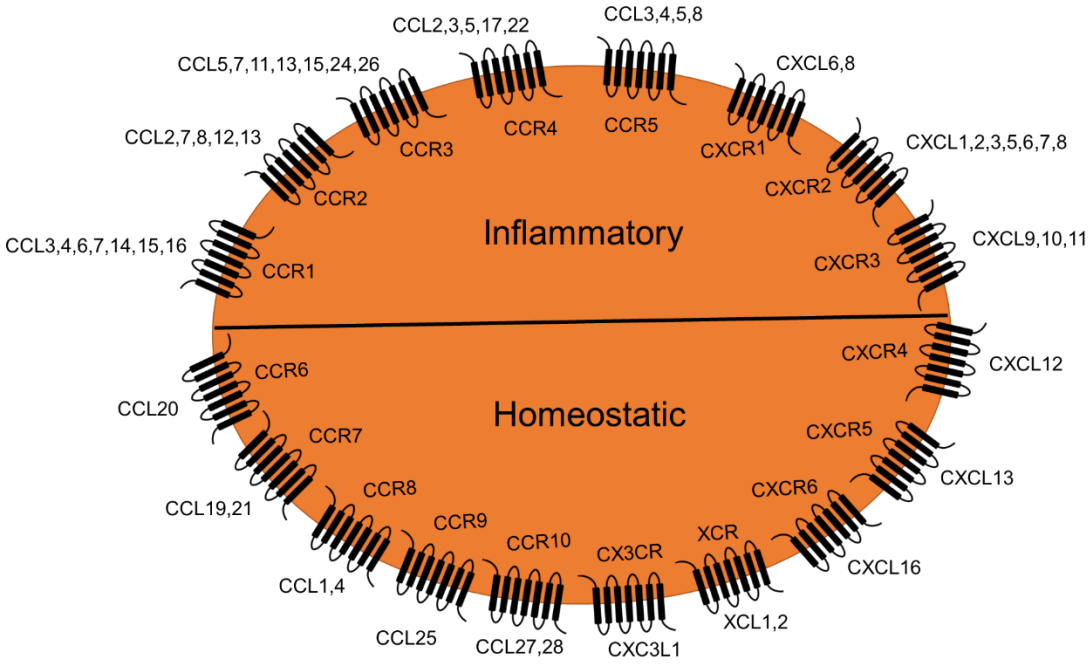

Figure 1.4. Chemokines and their respective cognate receptors (Image adapted from [48]). Chemokines and receptors are also grouped according to their main biological activity.

1.4.1 Chemokine Families

Chemokines are grouped into four families: CL, CCL, CXCL and CX_3CL, according to the spacing of the cysteine residues at the N-terminus end of the protein. The X in the motif corresponds to another amino acid besides cysteine, whilst C and L are abbreviations for cysteine and ligand respectively [49]. These cysteine residues are able to form disulphide bonds with other cysteines, to maintain the chemokines 3D tertiary structure (figure 1.5a) [50]. Most chemokines belong to either the CCL or CXCL families with only two chemokines belonging to CL and one CX_3CL [43]. Chemokine receptors are also categorised into the same four families as their corresponding chemokine ligand. R in the chemokine receptor nomenclature corresponds to receptor [49]. The CXCL family can also be further categorised into two separate subfamilies, according to the presence or absence of the ELR motif (Glu-Leu-Arg): ELR+ and ELR- respectively, which lies before the first cysteine residue of the CXC sequence [43, 51] (figure 1.5b).

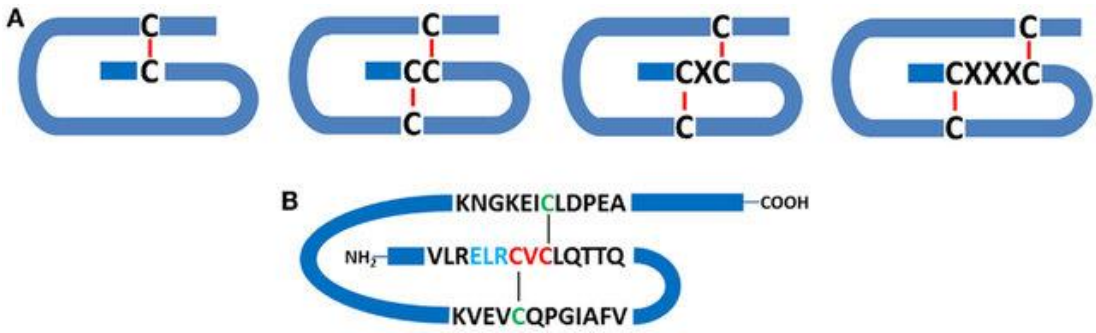

Figure 1.5. The four chemokine families and their respective motifs (Image taken from [52]). (A) The cysteine motifs of the four separate chemokine families: C, CC, CXC and CX_3C. (B) The presence of the ELR motif in the CXCL family.

1.4.2 Chemokine Structure

Chemokines are comprised of a short N-terminal tail, followed by an extended loop, and three β strands, and one α-helix present at the C-terminal tail [50]. The N-terminal tail is conserved amongst chemokines and is essential for receptor activation and affinity [53]. The extended loop is less conserved and displays greater variability amongst the different chemokines. The extended loop is important for chemokine receptor specificity as well as affinity [53, 54]. The three β strands and one α-helix provides structural stability to the chemokine [53, 55] (figure 1.6).

Chemokines have been proposed to bind to chemokine receptors in two steps. The first step involves the N-loop of the chemokine binding to both the N-terminal tail and extracellular loops of the receptor. In the second step the N-terminus of the chemokine interacts with the transmembrane domain for receptor activation [51, 53, 56-58]. This two-step binding model gives chemokines a broad binding site on the receptor.

Another key structural/functional component of chemokines is their ability to attach to glycosaminoglycans (GAGs) [53] which is largely facilitated through the electrostatic interactions between the basic residues of the chemokine and the GAGs acidic residues [50, 59].

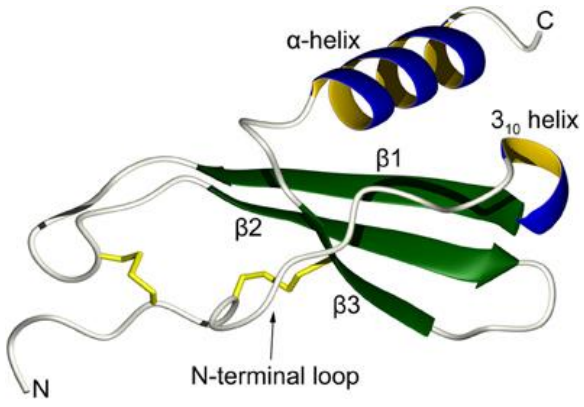

Figure 1.6. The general structure of a chemokine: an N-terminal loop, three β strands and the C-terminal α-helix (Image taken from [55]). The disulphide bonds (yellow) stabilise the N-terminal loop. The α-helix is folded over the β strands.

1.5 $G\alpha_i\backslash\beta\gamma$ Downstream Signalling

As previously mentioned, chemokine receptors are mainly coupled to and signal via the $G\alpha_i$ class of the Gα subunits. Unlike $G\alpha_s$, $G\alpha_i$ is an inhibitor of AC and blocks cAMP production [25]. Alternatively, in the canonical $G\alpha_i$ downstream signalling pathway: $G\alpha_i$ activates the tyrosine kinase Src (sarcoma non-receptor tyrosine kinase) [60], which modulates the activity of several kinases, including focal adhesion kinase (FAK) [61, 62], mitogen activated protein kinases (MAPK) [63, 64] and PI3K [65-67]. Each of these kinases is a regulator for a specific downstream signalling pathway which ultimately leads to cellular responses such as proliferation, survival and migration [12, 68, 69] (figure 1.7). Despite belonging to their own distinct pathway, cross-talk between these pathways is possible, such as, through the binding of FAK and PI3K [70-72] or the downstream activation of MAPK by FAK [73].

The Gβγ subunit on the other hand, binds and activates PLC2 at the cellular membrane [74, 75]. PLC2 is a phosphodiesterase and cleaves PIP_2, to produce two secondary messengers: IP_3 and diacyl-glycerol (DAG). IP_3 is hydrophilic, allowing it to detach from the membrane and bind the IP_3 channels on the endoplasmic reticulum (ER). This opens the IP_3 channels, causing an influx of calcium ions from the intracellular calcium stores and into the cytosol [51]. Calcium ions are key secondary messengers and alongside DAG activate protein kinase C (PKC) through binding to the C2 and C1 domains respectively [76] (figure 1.7). PKC activation, leads to the phosphorylation of serine/threonine residues on multiple downstream proteins, including c-Raf [77, 78] and MAPK/Erk kinase (MEK) [79] for the regulation of the MAPK signalling pathway. In addition to MAPK, PKC is also thought to regulate PI3K signalling [80-82], whilst the Gβγ subunit has been shown to be a director activator of PI3Kγ [83]. This again reaffirms the possibility of cross-talk downstream of the $G\alpha_i$ and Gβγ activation. Ultimately, the activation of both PKC and PI3Kγ is often important for promoting cell migration [84-87].

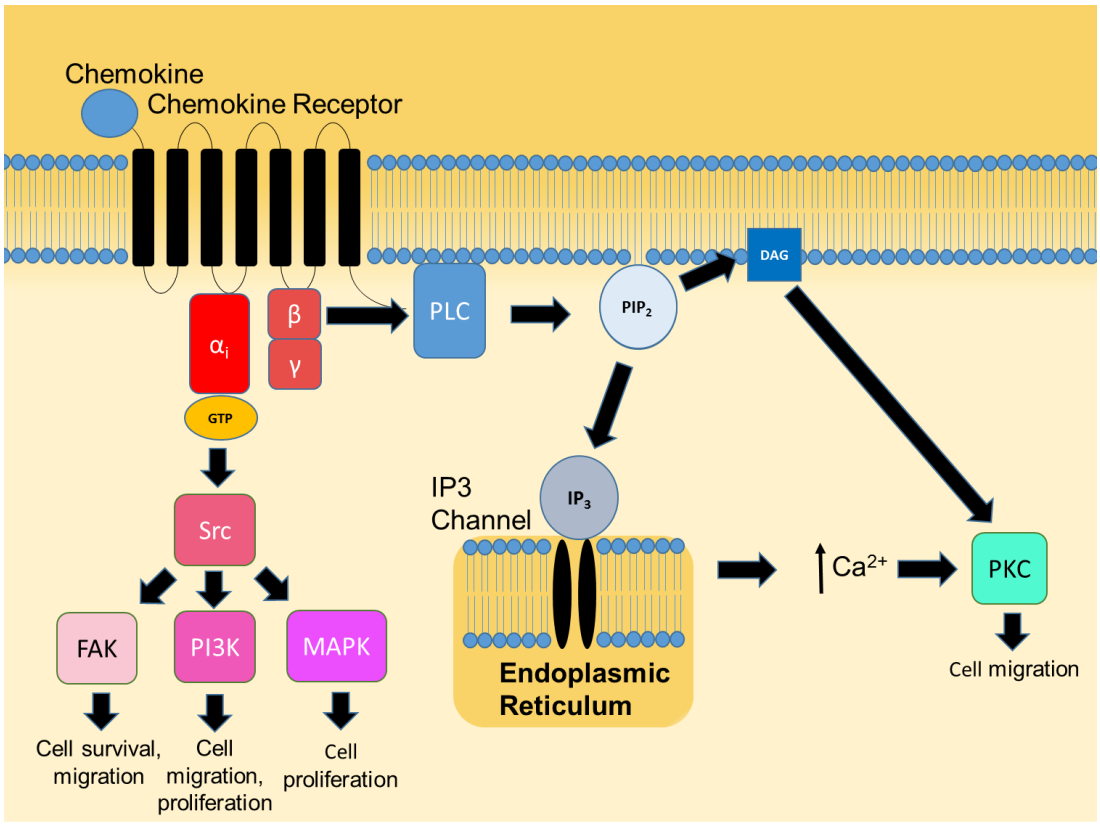

Figure 1.7. Canonical Gαi/βγ signalling pathway downstream of chemokine receptor activation (Image based on [88]). The $G\alpha_i$ signalling involves signal transduction through Src leading to FAK, PI3K and MAPK activation to induce various cellular responses. The Gβγ pathway activates PLC at the cell membrane to cleave PIP_2 to produce IP_3 and DAG. IP_3 opens the IP_3 channels on the endoplasmic reticulum releasing Ca^{2+} into the cytosol, which alongside DAG can activate PKC to promote cell migration [88].

1.6 Biased Signalling

G-protein signalling is ubiquitous for GPCRs however alternate modes of intracellular signalling involving Janus-family tyrosine kinase-Signal transducer and activator of transcription (JAK-STAT) [89-91] and β-arrestin have also been observed. β-arrestin signalling occurs following GPCR endocytosis whereby β-arrestin can act as a scaffold to mediate either

Extracellular signal-regulated kinase (ERK) [92] or Jun N-terminal kinase (JNK) [93] activation to initiate the MAPK signalling pathway [22].

The ability to utilize different signalling modes has allowed GPCRs to display a phenomena known as biased signalling. Signalling biases arise when a ligand induces a conformational change in the receptor which causes a particular signalling pathway to be preferentially activated over another pathway [94] (figure 1.8). Biased signalling has been detected in a numerous GPCRs such as chemokine, β-adrenergic and angiotensin receptors, with the β-arrestin and G-protein pathways most commonly investigated [95, 96]. No studies have explored the involvement of JAK-STAT in the biased signalling of GPCRs.

Signalling bias can be influenced by either the ligand, receptor or cell type [94] (figure 1.8). Many examples of different signalling biases have been provided from studies involving chemokine receptors, due to their large number of shared ligands and receptors [96, 97]. The chemokine receptor CCR7 is a particularly useful model for studying ligand bias as it has two known cognate ligands: CCL19 and CCL21 [94]. Activation of CCR7 by CCL19 in Human embryonic kidney-293 (HEK293) cells has been shown to exhibit greater β-arrestin 2 recruitment and receptor desensitisation compared to CCL21 [98]. In T-lymphocytes CCL21 was able to induce a greater chemotactic response than CCL19 [99], although in dendritic cells the opposite was shown, suggesting the presence of cell specific bias for both CCL19 and CCL21 as well [100]. Aside from receptor sharing chemokine receptors such as CXCR4 and ACKR3 (previously known as CXCR7) share ligands i.e. CXCL12, which allows the possibility for biases in receptor signalling to be observed. One such example is CXCL12s ability to recruit both β-arrestin and Gαi/βγ upon CXCR4 activation [101] whilst for CXCL12-ACKR3 activation only β-arrestin is recruited [102].

Biased signalling is a relatively new concept with most evidence provided from *in vitro* assays and often in heterologous cell expression systems, therefore the exact physiological relevance of biased signalling *in vivo* is not fully understood. It is likely that biased signalling enables tissues to exert a greater

degree of control over cellular responses thereby ensuring tighter spatial and temporal regulation [94, 97].

Improved understanding of the biological significance of biased signalling and its role in disease pathogenesis *in vivo* will allow the opportunity to develop drugs which can disrupt specific disease related pathways whilst simultaneously leaving normal pathways unaltered. This approach would therefore reduce the possibility of adverse side effects and at the same time maximise the therapeutic benefit [94, 97, 103].

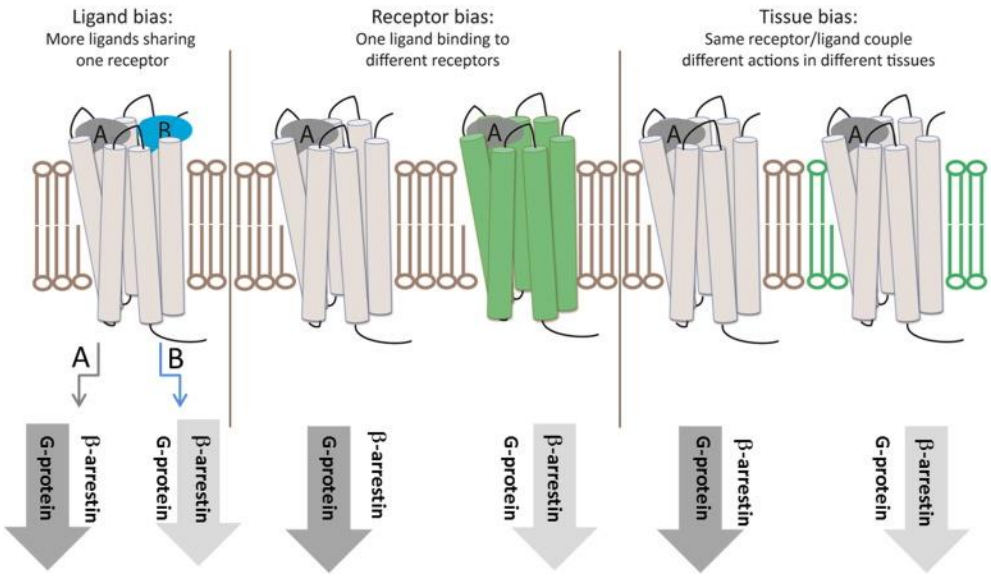

Figure 1.8. Outline of the three possible signalling biases for GPCRs: ligand, receptor and tissue (Image taken from [94]). Arrows (grey) highlight the preferentially activated G-protein or β-arrestin pathway.

1.7 Chemokine and Chemokine Receptor Oligomerisation

Although chemokines are monomeric proteins they are known to frequently form homodimers, as well as tetramers and even heterodimers. This coupling of chemokines is facilitated through interactions between β-strands, with dimer orientation dependent on the chemokine family [50]. Chemokine dimerization has been shown to influence biological effects such as CXCL12 monomers promoting colonic carcinoma cell migration whilst CXCL12 dimers inhibiting

this same migration despite both forms of CXCL12 activating CXCR4 [104]. In addition to chemokine dimerization, chemokine receptors can also exist as hetero and homodimers which can also impact on the downstream signalling pathway [105]. In HEK293 cells CXCR4/CXCR7 heterodimerisation amplified intracellular calcium signalling and regulated ERK activation in response to CXCL12 stimulation compared to HEK cells expressing CXCR4 alone [106]. Therefore the presence of chemokine and receptor oligomerisation provides an additional level of complexity to the biological nature of chemokines.

1.8 Chemokine Biological Activity

Chemokines are a chemoattractant for cells expressing chemokine receptors, often leukocytes and endothelial cells. This chemotaxis serves two broad functions in the human body: inflammation or homoeostasis [107].

During inflammation and/or infection, chemokines are secreted by stromal and epithelial cells in response to the presence of pro-inflammatory cytokines, lipopolysaccharides and viral particles within the tissue microenvironment [108-110]. Secreted chemokines attach to GAGs present on surface of endothelial cells to form a local concentration gradient within the tissue microenvironment [111]. This concentration gradient traffics neighbouring leukocytes towards these sites of infection and/or inflammation to mount an effective immune system response [109]. Chemokines associated with inflammation tend to exhibit greater receptor promiscuity which was originally presumed to ensure a robust immune response to disease [47]. The importance of a robust response is particularly pertinent when considering the molecular mechanisms deployed by viruses to mimic and manipulate the chemokine signalling network to avoid immune cell detection [112]. However notwithstanding receptor redundancy, chemokine receptors can be differentially expressed on leukocytes with CCRs commonly located on monocytes, T cells, eosinophils and basophils and play a key role in chronic inflammation [113, 114]. Whilst members of the CXCR family in particular CXCR1/2 are expressed on neutrophils and therefore are considered more important for acute inflammation [51, 114].

For homeostasis chemokines are constitutively secreted by stromal cells to promote leukocyte basal migration as part of the immunosurveillance process [115]. Homeostatic chemokines commonly traffic leukocytes to peripheral sites in the body such as the blood brain barrier, skin, lymph nodes, thymus and spleen, with the secondary lymphoid organs also involved in lymphocyte maturation [114, 116, 117]. Aside from immunosurveillance chemokines CXCL12, CXCL14 and CX_3CL1 are also expressed within the brain where they regulate neurogenesis [116]. Furthermore CXCL12 is also present at high levels in the bone marrow for the homing of hematopoietic stem cells to support the bone marrow stem cell niche [118].

These two inflammatory and homeostatic roles however are not always mutually exclusive and can vary depending on the tissue or disease state [119, 120]. Aside from inflammation and homeostasis chemokines also regulate angiogenesis, apoptosis [121], and phagocyte activation [122]. In angiogenesis the presence of ELR motif in the CXCL family determines whether the chemokine inhibits or promotes endothelial cell migration [123]. ELR+ chemokines: CXCL1, CXCL2, CXCL3, CXCL5, CXCL6, CXCL7, and CXCL8 promote endothelial migration and proliferation primarily through CXCR2 activation [43, 124]. Whilst, ELR- chemokines: CXCL4, CXCL9, CXCL10, CXCL11 and CXCL17 inhibit endothelial migration and proliferation often via CXCR3B [43]. There is however one notable exception CXCL12, which can promote endothelial migration through activation of both CXCR4 and ACKR3 even without ELR [43, 125, 126].

As chemokines play a vital role in regulating the migration of immune cells, dysregulation in chemokine signalling has been implicated in a range of autoimmune and inflammatory disorders including rheumatoid arthritis and multiple sclerosis [127] as well as atherosclerosis [128]. Moreover chemokine receptor overexpression has been identified in numerous different cancer types with the chemokine acting as a chemoattractant to promote cancer cell invasion and metastasis [48, 129-131]. Consequently the targeting of the chemokine signalling network to block abnormal cell migration in both immune and cancer cells is a highly sought area of research to treat inflammatory and immune associated diseases [132, 133].

1.9 Cell Migration

Cell migration can be defined as the ability of a cell to navigate through their surrounding external environment and includes responding to extracellular cues for directing movement (chemotaxis). Cell migration is particularly important in the evolution of multicellular organisms whereby cellular movement is tightly regulated both spatially and temporally for tissue and organ formation during early stages of development [134]. Cell migration is also crucial for other homeostatic processes, such as wound healing [135] and the immune system response [136] with the latter having been previously described. As coordinated cell migration is involved in a diverse range of biological processes it often takes place within differing tissue microenvironments and involves various different cell types [135-137]. This has therefore given rise to distinct modes of cell migration which can vary according to the cell type, external environment and even disease state, such as in cancer [138].

1.9.1 Cell Migration Modes

Cells suspended in aqueous environments such as leukocytes, have the tendency to migrate in an ‘amoeboid’ mode through the formation of actin filament (F-actin) rich protrusions known as pseudopods [139]. ‘Amoeboid’ migrating cells have a weak adherence to the external substrate and therefore migrate rapidly. In contrast mesenchymal cells such as fibroblasts reside in firmer and more stable environments and so adhere more strongly to the external substratum [140]. Mesenchymal cells migrate slower than ‘amoeboid’ cells despite also forming pseudopods (figure 1.9 and table 1.1). However unlike ‘amoeboid’ cells which migrate individually mesenchymal cells can migrate collectively as clusters [141]. Nonetheless despite differences in the migratory modes both involve the remodelling of the F-actin cytoskeleton and as such there is a significant overlap in some of their underlying molecular events [138].

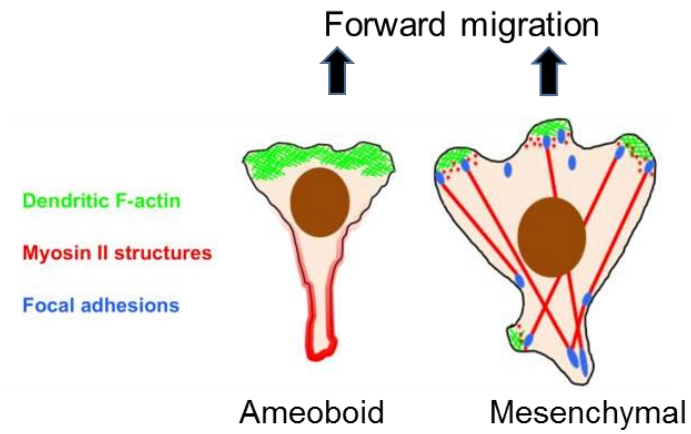

Figure 1.9. Two of the main modes of cell migration: amoeboid and mesenchymal (Image taken from [142]).

Table 1.1. Differing cellular characteristics between the amoeboid and mesenchymal migration modes

	Amoeboid	Mesenchymal
Migration speed	Fast, around 10 μm/min	Slow, < 1 μm/min
Polarity	Defined front and rear	Multiple lamellipodia
Migration mode	Squeezing through gaps in the ECM	Generate traction by adhering to the ECM
Adhesion	Weak, mostly interior.	Strong
Actin cytoskeleton organisation	Thick dendritic F-actin at the front and surrounding actin cortex elsewhere	Dendritic F-actin in lamellipodia. Thinner F-actin in the lamellum. Stress fibers inside cell.
Common receptors type used for chemotaxis	GPCRs	Receptor tyrosine kinases
Example cell type	Leukocytes	Fibroblasts

Table adapted from [142]**.** ECM refers to extracellular matrix.

1.9.2 Actin Polymerisation

In eukaryotic cells monomeric G-actin is a highly abundant protein, where it serves as a building block for actin filament (F-actin) formation. F-actin formation is the main process which drives both 'mesenchymal' and 'amoeboid' migration and is comprised of three steps: nucleation, elongation and steady state [143] (figure 1.10).

F-actin polymerisation begins with the aggregation of at least three G-actin monomers to form a stable actin nucleus structure known as nucleation. The actin nucleus can be then be further extended through the addition of G-actin monomers to the barbed (+) end for unidirectional F-actin polymerisation. F-actin polymerisation is directed towards and against the cell membrane causing the membrane to extend outwards to create pseudopods [144]. To maintain polymerisation G-actin monomers are removed from the pointed (-) end and added to the barbed (+) end at an equal rate thereby keeping F-actin polymerisation at a steady state or tread milling [143] (figure 1.10 below).

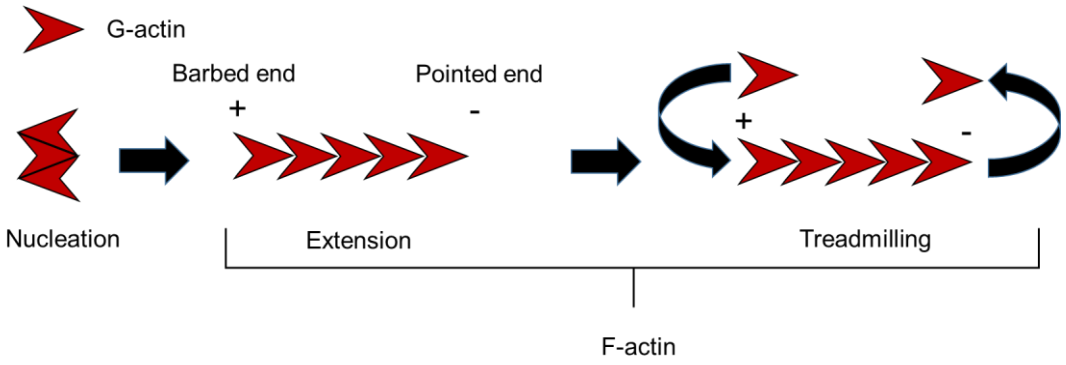

Figure 1.10. The three stages of actin polymerisation (Image adapted from [145, 146]). The process of F-actin formation is initiated by the aggregation of three G-actin monomers to form a nucleus. G-actin monomers are then added to the barbed end which extends the F-actin. During treadmilling the G-actin monomers are added and removed at an equal rate from the barbed and pointed ends respectively.

F-actin polymerisation is facilitated by formin, a dimeric protein which forms a ring like structure at the barbed end with its FH2 domains. Formin both removes and blocks protein capping to promote nucleation and polymerisation [147]. The FH1 domain of formin recruits profilin to the barbed end of the F-actin. Profilin binds and catalyses the exchange of ADP for ATP on the G-actin monomer which promotes F-actin stability, before trafficking the G-actin monomer to the barbed end to promote extension [148, 149] (figure 1.11a). Beside actin polymerisation at the barbed end, actin filaments can also be formed at a 45° angle at the sides. This F-actin branching is mediated by the actin related protein 2/3 (Arp2/3) which binds to the F-actin sides to initiate nucleation and polymerisation [145]. F-actin branching by Arp2/3, is dependent on both ATP and the recruitment of nucleation-promoting factors Wiskott-Aldrich syndrome protein (WASP) and WASP-family verprolin-homologous (WAVE) [150] (figure 1.11b).

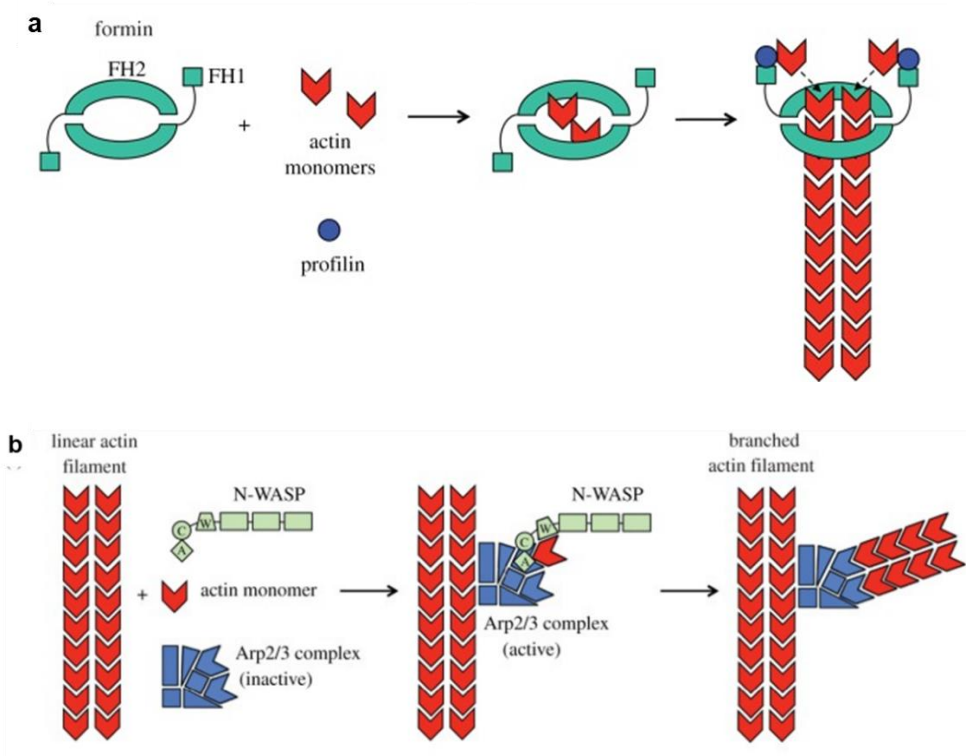

Figure 1.11. The molecular mechanisms facilitating F-actin polymerisation (Image adapted from [145]). (a) Formin's FH2 domain surrounds the barbed end of the F-actin, with the FH1 domain binding the profilin-G-actin associated complex. (b) The VCA (or WCA) domain of N-WASP binds both G-actin and Arp2/3 to initiate F-actin branching.

1.9.3 Leading Edge (Extension)

In migrating cells actin polymerisation occurs at the cellular membrane of a cells leading edge to form two types of pseudopods: lamellipodia and filopodia [140, 151, 152]. The formation of both the lamellipodia and filopodia are dependent on F-actin polymerisation, however, aside from this both their functions and molecular mechanisms differ [153-156].

1.9.3.1 Filopodia

Filopodia are thin structures around 100-300 nm in diameter and consist of between 10-30 parallel actin filaments. Filopodia are the sensors of the cell to the external environment and express higher levels of cell adhesion proteins such as integrins and cadherins [153, 154] (figure 1.12). Filopodia formation is regulated by Cdc42, a member of the Rho GTPase family, which together with PIP_2, activates WASP and N-WASP by disrupting interactions between the VCA and CRIB domains which cause WASP autoinhibition. The VCA domain of WASP is then free to interact with Arp2/3 to promote F-actin branching [157] (figure 1.11b). Formin and another actin binding protein enabled/vasodilator-stimulated phosphoprotein (ENA/VASP) are also present at the filopodia to block barbed end capping and promote F-actin extension [153]. Other proteins also involved in filopodia development are fascin, an F-actin cross linker for F-actin bundling and the insulin-receptor substrate p53 (IRSp53), an adaptor which localises Cdc42, WASP and ENA/VASP to the F-actin and also assists in membrane deformation [153, 157, 158].

1.9.3.2 Lamellipodia

Lamellipodia are large flattened cellular sheets which act as the mechanical force to propel the cell forward [155] (figure 1.12). Lamellipodia formation is regulated by another Rho GTPase Rac as well as Phosphatidylinositol (3,4,5)-trisphosphate (PIP_3), both of which recruit and activate WAVE2 at the leading edge [155, 156]. WAVE2 activation is facilitated by IRSp53 which has a Rac binding domain at the N-terminus and a Src-homology-3 (SH3) domain to bind WAVE2 at the C-terminus [155, 159]. Similar to WASP, WAVE2 then activates Arp2/3 using its VCA domain to promote F-actin branching [155].

1.9.3.3 Cellular Polarity

In order for pseudopods to only form at the leading edge the molecular events between the cells leading and trailing edges must differ. Hence migrating cells display substantial cellular polarity according to their signalling pathways [160-162] (figure 1.12).

PI3K is an important facilitator of cellular polarity through the phosphorylation of PIP_2 to produce PIP_3 which acts a binding site for proteins which have a pleckstrin homology domain e.g. guanine exchange factors (GEF), Akt and WAVE2 [155, 162]. Experiments using GFP-labelled Akt have demonstrated the localisation of PI3K/PIP_3 at the leading edge of migrating fibroblasts [163], neutrophils [164] and *Dictyostelium* [165], with the pharmacological blockade of PI3K shown to inhibit the chemotaxis of neutrophils [166] and *Dictyostelium* [167]. Interestingly phosphatase and tensin homolog (PTEN) which acts in opposition to PI3K by dephosphorylating PIP_3 to generate PIP_2 is preferentially located at the trailing edge of the cell [162].

PIP_3 acts as a localisation point for GEF at the leading edge of the cell for Rho GTPase activation and subsequent F-actin polymerisation [168]. Also as PIP_2 is able to bind profilin and block profilin-G-actin interactions [169], higher levels of PIP_3 at the leading edge could result in greater levels of profilin present in the cytosol which aids F-actin formation.

However despite evidence of PI3K being important for chemotaxis, one comprehensive study using 5 separate PI3K and one PTEN knockout in *Dictyostelium* showed no effect on chemotaxis [170]. This lead to the conclusion that off-target effects of the PI3K inhibitor LY294002 may have contributed to some of these chemotaxis defects [170]. This also suggests that in *Dictyostelium* there are other signalling mechanisms involved in chemotaxis which may include phospholipase A2, cyclic guanosine monophosphate and RasC [171]. Nonetheless the same authors did identify a role for PI3K in cellular speed confirming some importance of PI3K for cell migration [170].

Aside from the PIP_3, calcium ion levels are also polarised within migrating cells with low calcium ion levels present at the leading edge whilst higher levels found towards the rear [161] (figure 1.12) . Low levels of calcium increases the cells sensitivity to pulses of calcium at the boundary between the lamellipodia and lamella at the leading edge. These calcium pulses arise from either the ER or calcium channels on the cell surface which can activate various effectors including calmodulin and PKC [161, 172]. Calmodulin can activate the myosin light chain kinase (MLCK) which in turn phosphorylates myosin II to induce contraction. Myosin II contraction causes the F-actin to be pulled towards the cell interior, a process known as retrograde flow which regulates F-actin treadmilling [161]. Activation of PKC is able to modulate cell migration through the regulation of fascin, myosin II and p115RhoGEF for remodelling the actin cytoskeleton [173-175].

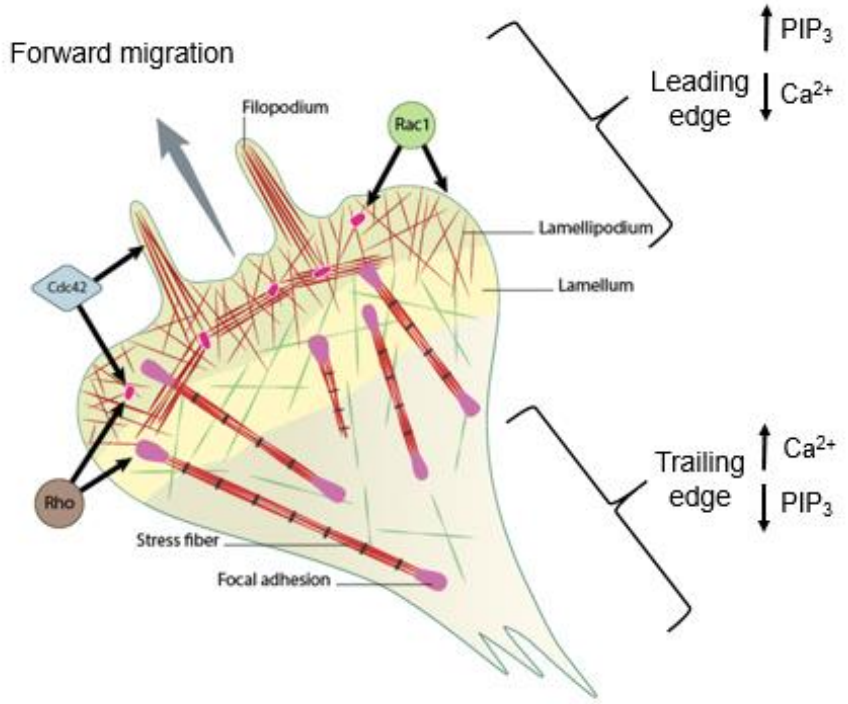

Figure 1.12. The molecular mechanisms involved in forward cellular migration (Image adapted from [176]). Cdc42 is important for the formation of filiopodia and nascent focal adhesions (small pink circles) [153, 177]. Whilst Rac1 is important for lamellipodia formation as well as nascent focal adhesions [155, 178]. Rho promotes the conversion of nascent focal adhesions to mature focal adhesions (long purple circles) [179]. Stress fibers connect mature focal adhesions within the cell for cellular contraction [155, 180]. During forward migration PIP_3 is present at higher levels at the leading edge whilst at the trailing edge Ca^{2+} levels are higher instead [161, 171].

1.9.4 Focal Adhesions (Traction)

During migration cells generate traction by adhering to the extracellular matrix (ECM) through the assembling of macromolecular structures on their cell surface known as focal adhesions (FAs) (figures 1.12 and 1.13). FAs are sites of adherence and actin polymerisation and function to counteract the F-actin retrograde flow caused by myosin II contraction [181, 182]. The activation of various transmembrane receptors including chemokine receptors are known to promote focal adhesion assembly [183-186].

1.9.4.1 Integrins

Cellular adherence often involves integrins, a group of transmembrane receptors which exist as αβ heterodimers [187]. Cells express a particular set of integrin subunits depending on the extracellular environment encountered. In the presence of collagen, cells express α1β1 and α2β1, whilst for laminin the α2β1, α3β1 and α6β1 subunits are expressed instead [188]. These distinct combinations of integrin subunits are able to activate specific signalling pathways which allows the cell to exert a greater flexibility and specificity over both its adherence and migration in response to its surroundings [188-190]

ECM and integrin binding causes the integrins to cluster which recruits talin to the cytoplasmic side of the β subunits. Upon arrival, talin disrupts the interaction between the α and β cytoplasmic tails of the integrin which shifts the integrin into a high ligand affinity state and enhances ECM binding [191]. Talin is often considered as an initiator of FA formation by recruiting FAK, vinculin and α-actinin (F-actin binding protein) [188]. Though this model was disputed by a separate study which alternatively identified FAK as being essential for talin recruitment and not the other way round [192]. However one review proposed a comprise between these two studies, in which at nascent FAs, talin recruitment is dependent on FAK, whilst at mature FAs, FAK is dependent on talin for retention [193].

1.9.4.2 Focal Adhesion Kinase

FAK recruitment to the FA is central to both FA assembly and its signal transduction, and is trafficked to the integrin's via its FAT (focal adhesion targeting) domain where it can bind both talin and paxillin [194] (figure 1.13). At the FA, the FAK FERM (four-point-one, ezrin, radixin, moesin) domain was originally thought to interact with the cytoplasmic tail of the β integrin subunit to cause a conformational change in FAK leading to Tyr397 autophosphorylation and the subsequent activation of FAK [68]. However more recently an alternative model has been suggested in which FAK is activated at the FA by neighbouring PIP_2 molecules instead [195-197].

Nevertheless the autophosphorylation of Tyr397 acts as a binding site for proteins with the SH2 (Src Homology 2) such as Src, PI3K, PLC-γ and Ras GTPase activating protein (GAP) [194, 198]. The recruitment and activation of Src by Ty397 is a particularly important event as Src is able to phosphorylate the Tyr576 and Tyr577 residues on the activation loop of FAKs kinase domain which initiates FAKs tyrosine kinase activity [199]. Both Src and FAK are then able to phosphorylate two FA adaptor proteins paxillin and p130cas which can form binding sites for CT10 sarcoma oncogene cellular homolog (Crk) [194, 200]. Crk is an effector for the atypical GEF, dedicator of cytokinesis 1 (DOCK1) which in turn can activate Rac to promote cell migration, survival and membrane ruffling, with the latter being a precursor to migration [201-203]. Besides paxillin and p130cas, FAK is also able to phosphorylate N-WASP to promote migration, possibly by blocking its nuclear localisation [204].

Besides Tyr397, Tyr576 and Tyr577, other FAK phosphorylated tyrosine residues are Tyr861 and Tyr925 which enhance SH3 and SH2 binding of p130cas and growth factor receptor-bound protein 2 (Grb2) respectively [194]. Grb2 is another adaptor protein which is able to activate Ras and initiate the MAPK signalling cascade [194]. Additionally FAK can directly regulate GEFs and GAPs to either promote or suppress Rho GTPase activity respectively, as a means of regulating F-actin formation [200]. Thus FAK localisation to the integrins is not only important for FA assembly but also for integrin signal transduction to regulate F-actin polymerisation. This allows the cell to coordinate an appropriate cellular response according to the ECM encountered.

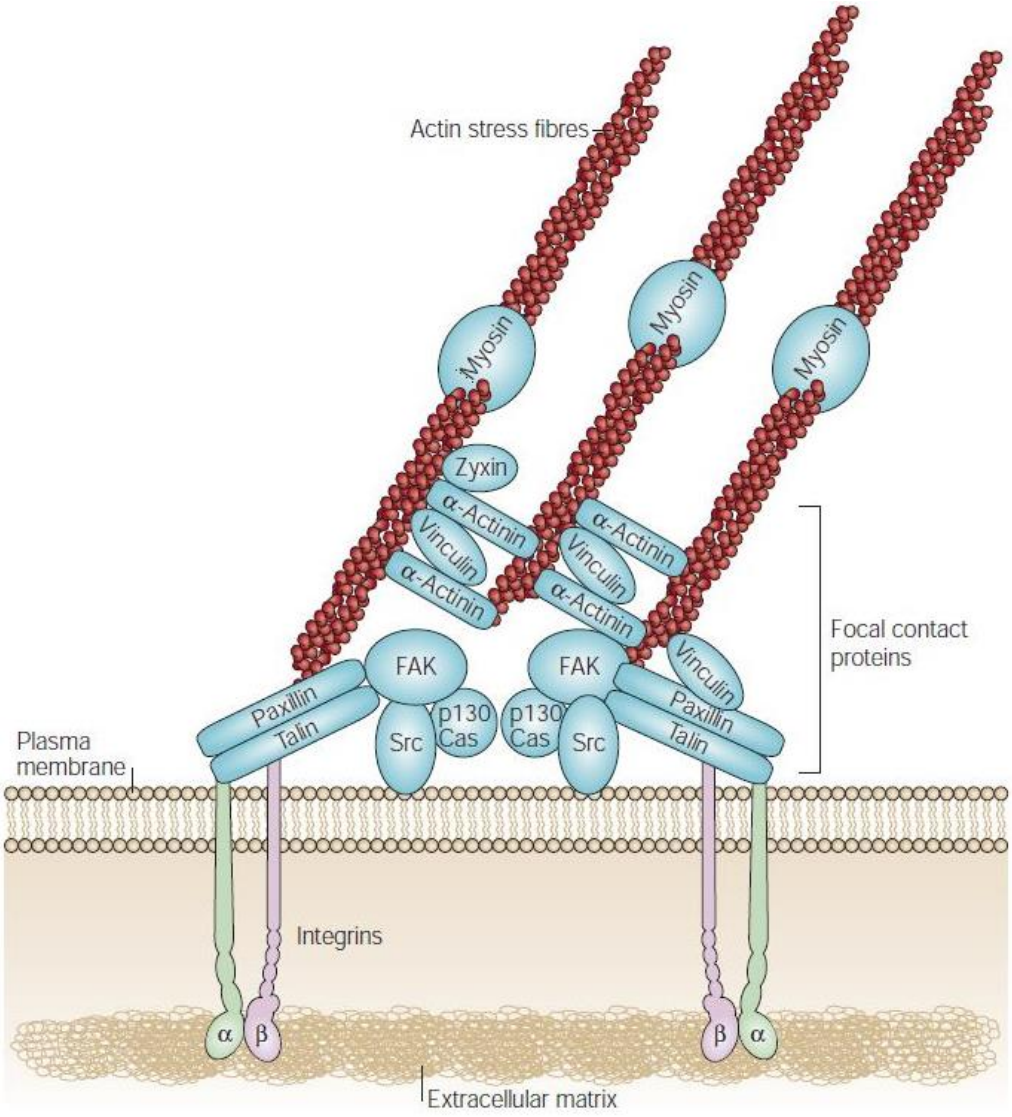

Figure 1.13. The (general) molecular composition of focal adhesions (Image taken from [194]).

1.9.4.3 Focal Adhesion Maturation

Nascent FAs are small structures which are formed at the leading edge of the cell and provide significant traction for cellular migration [205, 206]. The vast majority of these nascent FAs are disassembled, however a few can undergo maturation by elongating in the opposing direction to cellular migration where they become more important for cellular adherence [181] (see figure 1.12).

FA maturation involves the Rho GTPase RhoA, an effector of Rho-dependent protein kinase (ROCK) and formin activity. Among ROCKs downstream targets are myosin II light chain and LIM kinase both of which enhance stress fiber formation [179]. Stress fibers consist of 10-30 parallel F-actin bundles which span across the transverse, dorsal and ventral sides of the cell and often connect separate FAs (figure 1.12). Stress fiber contraction by myosin II is particularly important for FA maturation [180] and as such stress fiber formation is particularly characteristic of mesenchymal migration [140] (table 1.1). Overtime mature FAs will undergo either disassembly or remain to become sites for α5β1 integrin and tensin clustering. These sites are known as fibrillar adhesions and are found within the cell interior to promote stable adherence [207].

1.9.5 Trailing Edge (Retraction)

Cells migrate in a unidirectional manner and as such during migration the trailing edge of a cell needs to be retracted. This cellular retraction requires the focal adhesions located at the cellular edge to undergo disassembly [208]. The molecular mechanisms involved in FA disassembly are not as well understood as those involved in its assembly, however, several proteins associated with FA disassembly have been uncovered.

Although FAK is well known to be involved in FA formation many studies have shown that FAK is also important for FA disassembly [209-211]. At the FA site, FAK recruits dynamin to its FERM domain to initiate integrin endocytosis by either clathrin or caveolin [212, 213]. Dynamin endocytosis is also facilitated by the presence of Src which phosphorylates the Tyr231/597 residues of dynamin to enhance its GTPase activity [214]. At the FA, FAK may also activate p21-activated kinases to inhibit MLCK activity and thereby reducing FA stability [211]. Moreover the microtubules are also shown to be crucial for FA disassembly by trafficking endocytic related proteins to the FA [213].

As mentioned earlier (section: 1.8.3.3), calcium ion levels are higher at the trailing edge and as such Ca^{2+} modulated proteins are often associated with cellular retraction [215, 216]. Two particularly notable Ca^{2+} activated proteins

involved in FA disassembly are calpain and calcineurin. Calpain is a proteinase which cleaves FA adaptor proteins talin [216], FAK [217] and paxillin [218], whilst calcineurin facilitates intergrin endocytosis [215]. Furthermore, the presence of calcium ions at the trailing edge is thought to promote FAK retention at the FA [219] and interesting FAK can also bind calpain directly to promote FA turnover [220].

Both FA assembly and disassembly at the respective leading and trailing edges are key for cell migration with integrin endocytosis and recycling occurring at both edges to promote and maintain cell migration [221]. Moreover this recycling of integrins is also considered to be essential for the invasion of cancer cells [222, 223] with regulators of integrin activity such as FAK and Src, frequently dysregulated in cancer cells [224-226]. This therefore makes the FA signalling pathway a worthwhile area of study in cancer.

1.10 Cancer Metastasis

Cancer is a heterogeneous genetic disease characterised by uncontrolled cellular proliferation which gives rise to an abnormal cluster of cells known as a tumour [227]. The most widely accepted paradigm for metastasis is, over time some cancer cells within a primary (benign) tumour can acquire additional mutations allowing them to detach from their primary (tumour) site and invade the surrounding tissue to access the body's circulatory system. Once in circulation these cancer cells can travel to other sites within the body [227, 228]. Upon arriving at a new site, the cancer cell adheres to the blood vessel walls and migrates through the extracellular gaps between the endothelial cells, known as extravasation. The cancer cell then invades the new tissue site and grows to form a secondary tumour. This formation of a second tumour is termed metastasis [227, 228] (figure 1.14).

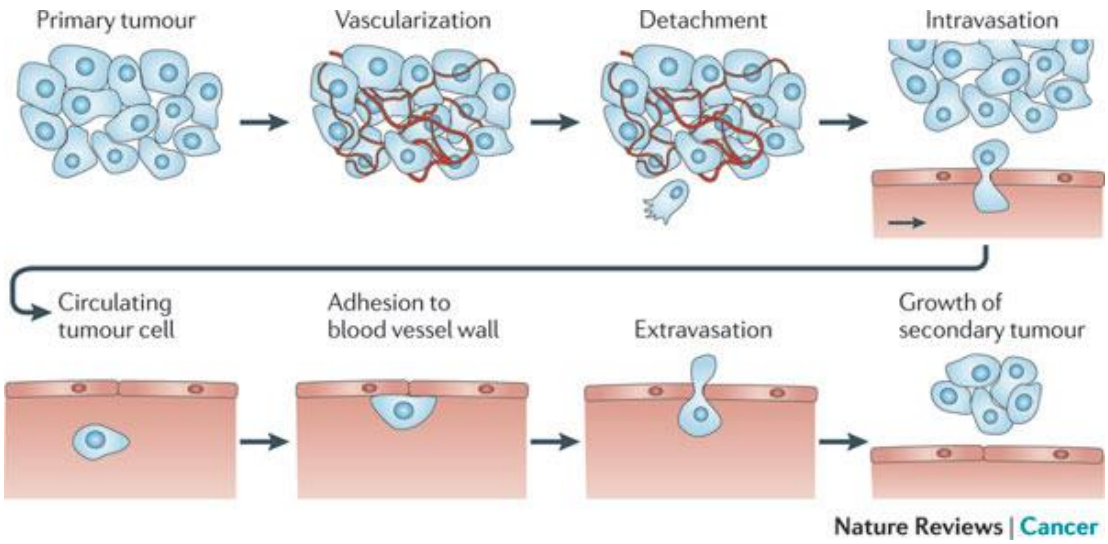

Figure 1.14. The sequence of events involved in cancer metastasis (Image taken from [228]). Tumour vascularization at the primary site is one of the first steps in cancer dissemination by suppling nutrients for tumour growth, as well as allowing the cancer cell access to the body's vascular system. Occasionally cancer cells detach from the primary tumour and enter the vascular system by intravasation. Circulating cancer cells can then attach and extravasate through the blood vessel walls and form a second tumour at a new site within the body [228].

Metastasis is the leading cause of fatality in cancer patients and is considered to be responsible for 90% of all cancer related mortality worldwide [229]. Its deadliness is further emphasised when comparing the five year survival rates between patients with stage IV (metastatic) tumours and those with stage I (benign) tumours. In the UK, breast cancer patients diagnosed with a stage I tumour have a 99% chance of surviving after five years whilst at stage IV this drops to just 15% [230]. Similar downward trends in survival rates for patients diagnosed with stage IV tumours is prevalent amongst other types of cancer as well (see table 1.2). This emphasises the need to block cancer metastasis as a strategy for improving the survival rates of cancer patients.

Table 1.2. List of carcinoma types and their common metastatic sites. The five year survival rates were for adults (15-99 years old) diagnosed with different stages of cancer in England and Wales

		Five year survival rate				
Cancer	**Main Sites of Metastasis**	**Stage I**	**Stage II**	**Stage III**	**Stage IV**	**Overall**
Bladder	Bone, liver, lung	87.9%	37.3%	23.8%	10%	75.9%
Bowel	Liver, lung, peritoneum	97.4%	84.7%	62.7%	7.5%	59.7%
Breast	Bone, brain, liver, lung	99.1%	87.6%	55.1%	14.7%	85.8%
Kidney	Bone, brain, liver, lung, adrenal gland	83.3%	82.9%	57.8%	5.9%	47.7%
Lung	Bone, brain, liver, other lung. adrenal gland	35.3%	20.9%	6.32%	UA	9.68%
Melanoma	Bone, brain, liver, lung, skin, muscle	100%	81.8%	52.4%	16.8%	89%
Ovary	Liver, lung, peritoneum	90%	42.8%	18.6%	3.5%	39.3%
Pancreas	Liver, lung, peritoneum	UA	UA	UA	UA	3.3%
Prostate	Bone, adrenal gland, liver, lung	100%	99.4%	93.3%	30.4%	87.4%

Information about the main sites of metastasis was obtained from the National Cancer Institute [231]. The five year survival rate data was from the Former Anglia Cancer Network, 2002-2006 [230] except for pancreatic cancer. The five year survival rate for pancreatic cancer was provided by the London School of Hygiene and Tropical Medicine, 2010-2011 [232]. All data on the five year survival rates were obtained for both sexes except for breast and prostate cancer which were from women and men only respectively. Data on Kidney cancer excludes the renal pelvis. UA corresponds to unavailable.

One of the reasons for the low survival rates for metastatic cancers is the cancers resistance to chemotherapy and/or radiotherapy as well as more targeted treatments [233]. This drug resistance can often arise as a result of mutations caused by the intrinsic genomic instability present in cancer cells due to their uncontrolled cell proliferation and defective DNA repair pathways [234-237]. Besides therapeutic agents and radiotherapy, for patients with solid tumours surgery is still the main treatment option [238, 239]. Nevertheless its efficacy is often limited to early-stage cancers as once the cancer has invaded the surrounding tissue and metastasised, removing all the cancerous tissue

using surgery alone is difficult [240-242]. Hence there is a greater likelihood of cancer recurrence in patients with higher stage tumours following surgery [241-243].

Due to the multiple mutational events required for a cancer to metastasize, many of the molecular mechanisms involved are not properly understood. Nevertheless, one feature common amongst all cancer types is their distinct pattern of metastasis. In prostate cancer the bone is the most common metastatic site (90% of cases) [244]. For pancreatic cancer it is the liver (85% of cases) [244]. Whist, in breast cancer there are a range of common sites including the bone, lung, liver and brain, although the bone is still the most frequent site (48% of cases) [244]. Some of this metastatic pattern can be partly explained by anatomy, such as blood flowing from the pancreas to the liver via the portal vein [245, 246]. However for more distant metastatic sites like the brain or site specific metastasis such as bone metastasis in breast cancer, this cannot be completely explained in terms of physiology alone and thus other contributing factors must be involved.

This has given rise to the ‘seed and soil’ hypothesis which was first proposed in 1889 by an English surgeon named Stephen Paget and was based on his observations of the non-random pattern of metastasis from the autopsy records of 735 women with breast cancer [247]. In this analogy the cancer cell is the seed whilst the pre-metastatic site is the soil. Therefore as certain seeds flourish within a particular type of soil the same concept is thought to occur for metastasis [248].

Within the pre-metastatic environment there are a myriad of different signalling molecules, such as growth, pro-survival, adhesion, proangiogenic factors and cytokines including chemokines. Many of which are considered crucial to the seeding of cancer cells for metastasis [249].

1.11 Chemokines and Cancer Metastasis

Cancer aetiology has identified inflammation as a key promoter of cancer progression [250] through two possible pathways: an extrinsic and an intrinsic pathway. The extrinsic pathway is caused by continuous exposure to toxic exogenous sources e.g. excessive alcohol intake or tobacco smoke which leads to persistent tissue damage and chronic inflammation within the tissue microenvironment [251]. Whilst the intrinsic pathway is instead a result of an accumulation in genetic abnormalities within a cell which causes oncogenesis and/or tumour suppressor loss leading to an upregulation in pro-inflammatory pathways [251, 252]. Both of these pathways can lead to elevated levels of chemokines and chemokine receptors through the increase in transcriptional activity of nuclear factor kappa light chain enhancer of activated B cells [253-258], hypoxia inducing factor [258-260] and activator protein 1 [256, 257].

The importance of chemokine overexpression in cancer metastasis was first discovered in 2001 from the seminal nature paper by Muller *et al*. (2001) [130]. In this study chemokines CXCL12 and CCL19/21 were found to be overexpressed at common sites of metastasis such as liver, lung, brain and lymph nodes whilst their respective cognate receptors CXCR4 and CCR7 were overexpressed on various breast cancer cells [130]. Since then CXCR4 overexpression has been further identified in at least 23 different cancer types and is often associated with a poor prognosis for cancer patients [261]. In addition to CXCL12 other particularly well-studied chemokines within the cancer research field are CCL2 [262], CCL5 [263] and CCL19/21 [264] with emerging chemokine signalling axis of interest involving CXCL9/10/11-CXCR3 [265] and CXCL8-CXCR1/2 [266].

Within the tumour microenvironment chemokines are commonly secreted by cancer associated fibroblasts, endothelial cells and tumour infiltrating leukocytes for the trafficking of immunosuppressive leukocytes such as regulatory T-cells and myeloid derived suppressor cells as well as endothelial cells to the tumour site [131, 267-269]. This helps to create an immunosuppressive environment and encourages blood vessel formation both of which support tumour survival and growth [131] (figure 1.15). At the pre-metastatic site chemokines also act as a chemoattractant for circulating cancer

cells which overexpress chemokine receptors [115, 130, 270]. In haematological cancers, the homing of leukemic cells to the bone marrow and lymph nodes by chemokines is thought to contribute to survival and drug resistance [271-273]. In cancer cells, chemokine signalling has also been shown to promote invasion, proliferation, survival, adhesion, and the secretion of vascular epidermal growth factors and matrix metalloproteinases [274-279].

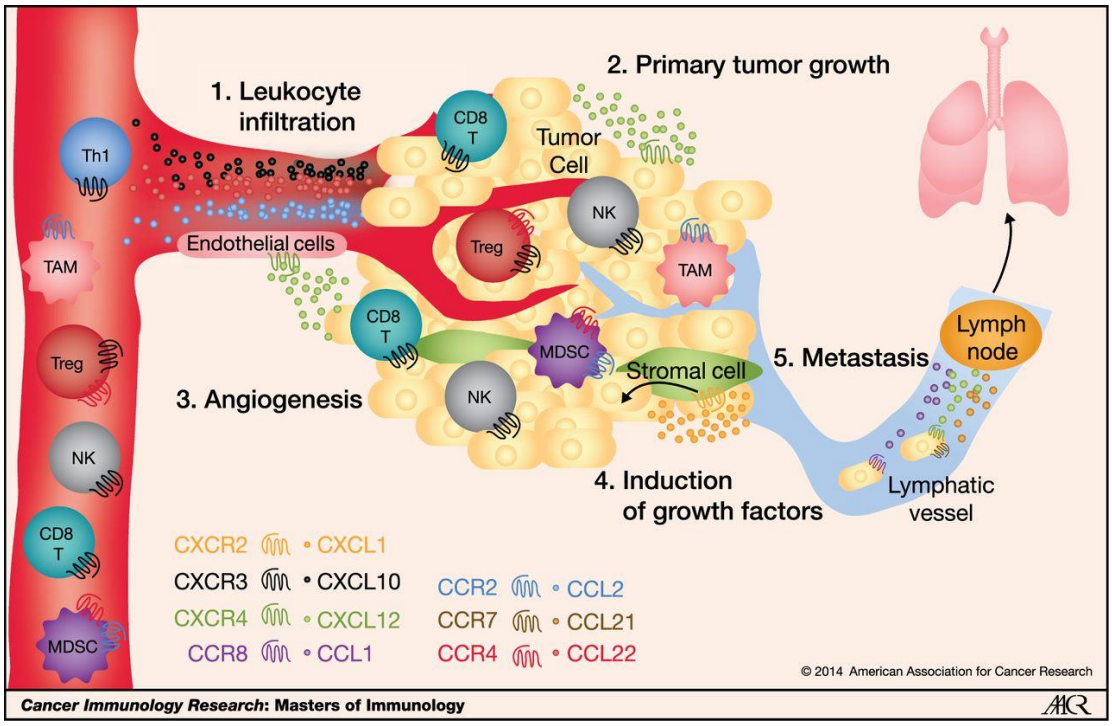

Figure 1.15. The various roles of the chemokine signalling axis in cancer progression (Image taken from [131]). Chemokines secreted at the primary tumour (yellow) are able to recruit leukocytes and endothelial cells to encourage tumour growth and vascularisation. Chemokine signalling also increases the production of growth factors at the tumour site. Chemokines expressed in the lymph nodes can recruit cancer cells from the primary tumour site and aid metastasis (pictured as the lungs). (TAM = Tumour associated macrophages, NK = Natural killer cells, MDSC = Myeloid derived suppressor cells, Th1 = Type 1 helper T-cells, CD8 T = CD8 T-cells and Treg = Regulatory T-cells) [131].

1.12 Chemokine Signalling: A Therapeutic Target for Cancer Treatment

GPCRs are the largest family of receptors in humans and their dysfunction underlies the pathogenesis of many diseases [280, 281]. To date, around 34% of all US Food and Drug Administration (FDA) approved drugs target GPCRs [282].

Successive preclinical *in vitro* and *in vivo* cancer models have demonstrated the therapeutic benefit in targeting chemokine signalling in several cancers including breast [130, 283-286], prostate [287, 288] and leukaemia [289, 290]. Hence there has been considerable interest from the pharmaceutical industry to develop and bring drugs which target the chemokine signalling network to clinical trial as a form of targeted treatment against cancer progression [291, 292].

1.12.1 Small Molecules Targeting Chemokine Signalling in Cancer Patients

CXCR4 is the most widely studied chemokine receptor in cancer, therefore it is unsurprising that most small molecules undergoing clinical trials are antagonists for CXCR4.

Currently the only licensed CXCR4 small molecule inhibiter used in cancer treatment is AMD3100 (licensed name plerixafor) which was approved in 2008 by the FDA to treat non-Hodgkin lymphoma and multiple myeloma (MM) [293]. AMD3100 is administered together with the granulocyte-colony stimulating factor for the mobilisation of hematopoietic stem cells into the blood stream for autologous stem cell transplantation following chemotherapy [294]. Since 2008, AMD3100 has undergone clinical trials in combination with different chemotherapy agents to enhance the treatment for acute myeloid leukaemia (AML) by blocking the retention of leukemic cells in the bone marrow [273]. Results from these studies demonstrated the successful mobilisation of leukemic cells into the circulatory system as well as improved remission rates [273, 295]. Other CXCR4 antagonists which have also completed phase II

clinical trials are Burixafor (previously known as TG-0054) and POL6326 both as alternatives to AMD3100 for the mobilisation of hematopoietic stem cells for MM and both non-Hodgkin's and Hodgkin's lymphoma [296, 297]. The results from both trials showed successful hematopoietic stem cell mobilisation and drug safety [296, 297].

Besides haematological cancers POL6326 also completed a clinical trial in combination with Eribulin for metastatic breast cancer however no results have been released (Trial registration ID: NCT01837095). Another CXCR4 inhibitor which has undergone clinical trials for solid tumours is the LY2510924 for small cell lung carcinoma, although no significant anti-tumour effect alongside carboplatin/etoposide was observed [298]. Whilst a clinical trial involving MSX-122 also for solid tumours was suspended with no reason given for the suspension (Trial registration ID: NCT00591682). Similarly, two other trials with LY2510924 in solid tumours (Trial registration ID: NCT02737072) and renal metastasis (Trial registration ID: NCT01391130.) were also cancelled, with the latter due to low efficacy [299]. However the clinical trial for AML with LY2510924 is still actively recruiting (Trial registration ID: NCT02652871).

Aside from the CXCL12-CXCR4 signalling axis another pathway being targeted is CXCL8-CXCR1/2 using the dual CXCR1 and CXCR2 inhibitor Reparixin. Reparixin is still in phase II clinical trial for triple negative breast cancer in combination with Taxol (Trial registration ID: NCT02370238) following a phase I study which reported favourable pharmacokinetics and no serious adverse effects or interference on Taxol anti-tumour activity [300].

1.12.2 Antibodies and Peptides Targeting Chemokine Signalling in Cancer Patients

Mogamulizumab is the only licensed monoclonal antibody used to target a chemokine receptor in cancer treatment. Mogamulizumab was first approved in 2012 by the Japanese Pharmaceuticals and Medical Devices Agency to target CCR4 positive adult T-cell leukaemia (ATL) in relapsed or refractory patients [301]. In 2018 the USA FDA approved the use of mogamulizumab for Non-Hodgkin lymphoma [302]. Whilst in Europe the European Medicine

Agency designated mogamulizumab as an orphan drug in 2016 and approved its use in 2018 also for the treatment of the cutaneous T-cell lymphoma subtype of Non-Hodgkin lymphoma [303].

For targeting CXCR4 the current leading antibody is MDX-1338 (or BMS-936564), developed by Bristol-Myers Squibb Co. MDX-1338 completed two phase I clinical trials, one as a monotherapy for treating patients with relapse AML and three subtypes of B-cell leukaemia (Trial registration ID: NCT01120457), and another as both a monotherapy and in combination with lenalidomide/dexamethasone or bortezomib/dexamethasone for relapse MM (Trial registration ID: NCT01359657). Both trials aimed to establish MDX-1138 safety and tolerability in these patients [304] however neither has disclosed any results since.

The CCL2-CCR2 signalling axis is another therapeutic target which has enjoyed preclinical success with antibodies [287, 305, 306]. As a result this lead to the development of two antibodies: carlumab and MLN1202. Carlumab (CNTO888) is a high affinity antibody for CCL2 developed by Centocor and has completed two separate phase I clinical trials for advanced solid tumours and one phase II trial for metastatic prostate cancer as both a monotherapy and in combination with chemotherapeutic agents. Carlumab was well tolerated in patients but there was no significant improvement in the disease state [307-309]. Furthermore, in both of the carlumab trials, despite the initial reduction in CCL2 levels these levels rebounded following a week of treatment, which could have been a contributing factor for the lack of anti-tumour activity. Possible reasons provided for lack of robust reduction in CCL2 levels by carlumab were poor affinity for CCL2 in humans, low clearance rate of the carlumab-CCL2 complex and an increase in CCL2 secretion in response to carlumab [307-309].

An alternative strategy for blocking CCL2-CCR2 signalling was using the CCR2 antibody MLN1202 developed by Millennium Pharmaceuticals, which was in a phase II clinical trial involving solid tumours with bone metastasis (Trial registration ID: NCT01015560). MLN1202 was shown to be safe as well as 32% of patients displaying a reduction in urinary N-telopeptide (a bone

reabsorption and metastasis marker), suggesting some possible therapeutic benefit though this has yet to be confirmed [310].

Aside from antibodies, other biological therapeutic agents include nanobodies and peptides. Nanobodies consist of a single heavy chain and thus are much smaller than regular antibodies making them more soluble and easier for drug delivery [311]. This has led the biotech company Ablynx to develop the first CXCR4 nanobody ALX-0651 which was used for phase I clinical trial in healthy patients (Trial registration ID: NCT01374503). Although this trial was terminated the proof of principle was listed as having been established. There has been no further news on the status of ALX-0651 since.

Alternatively a CXCR4 peptide antagonist, CTCE-9908, underwent a phase I/II trial for solid tumours in which it demonstrated drug safety and a potential anti-tumour effect in ovarian cancer [312]. Nonetheless since these findings (2007) there appears to be have been no further development with CTCE-9908 in the clinic. Although CTCE-9908 is still actively used in preclinical models [313-315] and has apparently been granted orphan drug status by the FDA for osteogenic sarcoma [316].

1.12.3 Challenges in Targeting Chemokine Signalling

Despite nearly a decade of research into the therapeutic targeting of the chemokine signalling system for cancer treatment only two drugs worldwide have been licensed: AMD3100 and mogamulizumab, with only mogamulizumab used as a direct therapeutic agent against cancer progression.

Several published review articles have discussed the challenges surrounding the blocking of the chemokine signalling system for the therapeutic treatment of inflammatory diseases including cancer [291, 292, 317, 318]. One of the most commonly cited reason for clinical failure is the redundancy thought to underpin chemokine signalling [319, 320], which could be particularly problematic for targeting chemokine signalling axis associated with inflammation (figure 1.4) [48, 321].

Evidence from the immunostaining of cancers has shown that cancer cells often overexpress multiple different chemokine receptors [130, 322, 323] whilst within the tumour microenvironment a multitude of different chemokines can be expressed at any given time [320, 324-326]. This therefore renders the targeting of a particular chemokine or receptor ineffective as alternative chemokine receptors present on the cancer cells can become activated instead.

Nevertheless not all chemokines display promiscuity especially chemokines which are involved in more homeostatic roles, with many having cognate receptors also expressed on cancer cells e.g. CXCR4, CCR7 and CCR9 [115, 130, 327]. However receptors such as CXCR4 are widely expressed amongst leukocytes [328] whilst CCR7 is expressed on both dendritic cells [329] and T-lymphocytes [330]. Therefore their pharmacological blockade could provoke unwanted and toxic side effects especially when considering many immune cells like T-cells, natural killer cells and M1 macrophages play an important role in anti-tumour activity [331-333]. Thus disturbing some of these chemokine signalling axis may be particularly detrimental for the treatment of solid tumours [267, 324].

Aside from redundancy, other explanations have included inappropriate target selection, off-target effects and poor pharmacokinetics [133, 317, 319]. Regarding inappropriate target selection, some of the contributing factors could involve inter-tumour heterogeneity as a few studies have reported chemokine receptor expression being associated with a more favourable prognosis in certain cancers [334-337]. Therefore as some clinical trials involve a range of solid tumours this approach may not be the most effective method to establish a therapeutic benefit. Moreover most preclinical models rely on immunodeficient mice as a proof of concept for targeting chemokine signalling in cancer [284, 285, 287, 338]. Which as previously mentioned, as chemokine receptors are expressed on anti-tumour immune cells the lack of anti-tumour leukocytes *in vivo* could over exaggerate the efficacy of chemokine blockade on cancer progression and hence would not translate into the clinic.

In the case of small molecule inhibitors their off-target effects maybe a result of their allosteric binding inside the receptor transmembrane domain [132], as the transmembrane domain is more conserved amongst chemokine receptors and as such this may cause off-targeting and possibly reduce clinical efficacy [319].

As discussed in this section, despite the wealth of preclinical evidence for targeting chemokine receptors for cancer treatment this strategy has thus far been mainly unsuccessful, particularly for solid tumours [298, 299, 307-309]. Hence there is still an urgent need to identify alternative approaches to block chemokine driven progression of cancer. One option are dual receptor inhibitors such as Repaxirin which may offer a way of overcoming some receptor redundancy though this has not yet been proven in the clinic. Combination therapies involving checkpoint inhibitors is another possibility with mogamulizumab currently undergoing several such clinical trials (Trial registration ID NCT03309878 and NCT02476123).

Another therapeutic strategy is to target specific proteins which are acting downstream of chemokine signalling to promote cancer cell migration. However one obstacle to this approach is that many of these downstream signalling pathways are not particularly well understood, with the few published studies on these cell signalling pathways tending to focus on the CXCL12-CXCR4 signalling axis and often in breast cancer [339-343]. Nonetheless a few key proteins such as Src, PI3K, protein tyrosine kinase 2, Casitas B-lineage Lymphoma, ELMO (Engulfment and Cell Motility), FAK and SH2-containing phosphatase 2 have been identified as being important for breast cancer cell migration in response to CXCL12 [339-344]. Some of these findings are from single studies, with a few deriving their results from only one breast cancer cell model. Therefore these results do not always account for cell specific differences as despite the limited amount of studies investigating the downstream signalling pathways of chemokines evidence of cell specific biases have been observed [89, 340, 345].

In the breast cancer MCF-7 cells, CXCL12 migration was shown to be dependent on PKC signalling [340] whilst in another breast cancer model,

MDA-MB-231 cells this was not the case [342, 343]. Similar differences in the role of PKC in CXCL12 signalling have also been observed between the migration of the leukemic Jurkat cells and MCF-7 cells [340]. However one potential drawback when comparing some of these different cell types was the different approaches used to measure cellular migration i.e. the wound healing assay and chemotaxis. Which may have also influenced the molecular mechanisms involved in cell migration. Notwithstanding cell specific biases, it is also possible for different chemokine ligands to activate separate signalling pathways within the same cell type under very similar conditions. Such as the importance of Rac for CXCL12 but not CCL3 migration in MCF-7 and monocytic THP-1 cells [346], or Gβγ for CXCL11 but not CCL3 chemotaxis in THP-1 cells [347].

These studies begin to demonstrate the possibility for significant differences in the molecular machinery for cellular migration between distinct chemokine and cell types. Which, when considering the vast number of chemokines and proteins involved in cellular migration provides both a substantial challenge but also a great opportunity to develop targeted treatments against cancer metastasis. As such there is a need to further explore the molecular mechanisms which are involved in cell migration.

1.13 Research Aim

Chemokines are a large family of cytokines, which regulate leukocyte migration under both homeostatic and inflammatory conditions [107]. Dysregulation of the chemokine signalling network provides cancer cells with the opportunity to metastasize to other sites within the human body [115, 130]. As such chemokine receptor overexpression on cancer cells is often associated with a poor prognosis for cancer patients [115]. Despite many clinical trials attempting to block chemokine signalling to prevent cancer metastasis the vast majority have been unsuccessful [291]. With chemokine promiscuity and inappropriate target validation considered to be two of the main causes [317]. Consequently, there is still a need to find alternative strategies to successfully disrupt chemokine signalling for cancer treatment.

In cancer cells, chemokine signalling activates a downstream pathway to promote cell migration and invasion [348]. As such, one alternative is to identify other viable therapeutic candidates downstream of the chemokine receptor which are also essential for cancer cell migration. However, very little is known about the downstream molecular mechanisms and furthermore these downstream signalling pathways can differ depending on the chemokine and cancer cell type [340, 346, 347]. Therefore this is still an area of cancer research which warrants further study and subsequently forms the basis of the PhD work presented in this thesis.

To investigate the downstream signalling pathway, a pharmacological based approach was used to identify and assess the importance of particular proteins (commonly dysregulated in cancer) in chemokine driven cancer cell migration. The aim of this thesis was to initially identify chemokines signalling pathways important for carcinoma metastasis and thereafter use small molecules to interrogate their downstream molecular mechanisms to discover novel therapeutic targets.

The outline of the research objectives were as follows:

- Chapter 3

  The aim of this chapter was to identify chemokine signalling pathways important for the metastasis of carcinoma cells. This was achieved by screening a range of chemokine ligands to determine their effect on the migration, actin cytoskeleton and release of calcium from the intracellular stores in different cancer cell types.

- Chapter 4

  As chemokines signal via the heterotrimeric G-protein to induce chemotaxis [349]. The aim of this chapter was to explore the role of the heterotrimeric G-protein signalling pathway in the migration of leukemic and carcinoma cell types in response to two notable chemoattractants: CCL3 and CXCL12. To investigate the downstream signalling pathway several known $G\alpha_i/\beta\gamma$ effectors including FAK, PI3K and PLC were studied, due to their implication in the development of cancer [225, 350-352].

- Chapter 5

  Actin polymerisation is a principal driving force for both cell migration and cancer invasion [353, 354]. As such, in this chapter the involvement of cytoskeletal regulators DOCK, Arp2/3 and the microtubules in CCL3 and CXCL12 downstream signalling was investigated in different leukemic and carcinoma cell types.

Chapter 2.0 Materials and Methods

2.1 Tissue culturing

2.1.1 Reagents

The Dulbecco's Modified Eagle Medium (DMEM) and Rosewell Park Memorial Institute (RPMI) 1640 were supplied by Thermo Fisher Scientific (Loughborough, UK). Fetal Calf Serum (FCS) and glutamine were supplied by Life Technologies (Thermo Fisher Scientific), and non-essential amino acids by (Thermo Fisher Scientific). The G418 was obtained from Invitrogen (Thermo Fisher Scientific), with 500 µg/mL added to DMEM media for CHO-CCR5 subculture.

Adherent cell lines were harvested using 0.25% Tryspin/EDTA or Trypsin/PBS supplied by Life Technologies (Thermo Fisher Scientific) and 2 mM EDTA/PBS. Both the Ethylenediaminetetraacetic acid (EDTA) and phosphate buffered saline (PBS) (8.1 mM, Na_2HPO_4, 1.5 mM KH_2PO_4, 137 mM NaCl, and 2.7 mM KCL, with a pH 7.2) were obtained from Thermo Fischer Scientific.

Dimethyl sulfoxide (DMSO) was purchased from Sigma Aldrich (Poole, UK).

2.1.2 Cell culture

All the secondary mammalian cancer cell lines: MCF-7 (Michigan Cancer Foundation-7), MIA PaCa-2, MDA-MB-231, PC-3 (Prostate Cancer-3), Jurkat and THP-1 cells were obtained from American Type Culture Collection (ATCC), Teddington, UK.

In addition, Chinese Hamster Ovary cells transfected with pcDNA3 encoding human CCR5 (CHO-CCR5) and antibiotic resistance gene to Geneticin (G418) were also used in this thesis. The CHO-CCR5 cells have been previously described and were provided by J. McKeating, Reading, UK [355].

MCF-7, MIA PaCa-2, MDA-MB-231 and CHO-CCR5 were cultured in DMEM, supplemented with 10% v/v FCS, 2 mM glutamine and 10X non-essential

amino acids. CHO-CCR5 were also cultured with the same DMEM composition previously stated, but also contained 500 µg/ml of G418.

PC-3, THP-1 and Jurkat cells were cultured in RPMI 1640 Medium, supplemented with 10% v/v FCS, 2 mM glutamine and 10X non-essential amino acids.

2.1.3 Cell culture protocol

All cell lines were cultured in 75 cm^2 (ThermoFischer Scientific) cell culture flask and incubated at 37°C, 5% CO_2 and 100% humidity. All cell culture was performed under class 2 vertical laminar air flow cabinets at room temperature. All cell lines were subcultured as described in tables 2.1 and 2.2.

For storing cell lines, cells were harvested and spun down (12000 revolutions per minute (RPM) for 5 mins) after reaching 90% confluency. Supernatant was removed and cells were resuspended in freezing media (10% v/v DMSO and FCS) for cryopreservation. 1 mL of cells were loaded into 1.8 ml sterile Cryotubes (BioSigma (Cona, Italy)), before wrapped within several layers of tissue to retain moisture and ease the freezing process to minimise cellular damage from crystallisation. The cells were then frozen overnight at -80°C, and then placed in liquid nitrogen at -196°C for long term storage.

For defrosting cells, cells were quickly thawed and washed once in growth media (10 mL). Thereafter, cells were resuspended in growth media (10 mL) and seeded into a 25 cm^2 cell culture flask (Thermo Fischer Scientific) before being incubated at 37°C, 5% CO_2 and 100% humidity. Cells were harvested and reseeded into a 75 cm^2 cell culture flask after reaching 90% confluency.

2.1.4 Description of cell lines and subculture methods used

2.1.4.1 MCF-7 cells

MCF-7 cells are a mammalian epithelial cell line originating from the breast tissue and obtained from the pleural effusion site of a 69 year old Caucasian women diagnosed with breast adenocarcinoma [356]. MCF-7 cells express both oestrogen and progesterone receptors [357, 358], but do not overexpress HER-2 [359]. Thus MCF-7 cells are used as an *in vitro* model to understand hormone sensitive breast cancers. MCF-7 cells were harvested with 2 mM EDTA/ PBS (4 ml) and subcultured in DMEM growth media (10% v/v FCS, 2 mM glutamine and 10X non-essential amino acids). Cells were split 1:10, after reaching 95% confluency (every 3 to 4 days).

2.1.4.2 MDA-MB-231 cells

MDA-MB-231 cells are a mammalian epithelial cell line originating from the breast tissue and obtained from the pleural effusion site of a 51 year old Caucasian women diagnosed with breast adenocarcinoma [360]. MDA-MB-231 cells are thought to be insensitive to either oestrogen or progesterone and do not overexpress HER-2 [357, 361]. Therefore they are considered a model for the triple negative breast cancer subtype.

For harvesting MDA-MB-231 cells, cells were washed in PBS (5 ml), prior to the addition of 0.25% Trypsin/PBS or EDTA (1.5 ml). MDA-MB-231 cells were subcultured in DMEM growth media (10% v/v FCS, 2 mM glutamine and 10X non-essential amino acids) and split 1:10 after reaching 95% confluency (every 2 to 3 days).

2.1.4.3 MIA PaCa-2 cells

MIA PaCa-2 cells are a mammalian epithelial cell line originating from the pancreatic tissue of a 65 year old Caucasian male diagnosed with pancreatic carcinoma [362].

MIA PaCa-2 cells were harvested with 2 mM EDTA/ PBS (4 ml) and subcultured in DMEM growth media (10% v/v FCS, 2 mM glutamine and 10X non-essential amino acids). Cells were split 1:10, after reaching 95% confluency (every 3 to 4 days).

2.1.4.4 PC-3 cells

PC-3 cells are a mammalian epithelial cell line originating from the bone of a 62 year old Caucasian male diagnosed with grade IV metastatic prostate adenocarcinoma [363]. PC-3 cells express lower levels of the androgen receptor [364, 365] and are used as a model for the androgen insensitive prostate cancer subtype.

PC-3 cells were harvested with 0.25% Trypsin/EDTA (3 ml) after reaching 90% confluency (between 3-5 days) and split 1:10. PC-3 cells were subcultured in RPMI 1640 growth media (10% v/v FCS, 2 mM glutamine and 10X non-essential amino acids).

2.1.4.5 CHO-CCR5 cells

CHO-CCR5 cells are a mammalian epithelial cell line originating from the ovary of a female Chinese hamster. CHO cells are known for their ease of transfection and hence used to express recombinant genes and proteins [366]. The CHO cells were transfected with the pc3DNA plasmid which express human CCR5 and is resistant to G418 antibiotic.

CHO-CCR5 cells were harvested with 2 mM EDTA/ PBS (4 ml) and subcultured in DMEM growth media (10% v/v FCS, 2 mM glutamine, 10X non-essential amino acids and 500 µg/mL G418). Cells were split 1:10, after reaching 95% confluency (every 3 to 4 days).

2.1.4.6 THP-1 cells

THP-1 cells are a mammalian monocytic cell line originating from the peripheral blood of a 1 year old human male infant diagnosed with acute monocytic leukaemia [367].

THP-1 cells were subcultured in RPMI 1640 growth media (10% v/v FCS, 2 mM glutamine and 10X non-essential amino acids) and split either 1:2 or 1:3 every 3 to 4 days after reaching a confluency above $70x10^4$ cells mL^{-1}.

2.1.4.7 Jurkat cells

Jurkat cells are a mammalian T-lymphocyte cell line originating from the peripheral blood of a human male diagnosed with acute T cell leukaemia [368].

Jurkat cells were subcultured in RPMI 1640 growth media (10% v/v FCS, 2 mM glutamine and 10X non-essential amino acids) and split either 1:2 or 1:3 every 2 to 3 days after reaching a confluency above $150x10^4$ cells mL^{-1}.

2.1.4.8 Summary of cell lines and subculture methods used

Table 2.1. Adherent cells

Cell line	Origin	Characteristics	Cell subculture method
MCF-7	Human: Caucasian Female, 69 year old	Oestrogen and progesterone positive breast adenocarcinoma	- 4 ml of PBS/EDTA for harvesting cells. - Cells split (1:10) every 3 to 4 days.
MDA-MB-231	Human: Caucasian Female, 51 year old	Triple negative breast adenocarcinoma	- Washed in 4 ml PBS (room temp), before harvesting with 1.5 ml of 0.25% Trypsin/EDTA or PBS. - Cells split (1:10) every 2 to 3 days.
MIA PaCa-2	Human: Caucasian Male, 65 year old	Pancreatic carcinoma	- 4 ml of PBS/EDTA was used to harvest cells. - Cells split (1:10) every 3 to 4 days.
PC-3	Human: Caucasian Male, 62 year old	Androgen negative, prostate adenocarcinoma, grade IV	3 ml of 0.25% Trypsin/EDTA used to harvest cells. Cells split (1:10) every 3 to 5 days.
CHO-CCR5	Chinese Hamster Ovaries	Overexpresses human CCR5	- 4 ml of PBS/EDTA used to harvest cells. - Cells split (1:10) every 3 to 4 days.

Table 2.2. Suspension cells

Cell line	Origin	Characteristics	Cell culture method
THP-1	Human: 1 year old infant	Acute monocytic leukaemia	- Cells split (1:2 or 1:3) every 3 to 4 days.
Jurkat	Human: Male	Acute T-cell leukaemia	- Cells split (1:2 or 1:3) every 2 to 3 days.

2.2 Chemokines

Chemokines: CCL2, CCL4, CCL5, CCL8, CCL23, CXCL8, CXCL9 and CXCL12 were obtained from Peprotech, London, UK. Chemokines were diluted in purified water and aliquoted into 10, 1 and 0.1 µM working stocks and stored at -20°C.

CCL3 was a gift from a L.Czaplewski of British Biotech, and is the characterised CCL3 D26A isoform [369].

Pharmacological studies into chemokines has allowed the identification of some of the cognate receptors, cellular function and has also highlighted the potential for redundancy underpinning chemokine signalling. Improved understanding of chemokine pharmacodynamics allows the opportunity to explore the potential therapeutic benefits and feasibility in targeting the chemokine signalling network to treat inflammatory associated diseases.

There is however still some discrepancy within the chemokine research field as to which chemokines can be considered an endogenous ligand for a particular chemokine receptor including the chemokine signalling axis presented in figure 1.4 [48, 113]. Consequently a literature search for published pharmacological studies on the chemokines used for this thesis was undertaken to identify some of the key cognate receptors. This list of chemokines and their respective cognate receptors was then used as a reference for the results presented in this thesis (see table 2.3).

In table 2.4 is a list of all the small molecules which were used in this thesis and includes information on their respective protein targets, pharmacological properties, storage and concentrations used.

Table 2.3. List of chemokines and their pharmacological properties for identified cognate receptors

Chemokine	Chemokine receptor	Assay	Pharmacological properties
CCL2	CCR2	Receptor binding	K_i= 0.1 nM in CHO-K1-CCR2 cells [96] K_d = 0.04 nM in THP-1 cells [370]
		GTPγS binding	EC_{50} = 9 nM in CHO-CCR2B cells [370]
		Calcium flux	EC_{50} = 0.7 nM in 300.19-CCR2 murine pre-B cells [371] EC_{50} = 6.31 nM in CHO-K1-CCR2 cells [96] EC_{50} = 3 nM in CHO-CCR2B cells [370]
		Chemotaxis	EC_{50} = 2.2 nM in CD14+ monocytes [372] EC_{50} = 159 nM in primary hypothalamic neurons [373] EC_{50} = 1 nM in human primary monocytes [370] Dose response = 0.12-360 nM in HEK293-CCR2b cells [374]
		cAMP	EC_{50} = 0.794 nM in CHO-K1-CCR2 cells [96]
		BRET β-arrestin2 recruitment	EC_{50} = 3.16 nM in CHO-K1-CCR2 cells [96]
		Internalisation	EC_{50} = 15.3 nM in CHO-CCR2B cells [370]
		pERK phosphorylation	EC_{50} = 0.106 nM in CHO-CCR2B cells [9]
	CCR3	GTPγS binding	EC_{50} = 1.1 nM in CHO-CCR3 cells [370]
		Internalisation	EC_{50} = 4.1 nM in CHO-CCR3 cells [370]

Chemokine	Chemokine receptor	Assay	Pharmacological properties
CCL3	CCR1	Receptor binding	K_i = 0.15 ± 0.07 nM in retinoic acid differentiated HL60 cells [375] K_i = 0.056 ± 0.013 nM in Ba/F3-CCR1 murine ProB cells [375] K_d = 4 ± 0.8 nM in HEK293-CCR1 cells [374] K_d = 5-9 nM in HEK293-CCR1 cells [376]
		GTPγS binding	EC_{50} = 15 ± 25 pM in Ba/F3-CCR1 murine ProB cells [375] EC_{50} = 0.040 ± 0.04 nM in retinoic acid differentiated HL60 cells [372]
		Calcium flux	EC_{50} = 0.1-0.3 nM for CCR1 in retinoic acid differentiated HL60 cells [377]
		Chemotaxis	EC_{50} = 0.2 nM in HEK293-CCR1 cells [378] EC_{50} = 0.1 nM for CCR1 in retinoic acid differentiated HL60 cells [375] Dose response = 0.012-360 nM in HEK293-CCR1 cells [374] Dose response = 0.12-120 nM in HEK293-CCR1 cells [376]
	CCR5	GTPγS binding	EC_{50} = 3.9 ± 2.4 nM in Ba/F3-CCR5 murine ProB cells [375] EC_{50} = 1.3 nM in CHO-CCR5 cells [355] EC_{50} = 2.3 nM in CHO-CCR5-CD4 cells [355]
		Calcium flux	EC_{50} = 63.1 nM in CHO-K1-CCR5 cells [96]
		cAMP	EC_{50} = 0.025 nM in CHO-K1-CCR5 cells [96]
		BRET β-arrestin2 recruitment	EC_{50} = 2.51 nM in CHO-K1-CCR5 cells [96]
	Multiple	Receptor binding	IC_{50} = 7.4 nM in THP-1 cells [378]
		Calcium flux	EC_{50} = 4.7 nM in THP-1 cells [378]
		Chemotaxis	EC_{50} = 0.2 nM in THP-1 cells [378]

Chemokine	Chemokine receptor	Assay	Pharmacological properties
CCL4	CCR1	GTPγS binding	EC_{50} = 11.9 ± 1.7 nM in Ba/F3-CCR1 murine ProB cells [375] EC_{50} = 17.1 ± 2.7 nM in retinoic acid differentiated HL60 cells [375]
		Calcium flux	no response for CCR1 in retinoic acid differentiated HL60 cells [375]
		Chemotaxis	no response for CCR1 in retinoic acid differentiated HL60 cells [375] agonist in Ba/F3-hCCR1 cells [375] weak agonist = 30 nM in HEK-293-CCR1 cells [376]
	CCR5	Receptor binding	K_i = 0.398 nM in CHO-K1-CCR5 cells [96]
		GTPγS binding	EC_{50} = 5.8 ± 2.7 nM in Ba/F3-CCR5 murine ProB cells [375] EC_{50} = 3.4 nM in CHO-CCR5 cells [355] EC_{50} = 4.3 nM in CHO-CCR5-CD4 cells [355]
		Calcium flux	EC_{50} = 6.31 nM in CHO-K1-CCR5 cells [96]
		cAMP	EC_{50} = 0.794 nM in CHO-K1-CCR5 cells [96]
		BRET β-arrestin2 recruitment	EC_{50} = 7.94 nM in CHO-K1-CCR5 cells [96]
CCL5	CCR1	GTPγS binding	EC_{50} = 1.4 ± 0.2 nM in Ba/F3-CCR1 murine ProB cells [375] EC_{50} = 2.2 ± 0.7 nM in retinoic acid differentiated HL60 cells [369]
		Chemotaxis	EC_{50} = 0.6 nM in HEK293-CCR1 cells [378] Dose response = 6-360 nM in HEK293-CCR1 cells [376]
	CCR3	Calcium flux	ED_{50}s = 10 nM in AML14.3D10-CCR3 cells [379]

Chemokine	Chemokine receptor	Assay	Pharmacological properties
CCL5	CCR5	GTPγS binding	EC_{50} = 0.27 ± 0.13 nM in Ba/F3-CCR5 murine ProB cells [375] EC_{50} = 3.4 nM ± 0.27 in HEK293T-CCR5 cells [380] EC_{50} = 0.33 nM in CHO-CCR5 cells [355] EC_{50} = 0.5 nM in CHO-CCR5-CD4 cells [355]
		Calcium flux	EC_{50} = 2.3 nM in HEK293-CCR5 cells [380] EC_{50} = 80 nM in CHO-K1-CCR5 cells [96]
		cAMP	EC_{50} = 0.0501 nM in CHO-K1-CCR5 cells [8]
		BRET β-arrestin2 recruitment	EC_{50} = 7.94 nM in CHO-K1-CCR5 cells [96]
	Multiple	Receptor binding	IC_{50} = 1 nM in THP-1 cells [378]
		Calcium flux	EC_{50} = 13 nM in THP-1 cells [378]
		Chemotaxis	EC_{50} = 0.6 nM in THP-1 cells [378]
CCL8	CCR1	GTPγS binding	EC_{50} = 19.8 ± 2 nM in Ba/F3-CCR1 cells murine ProB cells [375]
		Chemotaxis	Dose response = 0.012-360 nM in HEK293-CCR1 [374]
	CCR2	Calcium flux	EC_{50} = 15.4 nM in 300.19-CCR2 murine pre-B cells [371]
		Chemotaxis	Dose response = 0.12-360 nM in HEK293-CCR2B [374]
		cAMP	EC_{50} = 3.98 nM in CHO-K1-CCR2 cells
		BRET β-arrestin2 recruitment	EC_{50} = 20 nM in CHO-K1-CCR2 cells [96]
	CCR3	GTPγS binding	EC_{50} = 1.10 nM in CHO-CCR3 cells [370]
		Internalisation	EC_{50} = 3.1 nM in CHO-CCR3 cells [370]
	CCR5	Receptor binding	K_d = 5 ± 2 nM in HEK293-CCR5 cells [381]
		GTPγS binding	EC_{50} = 5.5 nM in CHO-CCR5 cells [355]
		Calcium flux	EC_{50} = 39.8 nM in CHO-K1-CCR5 cells [96]
		Chemotaxis	EC_{50} = 0.12 nM in HEK293-CCR5 cells [381]
		cAMP assay	EC_{50} = 0.631 nM in CHO-K1-CCR5 cells [96]

Chemokine	Chemokine receptor	Assay	Pharmacological properties
CCL8	CCR5	BRET β-arrestin2 recruitment	EC_{50} = 100 nM in CHO-K1-CCR5 cells [96]
		Receptor binding	K_d = 2 nM in human peripheral blood monocytes [374]
CCL23	CCR1	Calcium flux	EC_{50} = 3-10 nM for CCR1 in retinoic acid differentiated HL60 cells [375]
		Chemotaxis assay	EC_{50} = 10-30 nM for CCR1 in retinoic acid differentiated HL60 cells [375]
		Receptor binding	K_i = 1 nM in HL-60-CXCR1 cells [382] K_d = 4.7 ± 0.095 nM in rat basophilic leukaemia-2H3-CXCR1 [383] K_d = 1.2 ± 0.54 nM in rat basophilic leukaemia-2H3-CXCR1 [384]
CXCL8	CXCR1	Calcium flux	EC_{50} = 2 nM in HL-60-CXCR1 cells [382] EC_{50} = 1.5 ± 0.1 nM in human neutrophils [385] agonist at 10 nM in rat basophilic leukaemia-2H3-CXCR1[384]
		PI hydrolysis	Dose dependent response = 0.1-1000 nM in rat basophilic leukaemia-2H3-CXCR1 [384]
		Chemotaxis	EC_{50} = 0.814 nM in human neutrophils [386] EC_{50} = 3.1 ± 1.1 in rat basophilic leukaemia -2H3-CXCR1 [385] Dose dependent response = 0.01-100 nM in rat basophilic leukaemia -2H3-CXCR1 [384]
		Internalisation	100 nM induced 50% CXCR1 internalisation after 60 mins in rat basophilic leukaemia-2H3-CXCR1 [384]

Chemokine	Chemokine receptor	Assay	Pharmacological properties
CXCL8	CXCR2	Receptor binding	K_i = 1 nM in HL-60-CXCR2 cells [382] K_d = 2.49 ± 0.13 nM in rat basophilic leukaemia -2H3-CXCR2 [383] K_d = 1.02 ± 0.94 nM in rat basophilic leukaemia -2H3-CXCR2 [384]
		Calcium flux	agonist at 10 nM in rat basophilic leukaemia -2H3-CXCR2 [384]
		PI hydrolysis	Dose dependent response = 0.1-1000 nM in rat basophilic leukaemia-2H3-CXCR2 [384]
		Chemotaxis	EC_{50} = 3.8 ± 0.2 in rat basophilic leukaemia -2H3-CXCR2 [385] - dose dependent agonism 0.01-100 nM in rat basophilic leukaemia-2H3-CXCR2 [384]
		Internalisation	100 nM induced 95% CXCR2 internalisation after 60 mins in rat basophilic leukaemia-2H3-CXCR2 [384]
CXCL9	CXCR3	GTPγS binding	EC_{50} = 260 nM in CHO-CXCR3 cells [387]
		Calcium flux	EC_{50} = 22 nM in rat basophilic leukaemia-CXCR3 [387]
		Chemotaxis assay	EC_{50} = 0.34 ± 0.05 nM in peripheral blood mononuclear cells from patients with chronic obstructive pulmonary disease [388] EC_{50} = 24.5 nM in H9 T lymphoma cells [387]

Chemokine	Chemokine receptor	Assay	Pharmacological properties
CXCL12	CXCR4	Calcium flux	EC_{50} = 1.6 nM in U87.CD4.CXCR4 cells [389] EC_{50} = ~2 nM in Fetal bovine heart endothelial cells [126] EC_{50} = 17 nM in HEK-293-CXCR4 cells [390]
		Chemotaxis	EC_{50} = 10-20 nM in human endothelial cells [126] EC_{50} = 7.9 nM in T-lymphoblast CCL-119 cells [391]
		Wound healing	EC_{50} = 508 nM in H1299 cells (human non-small cell lung carcinoma) [392]
		Dynamic mass redistribution	EC_{50} = 53 nM in Jurkat cells [390] EC_{50} = 73 nM in HEK-293-CXCR4 cells [390]
		S346/347-phosphyorylation	EC_{50} = 0.87 nM in HEK-293-HA-tagged CXCR4 cells [390]
		PRESTO-Tango β-arrestin recruitment	EC_{50} = 4.6 nM in HTLA cells [393]
		BRET β-arrestin recruitment assay	EC_{50} = 242 nM in HEK293T-CXCR4 cells [394]
	ACKR3 (previously known as CXCR7)	Receptor binding	K_d = 0.4 ± 0.1 nM in A0.01-CXCR7 T-cells [395]
		BRET β-arrestin2 recruitment	EC_{50} = 30 nM in HEK293T-CXCR7 cells [394]
		β-arrestin2 recruitment	EC_{50} = 18 ± 7 nM in CHO-CXCR7 cells [396]

Table 2.4. Details of small molecules used

Compound category	Compound	Protein target	Pharmacological properties	Supplier	Vehicle	Storage	Stock conc	Assay conc
Chemokine receptor antagonists								
	J113863	CCR1 CCR3	IC_{50} = 0.73 nM for CCL3 activation of CCR1 [397] IC_{50} = 0.58 nM for Eotaxin binding of CCR3 [397]	TOCRIS Bioscience (Bristol, England)	DMSO	4°C	10 mM	10 nM
	Maraviroc	CCR5	IC_{50} = 3.3 nM for CCL3 activation [398]	Pfizer (Sandwich, UK)	Ethanol	Room Temp	500 µM	10 nM
	AMD3100	CXCR4	CXCR4 IC_{50} = 5.7 nM Chemotaxis IC_{50} = 44 nM [396]	Santa Cruz (Dallas, USA)	DMSO	-20°C	100 mM	1 µM
Tyrosine kinase antagonists								
	FAK14	FAK	IC_{50} = 1 µM [399]	TOCRIS Bioscience	H_2O	-20°C	50 mM	1 µM
	PF562271	FAK	IC_{50} = 5 nM [400]	Abcam (Cambridge, UK)	DMSO	-20°C	10 mM	10 nM
	Masitinib	Lyn B	IC_{50} = 510 ± 130 nM [401]	Santa Cruz	DMSO	-20°C	100 mM	500 nM
	Bosutinib	Src	IC_{50} = 100 nM [402]	Selleck Chemicals (Munich, Germany)	DMSO	4°C	100 mM	250 nM-25 nM
	MNS	Src /Syk	IC_{50} = 29.3/2.5 µM [403]	Santa Cruz	DMSO	-20°C	1000 mM	10 µM

Compound category	Compound	Protein target	Pharmacological properties	Supplier	Vehicle	Storage	Stock conc	Assay conc
Serine/threonine kinase antagonists								
	Y27632	ROCK	ROCK1 K_i = 220 nM ROCK2 K_i = 300 nM [404]	TOCRIS Bioscience	H_2O	-20°C	2 mM	20 µM
	ZM336372	c-Raf	IC_{50} = 70 nM [405]	Santa Cruz	DMSO	-20°C	10 mM	1 µM
Phosphodiesterase antagonists								
	U73122	PLC/PIP_2	IC_{50} = 1-5 µM [406]	TOCRIS Bioscience	DMSO	-20°C	2 mM	1 µM-50 nM
ATPase pump antagonist								
	Thapsigargin	ER Ca^{2+} ATPase	IC_{50} = 30 nM [407]	Sigma Aldrich	DMSO	4°C		1%
Guanine nucleotide exchange factor antagonist								
	CPYPP	DOCK 1/2/5	DOCK 2 IC_{50} = 22.8 µM [408]	TOCRIS Bioscience	DMSO	-20°C	50 mM	5 mM-1 µM
PI3K antagonists								
	AS605240	PI3Kγ	IC_{50} = 8 nM [377]	Stratech Scientific (Ely, UK)	DMSO	-20°C	100 mM	2.5 µM
	LY294002	PI3K	IC_{50} = 1.4 µM [409]	Selleck Chemicals	DMSO	-20°C	25 mM	10 µM

Compound category	Compound	Protein target	Pharmacological properties	Supplier	Vehicle	Storage	Stock conc	Assay conc
G-protein antagonists								
	Gallein	Gβγ	IC_{50} = 241 ± 24 nM [410]	TOCRIS Bioscience	Ethanol	-20°C	6 mM	10 µM
	PTX	$G\alpha_i$	IC_{50} = 158 ± 40 pg/ml [411]	Sigma Aldrich	H_2O	4°C	0.1 µg/µL	100 ng/mL
	EHT 1864	Rac	Rac1 K_d = 40 nM Rac1b K_d = 50 nM Rac2 K_d = 60 nM Rac3 K_d = 230 nM [412]	Cambridge Biosciences (Cambridge, England)	H_2O	-20°C	10 mM	100 nM
Cytoskeletal effectors								
	CK666	Arp2/3	IC_{50} = 4 µM [413]	TOCRIS Bioscience	DMSO	-20°C	100 mM	10 µM
	Nocodazole	Microtubules	$\alpha\beta_{II}$ K_d = 0.52 ± 0.2 µM $\alpha\beta_{III}$ K_d = 1.54 ± 0.29 µM $\alpha\beta_{IV}$ K_d = 0.29 ± 0.04 µM [414]	TOCRIS Bioscience	Ethanol	-20°C	25 mM	3 µM
	Taxol	Microtubules	IC_{50} 1-10 nM [415]	Santa Cruz	DMSO	-20°C	100 mM	1 nM

2.3 Antibodies

Table 2.5. Primary antibodies

Antibody	Protein Target	Dilution factor	Supplier	Species raised in	Storage
MAB145	Human CCR1	1:100	R&D systems	Mouse	-20°C
HEK/1/85a/7a and 1/74/3j (abbreviated to 83a15j)	Human CCR5	1:500	Dr J.McKeating	Rat	4°C

Table 2.6. Secondary antibodies

Antibody	Antibody specificity	Dilution factor	Supplier	Species raised in	Storage
Anti-mouse IgG Tetramethylrhodamine (TRITC)	mouse	1:50	Sigma Aldrich	Goat	4°C
Anti-rat IgG Fluorescein isothiocyanate (FITC)	rat	1:50	Sigma Aldrich	Goat	4°C

2.4 Cellular migration experiments

2.4.1 The wound healing assay

Prior to cell seeding, 12 or 24 well plates were marked across the bottom with two parallel horizontal lines using a marker pen which served as a reference point for imaging the same scratches at different time points. Cells were seeded onto either a 12 or 24 well plate in 1 mL or 0.5 mL growth media respectively and incubated overnight at 37°C, 5% CO_2 and 100% humidity to form a confluent (100%) cell monolayer. The following day, growth media was removed and the cells were covered with 0.5 ml or 1 ml simple media to reduce cell proliferation. Three scratches were induced across the monolayer per well with either a 200 or 1000 µl pipette tip. After scratch induction, media was removed to clear cellular debris and cells were washed twice with 200 µl or 400 µl simple media. Each scratch was imaged using a Leica DMI6000 inverted microscope and Leica application suite, version 2.8.1.The image settings were at 77.7 ms exposure time, 0.75 saturation, 0.89 Gamma and 2.0X Gain and under 10x objective. After scratch imaging, chemokines and compounds were added to cells and incubated at 37°C, 5% CO_2 and 100% humidity for the designated time period. Following incubation the same scratches were reimaged using the previous imaging specifications. At the final time point all media was removed and cells were covered with 200 µl or 400 µl PBS.

To calculate cellular migration two approaches were used. The primary method involved measuring the scratch width before and after incubation using MS Powerpoint 2013. A ratio between the scratch width before and after incubation was taken to give a scale from 1 to 0. A value of 1 corresponded to no cellular migration, whilst 0 equated to full migration.

The alternative method was using ImageJ 1.48v. For this method, all images were cropped to show the scratch only. The cropped images were then converted to an 8-bit grey scale image and sharpened, with the edges of the cells marked and identified. To remove some of the background noise, the image was despeckled. The image background was then subtracted using the light background setting, with the rolling ball radius set at 10 µm pixel size, as

the largest size for all objects in the foreground. To measure the cell coverage, the threshold was adjusted to identify all objects considered as cells, with all objects/cells with pixel size: 0-infinity and circularity: 0-1 were counted. Cells at the edge of images and holes within cells were counted. From the particle analysis data, the percentage area (of cells) before incubation was divided by the percentage area (of cells) after incubation, to give a ratio of change in cell coverage (%). The closer the ratio was to 0, the more cellular migration.

2.4.2 Agarose spot assay

To make the agarose spot, low-melting point agarose (Sigma Aldrich) was diluted in PBS, to give a 0.5% agarose solution. The 0.5% agarose solution was heated on a hot plate, to dissolve the agarose particles, before being cooled to 40°C. Chemokine was prepared into a 0.1% BSA/PBS stock, and then diluted in molten 0.5% agarose solution (40˚C), to give a final concentration of 125 nM. For the control, 0.1% BSA/PBS was added to the 0.5% agarose solution.

Using a black marker, a line was marked across the middle, along the bottom of the 35 mm plate. One side was labelled as the control, whilst the other CXCL12 125 nM as shown in figure 2.1 (below).

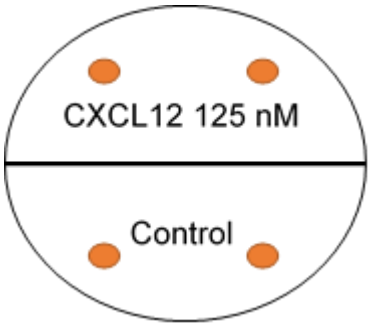

Figure 2.1. Agarose spot assay setup. Orange circles correspond to agarose spots.

2 mm was removed from the ends of 20 µl pipette tips, and two, 10 µl spots of either chemokine/agarose or PBS/agarose (control) were pipetted onto a 35 mm sterile plate. The plate was then incubated at 4°C for 5 mins to cool the agarose spots.

MDA-MB-231 cells were harvested with trypsin/PBS and prepared in 1 mL DMEM growth media, at a cell density of $17x10^4$ per mL cells. Cells were incubated at 37°C, 5% CO_2 and 100% humidity for 4 hrs allowing the cells to adhere to the base of the plate. After 4 hrs, DMEM growth media was removed and cells were covered with simple DMEM media, and then incubated at 37°C, 5% CO_2 and 100% humidity for 24 hrs.

Following incubation the edges of all four agarose spots were imaged using a Leica DMI6000 inverted microscope and Leica application suite, version 2.8.1. Cells within each spot were counted with the cell number used as a measurement of cellular migration.

2.4.3 Transwell migration assay

2.4.3.1 Suspension cells

Chemotaxis was measured using a microchemotaxis chamber (ChemoTx® System from Neuro Probe Inc.) with wells blocked with 30 µl of blocking buffer (1% BSA in simple RPMI) for 30 mins. Following blocking, 31 µl of chemokine diluted in working buffer (0.1% BSA in simple RPMI) or working buffer alone for controls, was added to each well. Cells were then harvested and adjusted to a concentration of $25x10^4$ cells mL^{-1} and $50x10^4$ cells mL^{-1} per well for Jurkats and THP-1 cells respectively, and resuspended in working buffer. Cells were then incubated with either vehicle or compounds for 30 mins at 37°C and 5% CO_2, prior to loading. 20 µl cells were then loaded onto a 5 µm pore polyvinylpyrollidone-free polycarbonate filter membrane and incubated for 4 hrs at 37°C and 5% CO_2 in a humidified chamber. After 4 hrs, the polyvinylpyrollidone-free polycarbonate filter membrane was removed and 10 µl was taken from the wells and loaded onto a Neubauer hemocytometer. Cells present in each well were counted, with the number of cells counted used as a measure of cellular chemotaxis. All conditions were performed in duplicates.

2.4.3.2 Adherent cells

Similar to suspension cells: chemotaxis was measured using a microchemotaxis chamber (ChemoTx® System from Neuro Probe Inc.). All wells were blocked with 30 µl of blocking buffer (1% BSA in simple RPMI) for 30 mins. Following blocking, 31 µl of chemokine diluted in working buffer (0.1% BSA in simple RPMI) or working buffer alone for controls, was added to each well. PC-3 cells were harvested with 3 ml of 0.25% Trypsin/EDTA and adjusted to a concentration of $10x10^4$ cells per mL^{-1} per well. 20 µl of cells were then loaded onto a 8 µm pore polyvinylpyrollidone-free polycarbonate filter membrane and incubated for 24 hrs at 37°C and 5% CO_2 in a humidified chamber. After 24 hrs, cells on the upper surface of the membrane were removed gently through swabbing with a cotton bud. Working buffer was removed from the wells and washed once with 31 µl of PBS. 31 µl of 4% paraformaldehyde was then added to the wells and the underside of the membrane was fixed for 5 mins. Following fixation, wells were washed with PBS (31 µl) and then 31 µl of crystal violet (Biocolor Ltd) was added. The underside of the 8 µm pore polyvinylpyrollidone-free polycarbonate filter membrane was stained for 30 mins. After 30 mins the membrane was washed with PBS to remove excess crystal violet. To account for the background staining from the crystal violet: a well which had been incubated with no cells was also fixed and then stained with crystal violet. To measure chemotaxis, all cells on the underside of the 8 µm pore polyvinylpyrollidone-free polycarbonate filter membrane were counted using a Leica DMI6000 inverted microscope with a 40x objective. The number of cells counted for each condition was subtracted against the number of cell shaped objects identified from the background stain, as a true measurement of cellular chemotaxis.

2.4.4 Time-lapse assay

PC-3 cells were harvested with 1.5 mL of 0.25% Trypsin/EDTA. PC-3 cells were sparse seeded onto a 24 well plate by pipetting 10 µl of cells into 1 mL of RPMI growth media. Cells were then incubated overnight at 37°C, 5% CO_2 and 100% humidity. Following incubation, growth media was removed and cells were recovered in 200 µl of fresh RPMI growth media. Cells were then incubated in the presence or absence of CXCL12 and inhibitors for 10 hrs at 37°C, 5% CO_2 and 100% humidity. During incubation cells were imaged every 4 mins with a Zeiss Axiovert 200M microscope and using AxioVision Rel 4.8 software at a 10x objective. Cell migration was analysed using ImageJ 1.48v with all the images set at 1 µm for the z plane and either 1.023 or 0.645 µm as the scale for the x/y plane: hence all the data was normalised. The distance was manually tracked for a least 10 cells per condition and the cellular velocity calculated as the distance (µm)/time (hrs).

2.5 Cellular signalling experiment

2.5.1 Intracellular calcium flux assay

Cells were harvested with appropriate agent and centrifuged at 12000 rpm for 5 mins. Thereafter cells were washed twice and resuspended in calcium flux buffer (reagents: 137 mM NaCl, 5 mM KCl, 1 mM MgCl, 1.5 mM $CaCl_2$, 10 mM Hepes and 25 mM D-glucose (pH 7.4)) (4°C). Cells were then incubated with 4 µM of Fura-2 AM (Invitrogen, ThermoFischer Scientific) alongside vehicle or compounds for 30 mins in the dark, at 37°C, 5% CO_2 and 100% humidity. For experiments involving PTX, MCF-7 cells were seeded and incubated overnight in two separate 25 cm^2 cell culture flasks to reach a 95% confluency. After incubation growth media was removed and the cells were incubated for a further 16 hrs with PTX in simple DMEM (100 ng/mL) or simple DMEM alone as a control. Following 16 hrs the cells were detached and harvested as per usual.

Cells were then washed twice with calcium flux buffer (4°C) to remove excess Fura-2 AM. 100 µl of cells were then added to each well of the 96 well black plate and loaded into the Fluorometer. The Fluorometer microinjector pump

was cleaned with H_2O (room temperature) twice, both before and after chemokine priming. The Fluorometer ran under BMG Labtech FLUOstar OPTIMA/POLARstar program with the Gain threshold set at 30%. Cells were excited at both 340 and 380 nm and the emission was measured at 510 nm at 1.46 secs intervals over a 73 secs assay running time. Chemokines were injected after 15 secs of the assay running time.

The intracellular calcium levels were measured as a ratio between the relative fluorescent units (at 510 nm) of the calcium bound Fura-2 (340 nm) and unbound Fura-2 (380 nm). Intracellular calcium fluctuations were quantified using two approaches: one by subtracting the difference between the 340:380 ratio prior to chemokine stimulation (background fluorescence) and the peak 340:380 ratio after chemokine stimulation (maximal fluorescence). Alternatively the 340:380 ratio data points were all normalised to the first data point (0 secs) which was defined as 100%. GraphPad Prism 6 was then used to measure the Area under Curve with the baseline set at 100% and only peaks above this baseline measured.

2.6 Cellular proliferation experiment

2.6.1 MTS cytotoxicity assay

Cells were seeded in growth media (200 µl) at the appropriate cell density onto either a round or flat bottomed clear 96 well plate (Sterilin Ltd, UK) depending on suspension or adherent cell type respectively. Control wells contained growth media only to measure background absorbance. 100 µl of PBS was added to surrounding wells to prevent loss of media during incubation. Cells were incubated in the presence or absence of compounds for the designated time at 37°C, 5% CO_2 and 100% humidity.

After incubation 10 µl of MTS reagent (3-(4,5-Dimethylthiazol-2-yl)-5-(3-carboxymethoxyphenyl)-2-(4-sulfophenyl)-2H-tetrazolium from CellTiter 96 AQ_{ueous} Non-Radioactive Cell Proliferation Assay (Promega)) was added to each well and incubated for at least one h.

During incubation the NAD(P)H dehydrogenase in viable cells metabolises the MTS tetrazolium into formazan, which is a purple coloured compound soluble in media. The concentration of formazan can be quantified by measuring it's absorbance at 492 nm using a BMG Labtech FLUOstar fluorometer. The absorbance readings are directly proportional to the number of viable cells allowing changes in cellular proliferation to be detected.

After incubation the absorbance of the plate was read at 492 nm. Cellular proliferation was measured against the absorbance reading of the media (background) whilst compound cytotoxicity was assessed against the control (cells only).

2.7 Cellular imaging experiments

2.7.1 Immunofluorescence

Cells were detached after reaching 90% confluency and seeded onto a glass coverslip in a 12 well plate containing growth media (1.5 ml) and incubated at 37°C, 5% CO_2 and 100% humidity overnight. Following incubation growth media was removed and 500 µl of PBS (4°C) was added. Cells were washed twice with PBS (4°C) and incubated with the primary antibody for 1 h at 4°C, except for the control cells which were incubated with PBS (4°C) only. After incubation the primary antibody was removed and the cells were washed twice with PBS (4°C) and then incubated with the secondary antibody for 1 h at 4°C in the dark. Following 1 h the cells were washed twice with PBS (4°C) and fixed with 4% Paraformaldehyde and then mounted onto glass slide using DPX (Thermo Fisher Scientific) or alternatively fixed with glycerol and imaged thereafter. All cells were imaged using Leica DMI6000 inverted microscope and Leica application suite, version 2.8.1.

2.7.2 Phalloidin Staining

Cells were harvested using the appropriate agent after reaching 90-95% confluency. MCF-7 and CHO-CCR5 cells were seeded onto a 12 well plate with glass coverslips whilst PC-3 cells were seeded onto a 12 well plate. All cells were grown in 1.5 ml growth media and incubated overnight at 37°C, 5% CO_2 and 100% humidity. After cells had reached 70-80% confluency the growth media was removed and cells were washed twice with simple media (400 µl). Chemokines and inhibitors were added to the cells and incubated for 24 hours at 37°C, 5% CO_2 and 100% humidity. After 24 hrs the media was removed and cells were washed twice with 500 µl of PBS (4°C), and fixed with 100 µl of 4% Paraformaldehyde for 5 mins. After fixing cells were washed once more with 500 µl PBS (4°C) and then permeabilized with 200 µl, 0.1% Triton x-100 (FischerBiotech) for 10 mins. Following permeabilized, cells were washed with 500 µl PBS (4°C) and stained with 200 µl Phalloidin CruzFluor TM^{594} conjugate (Santa Cruz) (diluted 1:1500 in 1% BSA/PBS) and incubated for 30 mins in the dark at room temperature. Cells were washed again with 500 µl PBS (4°C) and either mounted with DPX onto glass slide or recovered with 500 µl PBS in the 12 well plate. All fixed cells were imaged using a Leica DMI6000 inverted microscope and Leica application suite, version 2.8.1.

2.7.3 Phalloidin Staining: ImageJ analysis

All images were converted to 32-bit grayscale using ImageJ 1.48v and the contrast enhanced to 0.4% saturated pixels to identify cells easier. All clearly visible cells were drawn around using freehand selection and measured for area, shape descriptors, integrated density and mean gray value. The cellular fluorescence was calculated using the corrected total cell fluorescence (CTCF) equation:

CTCF = integrated density of selected cell – (area of selected cell x mean fluorescence of background readings).

Two background readings were taken for each image: a high and a low fluorescence reading. A mean was then taken from these two background readings. A minimum of six images for each condition was taken.

2.8 Data and Statistical Analysis

All data collected was analysed using GraphPad Prism 6 (GraphPad software). Post hoc statistical analysis was performed using one-way analysis of variance (ANOVA) or Kruskal Wallis test with the appropriate multiple comparison test applied as stated in figure legend. In appropriate cases datasets were compared using an unpaired Student's t-test or Wilcoxon Signed Rank Test. 95% was deemed a value for significance in all statistical tests performed with p-values ≤0.05 = *, ≤0.01 =**, ≤0.001= *** and ≤0.0001= ****. Dose response curves were fitted and analysed using a non-linear regression dose-concentration response curve assuming a Hill coefficient of 1. All data was formatted to the mean and ± standard error of means (S.E.M.) for a minimum 3 independent experiments unless stated otherwise.

Chapter 3.0 Screening for chemokine signalling pathways involved in carcinoma metastasis

3.1 Introduction

Chemokines are small extracellular proteins which are synthesised and secreted by cells upon detection of inflammatory, bacterial and viral molecules present in the tissue microenvironment [108-110]. Secreted chemokines have the ability to bind to GAGs on neighbouring stromal cells which retains their presence in the tissue microenvironment to form a local concentration gradient [416]. This chemokine concentration gradient serves as a chemoattractant for immune cells expressing chemokine receptors and forms the basis for mounting an immune system response towards the infection and/or tissue damage or alternatively for immunosurveillance as part of the body's homeostasis [417]. This immune system response is vital for the survival of multicellular organisms and therefore tightly regulated. However over time aberrations within this process can occur caused by the dysregulation of upstream regulators of chemokine receptor expression or due to chronic inflammation from the external environment leading to chemokine overexpression. Both can give rise to inflammatory associated diseases such as rheumatoid arthritis, atherosclerosis and cancer metastasis [113].

Clinical data from cancer patients has shown that chemokines are often overexpressed at the sites of metastasis such as lung, liver and brain [115], whilst chemokine receptors are overexpressed on metastatic cancer cells including breast [418, 419], pancreatic [420] and prostate [421]. Hence dysregulation in chemokine signalling is often associated with a poorer prognosis [115]. This has therefore generated much interest in targeting both chemokines and receptors to block cancer metastasis but to date this approach has been ineffective. There have been several reasons cited for the lack of clinical efficacy, with chemokine signalling redundancy considered as one of the main challenges [319, 320]. As cancer cells frequently overexpress

several chemokine receptors whilst sites of metastasis inhabit a variety of different chemokines. Therefore targeting just one receptor or chemokine is ineffective as alternative chemokine signalling pathways could become activated instead.

However the extent of this chemokine redundancy is starting to be questioned due to the emergence of many studies identifying evidence of biased signalling in both chemokines and receptors [96, 97]. Biased signalling has been shown to give rise to differences in cellular physiology in a few notable examples. Such as for CCR2, whereby activation by CCL2 induces actin polymerisation whilst CCL11 activation blocks actin polymerisation [422] or CXCL8 inducing respiratory burst in neutrophils via CXCR1 but not CXCR2 [423]. Though biased signalling is not merely dependent on just the ligand and receptor, it can also be influenced by the cell type, commonly referred to as tissue bias [424]. Tissue bias has been recognised within the CCL19-CCR7 signalling axis whereby CCL19 induces chemotaxis in dendritic cells [100] but not to the same extent in T-lymphocytes [99].

Despite a handful of examples demonstrating the role of biased signalling in normal cellular behaviour even less is known about the role it could play in disease states such as cancer metastasis. This evidence of biased signalling in chemokines could imply that the low clinical success rate in treating cancer is due to targeting inappropriate chemokine signalling pathways rather than any functional redundancy.

Although many clinical studies have identified a variety of different chemokines associated with cancer metastasis, numerous published target validation studies have tended to focus on chemokines such as CCL2, CCL5, CCL19, CCL21 and especially CXCL12 particularly for breast cancer [425-427] and to a lesser extent prostate [262, 263, 421, 427] and pancreatic cancer [262, 420, 428-430] amongst a family of 50 known chemokines. Consequently there are still many chemokines yet to be properly validated as therapeutic targets for blocking cancer metastasis.

3.2 Chapter Aim

- Identify chemokine signalling pathways involved in carcinoma metastasis for therapeutic targeting.

- Explore the extent of functional redundancy within chemokine signalling.

3.3 Immunofluorescence staining for CCR5 and CCR1 in different carcinoma cell types

Chemokine receptors are frequently overexpressed on different carcinoma cell types, whilst in normal epithelial cells their expression is either low or absent [287, 418]. This has made the chemokine receptor a promising therapeutic target.

There are currently 23 known chemokine receptors, with 4 considered atypical and do not signal via $G\alpha_i/\beta\gamma$, and as such are not considered important for cell migration [35, 431]. Amongst the "typical" chemokine receptors, their expression on cancer cells can be dependent on the cell type [130].

To identify chemokine signalling pathways which could be important carcinoma metastasis, two chemokine receptors CCR5 and CCR1 were stained for on four separate carcinoma cell types: MCF-7 and MDA-MB-231 (both breast), PC-3 (prostate) and MIA PaCa-2 (pancreatic). CCR5 and CCR1 are normally expressed on leukocytes and are involved in inflammation [48, 432]. Both receptors have overlapping cognate ligands CCL3, CCL5 and CCL8 which allows us to identify any chemokine specific bias in cancer cell migration.

CCR5 expression has been identified on several cancer cell lines including MCF-7, MDA-MB-231, MIA PaCa-2 and PC-3 [338, 420, 433, 434]. Nonetheless there have been conflicting reports on chemokine receptor expression on the same cell lines [435, 436]. The immunofluorescence stain was therefore performed to gain insight into possible receptor expression prior to the chemokine screen. Furthermore CCR5 was also stained for on the CHO-CCR5 cells as a control for the CCR5 antibody 83a15j.

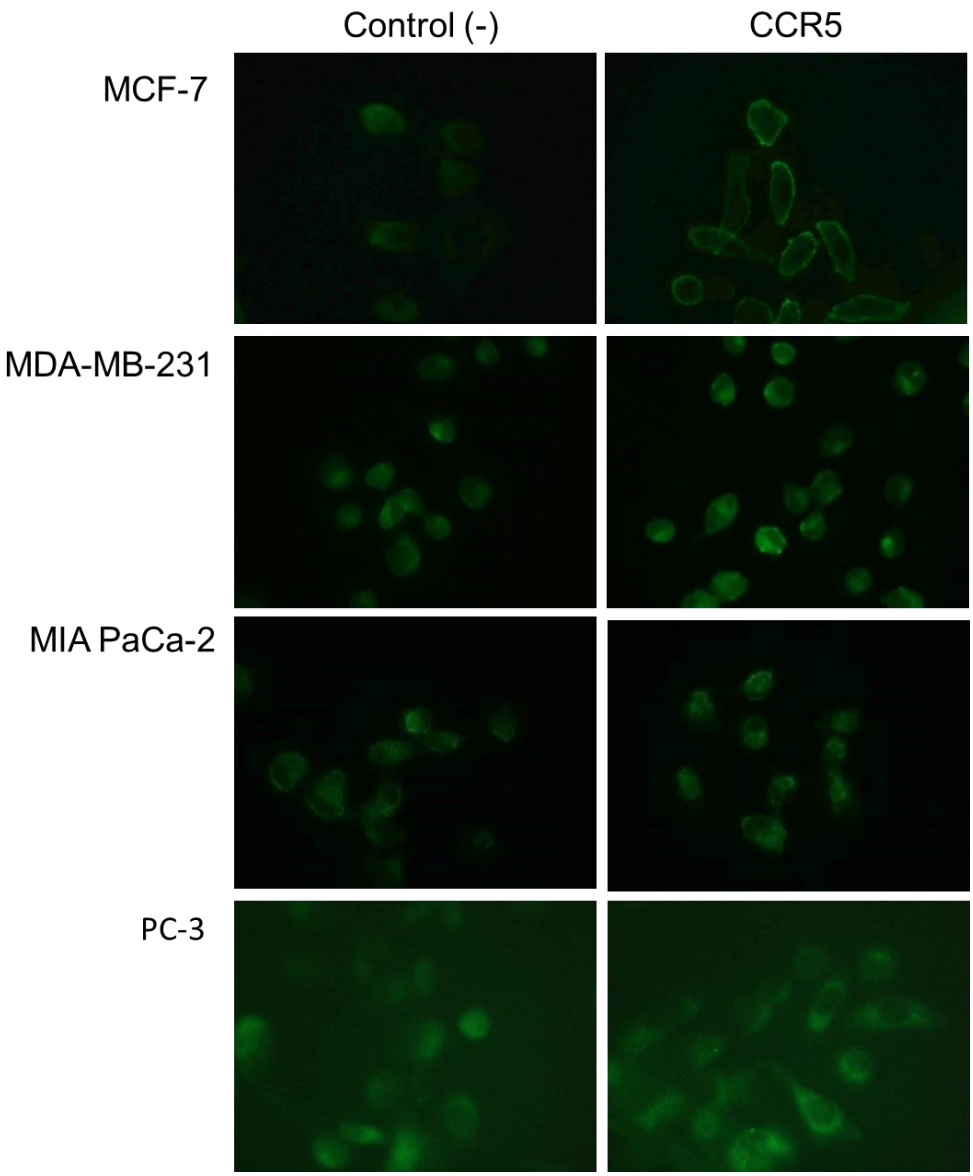

Figure 3.1. Immunofluorescence staining of CCR5. Anti-CCR5 stain (83a15j) counterstained using anti-rat FITC. Control (-) was anti-Rat FITC alone. All images are representative of the cell population and were taken at 63x objective with a Leica DMI6000 inverted microscope and using Leica application suite.

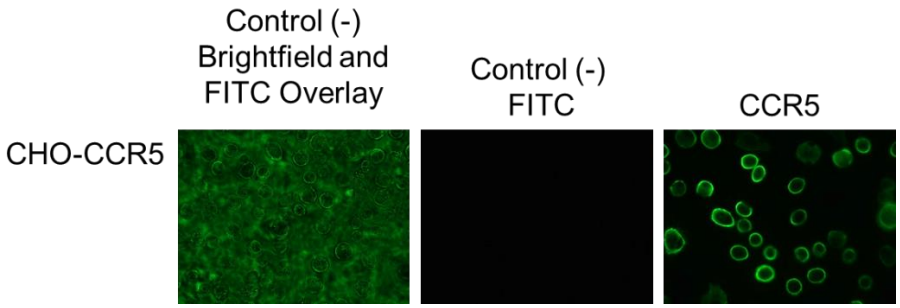

Figure 3.2. Immunofluorescence staining of CCR5. CHO-CCR5 cells express CCR5. Anti-CCR5 stain (83a15j) counterstained using anti-rat FITC. Control (-) was anti-rat FITC alone. Images are representative of the cell populations and were imaged at 63x objective with a Leica DMI6000 inverted microscope and using Leica application suite.

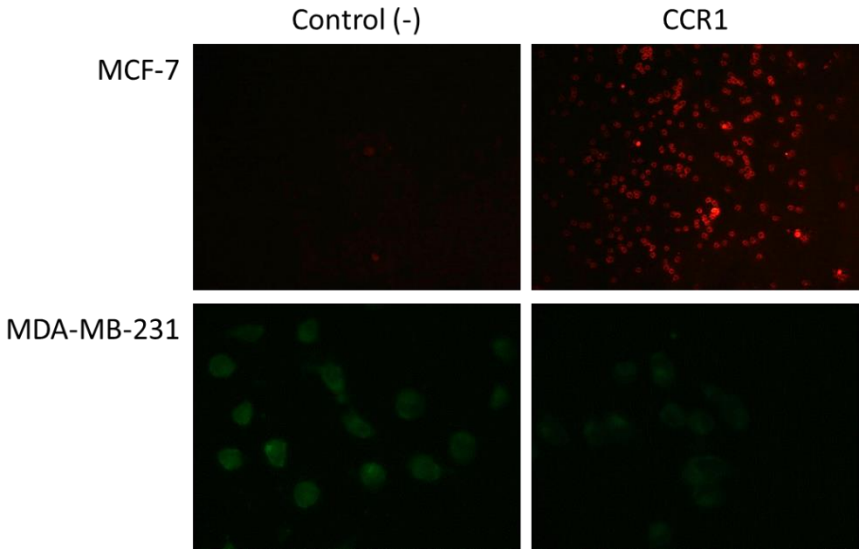

Figure 3.3. Immunofluorescence staining of CCR1. Images are representative of the cell populations. Anti-CCR1 stain (MAB145) counterstained with anti-mouse TRITC in MCF-7 cells and anti-mouse FITC in MDA-MB-231 cells. Control (-) was anti-mouse TRITC and anti-mouse FITC for MCF-7 and MDA-MB-231 cells respectively. MCF-7 cells were imaged at 10x objective and MDA-MB-231 cells were imaged at 63x objective with a Leica DMI6000 inverted microscope and using Leica application suite.

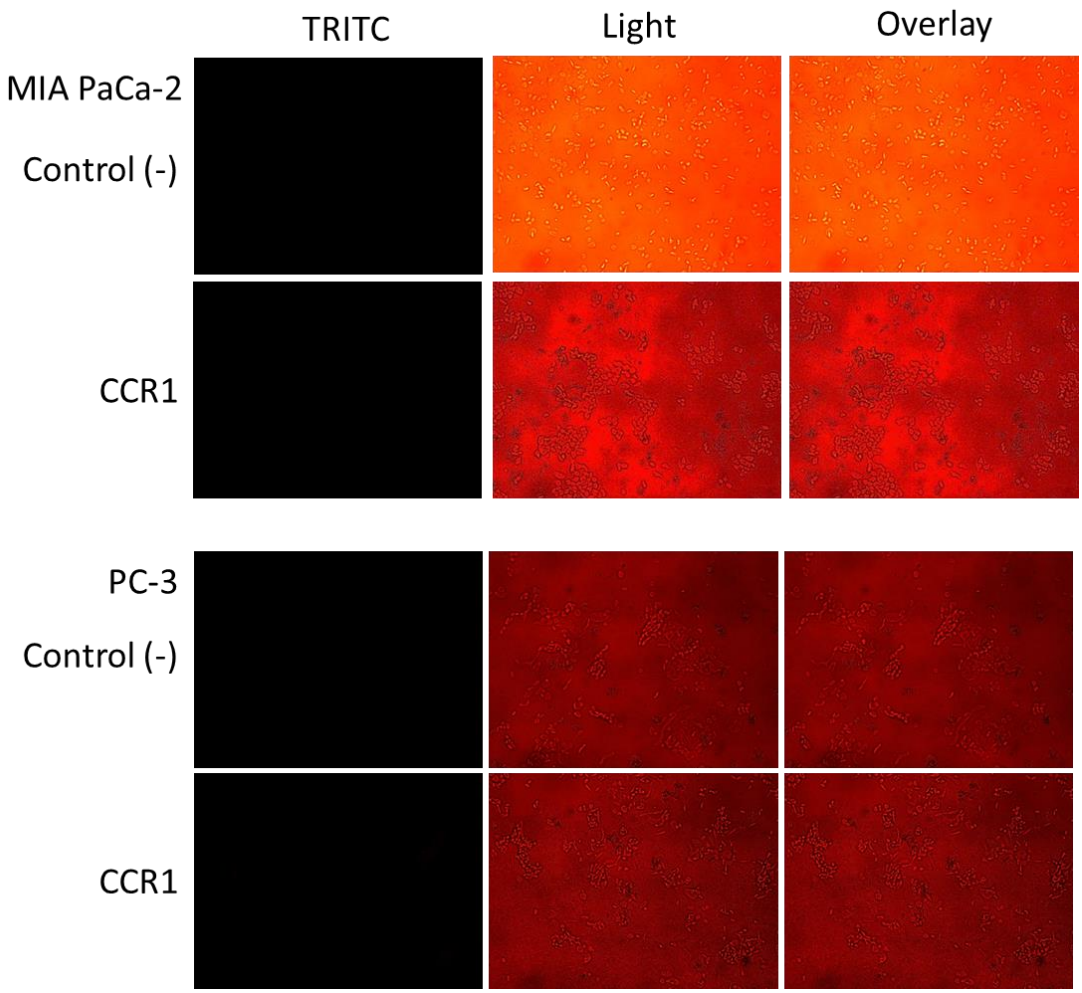

Figure 3.4. Immunofluorescence staining of CCR1. MIA PaCa-2 and PC-3 cells do not express CCR1. Anti-CCR1 stain (MAB145) counterstained with anti-mouse TRITC. Control (-) was TRITC alone. Images are representative of the cell population and were taken at 10x objective with a Leica DMI6000 inverted microscope and using Leica application suite.

Staining for CCR5 with 83a15j identified possible CCR5 expression on MCF-7, MIA PaCa-2, MDA-MB-231 and PC-3 and unsurprisingly in stably transfected CHO-CCR5 cells (figures 3.1 and 3.2). Immunofluorescence staining for CCR1 using MAB145 showed some CCR1 expression in MCF-7 cells but only within a small area of collected cells which may indicate that CCR1 is only expressed in a small subset of MCF-7 cells (figure 3.3). None of the other cell lines showed any clear evidence of CCR1 expression (figures 3.3 and 3.4).

3.4 CCL2 and CCL3 promote scratch closure in PC-3 and MCF-7 cells respectively after 24 hrs

To identify chemokine signalling pathways involved in carcinoma metastasis a screen of seven different chemokines: CCL2, CCL3, CCL4, CCL8, CCL23, CXCL9 and CXCL12, was devised for testing in four separate secondary carcinoma cell lines: MCF-7 and MDA-MB-231, MIA PaCa-2 and PC-3. Amongst the selected chemokines, many of the CC chemokines are ligands for the same receptors (see table 3.1) allowing us to identify potential ligand or receptor redundancy in chemokine signalling. The four different carcinoma cell types, cover three types of carcinoma and two breast cancer subtypes: hormone positive (MCF-7) and triple negative (MDA-MB-231), as well as exhibiting varying degrees of invasiveness. These phenotypic differences allow us to observe any carcinoma specific effects and potentially prognostic significance in chemokine signalling.

Table 3.1. Chemokines (screened), cognate receptors and published studies on MCF-7, MDA-MB-231, MIA PaCa-2 and PC-3 cell migration *in vitro*

Chemokines	Chemokine receptors	MCF-7	MDA-MB-231	MIA PaCa-2	PC-3
CCL23	CCR1				
CCL3	CCR1, 5	CTX [437] WH [346]			
CCL4	CCR1, 5	CTX [437]			WH [438] CTX [438]
CCL8	CCR1, 2, 3, 5				
CCL2	CCR2, 3	CTX [437, 439] WH [439]	CTX [440]	CTX [441]	CTX [278, 441]
CXCL9	CXCR3				
CXCL12	CXCR4, 7	WH [340, 346]	AS [442] WH [443]	CTX [444-446] CTX [447]	AS [448] CTX [278, 448] WH [448]

References in green highlight studies which showed a promotion of cell migration, whilst red studies showed no effect on cell migration and orange mixed depending on endogenous or exogenous chemokine source. Abbreviations: AS = Agarose spot, CTX = Chemotaxis, WH = wound healing assay. Chemokines and their listed cognate receptors were based on the published studies listed in table 2.3.

One of the methods commonly used by researchers to understand carcinoma metastasis is using the wound healing assay, an assay which partly mimics the *in vivo* wound healing process *in vitro*. Wound healing *in vivo*, is a process comprised of four main stages, beginning with haemostasis, whereby following injury, platelets and fibrin, aggregate to clot the blood [135, 449]. Thereafter, leukocytes flood the injured area, removing cellular debris, foreign particles or any microorganisms as part of the inflammatory stage. During the proliferative stage, the wound is contracted by myofibroblasts, and the extracellular matrix is assembled, with angiogenesis and re-epithelialisation occurring within the injury site [135, 449]. The final stage involves remodelling of the collagen from type III to type I giving rise to denser collagen fibres to strengthen the epithelium. As a chemoattractant, chemokines play a vital role in regulating wound healing by recruiting leukocytes, endothelial cells, and keratinocytes for inflammation, angiogenesis and re-epithelialisation respectively [450].

The wound healing assay is particularly useful for understanding collective migration of adherent cells, but it can also measure cell proliferation, spreading and survival. The assay involves adherent cells forming a 100% confluent cellular monolayer on the bottom of the well. Scratches are then introduced across the monolayer, normally with a pipette tip, and thereafter are imaged either continuously or at specific timepoints, to track cellular migration. The advantage of the assay lies not only in its simplicity, but as the cells grow to form a sheet, it simulates how cells normally exist within the epithelium [451] and how carcinoma cells invade the surrounding tissue [141, 452]. For these reasons the wound healing assay was used as a model to screen the seven separate chemokines for their involvement in carcinoma cell migration.

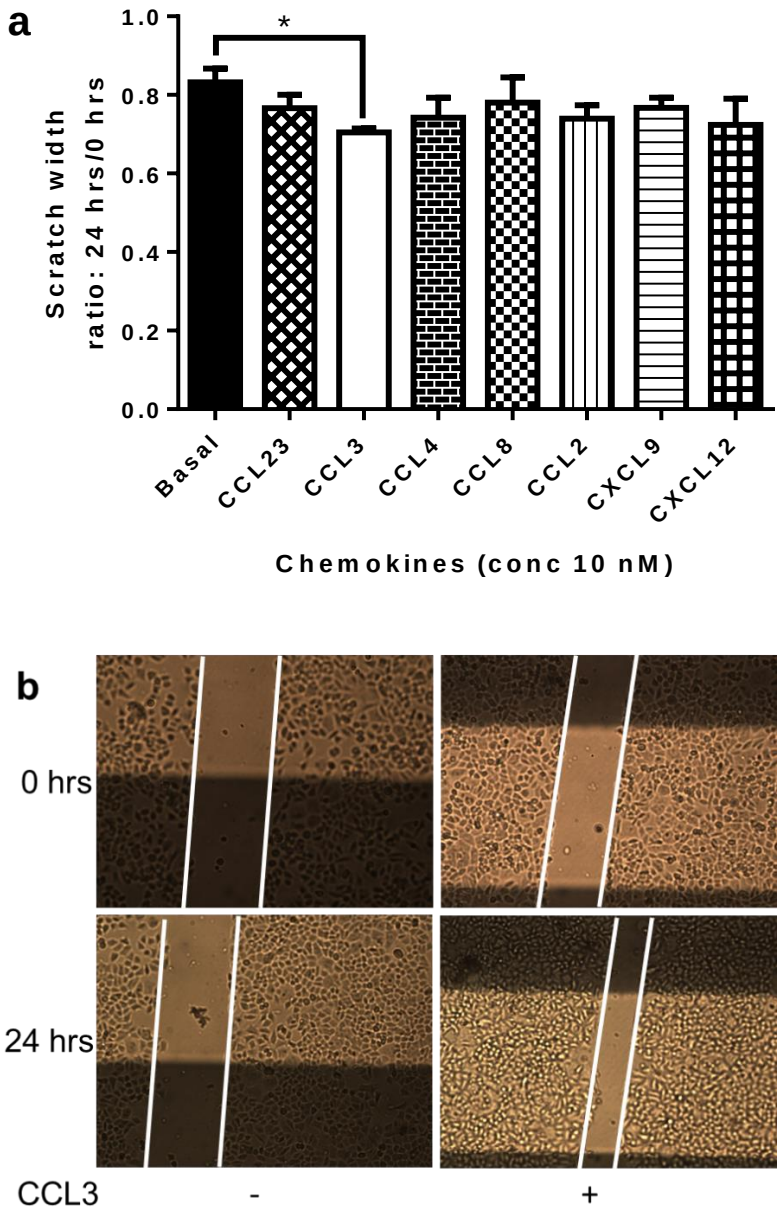

Figure 3.5. Chemokine screening in the wound healing assay of MCF-7 cells. (a) CCL3 (10 nM) promotes MCF-7 scratch closure after 24 hrs. A value of 1 denotes no migration, whilst 0 denotes complete migration. (b) Representative image of CCL3 (10 nM) scratch closure in MCF-7 cells after 24 hrs. MCF-7 cells treated with CCL3 (24 hrs) had a scatch width ratio of 0.58 compared to 0.89 for the basal. All images were taken at 10x objective with a Leica DMI6000 inverted microscope and using Leica application software. Results represent the mean $^{\pm}$ S.E.M. of four independent experiments (One-way ANOVA, Uncorrected Fisher's LSD, with * = $p \leq 0.05$).

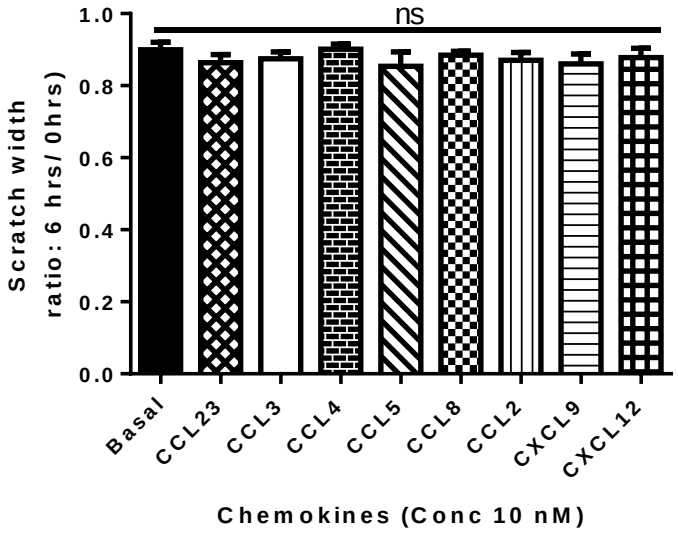

Figure 3.6. Chemokine screening in the wound healing assay of MDA-MB-231 cells for 6 hrs. A value of 1 denotes no migration, whilst 0 denotes complete migration. Results represent the mean ± S.E.M. of at least five independent experiments. (One-way ANOVA, Uncorrected Fisher's LSD, ns = p value≥0.05 of no significance).

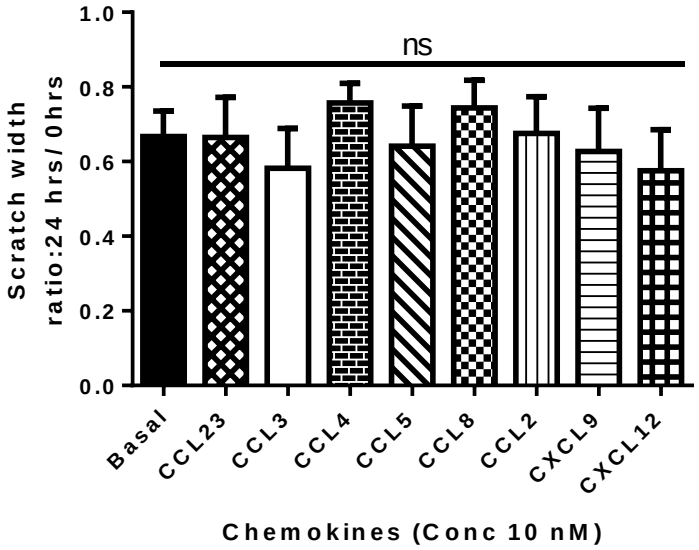

Figure 3.7. Chemokine screening in the wound healing assay of MDA-MB-231 cells for 24 hrs. A value of 1 denotes no migration, whilst 0 denotes complete migration. Results represent the mean ± S.E.M. of at least three independent experiments. (One-way ANOVA, Uncorrected Fisher's LSD, ns = p value≥0.05 of no significance).

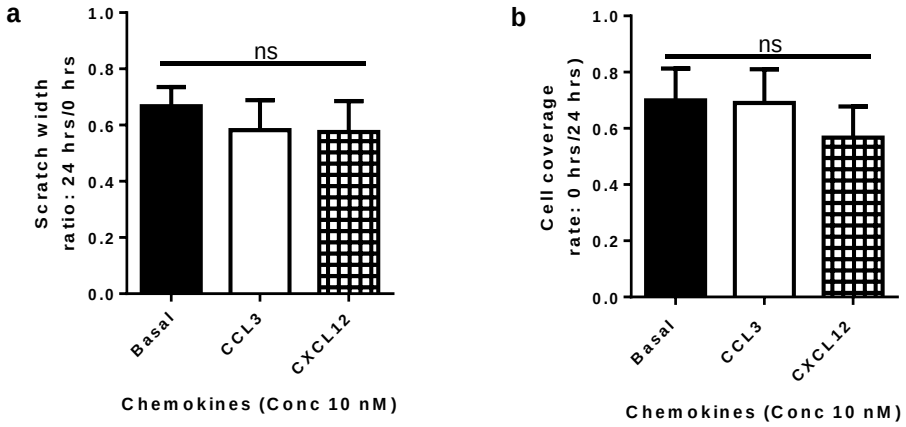

Figure 3.8. CCL3 (10 nM) and CXCL12 (10 nM) do not affect MDA-MB-231 scratch closure after 24 hrs. (a) Cell migration was assessed by measuring changes in scratch width. (b) Cell migration was assessed by measuring changes in cell coverage. A value of 1 denotes no migration, whilst 0 denotes complete migration. Results represent the mean ± S.E.M. of at least four independent experiments. (One-way ANOVA, Uncorrected Fisher's LSD, ns = p value≥0.05 of no significance).

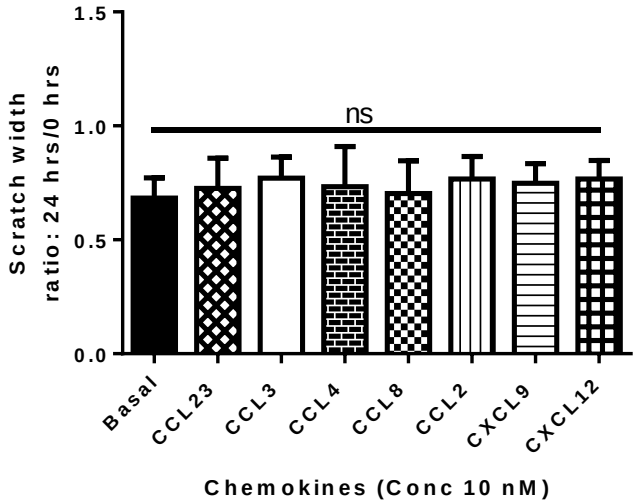

Figure 3.9. Chemokine screening in the wound healing assay of MIA PaCa-2 cells for 24 hrs. A value of 1 denotes no migration, whilst 0 denotes complete migration. Results represent the mean ± S.E.M. of at least three independent experiments. (One-way ANOVA, Uncorrected Fisher's LSD, ns = p value≥0.05 of no significance).

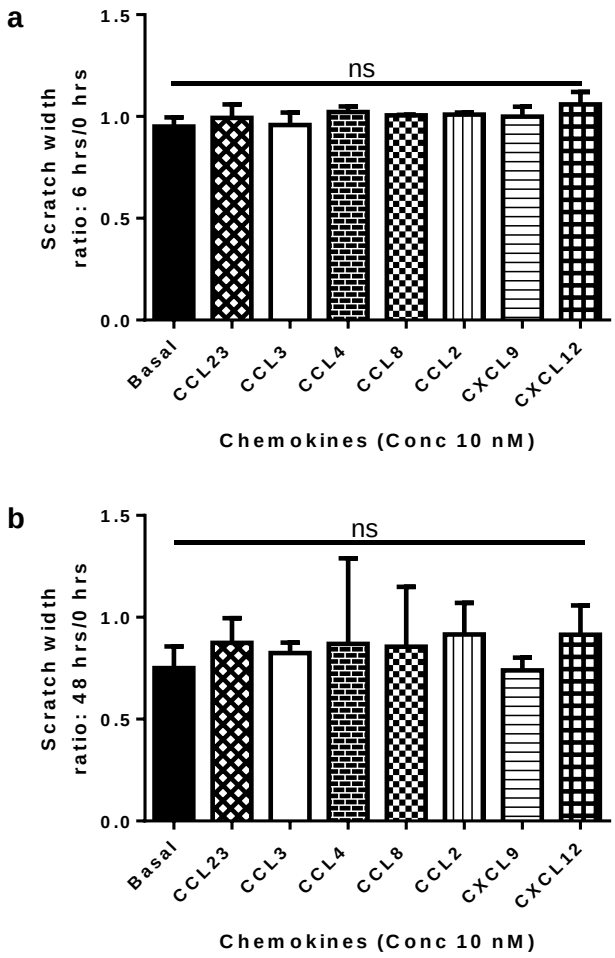

Figure 3.10. Chemokine screening in the wound healing assay of MIA PaCa-2 cells. MIA PaCa-2 cells were treated with chemokines (10 nM) for 6 hrs (a) and 48 hrs (b). A value of 1 denotes no migration, whilst 0 denotes complete migration. Results represent the mean ± S.E.M. of at least two independent experiments. (One-way ANOVA, Uncorrected Fisher's LSD, ns = p value≥0.05 of no significance).

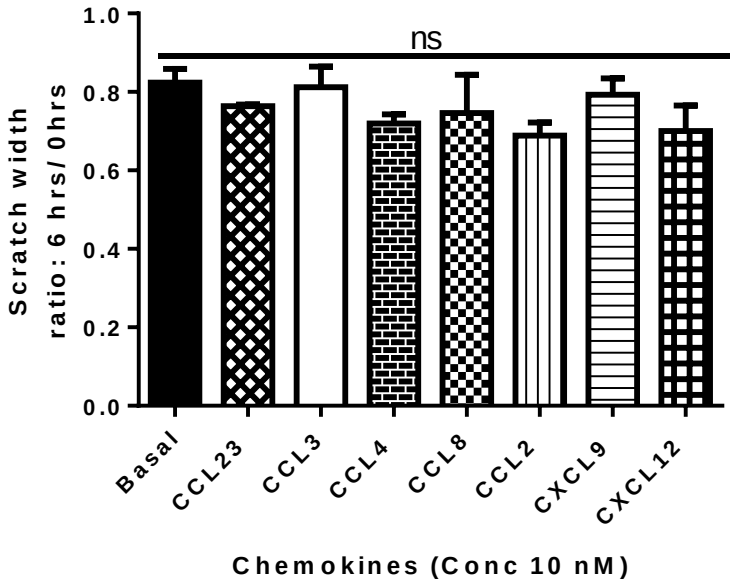

Figure 3.11. Chemokine screening in the wound healing assay of PC-3 cells for 6 hrs. A value of 1 denotes no migration, whilst 0 denotes complete migration. Results represent the mean ± S.E.M. of at least two independent experiments. (One-way ANOVA, Uncorrected Fisher's LSD, ns = p value≥0.05 of no significance).

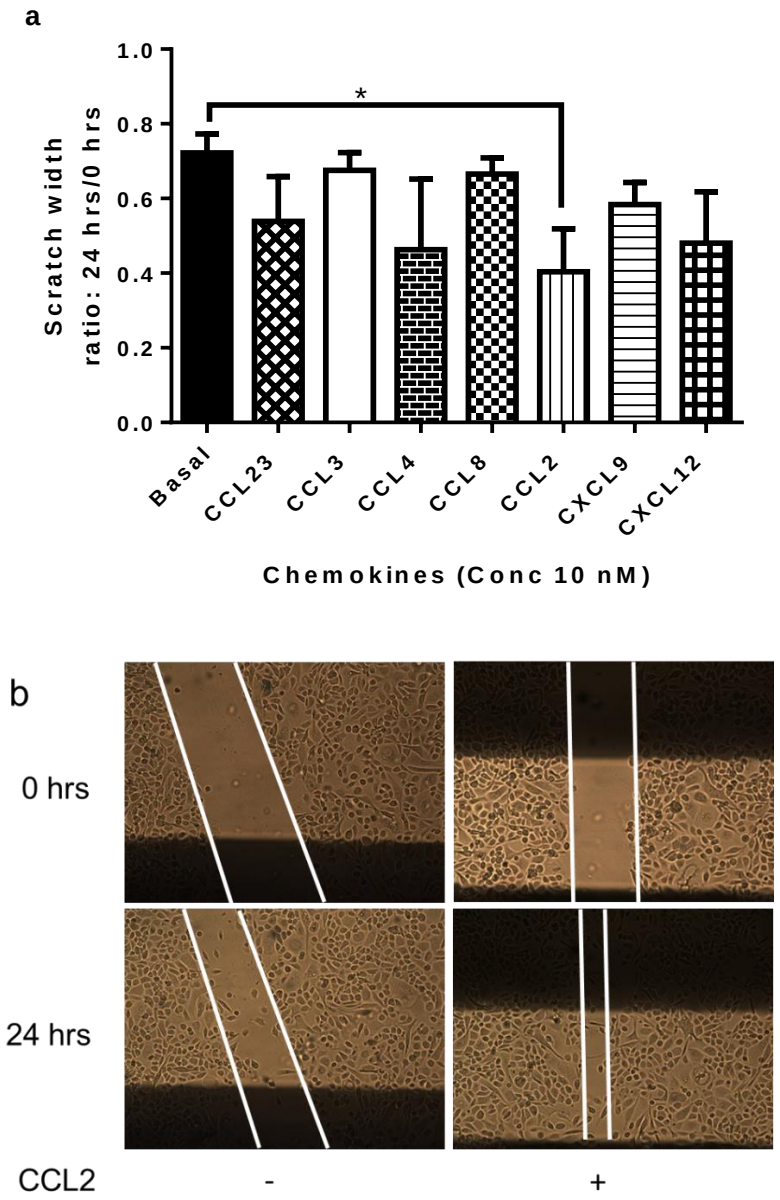

Figure 3.12. Chemokine screening in the wound healing assay of PC-3 cells for 24 hrs. (a) CCL2 (10 nM) promotes PC-3 scratch closure after 24 hrs. A value of 1 denotes no migration, whilst 0 denotes complete migration. (b) Representative image of CCL2 scratch closure in PC-3 cells after 24 hrs. PC-3 cells treated with CCL2 (24 hrs) had a scratch width ratio of 0.3704 compared to 0.723 for the basal. All images were taken at 10x objective with a Leica DMI6000 inverted microscope and using Leica application software. Results represent the mean ± S.E.M. of at least four independent experiments. (One-way ANOVA, Uncorrected Fisher's LSD, * = p≤0.05).

From the chemokine screen, CCL2 (10 nM) and CCL3 (10 nM) showed significant increases in PC-3 and MCF-7 scratch closure against the basal after 24 hrs respectively ($p \leq 0.05$), suggesting that both are able to promote cell migration in their respective cell type (figures 3.5a-b and 3.12a-b). With regards to the kinetics of CCL2 signalling in PC-3 cells, after 6 hrs there was a mean difference of 0.135 in scratch width ratio between CCL2 and the basal (figure 3.11) which then increased to 0.305 following 24 hrs. This implies that CCL2 is inducing some migration in PC-3 cells after 6 hrs and that the kinetics of this signalling pathway continues over a 24 hrs period.

Amongst the remaining chemokines screened, none had a significant effect on scratch closure in the different carcinoma cell types at any time point (figures 3.5-3.12). Although CXCL12 (10 nM) tended to display greater scratch closure in both PC-3 and MCF-7 cells after 24 hrs (figures 3.5a and 3.12a), with a similar trend also shown in PC-3 cells for CCL4 and possibly CCL23 after 24 hrs (figure 3.12a). CCL5 (10 nM) was also tested on MDA-MB-231 cells as previous studies have identified it as a promoter of MDA-MB-231 migration [338, 453], though no effect on scratch closure after either 6 hrs or 24 hrs was detected (figure 3.6 and 3.7).

Unlike MCF-7 cells, MDA-MB-231 cells did not form clear and distinct scratch edges. So an additional approach was used by measuring the change in cell coverage of CCL3 and CXCL12 scratch closure after 24 hrs. Similar to scratch width measurements (figure 3.8a) there was no significant difference in the cell coverage between either CCL3 or CXCL12 and the basal after 24 hrs (figure 3.8b). This demonstrates that measuring changes in scratch width is still a valid method for assessing scratch closure.

3.5 CCL3 promotes MCF-7 scratch closure through the activation of both CCR1 and CCR5

CCL3 has at least two known cognate receptors: CCR1 and CCR5 [47] (tables 2.3 and 3.1). To further explore the molecular mechanism underpinning CCL3 driven migration in MCF-7 cells, two small molecule inhibitors were used to block CCR1 and CCR5, either separately or at the same time, to establish whether one receptor is primarily involved or if there is functional redundancy between the two.

For targeting CCR5, the allosteric inhibitor for CCR5, maraviroc was used. Since 2007, maraviroc has been used as a licensed drug for treating HIV-1: by blocking viral entry into lymphocytes via CCR5 [454]. Crystallography data has revealed that maraviroc binds deep inside CCR5s transmembrane domain, and inside this pocket maraviroc, interacts with the Tyr248 residue in helix 6 through its benzene ring. This hydrophobic interaction is thought to stabilise CCR5s inactive conformation upon ligand binding [33]. Maraviroc is therefore considered to be an inverse agonist rather than an antagonist [455].

To block CCR1 another potent allosteric inhibitor J113863 was used. J113863 has been shown to block CCL3 binding to CCR1 in CHO cells with an IC_{50} of 0.9 nM, as well as, intracellular calcium signalling in U937 cells expressing CCR1 with an IC_{50} of 0.73 nM [397]. CCR1 shares structural homology with CCR2, CCR3 and CCR5, therefore J113863 may have off-target effects. This was highlighted in a very recent study by showing that J113863 was able to bind to and activate both CCR5 and CCR2 by displacing CCL4 (pIC_{50} = 5,9 ± 0.1) and CCL2 (pIC_{50} = 5.5 ± 0.1), as well as, having a pEC_{50} of 8.2 ± 0.1 and 6.4 ± 0.1 in increasing intracellular calcium respectively. In cell migration, J113863 was an agonist for CCR2, whilst for CCR5, J113863 acted as an antagonist for CCL4 [456]. Although Corbisier *et al.* (2017) identified J113863 as an agonist for CCR2 and CCR5, this was only achieved at concentrations over a 1000 fold greater than the $IC_{50} \approx 1$ nM. Indicating that J113863 is a weak agonist. However J113863 does appear to be a potent antagonist for CCR5 induced chemotaxis by fully blocking CCL4 chemotaxis in CCR5-L1.2 cells above 1 nM concentration [456].

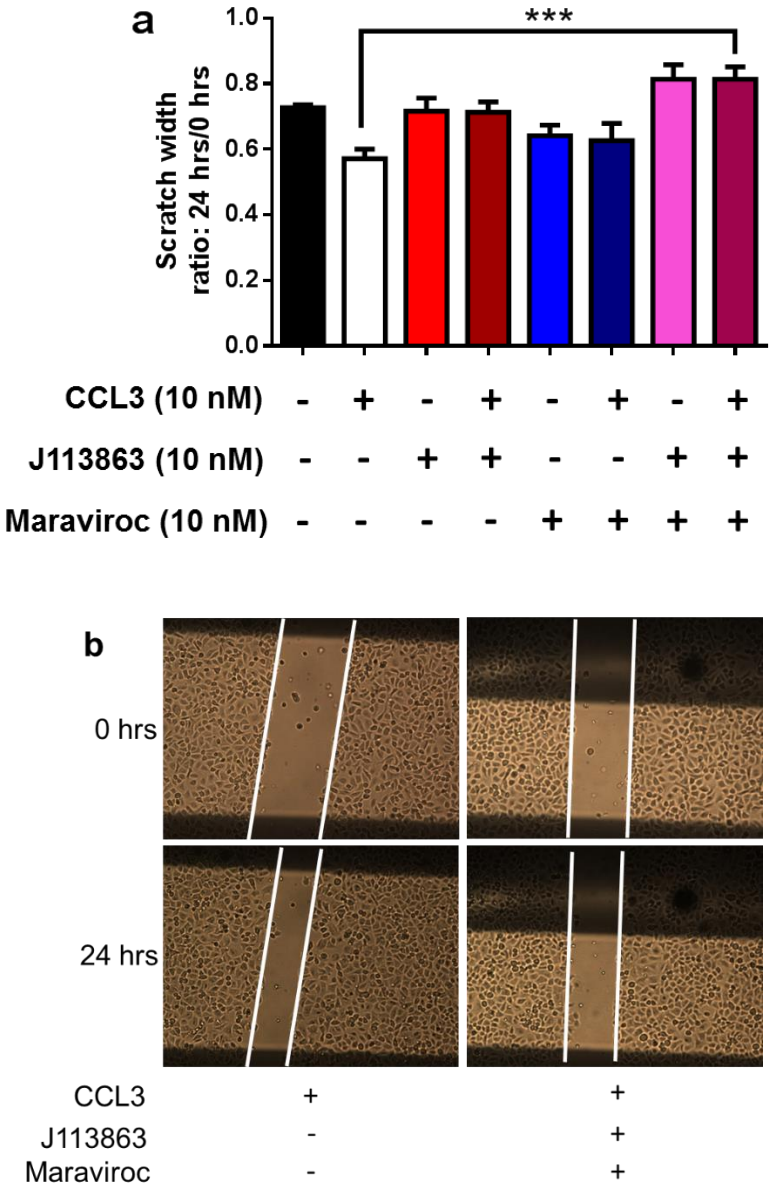

Figure 3.13. Scratch closure of MCF-7 cells after 24 hrs. (a) J113863 (10 nM) and Maraviroc (10 nM) together inhibit CCL3 (10 nM) induced scratch closure in MCF-7 cells after 24 hrs. (b) Representative image of CCL3 scratch closure in MCF-7 cells after 24 hrs. MCF-7 cells treated with CCL3 as well as Maraviroc and J113863 had a scratch width ratio of 0.84 compared to 0.53 when treated with CCL3 alone. Cells were imaged at 10x objective with a Leica DMI6000 inverted microscope and using Leica application suite. CCR1 inhibitor: J113863. CCR5 inhibitor: Maraviroc. Results represent the mean ± S.E.M. of at least three independent experiments. (One-way ANOVA, Tukey's test, *** = $p \leq 0.001$).

When using J113863 (10 nM) and Maraviroc (10 nM) to target CCR1 and CCR5 respectively in MCF-7 cells treated with CCL3 (10 nM). The data showed that only when both J113863 and Maraviroc were added at the same time was CCL3 scratch closure significantly inhibited ($p \leq 0.001$ n=5) (figure 3.13). Neither Maraviroc nor J113863 were able to significantly inhibit CCL3 scratch closure independently. Although the addition of J113863 alone did show some inhibition on CCL3 scratch closure, which could suggest that CCL3 relies more on CCR1 activation than CCR5 to drive MCF-7 cell migration. Overall, the data suggests that CCL3 utilises both CCR1 and CCR5 to promote MCF-7 cell migration, indicating significant receptor redundancy underlying this process.

3.6 Maraviroc and J113863 show no cytotoxicity in MCF-7 cells after 25 hrs

To ensure that the inhibitory effects of J113863 and Maraviroc on MCF-7 scratch closure was not a result of compound cytotoxicity, the MTS cell proliferation assay was used to measure cytotoxicity. This cell proliferation assay works by measuring the absorbance of formazan (a product of MTS tetrazolium metabolisation by NAD(P)H dehydrogenase) for quantifying the number of viable cells. To determine cellular proliferation, the background (growth media) was measured against the control (cells only). Whilst for identifying compound cytotoxicity, all the conditions tested were assessed against the control.

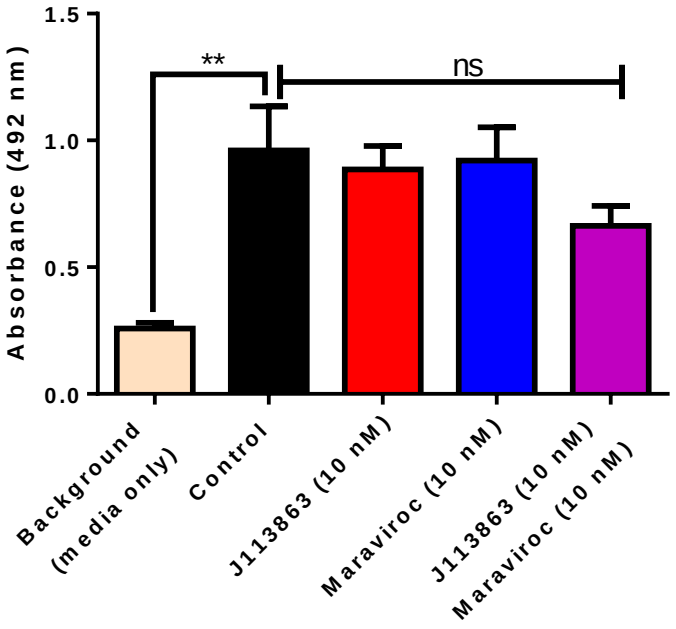

Figure 3.14. Cell proliferation assay in MCF-7 cells. J113863 (10 nM) and Maraviroc (10 nM) does not cause cytotoxicity in MCF-7 cells after 24 hrs incubation and 1 hrs MTS metabolisation. CCR1 inhibitor: J113863. CCR5 inhibitor: Maraviroc. Results represent the mean ± S.E.M of four independent experiments (One-way ANOVA, Dunnett's test, ** = p≤0.01, ns indicating a p value≥0.05 of no significance).

The data from the MTS assay on J113863 and Maraviroc showed no significant evidence of cytotoxicity in MCF-7 cells either independently or together following 25 hrs incubation (figure 3.14). This confirms that the inhibition observed for J113863 (10 nM) and Maraviroc (10 nM) on the scratch closure of MCF-7 cells in response to CCL3 was not due to any significant cellular cytotoxicity.

3.7 PC-3 cells do not migrate towards CCL2 or CXCL12 in the transwell migration assay. Agarose spot cannot be used to measure migration in MDA-MB-231 cells

The wound healing assay is one of the most commonly used method to assess for cellular migration. However one of its biggest limitations is it can only measure non-directed migration (chemokinesis) and not chemotaxis as no concentration gradient can be formed within the assay.

Chemokines function as a chemoattractant to promote cancer metastasis [115]. Therefore to assess for chemotaxis, two chemotaxis migration assays were used: the transwell migration and agarose spot.

Several published studies have used these assays to observe chemokine induced chemotaxis in the same cancer cell lines used in the wound healing assays presented in this thesis (see table 3.1). The transwell migration assay relies on a semi-permeable membrane to generate a concentration gradient. Cells are seeded on top of the membrane with the chemoattractant underneath. The number of cells counted on the underside of the membrane is used to quantify chemotaxis. The agarose spot assay on the other hand uses the diffusion of chemokines into the surrounding media from a chemokine concentrated agarose spot. The number of cells which enter the agarose spot is used as a measurement of chemotaxis [442, 448].

For the transwell migration assay the PC-3 cells were used as the cellular system to identify CCL2 and CXCL12 induced chemotaxis. Both CCL2 and CXCL12 were selected as they displayed the greatest effect on scratch closure (figure 3.12). For the agarose spot CXCL12 was used as the chemoattractant for MDA-MB-231 cells to try and reproduce the data from Vinadar. V *et al*. (2011) [442].

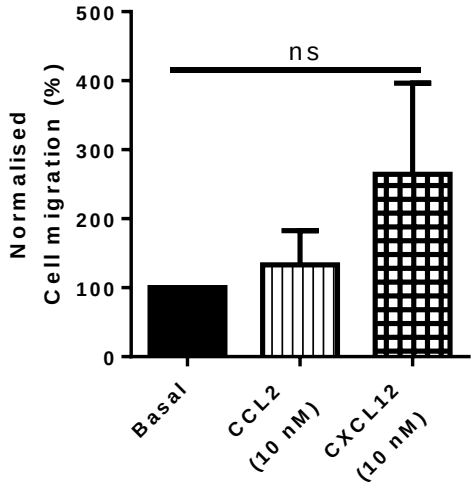

Figure 3.15. Transwell migration assay in PC-3 cells. CCL2 (10 nM) and CXCL12 (10 nM) do not induce chemotaxis in PC-3 cells after 24 hrs. Data was normalised to the basal. Results represent the mean ± S.E.M. of four independent experiments. (Kruskal Wallis test, Dunn's multiple comparisons test, ns indicating a p value≥0.05 of no significance).

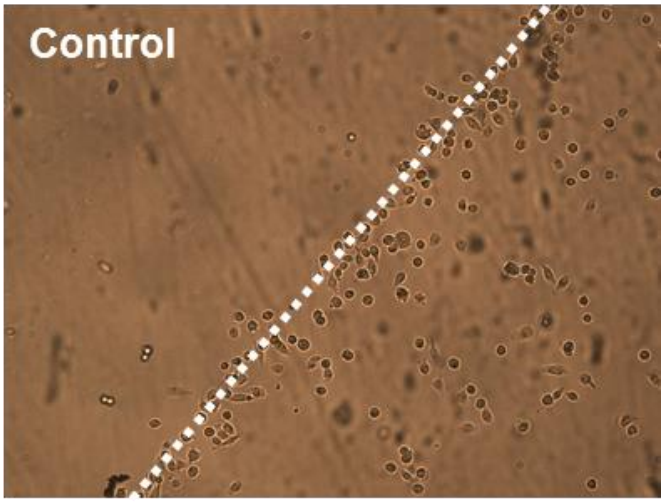

Figure 3.16. Agarose spot assay in MDA-MB-231 cells. Representative image of the control agarose spot (0.1% BSA/PBS) after 24 hrs. White line shows the edge of the agarose spot and the MDA-MB-231 cells. No image was able to be obtained for the CXCL12 agarose spot (125 nM).

Using the transwell migration assay, neither CCL2 (10 nM) nor CXCL12 (10 nM) demonstrated any significant evidence of chemotaxis in PC-3 cells after 24 hrs (figure 3.15). For the agarose spot, no meaningful data on MDA-MB-231 cell migration in response to CXCL12 (125 nM) was obtained (figure 3.16). The lack of useable data was due to the agarose spots not remaining properly fixed to either the plastic or glass bottom during the experiment. This caused the agarose spots to be easily dislodged and move, which prevented any cell migration between the control and CXCL12 agarose spots from being measured. As such no images of the CXCL12 agarose spot are presented in this thesis.

Overall, neither approach appears to be effective in detecting chemokine induced chemotaxis in either of these two cell lines.

3.8 Characterising chemokine signalling in MCF-7 and PC-3 cells

Chemokine receptors are primarily coupled to $G\alpha_i$ [36-39]. In the canonical $G\alpha_i/\beta\gamma$ pathway, the $G\beta\gamma$ subunit binds and activates PLC, which in turn cleaves PIP_2 into DAG and IP_3. IP_3 opens the IP_3 channels on the ER releasing calcium ions into the cytosol to act as a secondary messenger for signal transduction [88]. For many years now researchers have utilized this downstream release of calcium from the intracellular stores as a marker for chemokine receptor activation by using the fluorescent dye Fura-2 AM [457, 458]. Fura-2 AM has a high affinity for calcium ions and is ratiometric as it can be excited at both 340 and 380 nm depending on whether it is bound or unbound to Ca^{2+} respectively. Despite having two excitation states, Fura-2 AM still emits light at 510 nm [459]. Therefore the levels of intracellular calcium before and after receptor activation can be detected by measuring the difference in fluorescence levels between the two excitations states (340 and 380 nm) at 510 nm.

To confirm whether MCF-7 cells express CCR1 and/or CCR5, increases in intracellular calcium was measured in response to varying doses of CCL3. To

identify whether PC-3 cells express CCR2, changes in intracellular calcium levels were measured in response to CCL2 stimulation.

In addition the remaining chemokines were screened to firstly identify whether the PC-3 and MCF-7 cells expressed any other chemokine receptors such as CXCR3. Secondly to compare the efficacy levels of the different chemokines with respect to receptor activation as this may explain functional differences between the different chemokines.

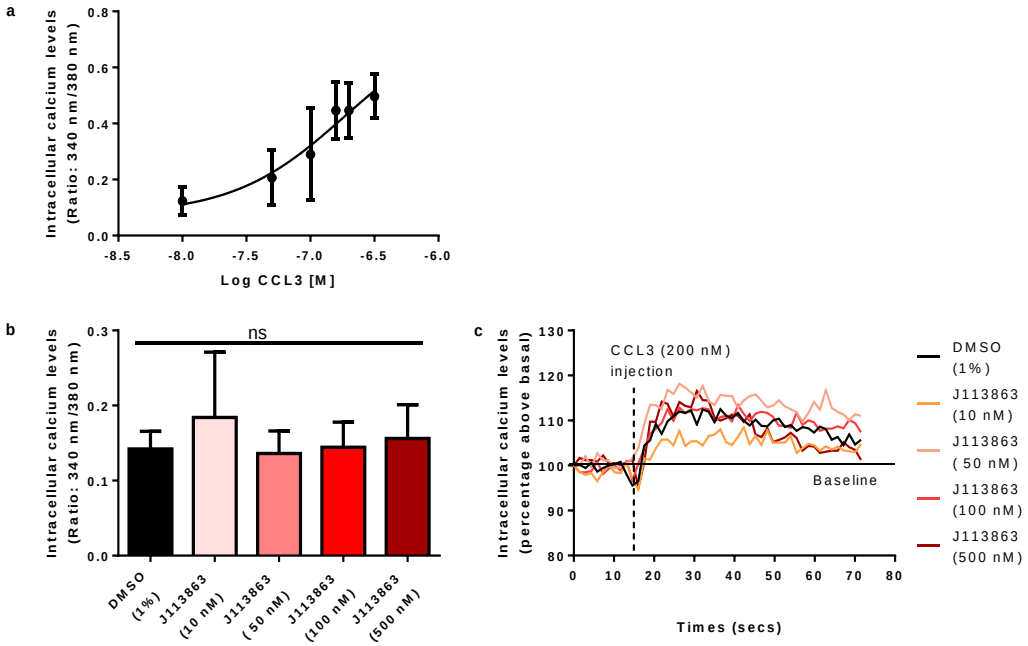

Figure 3.17. Increases in intracellular calcium in MCF-7 cells. (a) CCL3 dose dependent increase in intracellular calcium in MCF-7 cells (n=3). (b) J113863 inhibition of CCR1 does not block CCL3 (200 nM) intracellular calcium signalling in MCF-7 cells (n=5). (c) Representation of an intracellular calcium measurement trace following CCL3 stimulation in MCF-7 cells pretreated (30 mins) with different concentrations of J113863 (CCR1 inhibitor) after 70 secs. Results represent mean ± SEM of at least three independent experiments. (One-way ANOVA, Dunnett's test, ns indicating a p value≥0.05 of no significance).

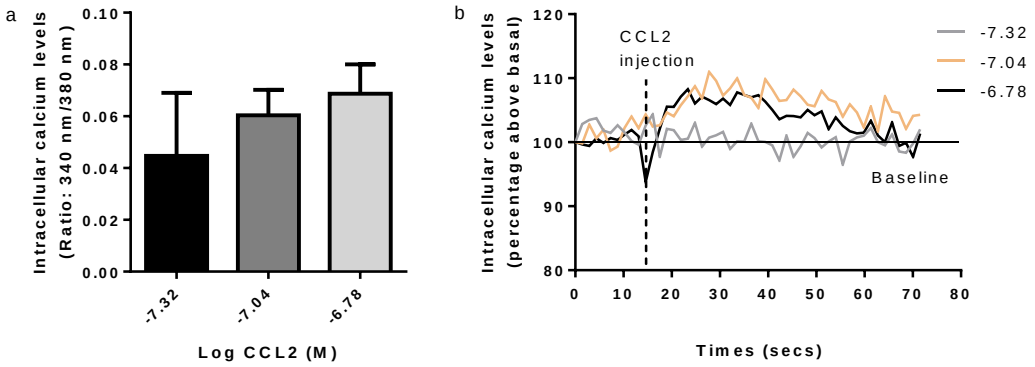

Figure 3.18. Increases in intracellular calcium towards varying concentrations of CCL2 in PC-3 cells. (a) CCL2 induces a weak increase in intracellular calcium in PC-3 cells. (b) Representation of an intracellular calcium measurement trace following CCL2 injection in PC-3 cells at concentrations of 50, 100 and 200 nM after 70 secs. Results represent the mean ± SEM of three independent experiments.

The results showed that CCL3 was able to induce a dose dependent increase in intracellular calcium in MCF-7 cells, with an EC_{50} of 184.8 nM (figure 3.17a). This firstly indicates that MCF-7 cells express either CCR1 and/or CCR5 and secondly that the receptors are functional. To gain further detail on whether CCL3 was signalling through either CCR1 or CCR5, the CCR1 antagonist J118363 was used at a range of concentrations to ensure maximal effect on CCL3 intracellular calcium increase in MCF-7 cells. The data from this experiment showed no inhibition of CCL3 signalling by J113863 at any concentration (figure 3.17b and c).

There are two possible explanations for this result. The first explanation is that CCL3 signals through CCR5 only, or secondly that there is functional redundancy between CCR1 and CCR5, similar to what was observed in the wound healing assay (figure 3.13). In order to confirm which one of these hypothesis is correct the activation of CCR5 would need to be blocked. Unfortunately, as the CCR5 inhibitor maraviroc has been shown to increase

intracellular calcium in THP-1 cells [460], the use of maraviroc to block CCR5 activation was not possible for the intracellular calcium flux assay.

Additionally the PC-3 cells were stimulated with three separate concentrations of CCL2: 50, 100 and 200 nM. However, only a small increase in intracellular calcium was measured in response to CCL2 (200 nM), with a mean of 0.069 (figure 3.18). This suggests that PC-3 cells could express some functional CCR2 and/or CCR3.

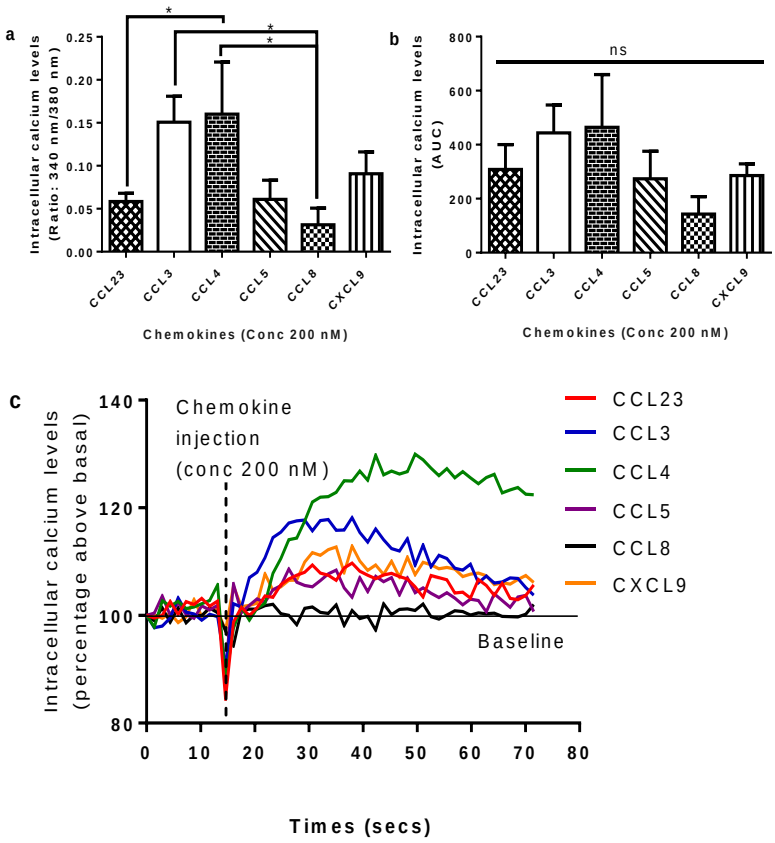

Figure 3.19. Chemokine screening in MCF-7 cells with the intracellular calcium flux assay. (a) Chemokine increases in intracellular calcium in MCF-7 cells when measuring the difference between the peak and base readings (n=3). (b) Chemokine increases in intracellular calcium in MCF-7 cells measured using the area under the curve (AUC). (c) Representation of an intracellular calcium measurement trace following chemokine injection in MCF-7 cells after 70 secs. Results represent the mean ± S.E.M. of at least three independent experiments (One-way ANOVA, Uncorrected Fisher's LSD, *=p≤0.05, ns = p≥0.05 of no significance).

When quantifying changes in intracellular calcium using the peak and base readings, MCF-7 cells were shown to significantly respond to CCL3 and CCL4 (200 nM) stimulation ($p \leq 0.05$, n=3). Furthermore a possible response to CXCL9 (200 nM) was also detected with a mean of 0.0907 ± 0.025 (figure 3.19a). This suggests that MCF-7 cells could be expressing functional CCR5 with the evidence from the immunofluorescence stain also suggesting possible CCR5 expression (figure 3.1).

One limitation with measuring the difference between the peak and base readings to quantify increases in intracellular calcium, is that it cannot measure differing responses, such as whether the increase in intracellular calcium is high and short-lived or lower and more prolonged. As such the same data was remeasured using the area under a curve (AUC) to see if the chemokines induced different responses.

When measuring the AUC the trend was similar to measurements made using the peak and base readings, however, this time there was no significant difference between the increases in intracellular calcium amongst the chemokines screened (figure 3.19b). This suggests that the overall increase in intracellular calcium is similar between the chemokines with perhaps the exception of CCL8. This indicates that the chemokines are inducing differing responses in MCF-7 cells. Which was also observed from the intracellular calcium measurement traces (figure 3.19c). From these traces CCL3 stimulation appears to induce a higher and shorter-lived increase in intracellular calcium, whilst CCL5, CCL23, and CXCL9 displayed a lower but prolonged increase in intracellular calcium. CCL4 stimulation also showed a prolonged response although it was much higher than any of the other chemokines screened. Amongst the chemokines screened only CCL8 showed no detectable increase in intracellular calcium in MCF-7 cells. These results suggest that different chemokines have differing levels of efficacy and produce distinct responses within the same cell type.

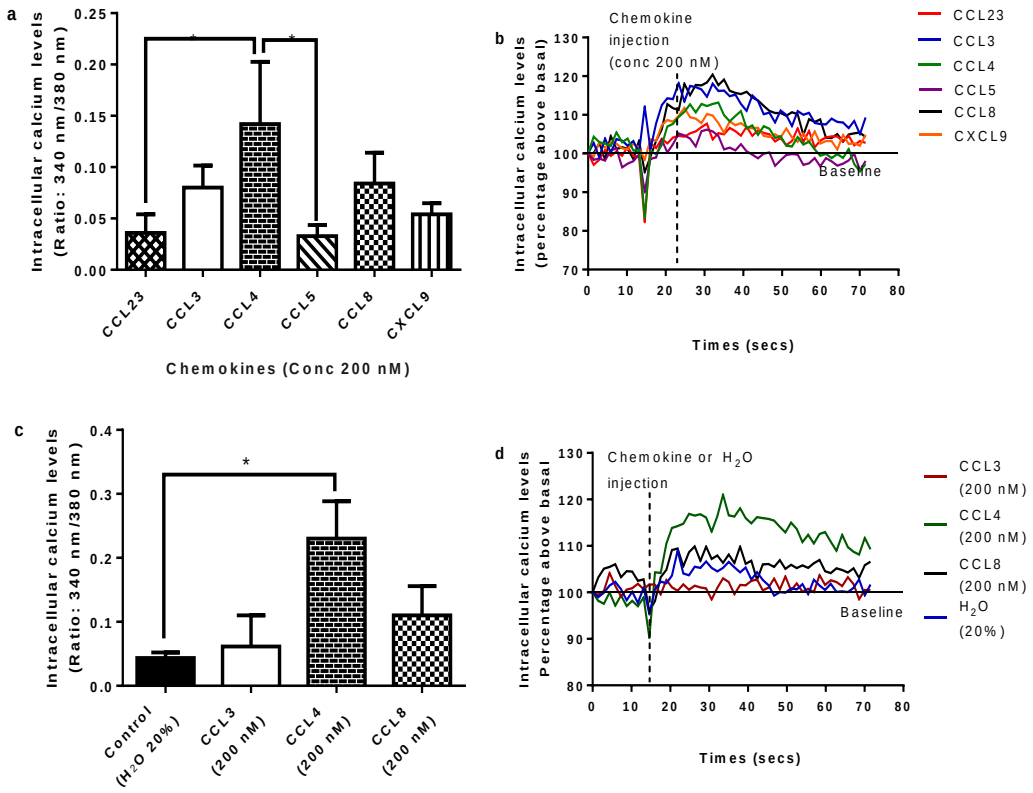

Figure 3.20. Chemokine screening in PC-3 cells with the intracellular calcium flux assay. (a) Chemokine increases in intracellular calcium in PC-3 cells when measuring the difference between the peak and base readings (n≥4). (One-way ANOVA, Uncorrected Fisher's LSD, * = p≤0.05). (b) Representation of an intracellular calcium measurement trace following chemokine injection (200 nM) in PC-3 cells after 70 secs. (c) CCL4 (200 nM) induces significant increase in intracellular calcium when measuring the difference between the peak and base readings (n≥2). One-way ANOVA, Dunnett's test, * = p≤0.05). (d) Representation of an intracellular calcium measurement trace following chemokine or H_2O injection in PC-3 cells after 70 secs. Results represent the mean ± S.E.M. of at least two independent experiments.

In PC-3 cells only CCL4 (200 nM) displayed a significant increase in intracellular calcium compared to the other chemokines screened (p≤0.05) (figure 3.20a). As a control increases in intracellular calcium from CCL3, CCL4

and CCL8 were measured against the background stimulation (injection of H_2O), which confirmed that PC-3 cells respond to CCL4 and that they likely express CCR5. ($p \leq 0.05$, $n=3$) (figures 3.20c and d). None of the other chemokines demonstrated any obvious increase in intracellular calcium. This indicates that CCL3, CCL5 and CCL8 have a lower level of efficacy than CCL4 in PC-3 cells. For CCL23 and CXCL9 the results from the intracellular calcium flux assay may suggest that PC-3 cells do not express their cognate receptors CCR1 and CXCR3 respectively and hence why no clear increases in intracellular calcium was detected.

3.9 Screening for chemokines involved in carcinoma cell actin polymerisation

Actin polymerisation is a key component and driving force for cell physiological changes such as adhesion, spreading and migration [143, 179, 461]. The process of actin polymerisation begins with G-actin nucleation which is elongated further to form F-actin. Elongated F-actin extends towards the cell membrane and forces protrusions to arise, allowing cells to migrate [143]. This cellular migration is maintained when actin polymerisation is at a steady state [179]. At the surface of a cells leading edge, F-actin can form two types of protusions: filopodia and lamellipodia. The filopodia function as sensors, allowing changes in the external environment to be detected by the cell [153, 154]. Whilst the lamellipodia is considered to be the mechanical force behind cell migration [155]. Besides the lamellipodia and filopodia, another F-actin structure also formed within the cell are the stress fibers which function to generate traction for cell migration [143, 179]. Due to the importance of actin polymerisation in cell migration, these chemokines were further investigated to determine if they were able to form identifiable F-actin structures in the different carcinoma cell lines. For imaging intracellular F-actin structures, researchers commonly use the bicyclic peptide phalloidin, which is a toxin originally derived from the death cap mushroom. Phalloidin has a high affinity for F-actin but not G-actin and is commonly conjugated to a fluorophore to give high quality and detailed images of the F-actin cytoskeleton [462].

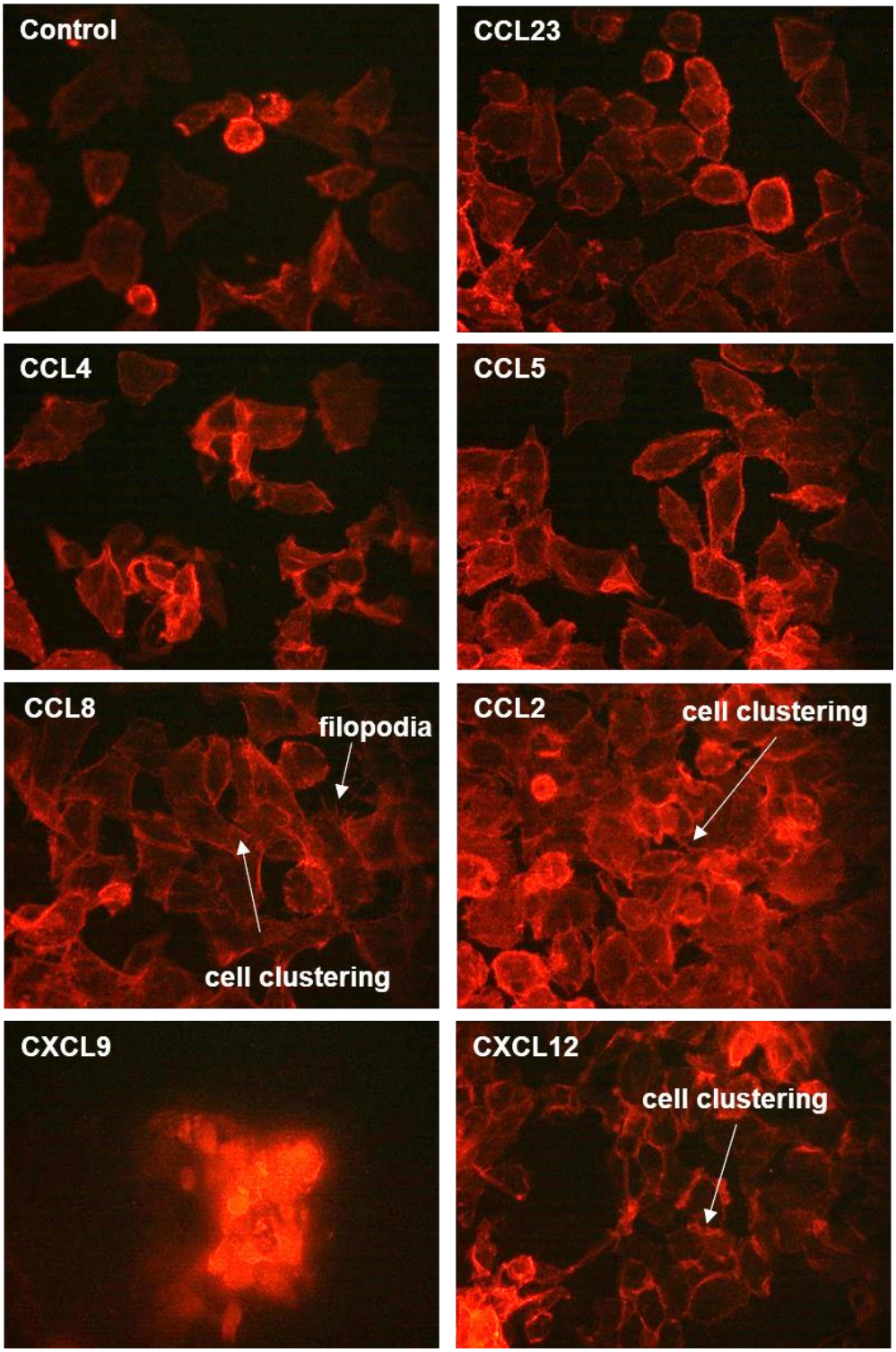

Figure 3.21. Phalloidin actin staining of MCF-7 cells in the absence and presence of different chemokines (10 nM) over 24 hrs. MCF-7 cells were fixed and stained with Phalloidin CruzFluor TM^{594} conjugate (red) for imaging the F-actin cytoskeleton. Images are a representation of the cell population and were taken at 63x objective with a Leica DMI6000 inverted microscope and using Leica imaging suite.

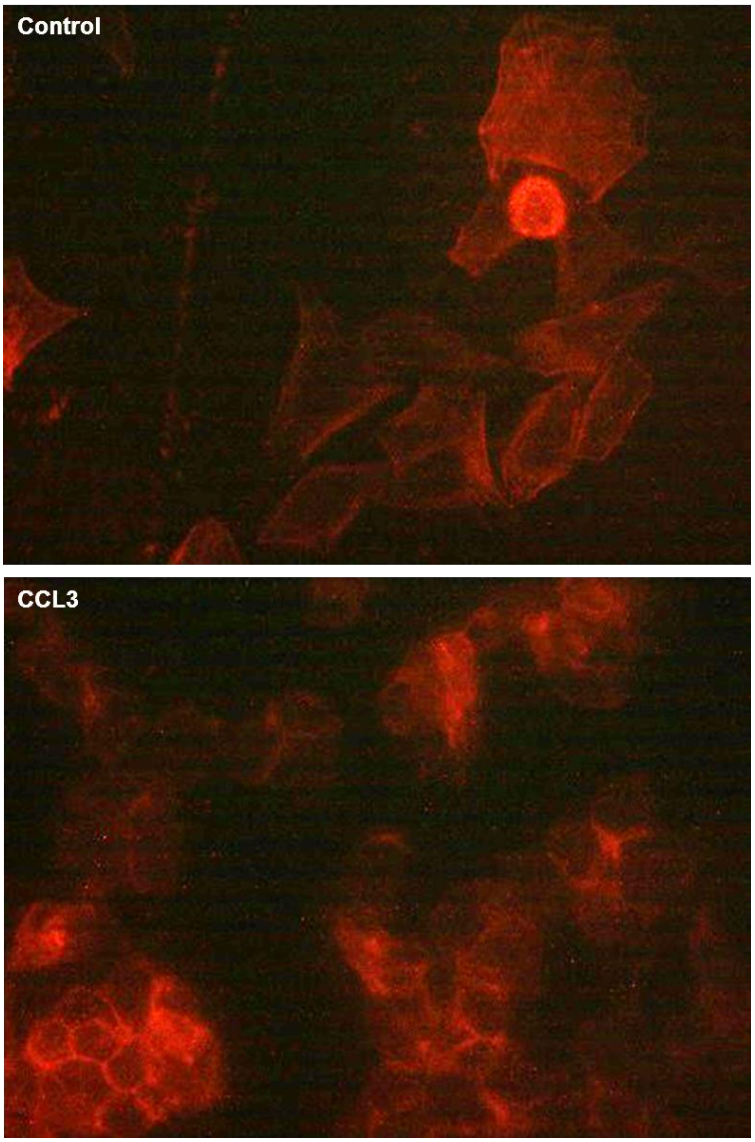

Figure 3.22. Phalloidin actin staining of MCF-7 cells in the absence and presence of CCL3 (10 nM) over 24 hrs. MCF-7 cells were fixed and stained with Phalloidin CruzFluor TM^{594} conjugate (red) for imaging the F-actin cytoskeleton. Images are a representation of the cell population and were taken at 63x objective with a Leica DMI6000 inverted microscope and using Leica imaging suite.

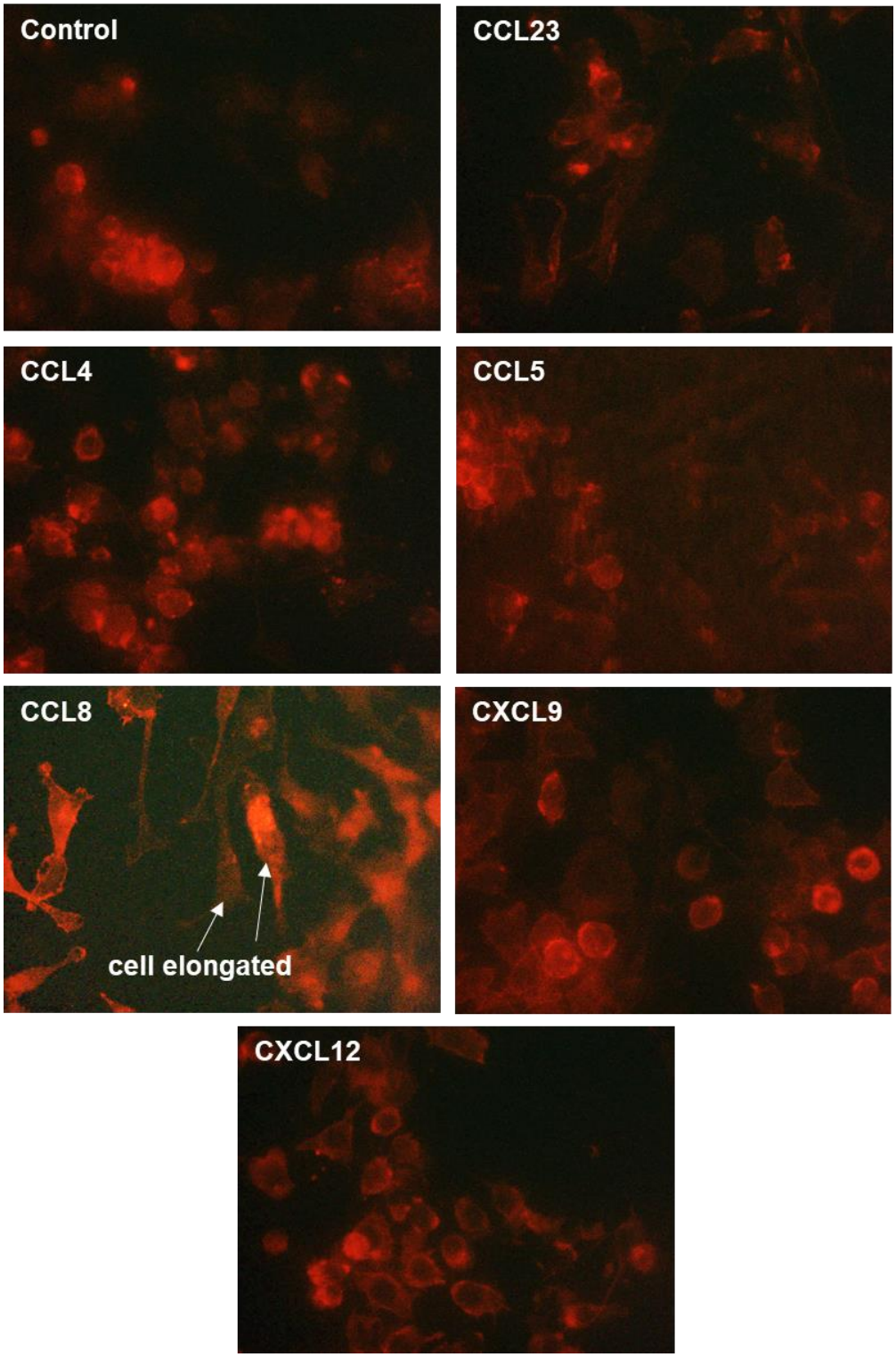

Figure 3.23. Phalloidin actin staining of MDA-MB-231 cells in the absence and presence of different chemokines (10 nM) over 24 hrs. MDA-MB-231 cells were fixed and stained with Phalloidin CruzFluor TM^{594} conjugate (red) for imaging the F-actin cytoskeleton. Images are a representation of the cell population and were taken at 63x objective with a Leica DMI6000 inverted microscope and using Leica imaging suite.

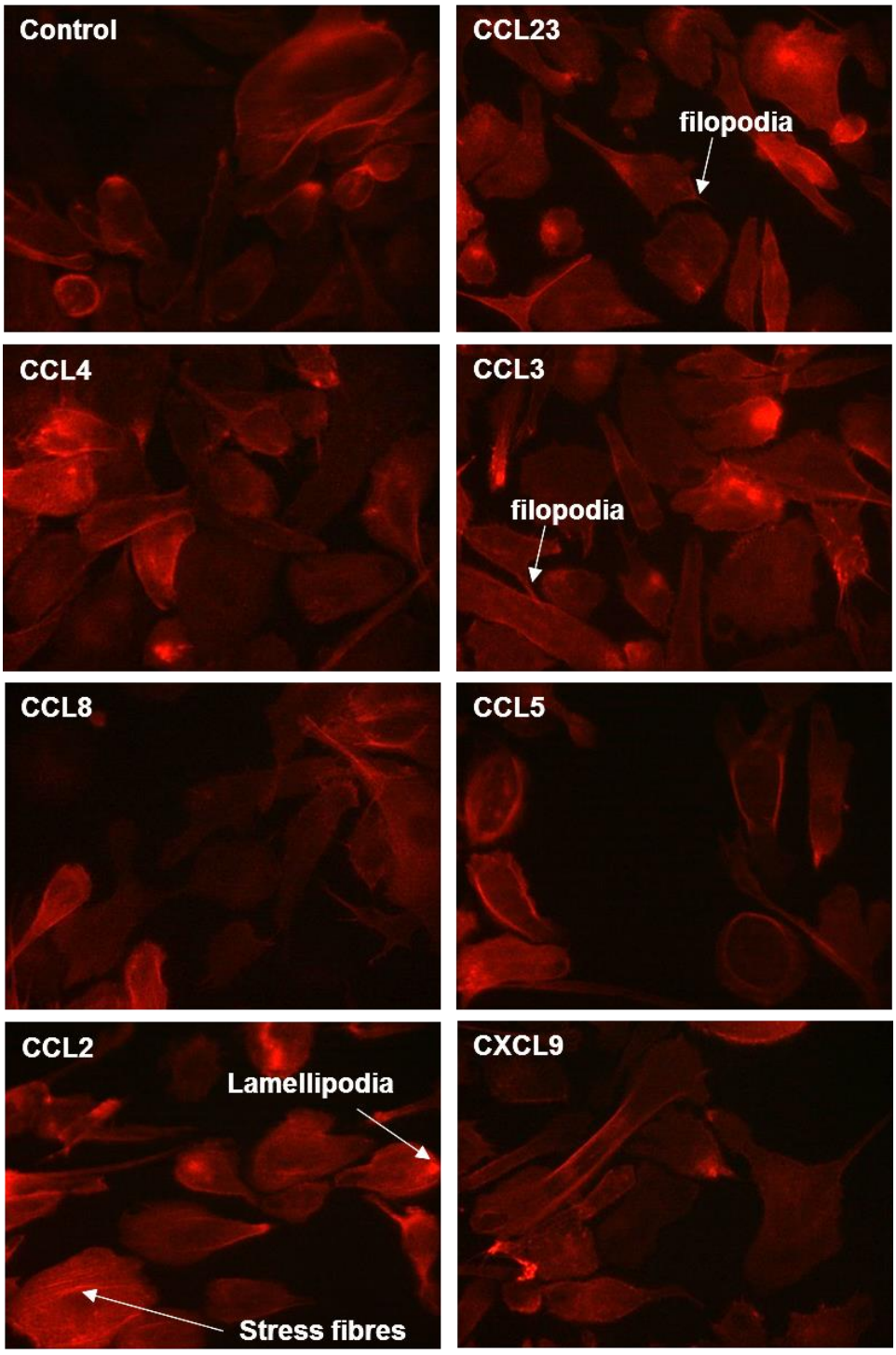

FFigure 3.24. Phalloidin actin staining of PC-3 cells in the absence and presence of different chemokines (10 nM) over 24 hrs. PC-3 cells were fixed and stained with Phalloidin CruzFluor TM^{594} conjugate (red) for imaging the F-actin cytoskeleton. Images are a representation of the cell population and were taken at 63x objective with a Leica DMI6000 inverted microscope and using Leica imaging suite.

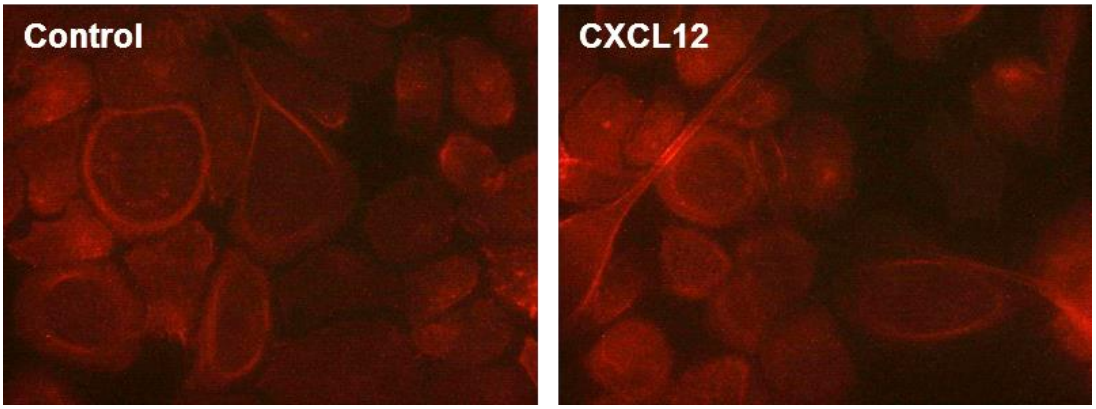

Figure 3.25. Phalloidin actin staining of PC-3 cells in the absence and presence of CXCL12 (10 nM) over 24 hrs. PC-3 cells were fixed and stained with Phalloidin CruzFluor TM^{594} conjugate (red) for imaging the F-actin cytoskeleton. Images are a representation of the cell population and were taken at 63x objective with a Leica DMI6000 inverted microscope and using Leica imaging suite.

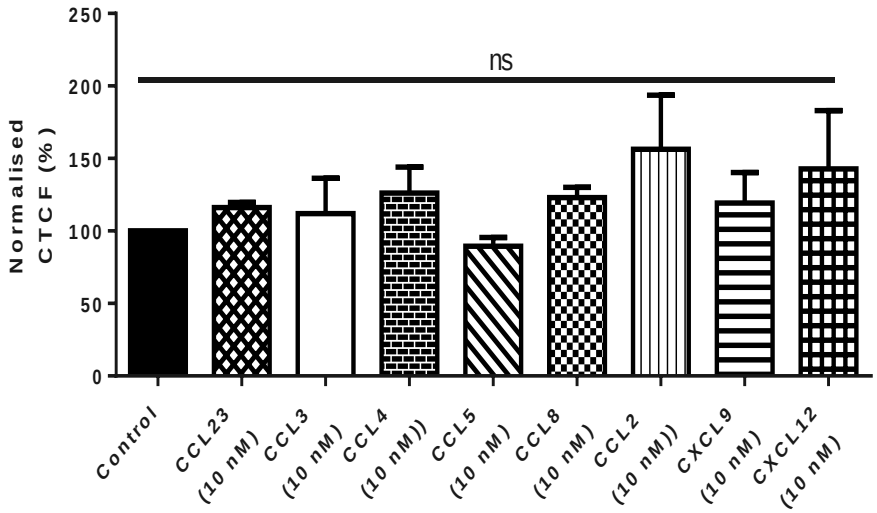

Figure 3.26. Quantification of actin polymerisation on PC-3 cells after 24 hrs. ImageJ 1.48v was used to calculate the corrected to cellular fluorescence (CTCF) for all images from the phalloidin stain before being normalised to the control. Results represent the mean ± S.E.M of at least three independent experiments. (Kruskal Wallis test, Dunn's multiple comparisons test, ns = p≥0.05 of no significance).

Amongst the cell lines imaged, the PC-3 cells provided the most detailed images, allowing for stress fibers, lamellipodia and filopodia to be occasionally identified, due to their larger size (figure 3.24). In MCF-7 and MDA-MB-231 cells, F-actin structures were difficult to identify and subsequently these cell lines appear to be unsuitable models for imaging the actin cytoskeleton (figures 3.21-3.23). Preliminary data with MDA-MB-231 cells, showed cells treated with CCL8 appeared to have a more elongated morphology than the control (figure 3.23) Overall, chemokine stimulation (10 nM) induced no obvious changes to cellular morphology in any of the cell lines over 24 hrs.

Nonetheless when looking at the cellular fluorescence levels some notable differences following chemokine stimulation were identified. For MCF-7 cells treatment with CXCL12 frequently displayed a greater level of fluorescence, though this was often in cells which were heavily clustered together (figure 3.21). Hence, it is unclear whether this was a genuine effect or merely a result of cell clustering as a similar effect was also observed amongst the other chemokines. In MDA-MB-231 cells, greater fluorescence levels were observed for cells incubated with CCL4, CCL8 and CXCL12 (figure 3.23). Whilst in PC-3 cells, treatment with CCL2 consistently displayed higher levels of fluorescence (figure 3.24). Consequently, the fluorescence levels of CCL2 and the other chemokines in the PC-3 cells were quantified using ImageJ 1.48v software by measuring the corrected total cellular fluorescence. From the data analysis none of the chemokines showed a significant difference in fluorescence levels against the control. However both CCL2 and CXCL12 did have a trend towards greater levels of fluorescence (figure 3.26).

3.10 CCL3 induces cellular elongation in CHO-CCR5 cells

Previous results showed that CCL3 promoted MCF-7 cell migration in the wound healing assay, but showed no observable changes to the F-actin cytoskeleton when stained with phalloidin. One explanation is that MCF-7 cells are a poor model for actin staining, therefore the CHO-CCR5 cells were used as an alternative model to characterise the effects of CCL3 on the actin cytoskeleton. CHO cells are commonly used for actin staining due to their larger size, allowing F-actin structures to be easily identified [184, 463]. Also, CHO-CCR5 express high levels of CCR5 so any effects should be enhanced here.

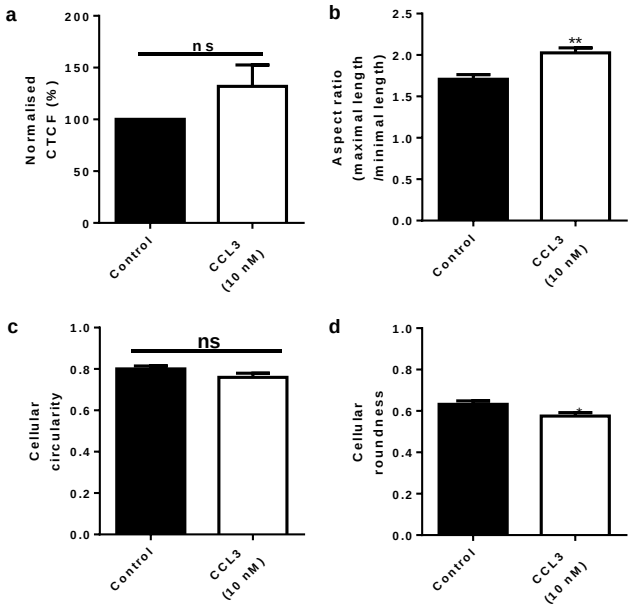

Figure 3.27. Quantification of actin staining on CHO-CCR5 cells after 24 hrs. (a) CTCF was measured in the absence and presence of CCL3 (10 nM) using ImageJ 1.48v. Results were normalised to the control. (Wilcoxon signed-rank test). (b) Aspect ratio was measured in the absence and presence of CCL3 (10 nM) using ImageJ 1.48v. (c) Cell circularity was measured in the absence and presence of CCL3 (10 nM) using ImageJ 1.48v. (d) Cell roundness was measured in the absence and presence of CCL3 (10 nM) using ImageJ 1.48v. Results represents the mean ± S.E.M. of at least 10 independent experiments (Student's t-test, ** = p≤0.01, * = p≤0.05 and ns = p≥0.05 of no significance).

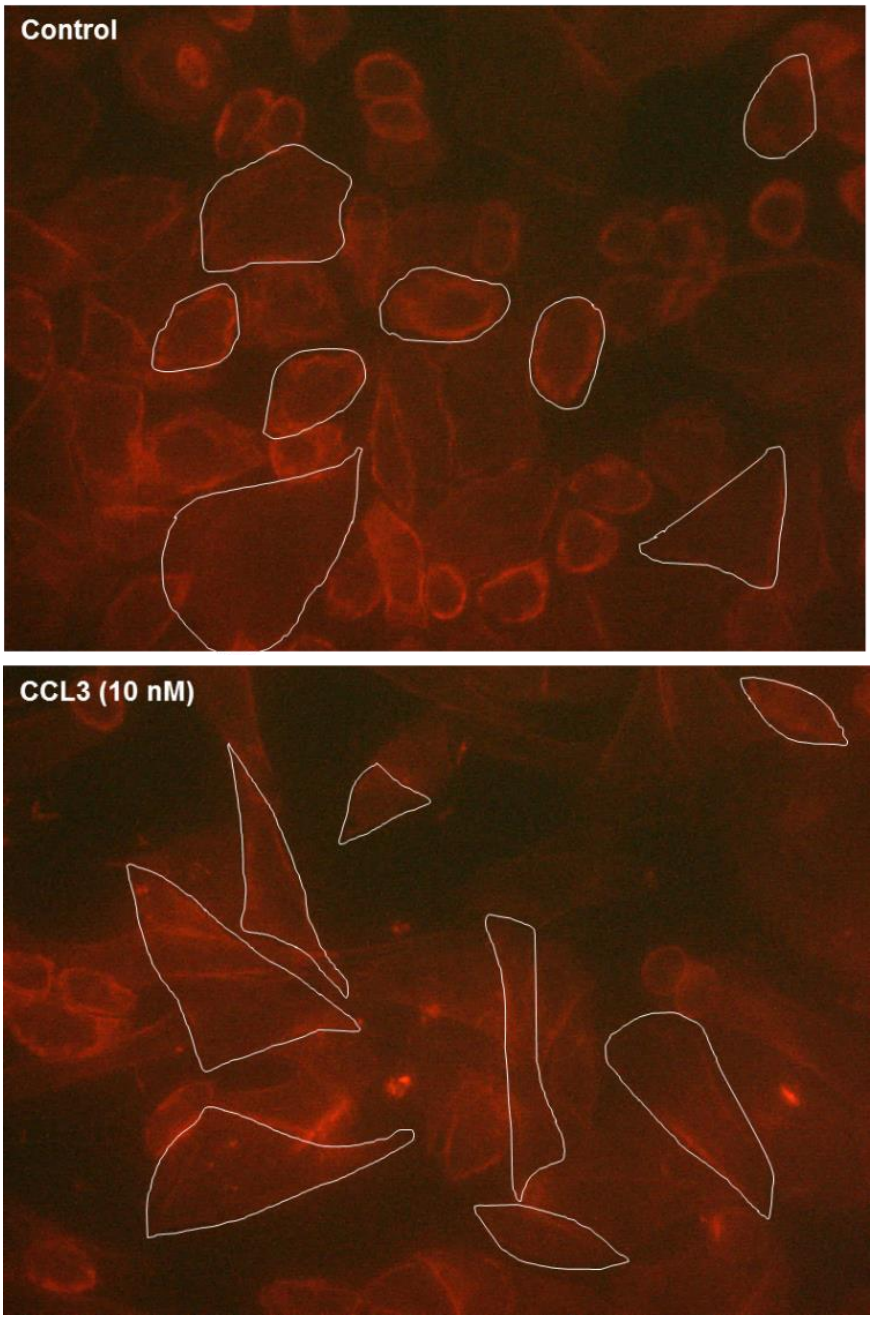

Figure 3.28. CCL3 promotes cellular elongation in CHO-CCR5 cells. CHO-CCR5 cells were stimulated with 10 nM of CCL3 for 24 hrs. Following 24 hrs, CHO-CCR5 cells were fixed and stained with Phalloidin CruzFluor TM^{594} conjugate (red) for imaging the F-actin cytoskeleton. Cells outlined in white are a representation of the cell populations. Images were taken at 63x objective with a Leica DMI6000 inverted microscope and using Leica imaging suite.

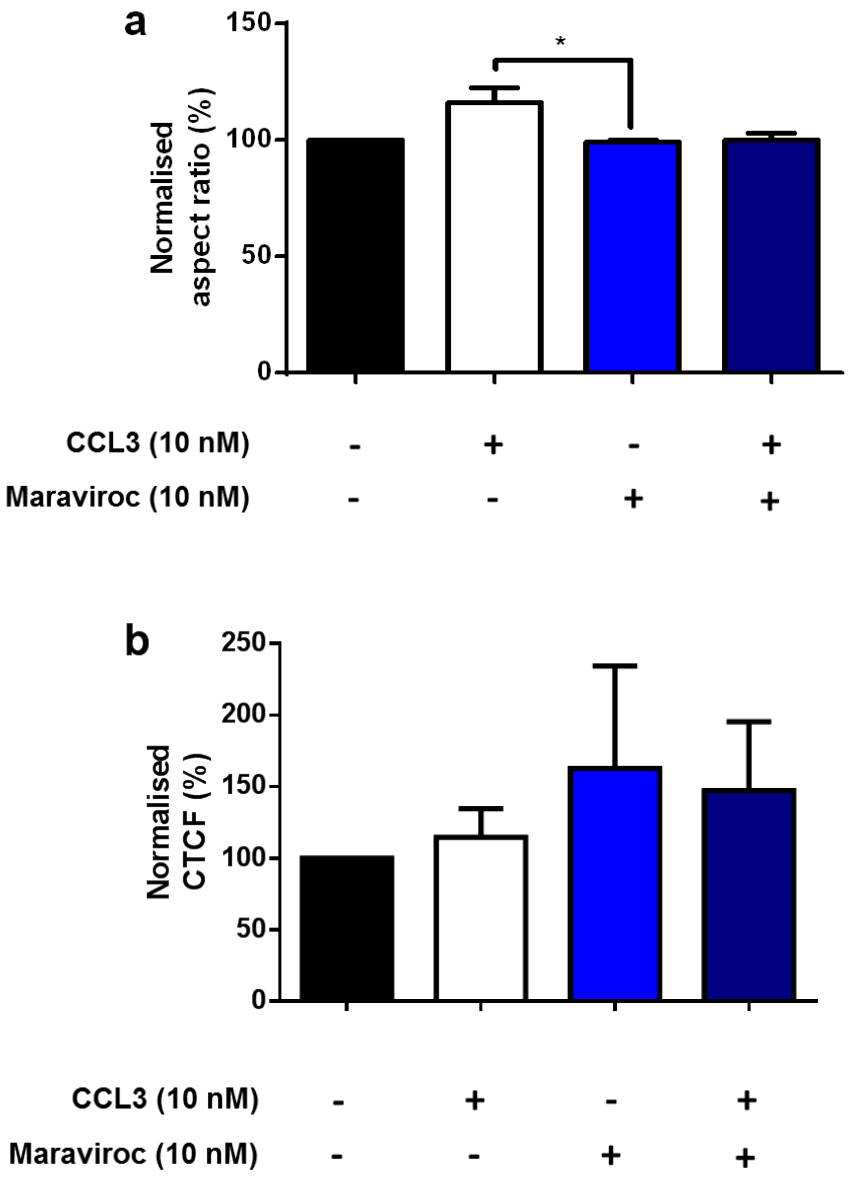

Figure 3.29. Quantification of actin staining on CHO-CCR5 cells after 24 hrs. (a) Maraviroc (10 nM) does not significantly inhibit CCL3 (10 nM) induced cellular elongation (aspect ratio) in CHO-CCR5 cells after 24 hrs. (b) Maraviroc (10 nM) shows no inhibitory effect on CTCF in CHO-CCR5 cells after 24 hrs. CCR5 inhibitor: Maraviroc. Results were normalised to control (absence of CCL3 and Maraviroc) and represent the mean ± S.E.M. of at least 4 independent experiments. (Kruskal-Wallis test, Dunn's multiple comparisons test, * = p≤0.05).

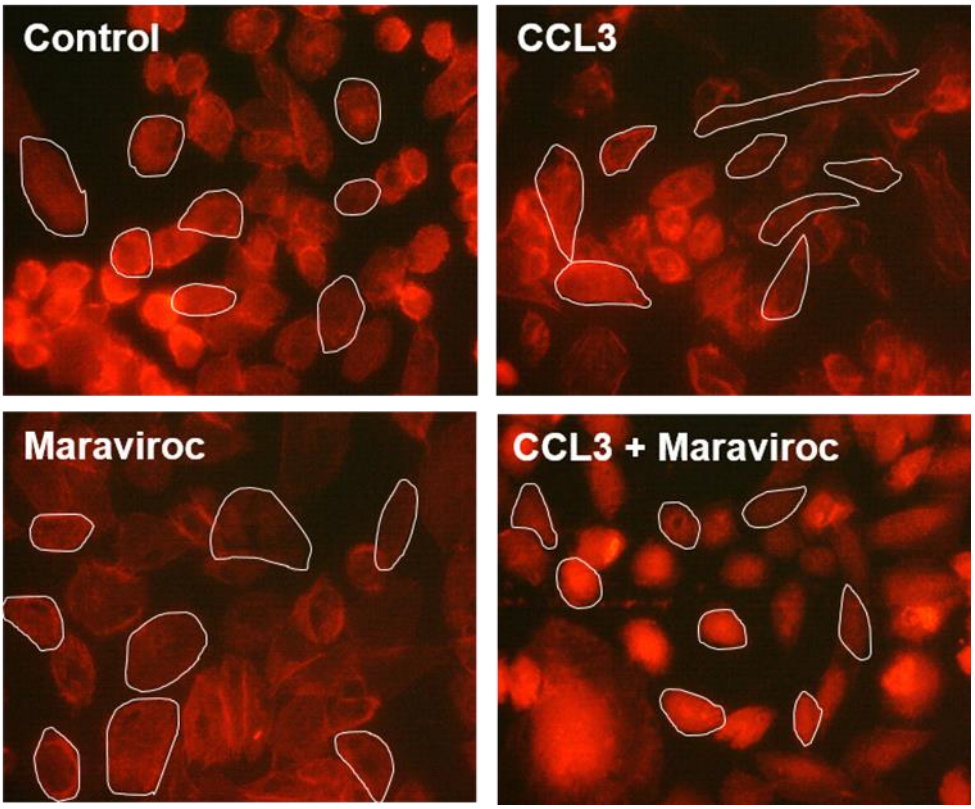

Figure 3.30. CHO-CCR5 cells stimulated with CCL3 (10 nM) in the presence and absence of Maraviroc (10 nM) after 24 hrs. CCR5 inhibitor: Maraviroc. Cells were fixed and stained with Phalloidin CruzFluor TM^{594} conjugate (red) for imaging F-actin. Cells outlined in white are a representation of the cell populations. Images were taken at 63x objective with a Leica DMI6000 inverted microscope and using Leica imaging suite.

From the ImageJ shape descriptors, the aspect ratio was shown to be significantly higher ($p \leq 0.01$, n=10) and the cell roundness significantly lower ($p \leq 0.05$, n=10) in CHO-CCR5 cells in the presence of CCL3 (10 nM) after 24 hrs (figure 3.27b and d). Whilst no significant change was measured in cell circularity (figure 3.27c). The aspect ratio is the ratio of the cells maximal length/minimal length, thus the higher value the more elongated the cell is, which was observed from the images (figure 3.28). The cellular roundness measures both cellular elongation and size. From the data it would appear that although CCL3 is able to induce some elongation of CHO-CCR5 cells generally these cells still retain their shape.

CHO-CCR5 cells only express one chemokine receptor CCR5 and so to confirm whether CCL3s effects on cellular elongation was genuine, maraviroc (10 nM) was used in an attempt to block this effect. Although maraviroc did not significantly block CCL3s effect on the aspect ratio there was a trend in inhibition which could also be observed from the images (figure 3.29a and 3.30). Furthermore there was a significant difference in cellular elongation between maraviroc alone and CCL3 alone suggesting that CCL3 is most likely inducing some changes to the cellular shape.

Besides analysing cell shape descriptors, changes to CTCF upon CCL3 stimulation was also measured. When looking at changes to CTCF no significant difference was detected although CHO-CCR5 cells incubated with CCL3 had a mean difference of 31.88% ± 20.65 above the control (figure 3.27a). Nonetheless when using maraviroc there was no reversal of this trend (figure 3.29b). Suggesting that CCL3 has either no genuine effect on actin polymerisation or that the approach was not sensitive enough to detect or measure these changes.

3.11 Maraviroc shows no cytoxicity in CHO-CCR5 cells after 25 hrs

To confirm the absence of a cytotoxic effect by maraviroc on CHO-CCR5 cells. The CHO-CCR5 were treated with maraviroc (10 nM) for 24 hrs using the MTS reagent to identify any effects on cellular viability. The results from this MTS assay showed no evidence of cytotoxicity (figure 3.31).

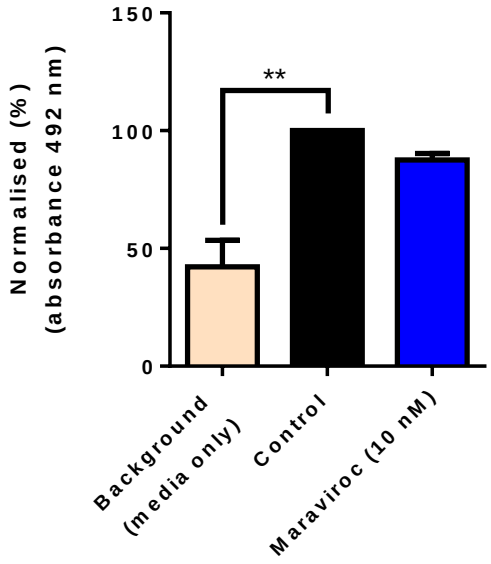

Figure 3.31. Cell proliferation assay in CHO-CCR5 cells. Maraviroc (10 nM) does not cause cytotoxicity in CHO-CCR5 after 24 hrs and 1 hrs MTS metabolisation (data from Wing Yee Lai). CCR1 inhibitor: J113863. CCR5 inhibitor: Maraviroc. Results represent the mean ± S.E.M in four independent experiments (Kruskal-Wallis test, Dunn's multiple comparisons test, ** = $p \leq 0.01$ and ns = $p \geq 0.05$ of no significance).

3.12 Discussion

The chemokine signalling network is frequently dysregulated in many carcinoma types which as a result leads to the ectopic migration of cancer cells to other sites within the body [115, 130]. Cancer dissemination is often fatal for the patient and therefore blocking chemokine signalling could be therapeutically beneficial for improving the survival rates of cancer patients. Unfortunately however this strategy has been particularly unsuccessful for carcinomas, with chemokine promiscuity and/or inappropriate target selection being two of the main issues [317].

The main objective of this chapter was to identify chemokine signalling pathways involved in the invasion of carcinoma cells for potential therapeutic targeting. The second aim was to establish the extent of functional redundancy underlying chemokine signalling in cancer cells.

To identify chemokine signalling pathways involved in carcinoma cell migration, seven different chemokine ligands were screened using the wound healing assay. From the screen CCL2 and CCL3 were identified as being involved in PC-3 and MCF-7 cell migration respectively (figures 3.5a and 3.12a) which corresponds with results from previous studies [278, 346, 437, 441].

The results from the intracellular calcium flux assay suggest that both PC-3 and MCF-7 cells express CCR5 (figures 3.19a-c and 3.20a-d). Therefore the different responses to CCL3 in the wound healing assay by MCF-7 and PC-3 cells could imply that CCL3 has a cell specific bias for promoting migration in MCF-7 cells. Although it may also be possible that the differences between the PC-3 and MCF-7 cells could be caused by different expression levels of CCR5 and/or CCL3 efficacy, as CCR5 expression was not quantified nor was different concentrations of CCL3 used.

In MCF-7 cells neither CCL4 nor CCL8 had any effect on scratch closure indicating that CCL3 could also be a biased agonist for CCR5 in promoting MCF-7 cell migration. When measuring increases in intracellular calcium both CCL4 and CCL3 demonstrated similar levels of efficacy in MCF-7 cells (figure 3.19a and b). However, due to differences in the kinetics and chemokine

concentration used to measure intracellular calcium levels (70 secs and 200 nM) and scratch closure (24 hrs and 10 nM), the efficacy levels of CCL3 and CCL4 between these two assays may not be comparable. Therefore efficacy cannot be rule out as a contributing factor for the differing responses to CCL3 and CCL4 in the wound healing assay. CCL8 on the other hand showed no receptor activation in MCF-7 cells which could be why no effect on scratch closure was observed.

Similarly in PC-3 cells, CCL8 also showed no effect on scratch closure unlike CCL2. Both CCL2 and CCL8 can activate CCR2 and CCR3 which may suggest that CCL2 is a biased agonist for CCR2 in PC-3 cell migration. Nonetheless data from the intracellular calcium flux assay was unable to properly establish the activation of CCR2 by either CCL2 or CCL8 in PC-3 cells (figures 3.18 and 3.20). Therefore CCR2 and CCR3 expression on PC-3 cells would need to be established using antibodies.

When probing the molecular mechanisms behind CCL3s activity in MCF-7 cell migration, the role of both CCR5 and CCR1 appeared to be redundant (figure 3.13). Evidence from the intracellular calcium flux assay also suggested that CCR1 could be functionally redundant for CCL3 signalling (figure 3.17b). Although to confirm this CCR5 activation would also need to be blocked as well. However as experimental data from Dr. Richard Jacques has shown that maraviroc acts as an agonist by increasing intracellular calcium in THP-1 cells [460], the use of maraviroc would not have been appropriate. Alternatively, siRNA could be used to knock down CCR5 expression instead.

Aside from CCL3 and CCL2 no other chemokines were identified as being involved in scratch closure, which contradicts the results from several previously published studies especially regarding CXCL12 (see table 3.1). Therefore there is a worrying lack of reproducibility with the wound healing assay. One explanation for this could be the narrow window available to measure differences in scratch closure between the basal and chemokine treatment. This was particularly evident in the less invasive cell lines such as the MCF-7 cells, with the mean difference in scratch width ratio between the basal and CCL3 just 0.127. As such, variability between batches of the same

cell line e.g. migration speed, chemokine efficacy and chemokine receptor expression, could have easily eroded this difference. Another issue surrounding the wound healing assay is the lack of sensitivity for more invasive cell types such as the PC-3 and MDA-MB-231 cells. As the higher basal migration could have concealed chemokine induced migration, especially if the cognate receptor was only expressed on a subset of cells such as CCR5 on MDA-MB-231 cells [338]. Therefore one alternative and perhaps a more sensitive approach would be to measure chemotaxis rather than scratch closure for detecting chemokine induced migration. As a consequence the effects of both CXCL12 and CCL2 on PC-3 chemotaxis were assessed using the transwell migration assay. Furthermore the agarose spot assay was used to measure the actions of CXCL12 on MDA-MB-231 cell migration.

Using the transwell migration assay no clear evidence of chemotaxis was measured for either CXCL12 or CCL2 in PC-3 cells (figure 3.15). Whilst for the agarose spot no meaningful data was collected (figure 3.16). Both of these approaches have been successfully used in previous studies to detect chemokine induced migration [278, 442, 448, 464].

The possible sources for the differing outcomes could have been the chemokine concentration, incubation time and cell density used. For the transwell migration assay two separate cell concentrations $25x10^4$ and $10x10^4$ per mL^{-1} were used (the data presented in this thesis was $10x10^4$ per mL^{-1}). Although PC-3 cells suspended at a cell density of 25x10^4 per mL^{-1} did display greater migration this did vary. CCL2 and CXCL12 were also tested at a concentration of 1 nM but this had no effect on migration whatsoever. Lastly PC-3 cells were incubated for 24 hrs, which was similar to another published study [278]. As such there is currently no definitive answer as to why this approach did not reproduce similar results as published in the wider literature. For the agarose spot assay all conditions were kept the same as in Vinadar. V *et al*. (2011). However the main issue with the agarose spot assay was the inability to fix the agarose spot to either glass or plastic which prevented any cell migration from being measured. From trialling these two techniques it would appear that neither are easily reproducible.

Other approaches which can be used to study chemotaxis instead include the Boyden chamber and the under the agarose cell migration assay. The Boyden chamber has been tried and tested for measuring chemokine induced chemotaxis [465]. Whilst no studies to our knowledge have used the under agarose assay to measure cellular migration in response to chemokine stimulation. Another approach is the Oris^{TM} migration assay which similar to the wound healing assay measures the movement of cells into a cell free zone and has already shown promising results in the lab with the PC-3 cells in response to CXCL8 and CXCL12. However one important limitation with these assays is that all migration is assessed in 2D rather than 3D which can lead to different cellular behaviour and gene expression [466, 467]. Therefore 3D migration models such as the spheroid invasion assay could be used to more accurately emulate *in vivo* metastasis and are already being used to study chemokine induced chemotaxis [468].

As an additional complementary experiment to the wound healing assay the effects of chemokine stimulation on the actin cytoskeleton of MCF-7, PC-3 and MDA-MB-231 cells for 24 hrs was explored using phalloidin staining. Overall neither PC-3 nor MCF-7 cells showed any obvious morphological differences following chemokine treatment (figures 3.21, 3.22, 3.24 and 3.25), although preliminary data with MDA-MB-231 cells showed cells treated with CCL8 had a more elongated morphology (figure 3.23). In PC-3 cells, treatment with CCL2 and CXCL12 tended to have higher levels of fluorescence when measuring the CTCF (figure 3.26). Interesting this trend also correlates with the wound healing assay data as both CCL2 and CXCL12 displayed greater levels of scratch closure after 24 hrs as well (figure 3.12a). Quantifying phalloidin fluorescence to measure F-actin formation was not a sensitive approach and as such western blotting or flow cytometry would be a more reliable and accurate way to detect changes in F-actin polymerisation. Also to truly determine an association between F-actin remodelling and scratch closure an F-actin inhibitor such as Cytochalasin D would need to be used to see if both of the observed effects for CCL2 and CXCL12 could be reversed.

To investigate the role of the CCL3-CCR5 signalling axis in the remodelling of the actin cytoskeleton the CHO-CCR5 cells were used, as they are a proven

cellular model for observing stress fiber formation [184]. From both the images and data analysis CCL3 stimulation was able to induce cellular elongation in the CHO-CCR5 cells (figures 3.27b and 3.28), which although not significantly blocked using maraviroc some inhibition was observed (figures 3.29a and 3.30). CCL3 treatment did show higher levels of fluorescence however maraviroc was unable to inhibit this effect and therefore as previously discussed the CTCF is not a reliable method for quantifying F-actin levels. Cellular elongation and polarity is a common feature of migrating cells and requires alterations to the actin cytoskeleton [469]. The CHO-CCR5 cells can serve as an independent and additional model to elucidate the molecular mechanisms of the CCL3-CCR5 signalling pathway involved in cytoskeletal changes.

In summary the evidence from the chemokine screen did not identify substantial functional redundancy amongst the chemokine ligands within and between specific cell types in the wound healing assay. Though evidence of chemokine receptor redundancy was identified. Due to the lack of sensitivity and reproducibility of the cell migration assays used in this chapter, whether inappropriate target selection could be a contributing factor for the low clinical success rate in the targeting of chemokine signalling for cancer treatment was not established.

3.13 Conclusion

The main findings from this chapter were also follows:

- CCL3 and CCL2 promote scratch closure in MCF-7 and PC-3 cells respectively, with the CCL3 acting on both CCR1 and CCR5.

- CCL4 induces intracellular calcium signalling in both PC-3 and MCF-7 cells. CCL3 also induces receptor activation in MCF-7 cells.

- CHO-CCR5 cells can be used as a model to investigate CCL3 induced cellular elongation.

- The wound healing assay is not a reliable approach for assessing chemokine induced migration. Whilst using the transwell migration and agarose spot assays to identify carcinoma chemotaxis towards chemokines is not highly reproducible.

Chapter 4.0 Investigating the downstream molecular mechanisms of G-protein signalling via different chemokines and in different cancer cell types

4.1 Introduction

Chemokine receptors are members of the G-protein coupled receptor superfamily and signal downstream through the dissociation of the heterotrimeric G-protein (Gα/βγ subunits). There are four main classes of the Gα subunit based on their genomic sequence and downstream effectors: $G\alpha_s$, $G\alpha_q$, $G\alpha_{12}$ and $G\alpha_i$. [36]. Chemokine receptors are primarily coupled to the $G\alpha_i$ class. Upon receptor activation the G-protein is recruited to the second and third intracellular loops resulting in the exchange of GDP for GTP on the $G\alpha_i$ subunit [25]. This activates the G-protein leading to its dissociation into the $G\alpha_i$ and Gβγ subunits. $G\alpha_i$ is a negative regulator of adenylate cyclase and blocks cAMP generation [470]. Alternatively $G\alpha_i$ can activate Src, a regulator of FAK, PI3K and MAPK signalling. Gβγ meanwhile can bind to Phospholipase C (PLC) which in turn cleaves PIP_2 into IP_3 and DAG. IP_3 travels to and opens the IP_3 channels on the endoplasmic reticulum which results in release of calcium from the intracellular stores. Intracellular calcium together with DAG activate PKC [88]. The downstream signalling pathways of FAK, PI3K, MAPK and PKC control many cellular physiological changes including cell migration and their dysregulation is associated with cancer metastasis [471-474]. Consequently many of these proteins are considered valid targets for cancer therapy and could serve as alternative therapeutic targets to the chemokine ligand or receptor.

Within the Mueller lab differences in the downstream pathway have been observed for distinct chemokine families [346, 347] and cell types [340]. However in the wider scientific literature understanding of the downstream signalling pathway for individual chemokines in different cancer types remains somewhat limited. This therefore restricts the selection of viable therapeutic

targets for blocking chemokine downstream signalling within metastatic cancer cells.

4.2 Aim

To investigate and probe the molecular machinery downstream of chemokine G-protein signalling within different types of cancer. This will potentially allow the identification of any novel chemokine and cell type specific intracellular signalling transducers which could be used for selective therapeutic targeting of the chemokine signalling network.

4.3 PLC is a cell specific mediator of intracellular calcium signalling for CCL3 in MCF-7 cells and chemokine signalling in THP-1 cells

PLC is a key mediator of chemokine increases in intracellular calcium and is often overexpressed in breast [475] and colorectal cancers [476]. Therefore establishing whether PLCs role is ubiquitous for the downstream signalling of different chemokines within separate cancer cell types could identify its importance as a therapeutic target.

To elucidate the molecular mechanisms in chemokine downstream signalling, intracellular calcium levels were measured to determine whether a protein could be important for this particular signalling event. The initial aim was to characterise the role of PLC in the downstream signalling of different chemokines by using PC-3, MCF-7 and THP-1 cells as cellular models for intracellular calcium signalling, as they all express both CCR5 and CXCR4 [436, 477-479].

The most commonly used small molecule for probing PLCs role in cellular based assays is the U73122, which disrupts PIP_2 hydrolysis [406]. U73122 has been widely shown to effectively attenuate the release of calcium from the intracellular stores [480-483]. Although there have also been some concerns regarding the potential for off-target effects, such as on calcium channels [484], SERCA [485] and even PLC activation [486], although the latter occurring within a cell free assay. Currently there are not many commercially

available PLC inhibitors, and amongst them, U73122 is the most well validated inhibitor for the pharmacological blockade of PLC in cell based assays.

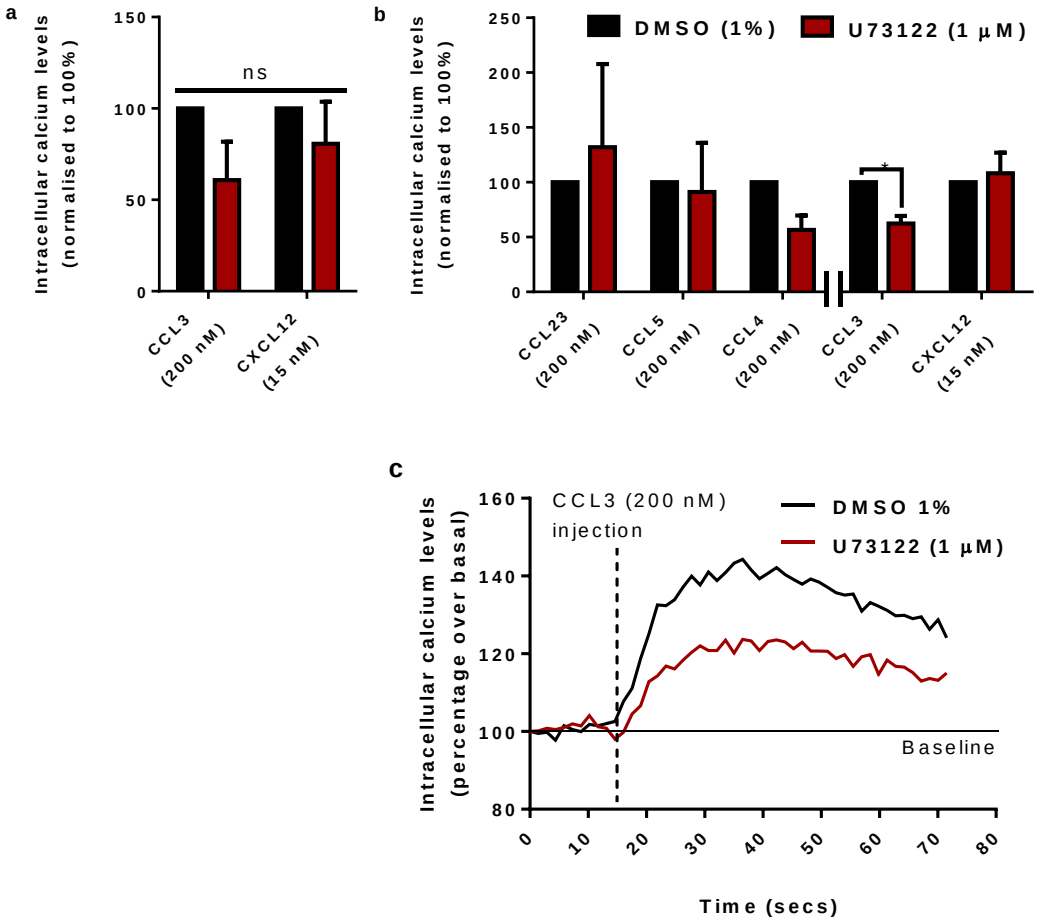

Figure 4.1. U73122 (1 µM) inhibition of PLC in the intracellular calcium flux assays of MCF-7 and PC-3 cells. (a) PC-3 cells were pretreated with U73122 (30 mins) prior to chemokine stimulation (n=3). (b) U73122 inhibits CCL3 intracellular calcium signalling in MCF-7 cells (n≥3). The double lines between CCL3 and CCL4 indicate separate experiments. (c) Representation of an intracellular calcium measurement trace following CCL3 stimulation in MCF-7 cells pretreated with U73122 (30 mins) after 70 secs. Data was normalised to the vehicle control (DMSO 1%) and represent the mean ± SEM of at least three independent experiments. (Wilcoxon Signed Rank Test, * = $p \leq 0.05$, and ns = $p \geq 0.05$ of no significance).

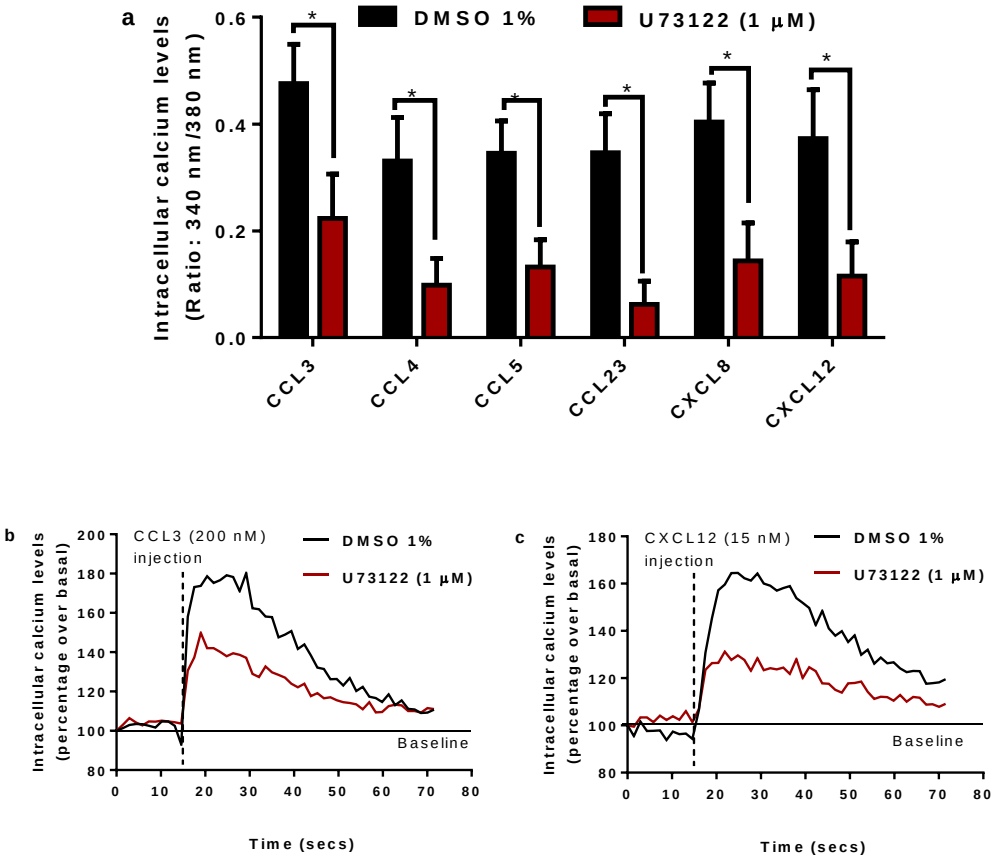

Figure 4.2. U73122 (1 µM) inhibition of PLC in the intracellular calcium flux assay of THP-1 cells. (a) U73122 inhibits chemokine intracellular calcium signalling in THP-1 cells. Representation of an intracellular calcium measurement trace following CCL3 (b) and CXCL12 (c) stimulation in THP-1 cells pretreated with U73122 (30 mins) after 70 secs. Data represents the mean ± SEM of at least four independent experiments (multiple t-tests, Holm-Šídák method, * = p≤0.05).

In THP-1 cells U73122 (1 µM) was able to significantly block increases in intracellular calcium amongst all the chemokines screened with the Student's t-test. Although multiple comparisons with the Holm-Šídák method showed no statistical significance this was likely obscured by the high standard deviation within the experiment (figure 4.2). This data implies that PLC is crucial for chemokine downstream signalling within THP-1 cells. In MCF-7 cells U73122 only significantly blocked increases in intracellular calcium from CCL3 (200

nM) indicating that PLC is important for CCL3 intracellular calcium signalling but not for CCL23, CCL5 or CXCL12 (figure 4.1b, c and d). For CCL4 signalling the U73122 did show a tendency to block increases in intracellular calcium. CCL3, CCL4 and CCL5 are all cognate ligands for CCR5 therefore the difference between PLCs importance in intracellular calcium signalling of CCL5 and that of CCL3 suggests that in MCF-7 cells, PLCs role is dependent on the chemokine ligand rather than the receptor. This was also observed for CCL3 and CCL23 intracellular calcium signalling as both chemokines activate CCR1 however U73122 only blocked CCL3 intracellular calcium signalling.

Blocking PLC activity in PC-3 cells displayed no significant effect on the increase in intracellular calcium of CCL3 (200 nM) or CXCL12 (15 nM). Though some reduction following CCL3 stimulation was observed with U73122 (figure 4.1a). Hence it appears that PLC is not crucial for CCL3 and CXCL12 intracellular calcium signalling in PC-3 cells.

4.4 U73122 blocks CCL3 increases in intracellular calcium in a concentration dependent manner in THP-1 cells

To ensure that the inhibition of chemokine intracellular calcium signalling by U73122 in THP-1 cells was due to a specific effect on PLC rather than a non-specific or off-target effect. A concentration response of U73122 at four separate concentrations: 50, 100, 500 nM and 1 µM was performed on CCL3 intracellular calcium signalling in THP-1 cells.

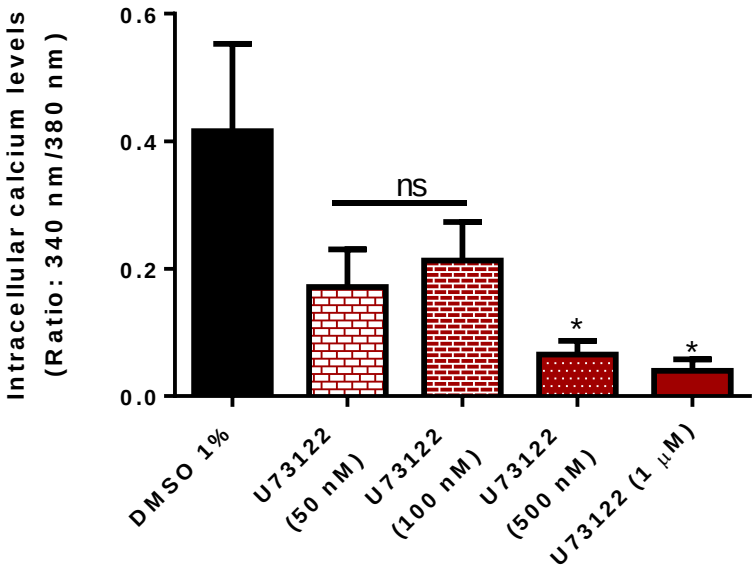

Figure 4.3. U73122 inhibits CCL3 (200 nM) intracellular calcium signalling in a concentration dependent manner in THP-1 cells. PLC inhibitor: U73122. Result represent the mean ± S.E.M. of at least three independent experiments. (One-way ANOVA, Dunnett's multiple comparisons test, * = $p \leq 0.05$, and ns = $p \geq 0.05$ of no significance).

The data from the concentration response of U73122 showed that U73122 was able to significantly inhibit CCL3 (200 nM) intracellular calcium signalling at both 500 nM and 1 µM, as well as having a moderate but non-significant inhibition on increases in intracellular calcium at 50 and 100 nM (figure 4.3). This demonstrates that U73122 inhibits increases in intracellular calcium in a concentration dependent manner and confirms a role for PLC in the downstream signalling pathway of chemokines in THP-1 cells.

4.5 U73122 is not cytotoxic in THP-1 after 2 hrs and in MCF-7 cells after 30 mins incubation

As an additional control the effects of U73122 was assessed on the cellular viability of THP-1 and MCF-7 cells using an MTS cell proliferation assay. Thereby excluding the possibility of compound cytotoxicity during the 30 mins pretreatment time prior to intracellular calcium measurements.

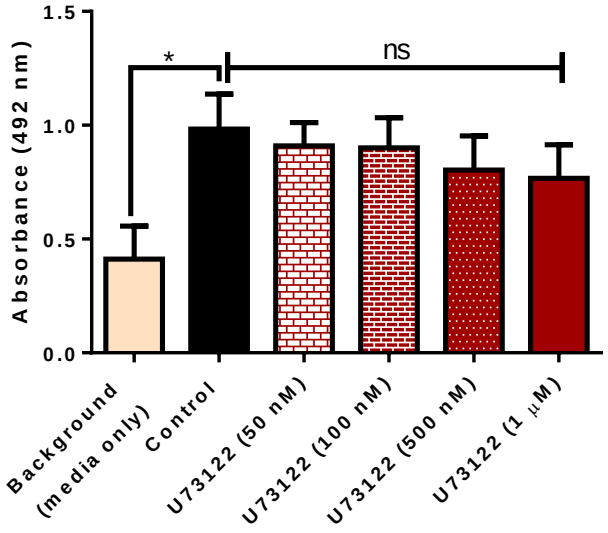

Figure 4.4. Cell proliferation assay of THP-1 cells. U73122 is not cytotoxic at concentrations of 50, 100, 500 nM and 1 μM in THP-1 cells after 2 hrs incubation with MTS reagent. PLC inhibitor: U73122. Result represent ± SEM of four independent experiments (One-way ANOVA, Dunnett's multiple comparisons test, * = $p \leq 0.05$ and ns = $p \geq 0.05$ of no significance).

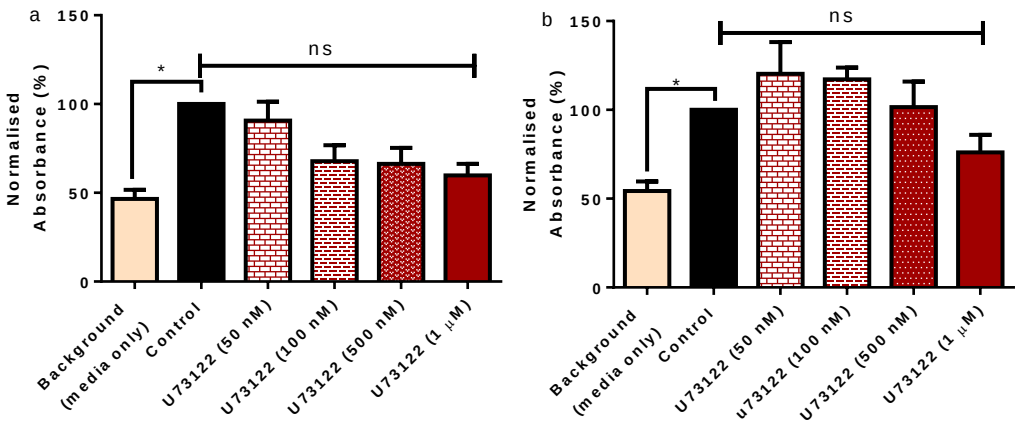

Figure 4.5. Concentration response of U73122 on MCF-7 cell proliferation. (a) U73122 is not significantly cytotoxic after 2 hrs incubation with MTS reagent. (b) U73122 is not cytotoxic after 30 mins incubation with MTS reagent. PLC inhibitor: U73122. Results were normalised to the control and represent ± SEM of four independent experiments (Kruskal-Wallis test, Dunn's multiple comparisons test, * = p≤0.05 and ns = p≥0.05 of no significance).

The results from the MTS assay showed that U73122 was not cytotoxic at any of the four concentrations (50, 100, 500 nM and 1 μM) in THP-1 cells and MCF-7 cells after 2 hrs incubation (figure 4.4). However in MCF-7 cells U73122 showed some decrease in cell viability at concentrations of 100, 500 nM, and 1 μM following 2 hrs incubation (figure 4.5a).

For the intracellular calcium flux assay U73122 was incubated for 30 mins prior to chemokine stimulation and the MTS assay was therefore repeated with U73122 incubated for 30 mins instead to see if there was still evidence of some possible cytotoxicity. After 30 mins incubation U73122 displayed no significant effect on MCF-7 cellular viability at any of the four concentrations tested. Although lower levels of absorbance were still observed with 1 μM of U73122 (figure 4.5b).

Overall the MTS assay data indicates that using U73122 at a concentration of 1 μM is still appropriate to functionally assess the role of PLC on intracellular

calcium signalling in THP-1 cells. For MCF-7 cells it is unlikely that U73122s effect on CCL3 intracellular calcium signalling was due to cytotoxicity as U73122 had no effect on CCL5, CCL23 and CXCL12 increases in intracellular calcium (figure 4.1b). However it appears that MCF-7 cells display some sensitivity towards to the effects of U73122 (1 μM).

4.6 CCL3 and CXCL12 do not signal through Gβγ in MCF-7 cells

In MCF-7 cells PLCs importance was shown to be specific to only CCL3. To establish whether the differing roles of PLC in CCL3 and CXCL12 intracellular calcium signalling in MCF-7 cells was a result of diverging signalling mechanisms upstream of PLC. The Gβγ subunit was targeted using the small molecule inhibitor gallein in MCF-7 cells prior to CCL3 or CXCL12 stimulation.

Gallein binds to the WD40 repeat structural motif of Gβγ which is the main protein binding site and thereby inhibits Gβγ intracellular activity [487]. Gallein has been shown to effectively block neutrophil [488] and T-lymphocyte chemotaxis [347]. For intracellular calcium signalling gallein was able to inhibit H1R agonism [489] however gallein had no such effect on glucose [490], CXCL11 or CCL3 [347]. Treatment with gallein alone has been shown not to induce increases in intracellular calcium [491].

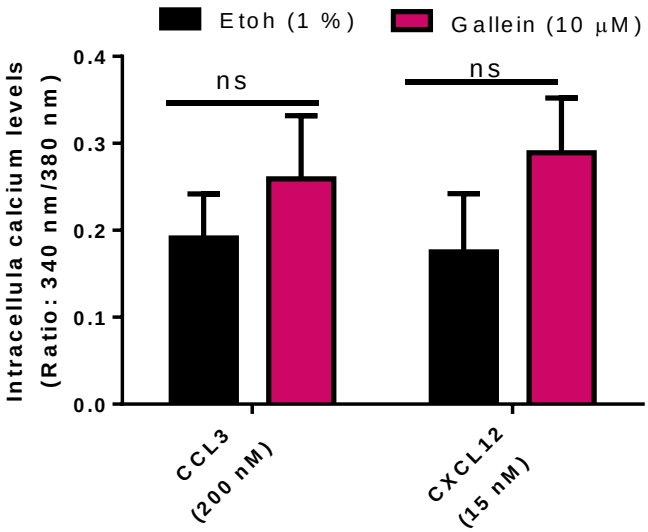

Figure 4.6. Gallein inhibition of Gβγ in the intracellular calcium flux assay of MCF-7 cells. Results represent the mean ± S.E.M. in at least four independent experiments (multiple t-tests, Holm-Sidak test, ns = p≥0.05 of no significance).

Incubating MCF-7 cells with gallein (10 µM) for 30 mins prior to chemokine stimulation did not inhibit CCL3 (200 nM) or CXCL12 (15 nM) intracellular calcium signalling compared to the vehicle control (etoh 1%) (figure 4.6). In contrast, upon CXCL12 simulation pre-incubation with gallein had a tendency to display a higher level of increase in intracellular calcium than the vehicle. The data shows that Gβγ is not important for the increases in intracellular calcium by CCL3 or CXCL12 in MCF-7 cells.

4.7 CCL4, CCL5 and CXCL12 signal through Gαi/βγ in MCF-7 cells

The results from the intracellular calcium flux assays with gallein conflicts with the current understanding of the canonical $G\alpha_i$ signalling pathway, whereby Gβγ is needed for PLC activation [74, 75]. Therefore it is possible to speculate that CCR1/5 and CXCR4 could be coupled to an alternative class of G-protein within MCF-7 cells, in particular $G\alpha_q$ which can also activate PLC to mobilise calcium from the intracellular stores [28]. To test this hypothesis pertussis toxin (PTX) was used to completely block $G\alpha_i/\beta\gamma$ coupling to the chemokine receptor.

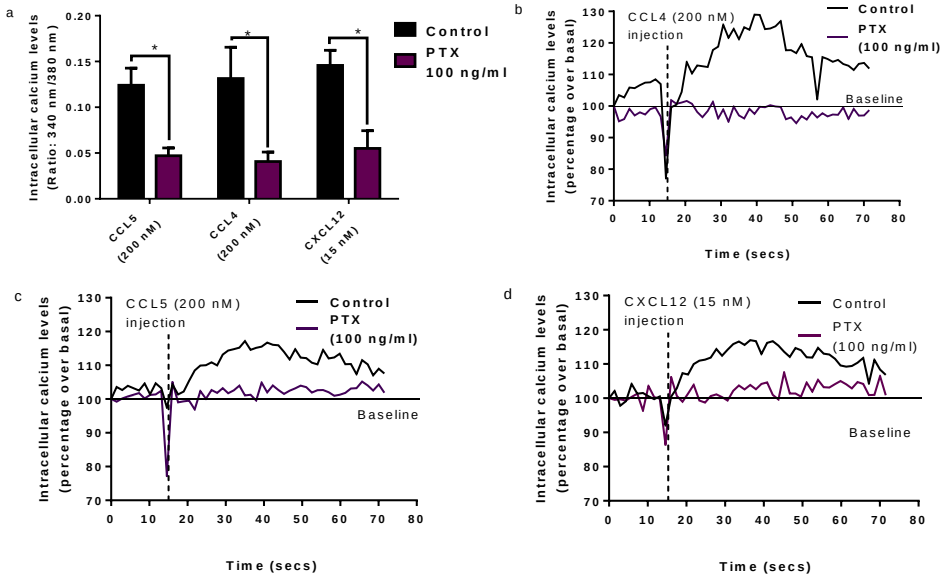

Figure 4.7. PTX inhibition of $G\alpha_i/\beta\gamma$ coupling in MCF-7 cells. (a) PTX (100 ng/ml) abolishes CCL4, CCL5 and CXCL12 intracellular calcium signalling in MCF-7 cells. (b) Representation of an intracellular calcium measurement trace following CCL4 stimulation in MCF-7 cells pretreated with PTX (16 hrs) after 70 secs. (c) Representation of an intracellular calcium measurement trace following CCL5 stimulation in MCF-7 cells pretreated with PTX (16 hrs) after 70 secs. Representation of an intracellular calcium measurement trace following CXCL12 stimulation in MCF-7 cells pretreated with PTX (16 hrs) after 70 secs. Results represent the mean ± S.E.M. in at least three independent experiments. (multiple t-tests, Holm-Sidak test, * = $p \leq 0.05$, ns = $p \geq 0.05$ of no significance).

The intracellular calcium measurement experiments with PTX showed that PTX (100 ng/ml) significantly abolishes the intracellular calcium signalling of CXCL12 (15 nM), CCL4 and CCL5 (200 nM) in MCF-7 cells (figure 4.7 a-d). The data confirms that in MCF-7 cells both CXCR4 and CCR5 are coupled to and signal via $G\alpha_i$.

4.8 FAK14 inhibits CXCL12 increases in intracellular calcium in THP-1 cells.

Aside from the PLC mediated signalling pathway, chemokine downstream signalling can also occur via the $G\alpha_i$-Src signalling axis [60]. Src is a tyrosine kinase which regulates the activity of a variety of downstream proteins including FAK and PI3K [61, 62, 65, 67]. In cancer, FAK is often overexpressed [471] whilst PI3K is frequently mutated [472]. Consequently FAK and PI3K are considered important for cancer progression and therefore could contribute to chemokine associated metastasis.

PI3K has been implicated in CXCL12 downstream signalling for T-cell leukaemia [340], breast [340, 342, 343], bile duct [492] and colon cancers [493], as well as, melanoma [494], glioblastoma [495] and multiple myeloma [496]. CXCL12 has also been shown to activate FAK within multiple myeloma [496], glioblastoma [497], leukaemia [498], breast [342, 343, 499], pancreatic [500], cervical [501], liver [501], prostate [502] and gastric cancers [503]. Despite the substantial evidence of FAK and PI3K activation downstream of CXCL12 signalling within cancer, much of this data especially for FAK is derived entirely from western blotting and therefore provides little insight into functionality, importance or the underlying molecular mechanisms involved.

To better understand the role of FAK and PI3K in chemokine downstream signalling both proteins were blocked within an intracellular calcium flux assay to see if they regulate CCL3 and CXCL12 mobilisation of calcium from the intracellular stores in PC-3, THP-1 and MCF-7 cells. CHO-CCR5 cells were also included as an additional cellular model for CCL3 signalling as much less is known about the roles of FAK and PI3K within the CCL3 signalling pathway.

To fully determine PI3Ks role two established PI3K inhibitors were used, the non-specific PI3K inhibitor LY294002 and the PI3Kγ inhibitor AS605240, thereby ensuring all PI3K isoforms were targeted. For blocking FAK kinase activity PF562271 was used, as it binds inside the ATP binding pocket of FAK [400]. FAK activation was also blocked using FAK14, which interacts with the Tyr397 residue to disrupt FAK autophosphorylation [399]. In addition to PF562271, another tyrosine kinase inhibitor masitinib was also used. Masitinib primarily targets Lyn B however it may also inhibit some FAK activity due to its ability to displace ATP within the tyrosine kinase domain [401, 504]. This range of FAK inhibitors allows the identification of potential functional differences in FAK activity as well as adding greater reliability to the results.

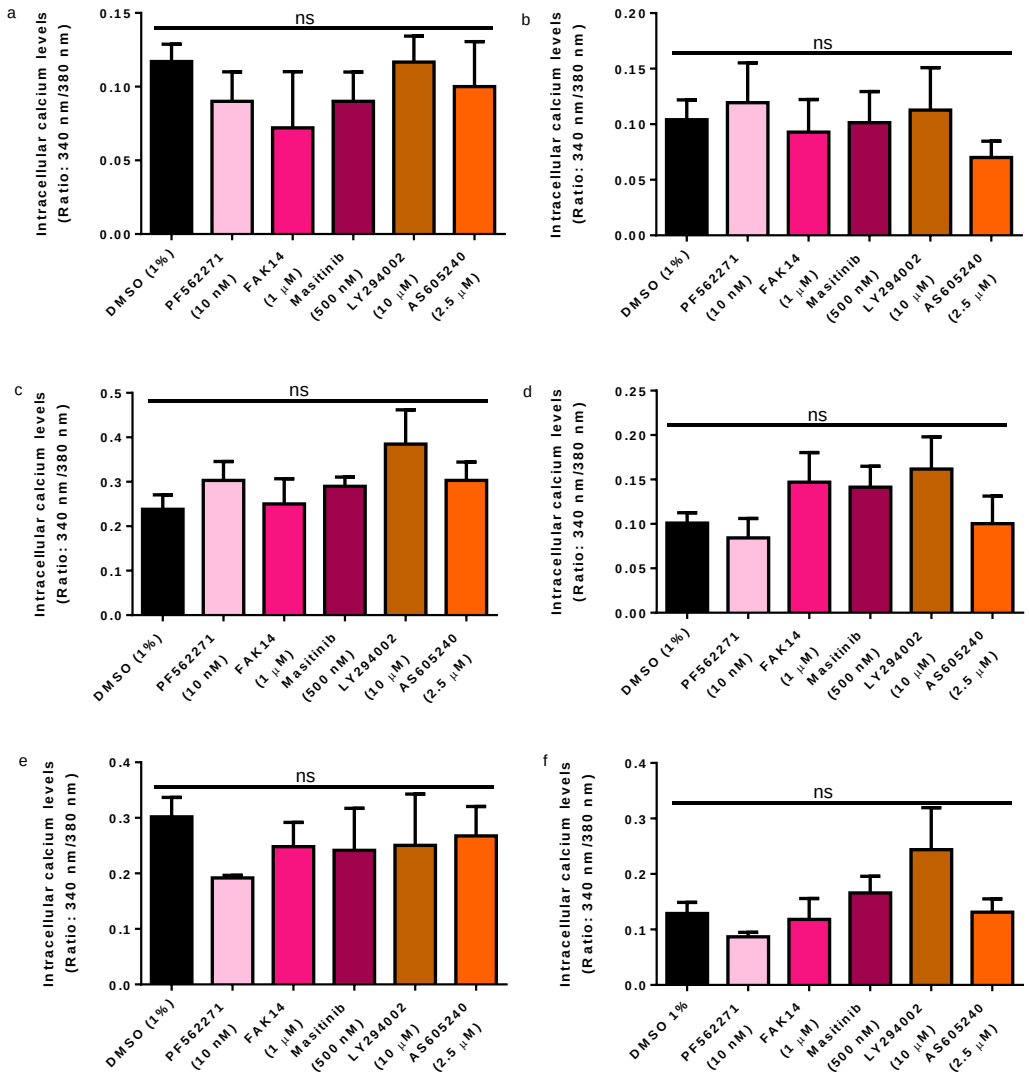

Figure 4.8. Inhibition of FAK and PI3K in CCL3 (200 nM) and CXCL12 (15 nM) intracellular calcium flux assays. PC-3 cells were pretreated with inhibitors (30) mins prior to CCL3 (a) or CXCL12 (b) stimulation. MCF-7 cells were pretreated with inhibitors (30 mins) prior to CCL3 (c) or CXCL12 (d) stimulation. (e) THP-1 cells were pretreated with inhibitors (30 mins) prior to CCL3 stimulation. (f) CHO-CCR5 cells were pretreated with inhibitors (30 mins) prior to CCL3 stimulation. FAK inhibitors: FAK14, Masitinib and PF562271. PI3K inhibitor: LY294002. PI3Kγ inhibitor: AS605240. Results represents the mean ± S.E.M. in at least 3 independent experiments. (One-way ANOVA, Dunnett's multiple comparisons test, Fischer's LSD Test, ns = p≥0.05 of no significance).

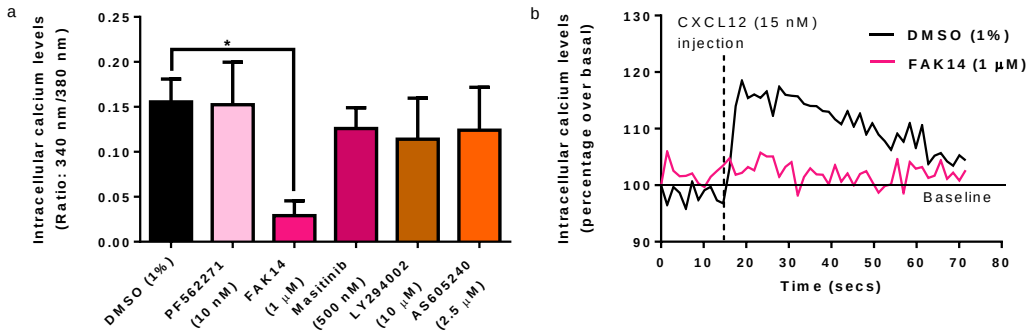

Figure 4.9. CXCL12 (15 nM) increases in intracellular calcium levels in THP-1 cells. (a) FAK14 (1 μM) abolishes CXCL12 intracellular calcium signalling in THP-1 cells. (b) Representation of an intracellular calcium measurement trace following CXCL12 stimulation in THP-1 cells pretreated with FAK14 (30 mins) after 70 secs. FAK inhibitors: FAK14, Masitinib and PF562271. PI3K inhibitor: LY294002. PI3Kγ inhibitor: AS605240. Results represents the mean ± S.E.M data in three independent experiments. (One-way ANOVA, Dunnett's multiple comparison test, Fischer's LSD Test, * = $p \leq 0.05$).

From the intracellular calcium measurement experiments only FAK14 (1 μM) was able to significantly attenuate CXCL12 (15 nM) signalling in THP-1 cells ($p \leq 0.05$, n=3, Fischer's LSD Test) (figure 4.9). None of the other compounds displayed any significant inhibitory effect on CCL3 (200 nM) or CXCL12 (15 nM) signalling in any of the cell lines used. In THP-1 cells incubation with PF562271 (10 nM) displayed a 30% lower increase in intracellular calcium than the vehicle control (DMSO 1%) in response to CCL3 stimulation (figure 4.8e). In CHO-CCR5 and MCF-7 cells incubation with LY294002 (10 μM) tended to show higher levels of intracellular calcium upon CCL3 stimulation compared to the vehicle alone (figure 4.8c and f).

These results indicate that FAK could be important for CXCL12 intracellular calcium signalling in THP-1, but not CCL3 or in MCF-7 or PC-3 cells.

4.9 FAK14 and U73122 show no additive effect on CXCL12 intracellular calcium signalling in THP-1 cells

The previous data indicated that CXCL12 intracellular calcium signalling in THP-1 cells is dependent on both PLC and FAK. To establish if PLC and FAK were acting on the same or two independent pathways both FAK14 and U73122 were used at lower concentrations to identify whether both inhibitors when added together would have a greater inhibitory effect on intracellular calcium signalling. An additive effect would indicate that both proteins are part of two independent pathways, hence the increase in inhibition.

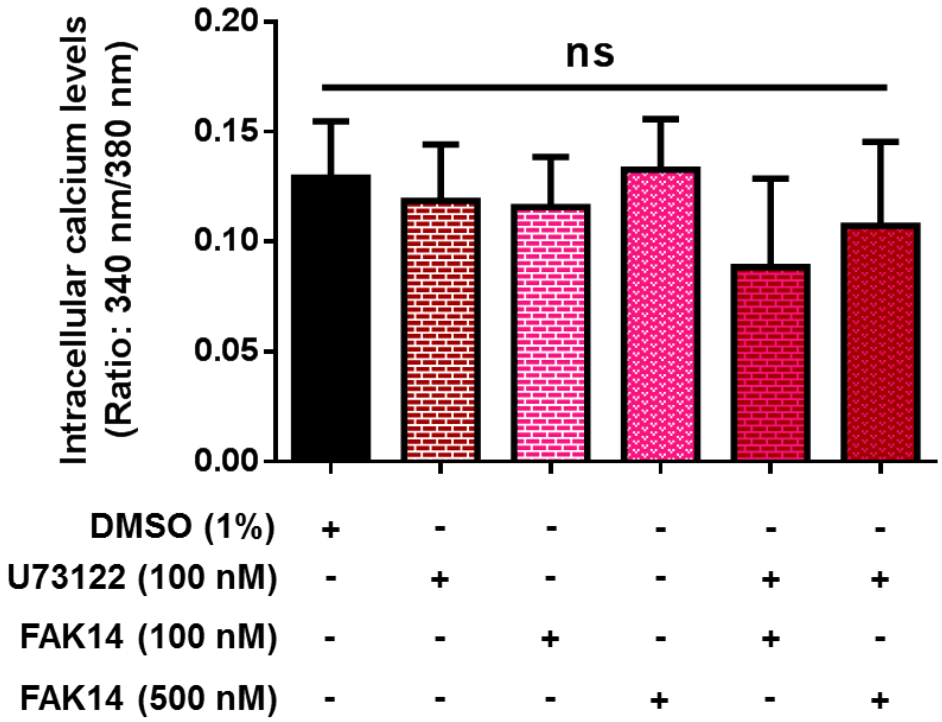

Figure 4.10. U73122 and FAK14 do not have an additive inhibition on CXCL12 (25 nM) intracellular calcium signalling in THP-1 cells. PLC inhibitor: U73122. FAK inhibitor: FAK14. Results represent the mean ± S.E.M. in five independent experiments. (One-way ANOVA, Dunnett's multiple comparisons test, ns = p≥0.05 of no significance).

Using concentrations of 100 nM for U73122, and 100 and 500 nM for FAK14 showed no significant inhibition on CXCL12 (25 nM) increases in intracellular

calcium in THP-1 cells when adding the compounds together (figure 4.10). However, incubating THP-1 cells with both FAK14 and U73122 did display lower increases in intracellular calcium compared to the other conditions. Neither FAK14 nor U73122 showed any inhibition against the vehicle control when added separately.

Overall, when added together neither U73122 nor FAK14 showed a significant additive effect. However as neither inhibitor showed any inhibition alone, whether FAK or PLC belong to the same or separate downstream signalling pathways could not be concluded from this experiment.

4.10 Src/Syk and c-Raf are important for CXCL12 intracellular calcium signalling in MCF-7 cells

Src is known to activate FAK and PI3K signalling but Src can also regulate the MAPK signalling pathway through the phosphorylation of Raf [64, 505]. Raf is a serine/threonine kinase and initiates a phosphorylation cascade by targeting MEK, which in turn phosphorylates ERK. Phosphorylated ERK translocates to the nucleus to regulate transcription factors such as FOXO, Elk and c-Fos, to increase cellular proliferation and cell survival [506].

The previous blockade of FAK and PI3K in CCL3 and CXCL12 intracellular calcium flux assays only identified the involvement of FAK in CXCL12 signalling in THP-1 cells (figure 4.9). Neither FAK nor PI3K were shown to be important for CCL3 intracellular calcium signalling or in MCF-7 cells.

To investigate whether CCL3 or CXCL12 could be increasing intracellular calcium through the activation of Src and/or MAPK signalling instead of PI3K or FAK, Src/Syk and c-Raf were targeted using MNS and ZM336372 respectively.

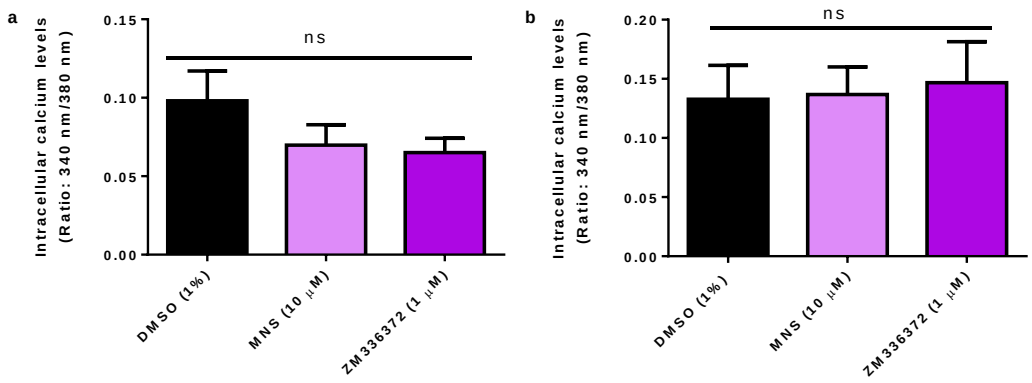

Figure 4.11. MNS (10 μM) and ZM336372 (1 μM) inhibition of Src/Syk and c-Raf respectively in the intracellular calcium flux assay. (a) MCF-7 cells were pretreated with MNS and ZM336372 (30 mins) prior to CCL3 (200 nM) stimulation. (b) CHO-CCR5 cells were pretreated with MNS and ZM336372 (30 mins) prior to CCL3 (200 nM) stimulation. Results represent the mean ± S.E.M. in at least 3 independent experiments. (One-way ANOVA, Dunnett's multiple comparisons test, ns = p≥0.05 of no significance).

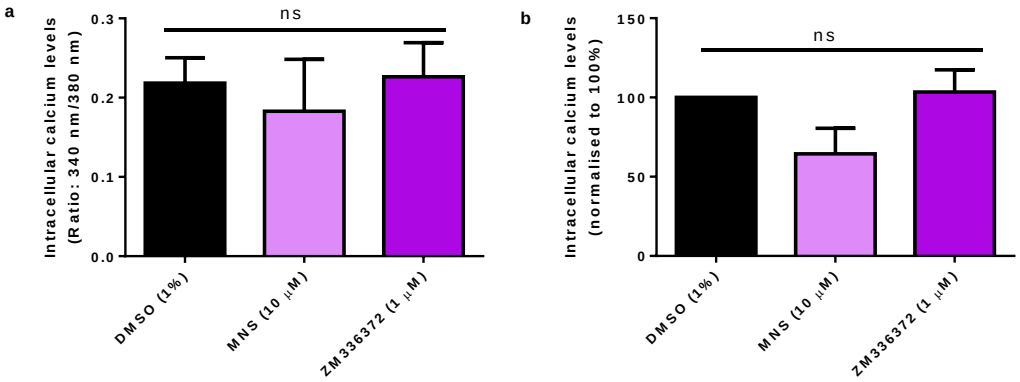

Figure 4.12. MNS (10 μM) and ZM336372 (1 μM) inhibition of Src/Syk and c-Raf respectively in the intracellular calcium flux assay of THP-1 cells. THP-1 cells were pretreated with MNS and ZM336372 (30 mins) prior to CCL3 (200 nM) (a) or CXCL12 (15 nM) (b) stimulation. Results for CXCL12 were normalised to the control (DMSO 1%) and analysed using the Kruskal-Wallis test, Dunn's multiple comparisons test. Results represent the mean ± S.E.M. in at least 3 independent experiments. (One-way ANOVA, Dunnett's multiple comparisons test, ns = p≥0.05 of no significance).

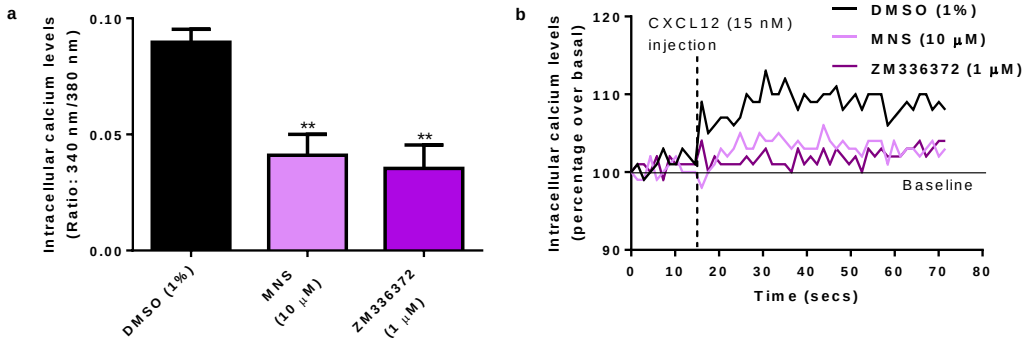

Figure 4.13. CXCL12 (15 nM) increases in intracellular calcium levels in MCF-7 cells. (a) MNS and ZM336372 inhibit CXCL12 intracellular calcium signalling in MCF-7 cells. (b) Representation of an intracellular calcium measurement trace following CXCL12 stimulation in MCF-7 cells pretreated with MNS or ZM336372 (30 mins) after 70 secs. Src/Syk inhibitor: MNS. c-Raf inhibitor: ZM336372. Results represent the mean ± S.E.M. of three independent experiments. (One-way ANOVA, Dunnett's multiple comparisons test, ** = p≤0.01).

From the intracellular calcium measurement experiments only MCF-7 cells showed a significant reduction of CXCL12 (15 nM) intracellular calcium signalling when treated with either MNS (10 μM) or ZM336372 (1 μM) (figure 4.13). Neither MNS nor ZM336372 had any effect on CXCL12 (15 nM) or CCL3 (200 nM) increase in intracellular calcium in THP-1 cells (figure 4.12c and d), or on CCL3 intracellular calcium signalling in MCF-7 and CHO-CCR5 cells (figures 4.12a and b). This suggests that Src/Syk and c-Raf are important for CXCL12 intracellular calcium signalling in MCF-7 cells but not in THP-1 cells or for CCL3.

4.11 U73122 inhibits CXCL12 chemotaxis of Jurkat cells

Chemokines primarily function as a chemoattractant and as such cell migration is a key cellular response to their signalling. In migrating cells, macromolecular structures known as focal adhesions (FA) are formed for adherence to the extracellular matrix and to generate traction [181, 182]. Within these FA, FAK can act as a scaffold for integrin binding, as well as binding to intracellular proteins such as Src, p130cas and paxillin for FA assembly [507]. Aside from FA formation, FAK and also PI3K can promote cell migration by regulating Rho GTPase activity [68, 508]. PI3K has been implicated in the migration of numerous different cancer cell types in response to chemokines [340, 342, 509-512]. But for FAK its role within chemokine cancer cell migration remains largely confined to a few studies [343, 498, 513]

To improve the understanding of FAKs role in chemokine stimulated migration, THP-1 cancer cells were used to model CCL3 and CXCL12 induced chemotaxis. The leukemic T-cell line, the Jurkat cells, was used as an additional cellular model to characterise the downstream signalling of CXCL12 chemotaxis. Jurkat cells express high levels of CXCR4 and as such display a high level of cellular mobility in response to CXCL12. This makes them an ideal model for studying CXCL12 chemotaxis.

To assess for cellular chemotaxis one of the most established methods used is the transwell migration assay. Transwell migration assays are comprised of two main components: the 96 well plate which contains the chemoattractant and a semipermeable membrane where cells are loaded onto. The semipermeable membrane is placed on top of the 96 well plate and the cells along with the chemoattractant are incubated together for a defined period of time. After incubation, the membrane and remaining cells are removed from the plate and the number of cells in each well are counted. The difference between the number of cells in the well with the chemoattractant and that of the buffer alone (the control) is used to measure chemotaxis.

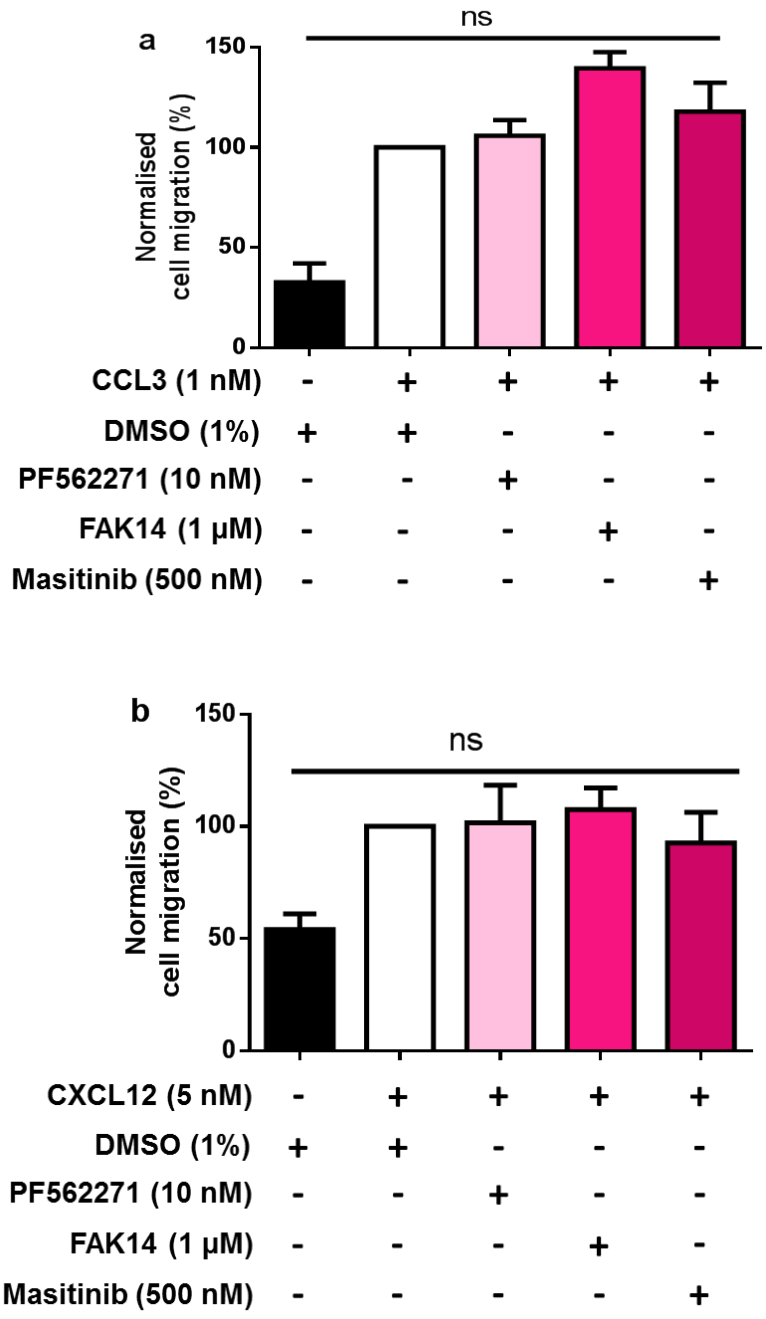

Figure 4.14. Inhibition of FAK in CCL3 (1 nM) and CXCL12 (5 nM) chemotaxis in THP-1 cells. (a) Treatment with FAK inhibitors does not inhibit CCL3 chemotaxis of THP-1 cells. (b) Treatment with FAK inhibitors does not inhibit CXCL12 chemotaxis of THP-1 cells after 4 hrs. FAK inhibitors: FAK14, Masitinib and PF562271. All results were normalised to DMSO (1 %) with CCL3 (1 nM) or CXCL12 (5 nM) and represent the mean ± SEM of three independent experiments. (Kruskal-Wallis test, Dunn's multiple comparisons, ns = p≥0.05 of no significance).

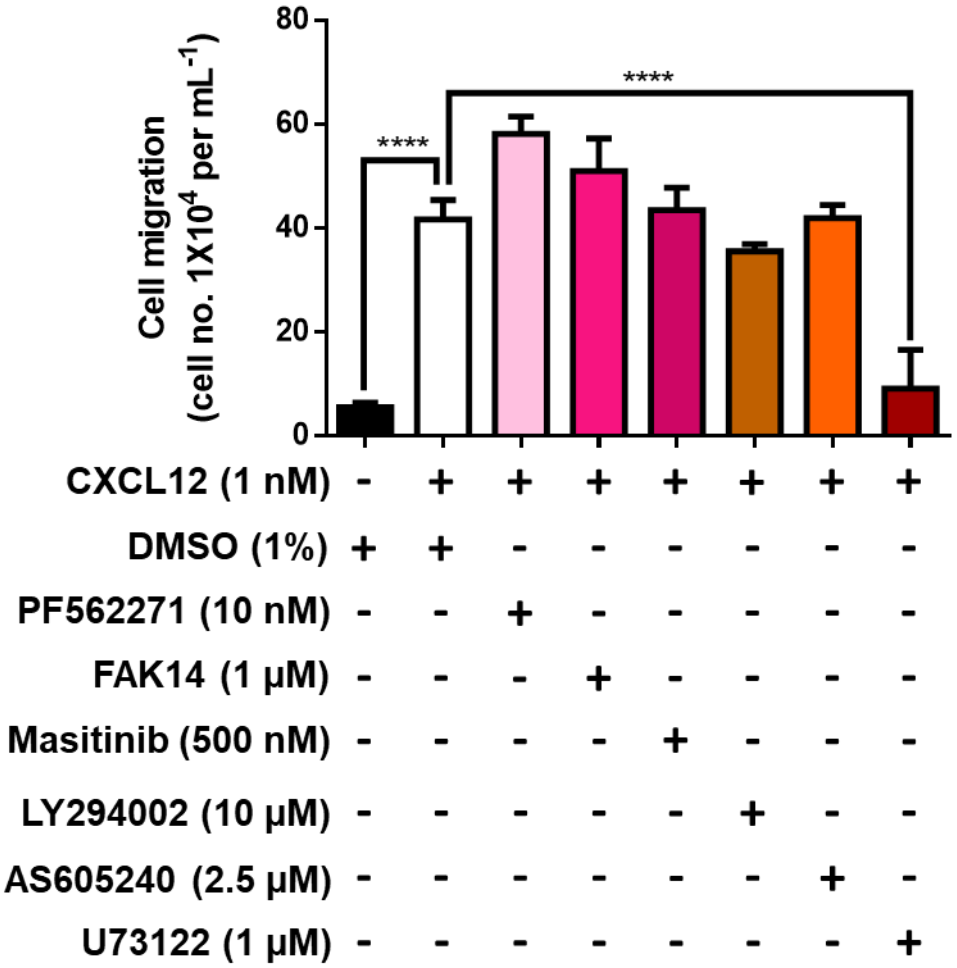

Figure 4.15. U73122 (1 µM) inhibition of PLC blocks CXCL12 (1 nM) chemotaxis in Jurkat cells after 4 hrs. PLC inhibitor: U73122. FAK inhibitors: FAK14, Masitinib and PF562271. PI3K inhibitor: LY294002. PI3Kγ inhibitor: AS605240. Results represent the mean ± SEM of at least three independent experiments. (One-way ANOVA, Dunnett's multiple comparisons test, **** = p≤0.0001).

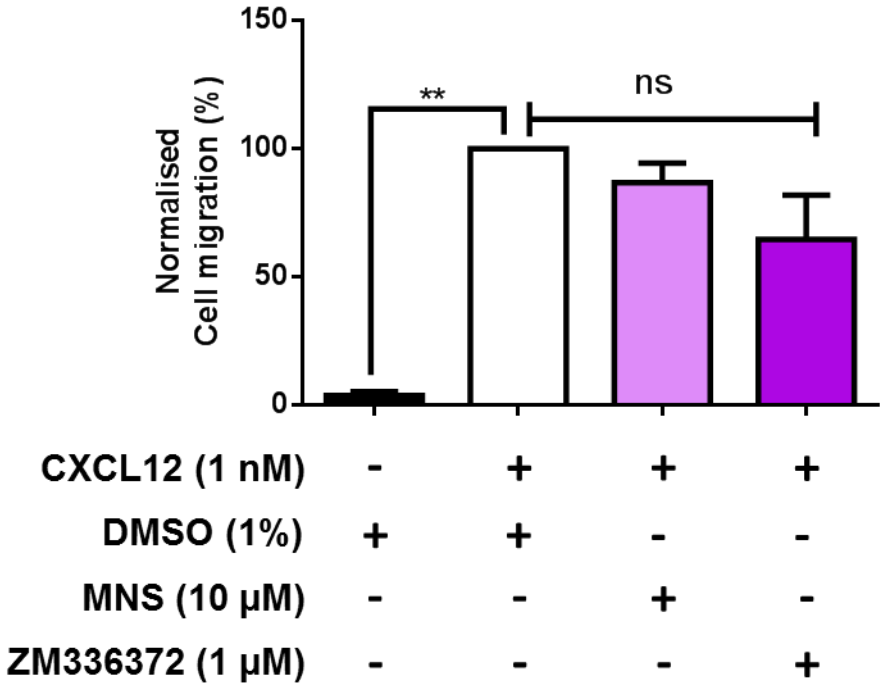

Figure 4.16. MNS (10 µM) and ZM336372 (1 µM) inhibition of Src/Syk and c-Raf respectively does not block CXCL12 (1 nM) chemotaxis in Jurkat cells after 4 hrs. All results were normalised to DMSO (1 %) with CXCL12 (1 nM) and represent the mean ± SEM in four independent experiments. (Kruskal-Wallis test, Dunn's multiple comparisons, ** = p≤0.01, ns = p≥0.05 of no significance).

FAK blockade showed no inhibition on THP-1 chemotaxis to either CCL3 (1 nM) or CXCL12 (5 nM) after 4 hrs (figure 4.14). In THP-1 cells incubation with FAK14 did display higher levels of cell migration towards CCL3 than the vehicle control. In Jurkat cells only U73122 (1 µM) was able to block CXCL12 (1 nM) induced chemotaxis (figure 4.14). FAK, PI3K, c-Raf or Src/Syk blockade in Jurkat cells showed no significant inhibition on CXCL12 (1 nM) chemotaxis after 4 hrs (figures 4.15 and 4.16). Though treatment with PF562271 (10 nM) did show higher levels of CXCL12 chemotaxis when compared to the vehicle control (figure 4.15).

Overall it appears that FAK is not important for promoting THP-1 chemotaxis towards CCL3 and CXCL12 or in Jurkat cells towards CXCL12. Whilst only PLC is crucial for CXCL12 chemotaxis of Jurkat cells.

4.12 U73122 is cytotoxic in Jurkat and THP-1 cells after 6 hrs and 29 hrs respectively

From the chemotaxis data U73122 (1 µM) was shown to significantly inhibit CXCL12 chemotaxis in Jurkat cells after 4 hrs (figure 4.15). To account for compound cytotoxicity as a possible cause for chemotaxis inhibition. All compounds used in the transwell migration assay were assessed for cellular cytotoxicity in both the THP-1 and Jurkat cell lines using the MTS cellular proliferation assay.

The data from the MTS identified that U73122 (1 µM) was cytotoxic in both THP-1 and Jurkat cells following 29 hrs and 6 hrs incubation respectively (figure 4.17). This indicates that U73122 inhibition on CXCL12 chemotaxis in Jurkat cells was due to cellular cytotoxicity rather than any functionality. None of the other compounds demonstrated any significant cytotoxicity in either cell line and as such were suitable to avoid cytotoxicity in the transwell migration assay.

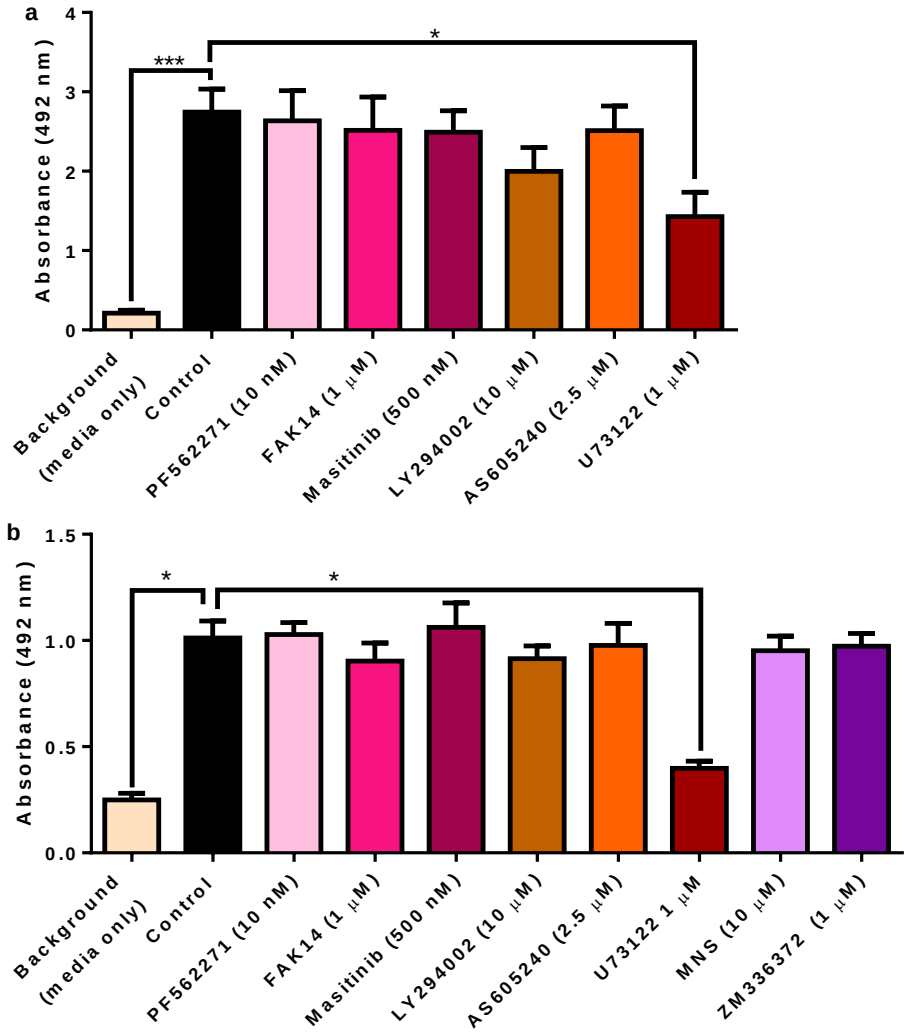

Figure 4.17. Cellular proliferation assay of THP-1 and Jurkat cells. (a) U73122 (1 μM) was significantly cytotoxic in THP-1 cells following 24 hrs incubation and 5 hrs MTS reagent metabolisation (n=3). (b) U73122 (1 μM) was significantly cytotoxic in Jurkat cells after 2 hrs incubation and 4 hrs MTS metabolisation (n=3). PLC inhibitor: U73122. FAK inhibitors: FAK14, Masitinib and PF562271. PI3K inhibitor: LY294002. PI3Kγ inhibitor: AS605240. Src/Syk inhibitor: MNS. c-Raf inhibitor: ZM336372. All results represent ± SEM of three independent experiments. (One-way ANOVA, Dunnett's multiple comparisons test, *** = p≤0.001 and * = p≤0.05).

4.13 PI3K is not important for CCL3 induced scratch closure of MCF-7 cells

The transwell migration assay is a reliable approach for measuring chemotaxis, but for the assay to be effective cells are required to be in suspension. For leukemic cells such as THP-1 and Jurkats, this mimics the *in vivo* environment. But for MCF-7 cells which are adherent this approach does not model their migratory mode as accurately.

MCF-7 cells are of epithelial origin and as such form cellular sheets. During cancer development some of these epithelial cells can adopt a mesenchymal phenotype by displaying a greater migratory behaviour and less adherence [514]. In the wound healing assay cells are grown as sheets and as such is a more applicable method for studying the migration of MCF-7 cells in response to chemokine stimulation.

A recent published study from the Mueller lab has shown that PI3K is important for CXCL12 induced migration in MCF-7 cells. However in this study PI3Ks role was determined by siRNA and not with the LY294002 [340]. To better understand the importance of PI3K in CCL3 induced migration in MCF-7 cells, both LY294002 and AS604520 were used in the wound healing assay of MCF-7 cells.

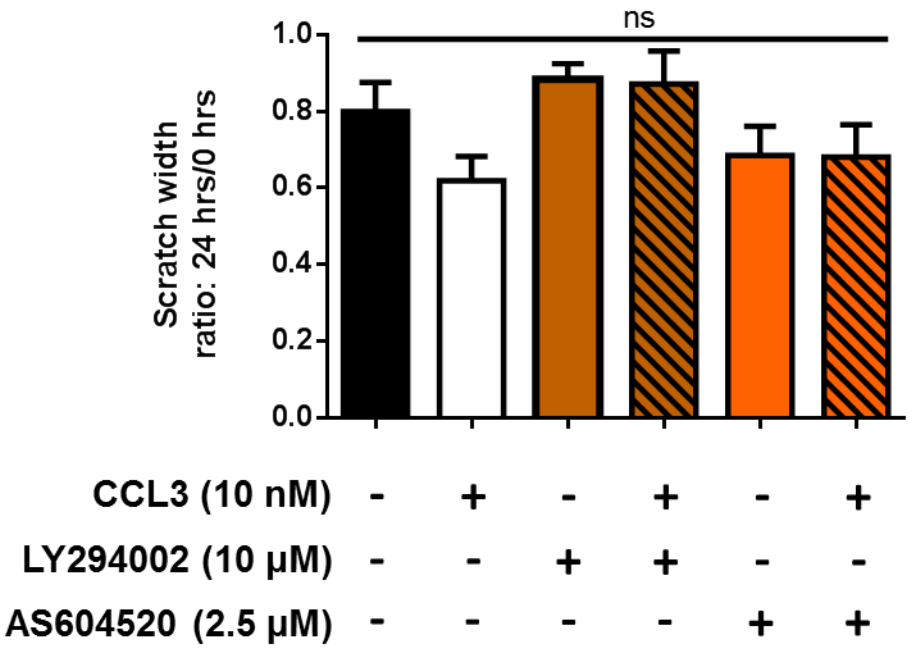

Figure 4.18. LY294002 (10 μM) and AS604520 (2.5 μM) inhibition of PI3K and PI3Kγ respectively does not block CCL3 (10 nM) scratch closure in MCF-7 cells after 24 hrs. A value of 1 denotes no migration, whilst 0 denotes complete migration. Results represent the mean ± SEM in four independent experiments. (One-way ANOVA, Tukey's test, ns = p≥0.05 of no significance).

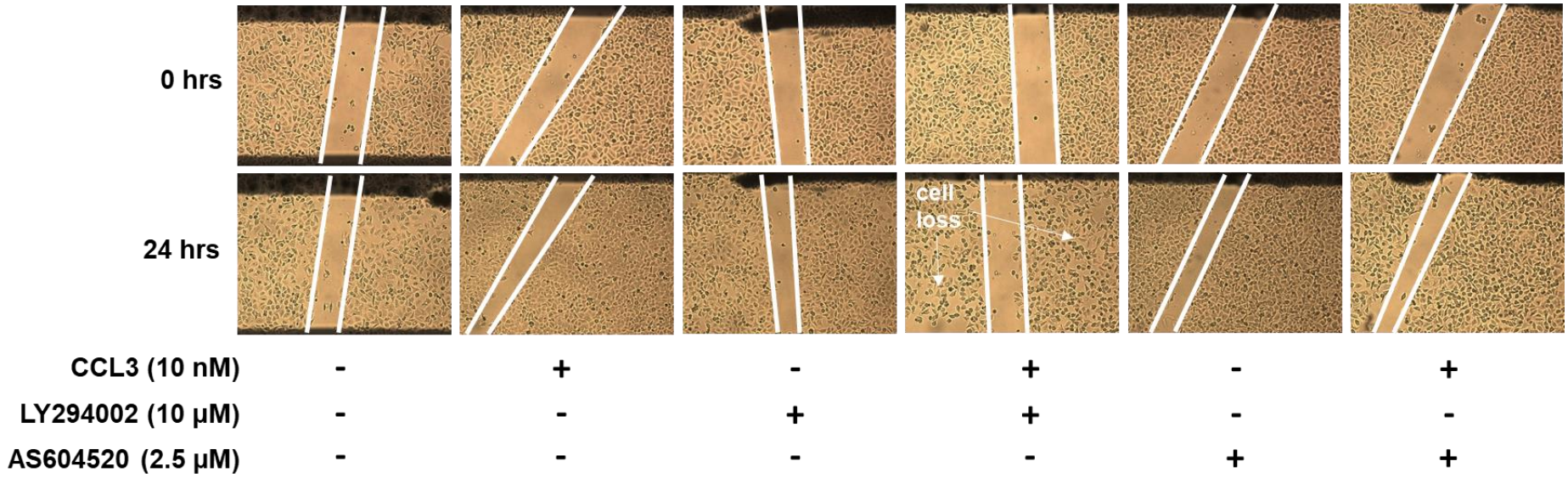

Figure 4.19. MCF-7 scratch closure in the presence and absence of CCL3 (10 nM) and respective PI3K and PI3Kγ inhibitors LY294002 (10 µM) and AS604520 (2.5 µM) after 24 hrs. Images are a representation of the cell population and were taken at 10x objective with a Leica DMI6000 inverted microscope and using Leica imaging suite.

When using LY294002 (10 μM) and AS604520 (2.5 μM) to block PI3K and PI3Kγ activity respectively, no significant inhibition on CCL3 (10 nM) scratch closure was detected (figure 4.18). However treatment with LY294002 did appear to reduce CCL3 induced scratch closure after 24 hrs. Although this could be due to cytotoxicity as two of the datasets showed observable cellular loss following LY294002 incubation (figure 4.19).

CCL3 treatment did show a tendency to enhance MCF-7 scratch closure after 24 hrs however it was not statistically significant. Also there was a similar level of scratch closure for AS604520 treatment alone when compared against CCL3 only. This raises substantial doubt as to whether CCL3 had any true effect on MCF-7 cell migration within this experiment.

4.14 None of the PI3K or FAK inhibitors were cytotoxic in MCF-7 cells following 25 hrs incubation

Due to the evidence of potential cellular cytotoxicity in MCF-7 cells following 24 hrs incubation with LY294002 (10 μM) in the wound healing assay (figure 4.19). An MTS assay was performed on the FAK and PI3K inhibitors to establish their effects on MCF-7 cell viability after 24 hrs.

Amongst the compounds tested none showed any significant effect on MCF-7 cell viability after 25 hrs incubation (figure 4.20). This confirms that the FAK and PI3K compounds used in this chapter are suitable to avoid cellular cytotoxicity for a 24 hrs wound healing assay experiment (at the concentration tested).

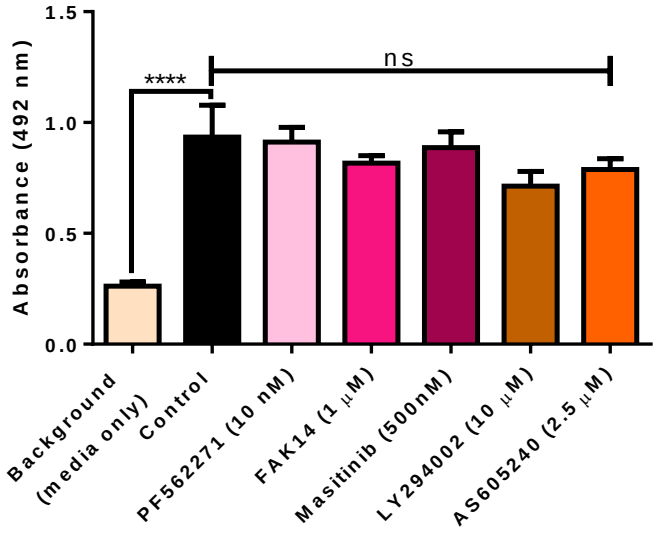

Figure 4.20. None of the compounds were significantly cytotoxic in MCF-7 cells following 24 hrs incubation and 1 hrs MTS metabolisation. FAK inhibitors: FAK14, Masitinib and PF562271. PI3K inhibitor: LY294002. PI3Kγ inhibitor: AS605240. All results represent ± SEM of at least three independent experiments. (One-way ANOVA, Dunnett's multiple comparisons test, **** = p≤0.0001 and ns = p≥0.05 of no significance).

4.15 FAK, PI3K and PLC do not affect the actin cytoskeleton in CHO-CCR5 and PC-3 cells.

The phalloidin staining of CHO-CCR5 cells identified that CCL3 induced greater cellular elongation (aspect ratio) following 24 hrs incubation (figure 3.27b). Furthermore CCL3 and CXCL12 both tended to exhibit higher levels of fluorescence (CTCF) in CHO-CCR5 and PC-3 cells respectively after 24 hrs (figures 3.26 and 3.27a).

As previously discussed, FAK and PI3K are known to effect the actin cytoskeleton by regulating the Rho GTPases family [68, 508]. Consequently both PC-3 and CHO-CCR5 cells were used to investigate whether the FAK and PI3K inhibitors would have any chemokine specific or non-specific effect on the actin cytoskeleton when stained with phalloidin. FAK is also known to

play a role in cell spreading [515] and so measurements of cell size (number of pixels) were also included to assess for any cellular spreading.

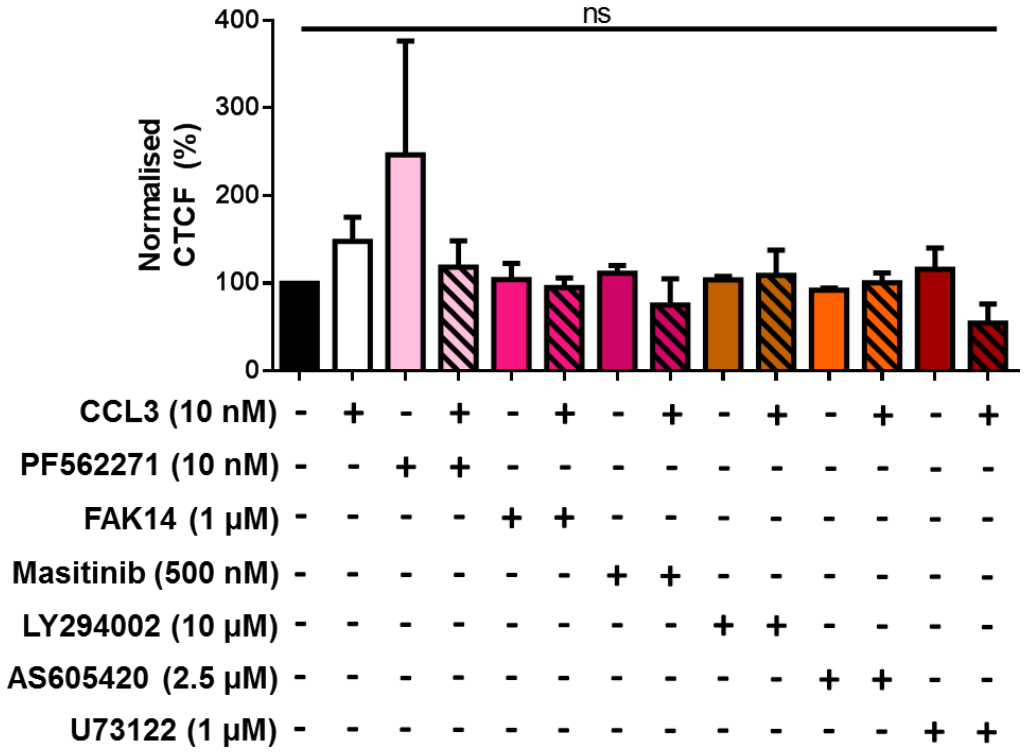

Figure 4.21. Inhibition of FAK, PI3K and PLC in the presence and absence of CCL3 (10 nM) does not affect the CTCF in CHO-CCR5 cells after 24 hrs. ImageJ 1.48v was used to calculate the CTCF for all images from the phalloidin stain, before being normalised to the control (absence of CCL3 and compounds). PLC inhibitor: U73122. FAK inhibitors: FAK14, Masitinib and PF562271. PI3K inhibitor: LY294002. PI3Kγ inhibitor: AS605240. Results represent the mean ± SEM of at least two independent experiments. (Kruskal-Wallis test, Dunn's multiple comparisons, ns = p≥0.05 of no significance).

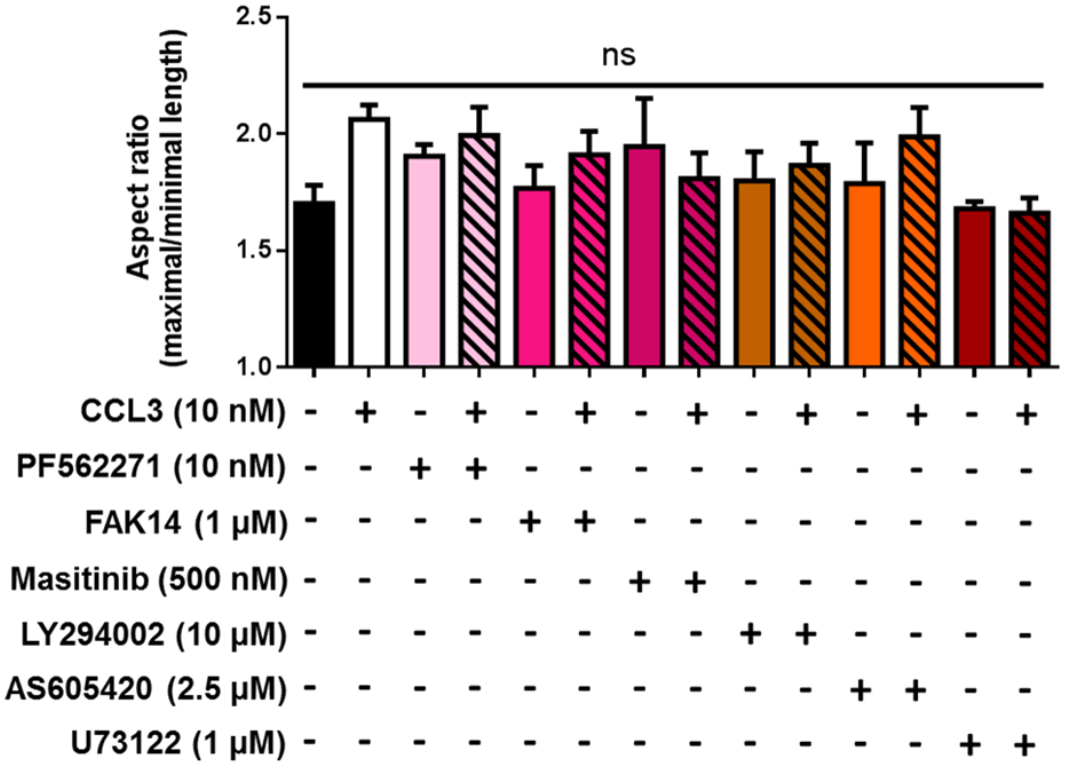

Figure 4.22. Inhibition of FAK, PI3K and PLC in the presence and absence of CCL3 (10 nM) does not affect the aspect ratio of CHO-CCR5 cells after 24 hrs. PLC inhibitor: U73122. FAK inhibitors: FAK14, Masitinib and PF562271. PI3K inhibitor: LY294002. PI3Kγ inhibitor: AS605240. Results represent the mean ± SEM of at least two independent experiments. (One-way ANOVA, Tukey's test, ns = p≥0.05 of no significance).

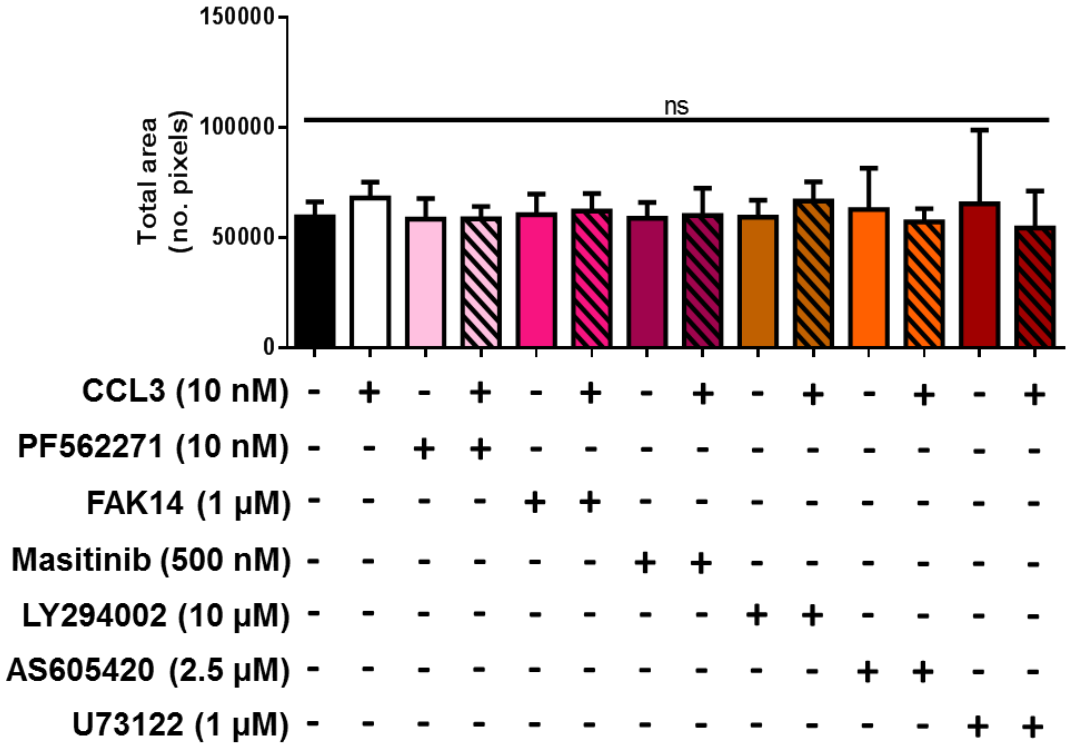

Figure 4.23. Inhibition of FAK, PI3K and PLC in the presence and absence of CCL3 (10 nM) does not affect the total area of CHO-CCR5 cells after 24 hrs. PLC inhibitor: U73122. FAK inhibitors: FAK14, Masitinib and PF562271. PI3K inhibitor: LY294002. PI3Kγ inhibitor: AS605240. Results represent the mean ± SEM of at least two independent experiments. (One-way ANOVA, Tukey's test, ns = p≥0.05 of no significance).

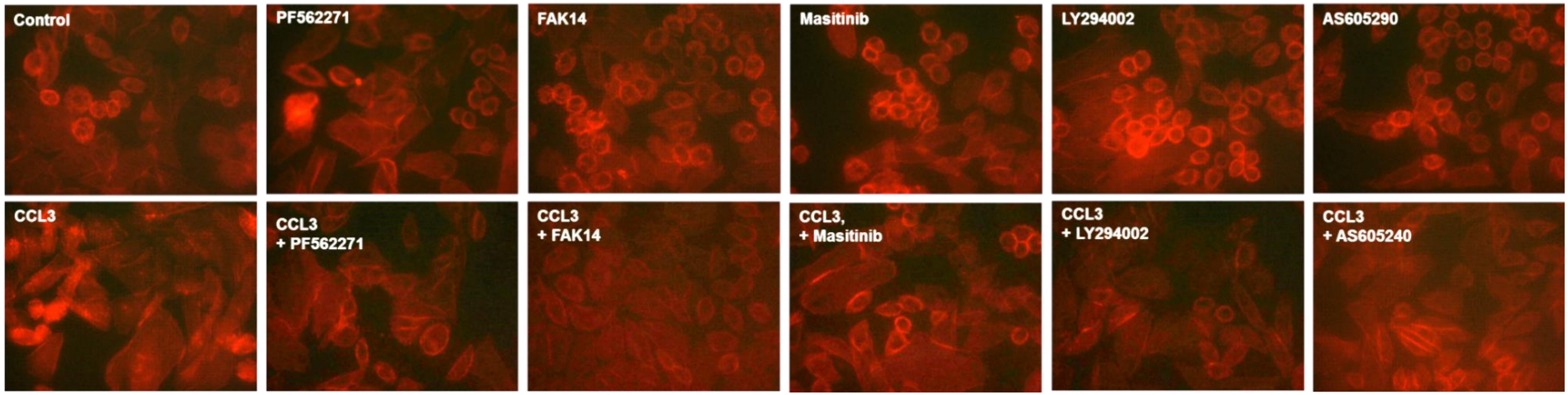

Figure 4.24. Phalloidin actin staining of CHO-CCR5 cells in the presence and absence of CCL3 (10 nM) with FAK and PI3K inhibitors after 24 hrs. FAK inhibitors: FAK14, Masitinib and PF562271. PI3K inhibitor: LY294002. PI3Kγ inhibitor: AS605240.CHO-CCR5 cells were fixed and stained with Phalloidin CruzFluor TM[594] conjugate (red) for imaging the F-actin cytoskeleton. Images are a representation of the cell population and were taken at 63x objective with a Leica DMI6000 inverted microscope and using Leica imaging suite.

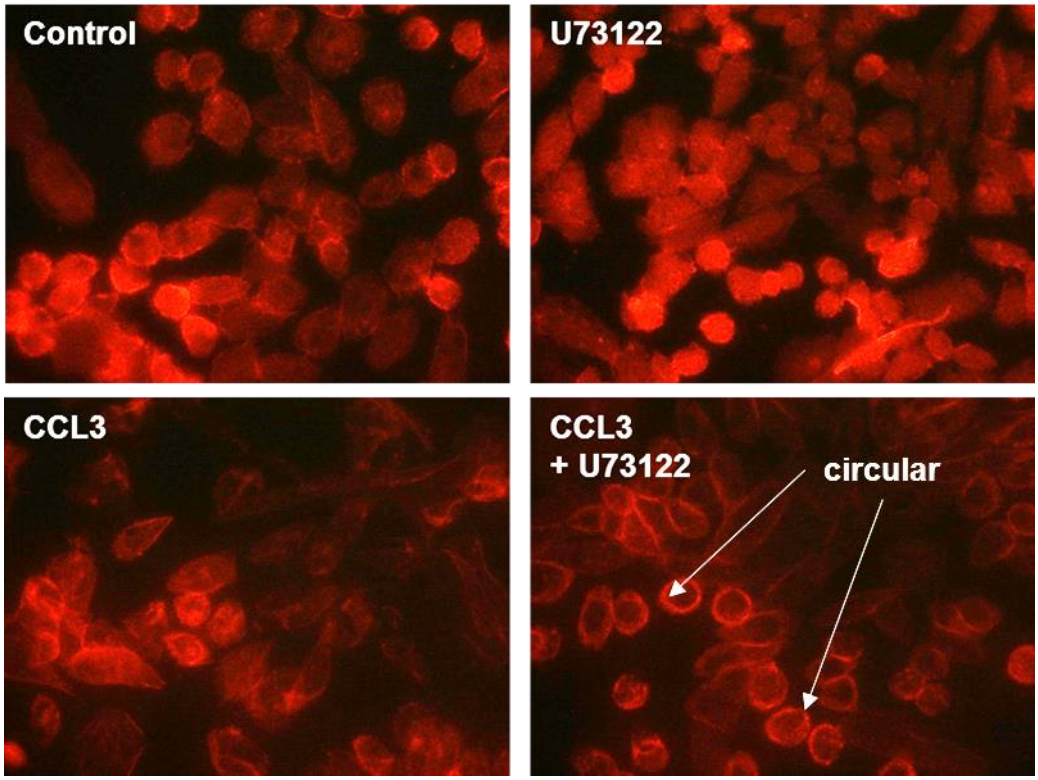

Figure 4.25. Phalloidin actin staining of CHO-CCR5 cells in the presence and absence of CCL3 (10 nM) and the PLC inhibitor U73122 (1 µM) after 24 hrs. CHO-CCR5 cells were fixed and stained with Phalloidin CruzFluor TM[594] conjugate (red) for imaging the F-actin cytoskeleton. Images are a representation of the cell population and were taken at 63x objective with a Leica DMI6000 inverted microscope and using Leica imaging suite.

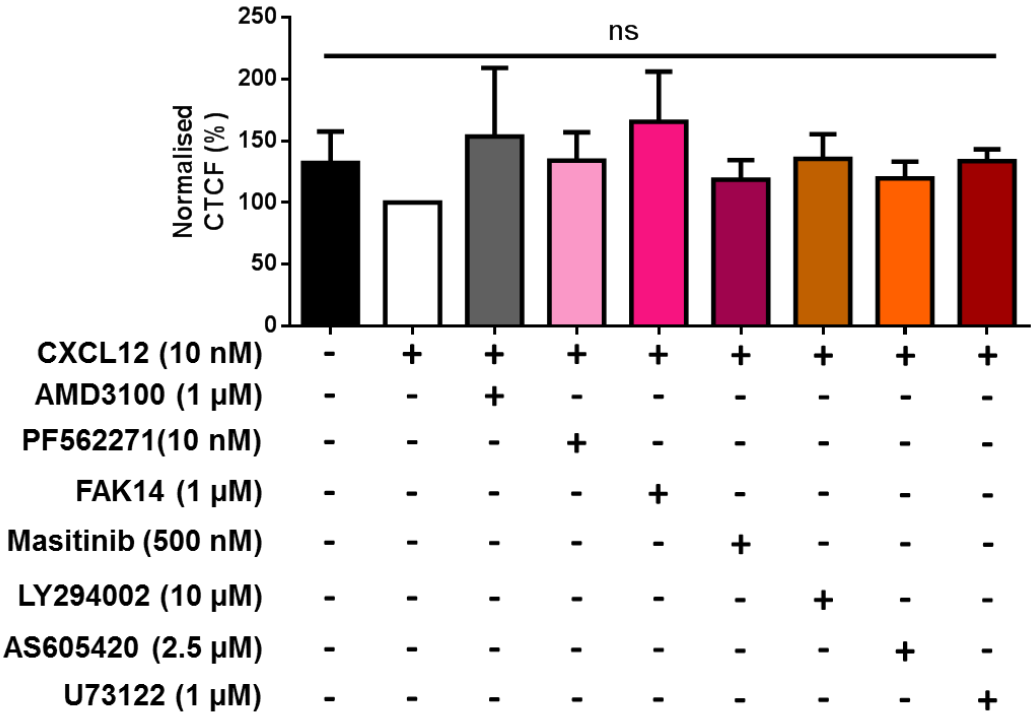

Figure 4.26. Inhibition of FAK, PI3K, PLC and CXCR4 in the presence of CXCL12 (10 nM) does not affect the CTCF of PC-3 cells following 24 hrs incubation. CXCR4 inhibitor: AMD3100. PLC inhibitor: U73122. FAK inhibitors: FAK14, Masitinib and PF562271. PI3K inhibitor: LY294002. PI3Kγ inhibitor: AS605240. All data represented was normalised to cells treated with the CXCL12 (10 nM) alone. Results represent ± SEM of at least two independent experiments. (Kruskal-Wallis test, Dunn's multiple comparisons, ns = p≥0.05 of no significance, ns = p≥0.05 of no significance).

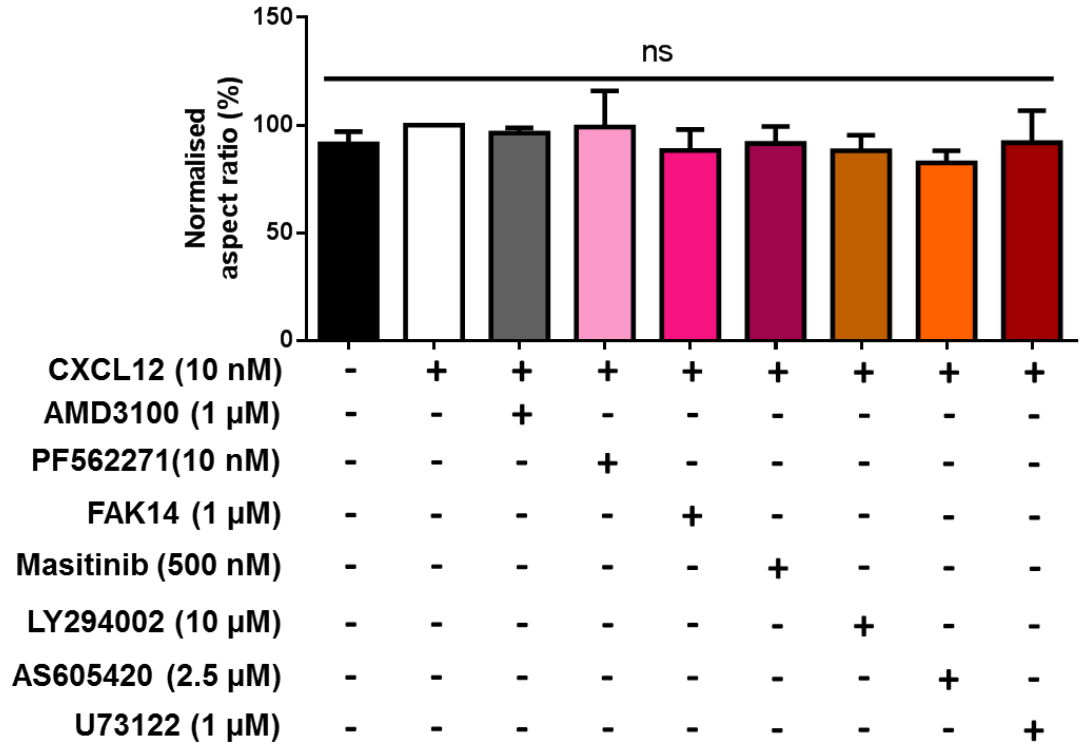

Figure 4.27. Inhibition of FAK, PI3K, PLC and CXCR4 in the presence of CXCL12 (10 nM) does not significantly affect the aspect ratio of PC-3 cells following 24 hrs incubation. CXCR4 inhibitor: AMD3100. PLC inhibitor: U73122. FAK inhibitors: FAK14, Masitinib and PF562271. PI3K inhibitor: LY294002. PI3Kγ inhibitor: AS605240. All data represented was normalised to cells treated with the CXCL12 (10 nM) alone. Results represent ± SEM of at least two independent experiments. (Kruskal-Wallis test, Dunn's multiple comparisons, ns = p≥0.05 of no significance).

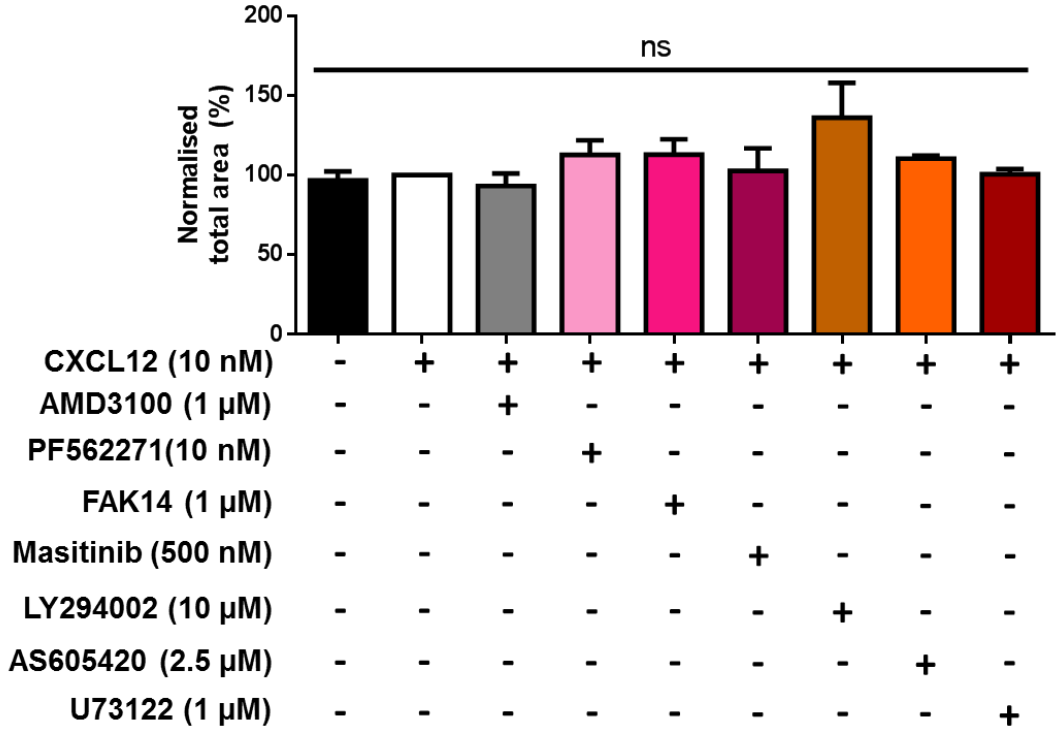

Figure 4.28. Inhibition of FAK, PI3K, PLC and CXCR4 in the presence of CXCL12 (10 nM) does not significantly affect the total area of PC-3 cells following 24 hrs incubation. CXCR4 inhibitor: AMD3100. PLC inhibitor: U73122. FAK inhibitors: FAK14, Masitinib and PF562271. PI3K inhibitor: LY294002. PI3Kγ inhibitor: AS605240. All data represented was normalised to cells treated with CXCL12 (10 nM) alone. Results represent ± SEM of at least two independent experiments. (Kruskal-Wallis test, Dunn's multiple comparisons, ns = p≥0.05 of no significance).

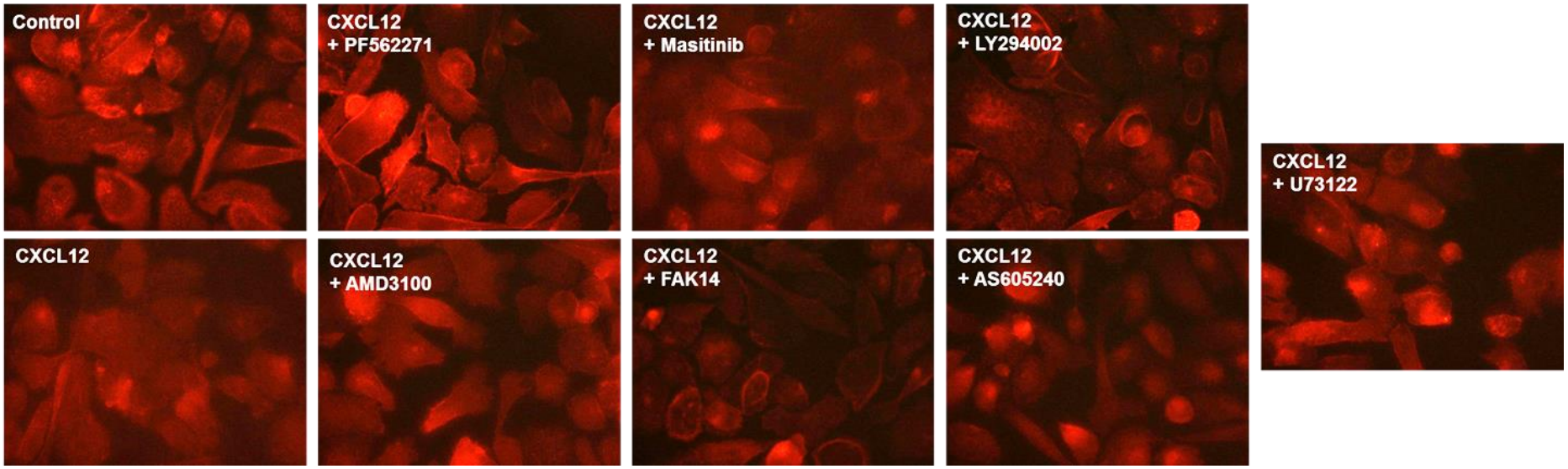

Figure 4.29. Phalloidin actin staining of PC-3 cells in the presence of CXCL12 (10 nM) with FAK, PI3K, PLC and CXCR4 inhibitors after 24 hrs. CXCR4 inhibitor: AMD3100. PLC inhibitor: U73122. FAK inhibitors: FAK14, Masitinib and PF562271. PI3K inhibitor: LY294002. PI3Kγ inhibitor: AS605240. PC-3 cells were fixed and stained with Phalloidin CruzFluor TM^{594} conjugate (red) for imaging the F-actin cytoskeleton. Images are a representation of the cell population and were taken at 63x objective with a Leica DMI6000 inverted microscope and using Leica imaging suite.

Amongst the compounds tested none showed a significant inhibitory effect on the actin cytoskeleton in either the presence of CXCL12 (10 nM) or in the presence and absence of CCL3 (10 nM) in PC-3 or CHO-CCR5 cells respectively when measuring for fluorescence (CTCF) and cellular elongation (aspect ratio) (figures 4.21, 4.22, 4.26 and 4.27). None of the compounds had any effect on PC-3 or CHO-CCR5 cell size when measuring the total area (no. pixels) (figures: 4.23 and 4.28).

Despite the absence of statistical significance some trends across the datasets were observed. In CHO-CCR5 cells incubating the compounds with CCL3 showed lower levels of CTCF compared to CCL3 alone except for PF562271, this was particularly evident for U73122 (1 μM) (figure 4.21). The effect of the compounds on the fluorescence levels of CCL3 could be clearly observed from the images (figures 4.24) although not with U73122 (figure 4.25). U73122 also showed a similar reduction in the aspect ratio compared to CCL3 alone (figure 4.22) which was evident from the images (figure 4.25).

In PC-3 cells treatment with both LY294002 (10 μM) and CXCL12 (10 nM) tended to have a larger area size when compared to treatment with either CXCL12 (10 nM) alone or the control (figure 4.28). However no clear evidence of this could be observed from the images (figure 4.29). A modest increase in cell size was also measured in PC-3 cells following treatment with either PF562271 (10 nM) and FAK14 (1 μM) together with CXCL12 (10 nM) (figure 4.28).

In summary from both the images and the data analysis of CHO-CCR5 phalloidin staining there was no evidence of FAK, PI3K or PLC playing a decisive role in CCL3 induced cellular elongation. Also none of the compounds showed any significant non-specific effects on F-actin formation, cellular elongation or cell size in either PC-3 or CHO-CCR5 cells following 24 hrs incubation.

4.16 U73122 is cytotoxic in CHO-CCR5 cells after 25 hrs incubation

Although none of the inhibitors demonstrated any significant effect on either F-actin formation, cellular elongation or cell size in the CHO-CCR5 cells after 24 hrs incubation. Their effects on the viability of CHO-CCR5 cells after 24 hrs was still performed in order to provide additional information on these compounds which could be a useful reference for other researchers looking to use these same compounds in other cell based assays.

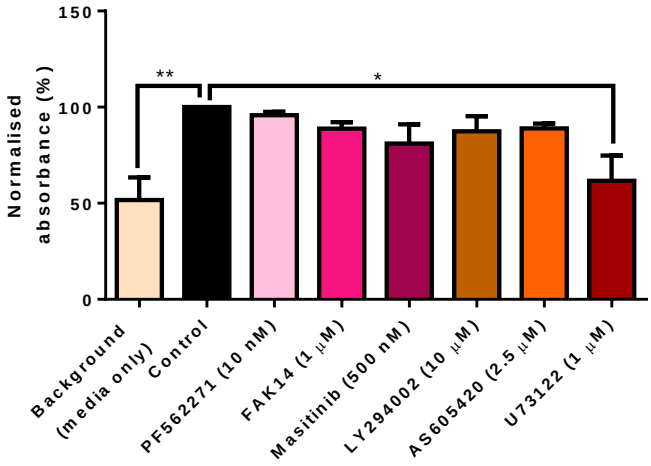

Figure 4.30. U73122 (1 µM) is cytotoxic in CHO-CCR5 cells after 24 hrs incubation and 1 hrs MTS metabolisation. PLC inhibitor: U73122. FAK inhibitors: FAK14, Masitinib and PF562271. PI3K inhibitor: LY294002. PI3Kγ inhibitor: AS605240. Results were normalised to the control and represent ± SEM of at least three independent experiments (data from Wing Yee Lai). (One-way ANOVA, Dunnett's multiple comparisons test, ** = p≤0.01 and * = p≤0.05).

When assessing for cell viability in the CHO-CCR5 cells following 25 hrs incubation, only U73122 (1 µM) was identified as being significantly cytotoxic (figure 4.30). All the other compounds tested displayed no effect on cell viability at their respective concentration. Therefore the results indicate that U73122 above 1 µM is unsuitable to be used on CHO-CCR5 cells for 24 hrs.

4.17 Discussion

Chemokine receptors are overexpressed in many different cancer types with their downstream signalling pathway inducing a variety of cellular responses which can contribute to metastasis [115, 130]. Targeted treatments against either the chemokine ligand or receptor have been unsuccessful at the clinical stage thus far possibly owing in a large part to chemokine ligand promiscuity and receptor redundancy. Hence there is still an urgent need to develop alternative approaches to therapeutically target the chemokine signalling network with the downstream signalling pathway being one alternative. Chemokines receptors are GPCRs and typically signal via the $G\alpha_i$ class [88]. Both the $G\alpha_i$ and $G\beta\gamma$ subunits activate various downstream effectors such as FAK, PI3K and PLC, all of which have been implicated in cancer dissemination [88, 225, 350, 352]. Consequently the aim of this chapter was to validate the downstream effectors of the $G\alpha_i/\beta\gamma$ as potential therapeutic targets to block cancer metastasis.

To build a detailed picture of the chemokine downstream signalling pathway in cancer PLC was blocked with U73122 in three separate cancer lines: MCF-7 (breast), PC-3 (prostate) and THP-1 (acute myeloid leukaemia), all of which had been stimulated with different chemokines. From these experiments PLC was identified as being crucial for chemokine intracellular calcium signalling in THP-1 cells (figure 4.2) whilst in MCF-7 cells this was only the case for CCL3 and perhaps CCL4 (figure 4.1b, c and d). In PC-3 cells PLC did not appear to be important (figure 4.1a). PLCs role in downstream signalling appears to be cell type and chemokine specific and therefore suggests that chemokines can display both a tissue and ligand specific bias for intracellular calcium signalling.

The PLC-PIP_2 signalling axis is considered the main downstream pathway for intracellular calcium mobilisation following chemokine receptor activation with limited evidence of any alternative pathways in the wider literature. However one possibility for intracellular calcium signalling to be independent of PLC activity is through the activation of the ryanodine receptors present on the ER. Studies in THP-1 and rat neonatal cardiomyocytes cells have shown that CCL3 and CXCL12 increases in intracellular calcium is reliant on the IP_3 channels and not the ryanodine receptors respectively [516, 517]. However in rat

microglia cells treated with lipopolysaccharides, CCL3 intracellular calcium signalling was shown to occur via the ryanodine receptors although for CCL5 it was still through the IP_3 channels [518]. To the contrary, in natural killer cells it was CCL5 but not CXCL12 which was shown to be partly dependent on the ryanodine receptors for intracellular calcium signalling [519]. Furthermore, blocking ryanodine receptors with ryanodine (10 μM) in both CHO-CCR5 and THP-1 cells actually enhanced CCL3 intracellular calcium signalling suggesting that the ryanodine receptors may regulate some release of calcium from the ER intracellular stores [517]. This therefore presents further evidence of chemokine and tissue specific biases which can influence the downstream signalling pathway.

To establish whether chemokine specific biases in PLC mediated intracellular calcium signalling in MCF-7 cells was due to differing molecular mechanisms upstream. The role of both Gβγ and $G\alpha_i$/βγ in the downstream signalling pathway of CCR1/5 and CXCR4 receptor activation was probed with gallein and PTX respectively. Treatment with gallein had no effect on CCL3 or CXCL12 intracellular calcium signalling (figure 4.6) whilst PTX abolished CCL4, CCL5 and CXCL12 intracellular calcium signalling (figure 4.7). Therefore in MCF-7 cells CXCR4 and CCR5 signalling occurs via $G\alpha_i$ though neither receptor appears to be dependent on Gβγ for the mobilisation of calcium from the intracellular stores.

It is widely understood that chemokines signal via the $G\alpha_i$ [36] with Gβγ activating PLC to mediate increases in intracellular calcium [88]. However the results using gallein contradict this, although two other studies have also reported similar results with gallein with the intracellular calcium flux assay [347, 520]. It is unclear for the reason behind this but one possibility is that gallein is ineffective in disrupting Gβγ-PLCβ interactions. Nonetheless a very similarly structured compound to gallein, M119, has been proven to disrupt Gβγ-PLCβ-3 interactions in both a cell-free [521] and cell based assay [522]. Alternatively the authors of Kerr. J *et al*. (2013) proposed that gallein binding could perhaps induce a conformational change in Gβγ which disrupts canonical binding and causes non-classical interactions as observed with other Gβγ inhibitors [347]. However one review reported that neither gallein

nor M119 binding induced a conformational change in Gβγ when analysed with nuclear magnetic resonance [487]. It is therefore possible that there are alternative effectors acting independently from Gβγ to induce increases in intracellular calcium and which likely involves the $G\alpha_i$ signalling pathway.

Based on these observations with gallein the importance of $G\alpha_i$ for intracellular calcium signalling was investigated by targeting Src/Syk, as well as three downstream effectors of Src: FAK, PI3K and c-Raf. From these intracellular calcium measurement experiments FAK was identified as being essential for CXCL12 intracellular calcium signalling in THP-1 cells (figure 4.9). Whilst c-Raf and Src/Syk were important for CXCL12 intracellular calcium signalling in MCF-7 cells (figure 4.13).

In THP-1 cells only FAK14 blocked CXCL12 increases in intracellular calcium whilst FAK inhibitors PF562271 and Masitinib had no effect (figure 4.9). FAK14 blocks FAK activation and thereby inhibits both its adaptor and kinase function whereas PF562271 and Masitinib inhibit the kinase activity only. This would therefore imply that in THP-1 cells CXCL12 intracellular calcium signalling relies on FAKs role as an adaptor rather than its kinase activity. In the wider literature FAK has been shown to mediate increases in intracellular calcium in platelets [523] and in ovarian cancer cells [524], with the authors of the latter proposing that FAK regulated PLC-γ phosphorylation to mediate intracellular calcium signalling [524]. As the data showed that both FAK and PLC were crucial for CXCL12 intracellular calcium signalling in THP-1 cells, whether both PLC-γ and FAK belonged to the same pathway was explored as both are known to interact with one another [525]. To achieve this FAK14 and U73122 were used at reduced concentrations to see if greater inhibition on CXCL12 intracellular calcium signalling would be observed. Using this approach no significant synergistic inhibition on CXCL12 intracellular calcium signalling with FAK14 and U73122 together was measured. However as no inhibition with either compound separately was observed this suggests that the concentrations were too low for a true additive effect to be detected (figure 4.10). Therefore to properly map this pathway co-immunoprecipitation could be used to identify FAK-PLC binding. Also, confirming the phosphorylation

status of FAK Tyr397 in the presence and absence of both CXCL12 and U73122 would identify if FAK was acting downstream of PLC.

CXCL12 intracellular calcium signalling in MCF-7 cells was shown to involve both Src/Syk and c-Raf (figure 4.13). As Src/Syk regulate c-Raf [63, 64, 526], it is therefore very likely that both Src/Syk and c-Raf are acting on the same pathway. Based on the findings in this chapter, the data would indicate that in MCF-7 cells CXCL12 intracellular calcium signalling is reliant on the $G\alpha_i$-Src/Syk-c-Raf signalling axis but not on Gβγ-PLC. The molecular mechanisms behind the $G\alpha_i$-Src/Syk-c-Raf mediated increases in intracellular calcium is not obvious, but if the mobilisation of calcium from the ER is independent of IP_3 production then alternative sources for this mobilisation of calcium could be the ryanodine receptors or calcium channels on the cell membrane. Ryanodine receptors are regulated by several effectors: Homer, AKAP, PKA, PP2A and calmodulin [527], however none are known to be activated by MAPK signalling. There are however a few examples of MAPK regulating transmembrane calcium channel activity [528, 529]. Therefore as the cells were incubated in a $CaCl_2$ containing buffer prior to chemokine stimulation, these calcium channels could be an additional mechanism for increases in intracellular calcium following CXCL12 stimulation.

None of the cell lines in this chapter showed any dependence on PI3K activity for intracellular calcium signalling in response to either CCL3 or CXCL12 (figure 4.8). Which is similar to the results from two other published studies which also used LY294002 [89, 347]. Nonetheless another study has shown that PI3K blockade using either wortmannin or LY294002 did abolish CX3CL1 intracellular calcium signalling in CHO cells [530] which suggests that PI3Ks role could be chemokine specific.

To investigate whether any of the observations made from the intracellular calcium measurement experiments had any functional relevance in the migration of cancer cells. THP-1 cells were treated with the three FAK inhibitors whilst Jurkat cells were treated with FAK, PIK3, PLC, Src/Syk and c-Raf inhibitors. Overall only PLC appeared to be important for CXCL12 chemotaxis in Jurkat cells, however, a follow up experiment using the MTS

reagent confirmed that this was due to cytotoxicity (figure 4.17b). U73122 (1 µM) also displayed cytotoxicity in THP-1 cells (figure 4.17a) and potential cytotoxicity in MCF-7 cells (figure 4.5a) and as such is not a reliable research tool for probing PLCs role within cell based assays. In Jurkat cells previous studies have shown that CXCL12 chemotaxis is dependent on PLC, Src, Raf and PI3K [340, 531], which besides PLC is a vast contrast to the results presented in this chapter (figure 4.15).

To block Src/Syk activity MNS (10 µM) was used, which is lower than the reported IC_{50} for Src inhibition at around 29.3 µM [403]. It is therefore unlikely that Src was fully blocked during Jurkat chemotaxis and hence why these results may have differed from the literature [340]. In Mills. SC *et al.* (2016) Raf inhibition was achieved using the pan-Raf inhibitor L779450, whilst for this thesis a c-Raf specific inhibitor (ZM336372) was used instead. Therefore the differences between these results would imply that for CXCL12 chemotaxis, Jurkat cells rely on the B-Raf and/or A-Raf isoforms rather than c-Raf for cellular migration.

In Mills. SC *et al.* (2016) the LY294002 was able to successfully block CXCL12 chemotaxis in Jurkat cells, however despite this, these results were unable to be reproduced in this chapter using a similar experimental approach. The only possible explanation for this could be the difference in the chemotactic response between the two batches of Jurkat cells. As for Mills. SC *et al.* (2016) the Jurkat chemotactic response towards CXCL12 was far superior with a mean $\approx 400x10^4$ per mL^{-1} compared to $\approx 40x10^4$ per mL^{-1} for the data presented in this chapter. Hence this migratory response was perhaps too low to detect the moderate inhibition on CXCL12 chemotaxis by LY294002 which was observed in Mills. SC *et al.* (2016) [340].

Aside from chemotaxis the effect of PI3K inhibition on MCF-7 scratch closure in response to CCL3 was also assessed. In this experiment PI3K was shown not to be important for CCL3 scratch closure using either LY294002 or AS605240 (figure 4.18). These results with the LY294002 agree with the findings from Mill. SC *et al*. (2016) on CXCL12 scratch closure in MCF-7 cells [340]. In addition there was no significant difference in scratch closure

measured between CCL3 treatment and the basal. This reemphasises the issue surrounding reproducibility using the wound healing assay, as previously discussed in chapter 3.

In the previous chapter the CHO-CCR5 cells were identified as a model for assessing CCL3 induced cellular elongation. As such, this model was used to assess the importance of FAK, PLC and PI3K on the remodelling of the actin cytoskeleton though neither FAK, PLC nor PI3K demonstrated a clear role in cellular elongation (figure 4.22 and 4.24). However the U73122 did show some inhibition on CTCF and the aspect ratio but this was once again likely due to cytotoxicity (figure 4.30). Aside from U73122 all the other compounds besides PF562271 showed a tendency to reduce the fluorescence levels of CCL3 stimulated CHO-CCR5 cells (figure 4.21). However as discussed in the previous results chapter, using the CTCF to quantify phalloidin fluorescence is not a sensitive enough approach to identify any specific changes to F-actin formation.

In addition to the CHO-CCR5 cells, a similar investigation was performed with the same compounds on the PC-3 cells to assess their effect on actin cytoskeleton in the presence of CXCL12. However contrary to the results from chapter 3 (figure 3.26), treatment with CXCL12 displayed lower levels of fluorescence compared to the basal and as a result the PC-3 cells were not a suitable model for assessing any CXCL12 specific effects on the actin cytoskeleton.

4.18 Conclusion

The main findings from this chapter were as follows:

- U73122 is a highly cytotoxic compound and not suitable for assessing PLCs role in cell based assays long term.

- FAK mediates CXCL12 intracellular calcium signalling but not chemotaxis in THP-1 cells.

- Src/Syk and c-Raf are involved in CXCL12 intracellular calcium signalling in MCF-7 cells.

- PLCs importance for intracellular calcium signalling is dependent on both the chemokine and cell type.

Chapter 5.0 The role of the cellular cytoskeleton in chemokine downstream signalling within different cancer types

5.1 Introduction

Chemokines are mediators of the immune system response by promoting leukocyte migration towards either sites of infection and inflammation or to the lymph nodes and peripheral sites in the body for immunosurveillance. Consequently chemokine signalling can induce the remodelling of the cellular cytoskeleton in leukocytes to promote chemotaxis [532].

The cellular cytoskeleton is composed of three distinct protein filaments: microtubules, intermediate filaments and F-actin. Microtubules provide structure, organelle arrangement and are important for chromatid segregation in cell division [533, 534]. F-actin is the most dynamic of the three cytoskeletal proteins and plays a crucial role in cellular migration, though the microtubules can also be involved [535]. The intermediate filaments provide additional support to both the microtubules and F-actin [534].

When cells migrate, F-actin polymerisation occurs at the leading edge of the cell giving rise to F-actin rich structures: lamellipodia and filipodia. F-actin polymerisation is promoted by Arp2/3 which initiates actin nucleation at Arp2/3 bound sites on the F-actin. Arp2/3 is activated by members of the WASP/WAVE family which in turn are regulated by members of the Rho GTPase family Rac and Cdc42, which initiate lamellipodia and filopodia formation respectively [153, 155].

A key hallmark of cancer cells is their enhanced ability to migrate allowing them to invade the surrounding tissue. As such many of the molecular mechanisms driving “normal” cellular migration are also associated with the invasiveness of cancer cells. Many cancers display elevated levels of Rho GTPases [536], WAVE [537] and Arp2/3 [538], with WAVE2 and Arp2 co-expressed in colorectal [539], breast [540] and lung cancer [541]. Whilst the knocking down

of WAVE [537] and the pharmacological blockade of Rac [542] has been shown to reduce cancer cell invasion. Hence the Rac-WAVE-Arp2/3 signalling axis is an attractive target for cancer therapy.

In chemokine signalling Rac has been shown to be important for the chemotaxis of CXCL12 but not CCL3 in cancer cells [346]. However aside from Rac and RhoA-ROCK signalling [322, 346, 543-545] the involvement and importance of other cytoskeletal regulators in chemokine induced chemotaxis of cancer cells is not properly understood.

5.2 Chapter Aim

To improve understanding of the molecular mechanisms regulating the cellular cytoskeleton in chemokine downstream signalling in both carcinoma and leukemic cell types.

5.3 DOCK1/2/5 is important for the intracellular calcium signalling of CCL3 and CXCL12 in MCF-7 and THP-1 cells, whilst Arp2/3 and Taxol are cell type or chemokine specific

Calcium is an important secondary messenger for both chemokine downstream signalling and cellular migration. Calcium ions can directly activate a variety of proteins such as PKC, calcineurin and calmodulin-dependent protein kinase II to regulate PI3K, FAK and MLCK activity for focal adhesion turnover and cytoskeletal remodelling [172]. As calcium ions can influence changes to the actin cytoskeleton, whether any of the regulators of the actin cytoskeleton could also influence intracellular calcium signalling as part of a possible feedback loop to regulate cell migration is not known. Therefore to explore this possibility of a feedback loop both Arp2/3 and members of the DOCK A subfamily DOCK1/2/5, a GEF for Rac, were blocked using two small molecule inhibitors CK666 and CPYPP respectively. CK666 blocks Arp2/3 nucleation activity by stabilising its inactive splayed structure [546]. CPYPP binds to the DHR-2 domain of DOCK1/2/5, to block guanine nucleotide exchange activity and subsequently Rac activation [408]. To see if

the cytoskeleton also influences chemokine signalling the role of the microtubules was investigated using the chemotherapeutic agent Taxol which stabilises the microtubules against depolymerisation [547].

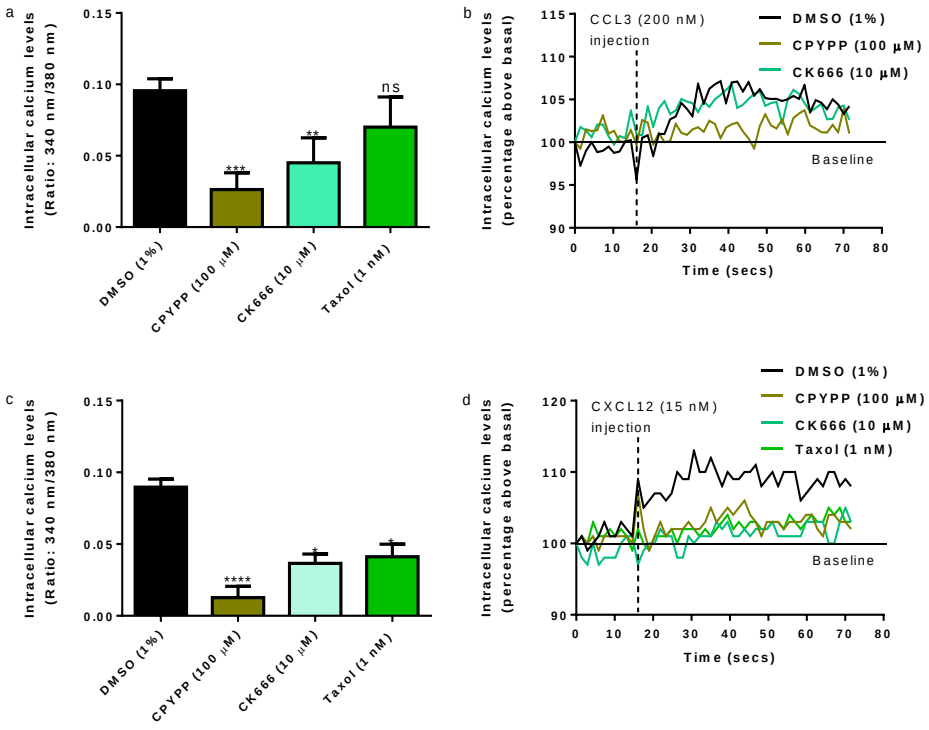

Figure 5.1. CPYPP and CK666 inhibition of DOCK1/2/5 and Arp2/3 respectively and Taxol microtubule stabilisation on CCL3 (200 nM) and CXCL12 (15 nM) intracellular calcium signalling in MCF-7 cells. (a) CPYPP (100 μM) and CK666 (10 μM) inhibits CCL3 intracellular calcium signalling in MCF-7 cells (n=4). (b) Representation of an intracellular calcium measurement trace following CCL3 stimulation in MCF-7 cells pretreated with CPYPP and Taxol (30 mins) after 70 secs. (c) CPYPP, CK666 and Taxol (1 nM) inhibit CXCL12 intracellular calcium signalling in MCF-7 cells (n≥2). (d) Representation of an intracellular calcium measurement trace following CXCL12 stimulation in MCF-7 cells pretreated with CPYPP, CK666 and Taxol (30 mins) after 70 secs. Results represents the mean ± S.E.M. in at least two independent experiments. (One-way ANOVA, Dunnett's multiple comparisons test, **** = p≤0.0001, *** = p≤0.001, ** = p≤0.01, * = p≤0.05, and ns = p≥0.05 of no significance).

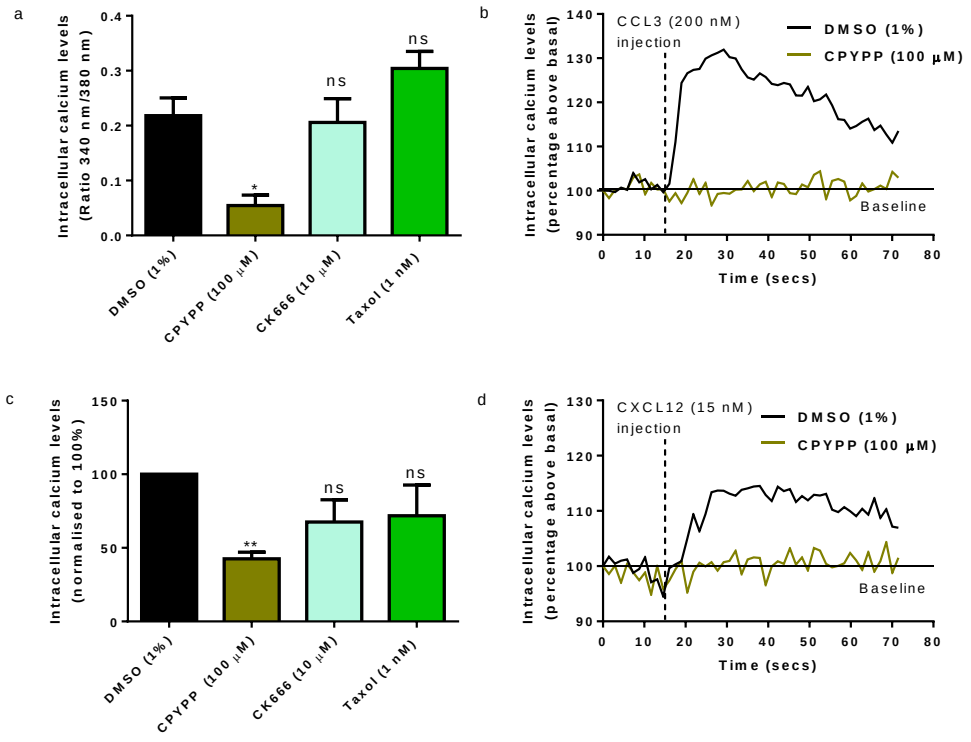

Figure 5.2. CPYPP and CK666 inhibition of DOCK1/2/5 and Arp2/3 respectively and Taxol microtubule stabilisation on CCL3 (200 nM) and CXCL12 (15 nM) intracellular calcium signalling in THP-1 cells. (a) CPYPP abolishes CCL3 intracellular calcium signalling in THP-1 cells (n=4). (One-way ANOVA, Dunnett's multiple comparisons test). (b) Representation of an intracellular calcium measurement trace following CCL3 stimulation in THP-1 cells pretreated with CPYPP (30 mins) after 70 secs. (c) CPYPP abolishes CXCL12 intracellular calcium signalling in THP-1 cells (n=7). (Kruskal-Wallis test, Dunn's multiple comparisons). Results for CXCL12 were normalised to the control (DMSO 1%). (d) Representation of an intracellular calcium measurement trace following CXCL12 stimulation in THP-1 cells pretreated with CPYPP (30 mins) after 70 secs. Results represent the mean ± S.E.M. in at least four independent experiments. (** = p≤0.01, * = p≤0.05, and ns = p≥0.05 of no significance).

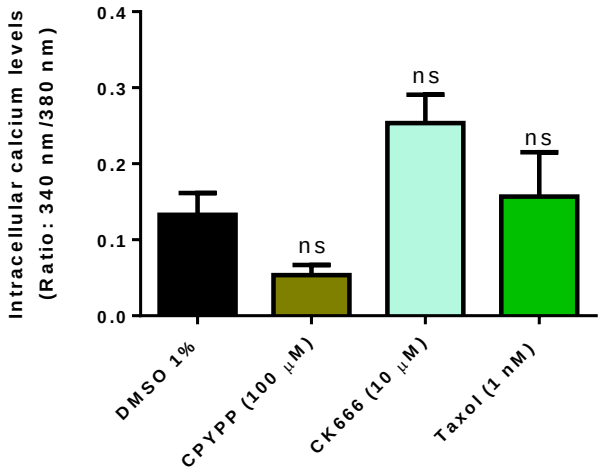

Figure 5.3. CPYPP and CK666 inhibition of DOCK1/2/5 and Arp2/3 respectively and Taxol microtubule stabilisation on CCL3 (200 nM) intracellular calcium signalling in CHO-CCR5 cells. Results represents the mean ± S.E.M. in three independent experiments. (One-way ANOVA, Dunnett's multiple comparisons test, ns = p≥0.05 of no significance).

When investigating the role of DOCK1/2/5, Arp2/3 and microtubules in CCL3 (200 nM) and CXCL12 (15 nM) intracellular calcium signalling, CPYPP (100 μM) was shown to abolish increases in intracellular calcium in response to both CCL3 and CXCL12 in MCF-7 and THP-1 cells (figure 5.1 and 5.2). In CHO-CCR5 cells CPYPP also showed a similar trend following CCL3 stimulation (figure 5.3).

CK666 (10 μM) showed inhibition on both CCL3 and CXCL12 intracellular calcium signalling in MCF-7 cells (figure 5.1). Whereas in CHO-CCR5 cells, CK666 tended to show higher increases in intracellular calcium following CCL3 stimulation (figure 5.3). Taxol displayed significant inhibition on CXCL12 intracellular calcium signalling in MCF-7 cells (figure 5.1c and d). In THP-1 cells Taxol displayed a trend of higher levels of CCL3 intracellular calcium signalling (figure 5.2c).

The data suggests that DOCK1/2/5 is essential in the downstream signalling of both CCL3 and CXCL12 in MCF-7 and THP-1 cells. For Arp2/3 its role in

chemokine intracellular calcium signalling was shown to be specific for MCF-7 cells only. The role of the microtubules appears specific to CXCL12 intracellular calcium signalling for MCF-7 cells suggesting that its role is both chemokine and cell specific.

5.4 Nocodazole does not inhibit CCL3 or CXCL12 intracellular calcium signalling in MCF-7, THP-1 or CHO-CCR5 cells.

Incubating MCF-7 cells with Taxol inhibited CXCL12 intracellular calcium signalling (figure 5.1a). To further probe the role of the microtubules in chemokine downstream signalling the microtubule disrupter nocodazole was used to see if similar effects to Taxol (microtubule stabiliser) would be observed or whether differences would arise.

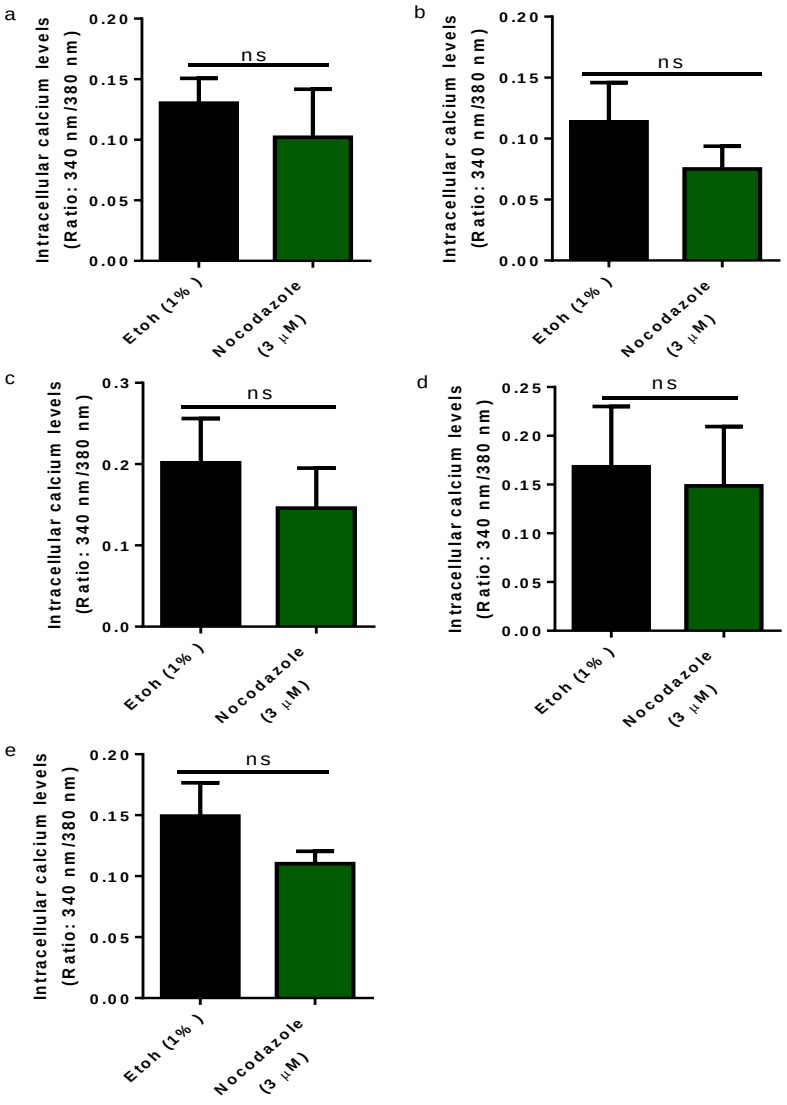

Figure 5.4. Nocodazoles (3 μM) disruption of microtubule polymerisation on CCL3 (200 nM) and CXCL12 (15 nM) intracellular calcium signalling. MCF-7 cells were pretreated with nocodazole (30 mins) prior to CCL3 (a) or CXCL12 (b) stimulation. THP-1 cells were pretreated with nocodazole (30 mins) prior to CCL3 (c) or CXCL12 (d) stimulation. (e) CHO-CCR5 cells were pretreated with nocodazole (30 mins) prior to CCL3 stimulation. Results represents the mean ± S.E.M. in at least three independent experiments. (Student's t-test, ns = p≥0.05 of no significance).

Using nocodazole (3 µM) to perturb microtubule polymerisation prior to CCL3 (200 nM) and CXCL12 (15 nM) stimulation, showed no significant effect on increases in intracellular calcium in MCF-7, THP-1 and CHO-CCR5 cells (figure 5.4). These results demonstrate that microtubule polymerisation is not important for CCL3 or CXCL12 intracellular calcium signalling in MCF-7, THP-1 and CHO-CCR5 cells.

5.5 CPYPP, Taxol and CK666 do not show any compound cytotoxicity in Jurkat cells after 6 hrs. CPYPP (5 mM) appears to be cytotoxic in THP-1 cells

To investigate whether CPYPPs inhibitory effect on chemokine increases in intracellular calcium in MCF-7 and THP-1 cells could be a result of cellular cytotoxicity, the effects of CPYPP on the cell proliferation of both THP-1 and MCF-7 cells was investigated. The Jurkat cell line was also included to establish whether the concentrations used for CPYPP, CK666 and Taxol in the intracellular calcium flux assay would also be suitable for assessing their effect on Jurkat chemotaxis after 4 hrs of treatment.

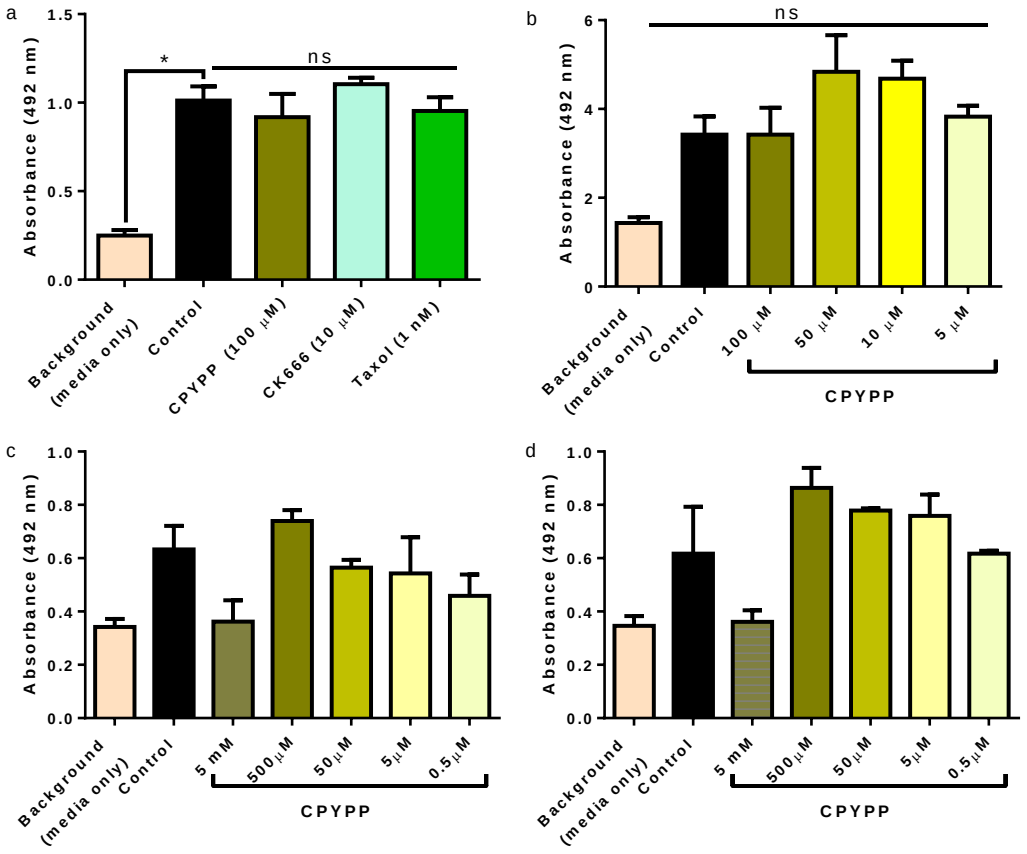

Figure 5.5. Compound cytotoxicity in THP-1 and Jurkat cells using the MTS cellular proliferation assay. (a) None of the compounds are cytotoxic in Jurkat cells after 2 hrs incubation and 4 hrs MTS metabolisation (n=3). (b) CPYPP is not cytotoxic in MCF-7 cells after 1 h incubation and MTS metabolisation (n=3). (c) CPYPP (5 mM) appears to be cytotoxic in THP-1 cells after 72 hrs incubation and 4 hrs MTS metabolisation. (Data from Wing Yee Lai, Georgia Eagleton and Veronica Youssef) (n=2). (d) CPYPP (5 mM) appears to be cytotoxic in Jurkat cells after 72 hrs incubation and 4 hrs metabolisation. (Data from Wing Yee Lai, Georgia Eagleton and Veronica Youssef) (n=2). DOCK1/2/5 inhibitor: CPYPP. Arp2/3 inhibitor: CK666. Microtubule stabiliser: Taxol. All results represent ± SEM of at least two independent experiments. (One-way ANOVA, Dunnett's multiple comparisons test, * = $p \leq 0.05$ and ns = p value≥ 0.05 of no significance).

In Jurkat cells neither CPYPP (100 µM), CK666 (10 µM) and Taxol (1 nM) were found to be cytotoxic following 6 hrs incubation (figure 5.5a). CPYPP also demonstrated no cytotoxicity in MCF-7 cells after 1 h incubation (figure 5.5b). Preliminary data from CPYPP concentration response experiments on THP-1 and Jurkat cell proliferation suggest that CPYPP is only cytotoxic at 5 mM and after 72 hrs (figures 5.5c and d).

This MTS data confirms that working concentrations of 100 µM for CPYPP, 1 nM for Taxol and 10 µM for CK666 are suitable for measuring chemotaxis in Jurkat cells. The data also confirms that the inhibitory effects of CPYPP on the intracellular calcium flux assays of MCF-7 and THP-1 cells was not due to any cytotoxicity.

5.6 CPYPP (100 µM) inhibits Thapsigargin increases in intracellular calcium in THP-1 cells

CPYPP (100 µM) was able to block CCL3 and CXCL12 intracellular calcium signalling in both MCF-7 and THP-1 cells. As well as displaying a similar effect in CHO-CCR5 cells.

To quantify changes in intracellular calcium levels Fura-2 AM fluorescence is measured both before and after chemokine receptor activation. CPYPP is a dark red coloured compound and frequently displayed lower levels of background fluorescence when added to the cells. As CPYPP is a relatively newly marketed compound no previous studies to our knowledge have reported using CPYPP in intracellular calcium flux assays before. To ensure that the inhibitory effects of CPYPP was not due to any quenching of the fluorescence, Triton x-100 was used to permeabilize the cell to release cytosolic Fura-2 AM into the $CaCl_2$ containing buffer to increase fluorescence levels independent of any cellular signalling. Furthermore to confirm that CPYPP was not depleting the intracellular calcium stores prior to receptor activation the ER Ca^{2+} ATPase inhibitor Thapsigargin was used to induce calcium release from the intracellular stores independent of any chemokine signalling.

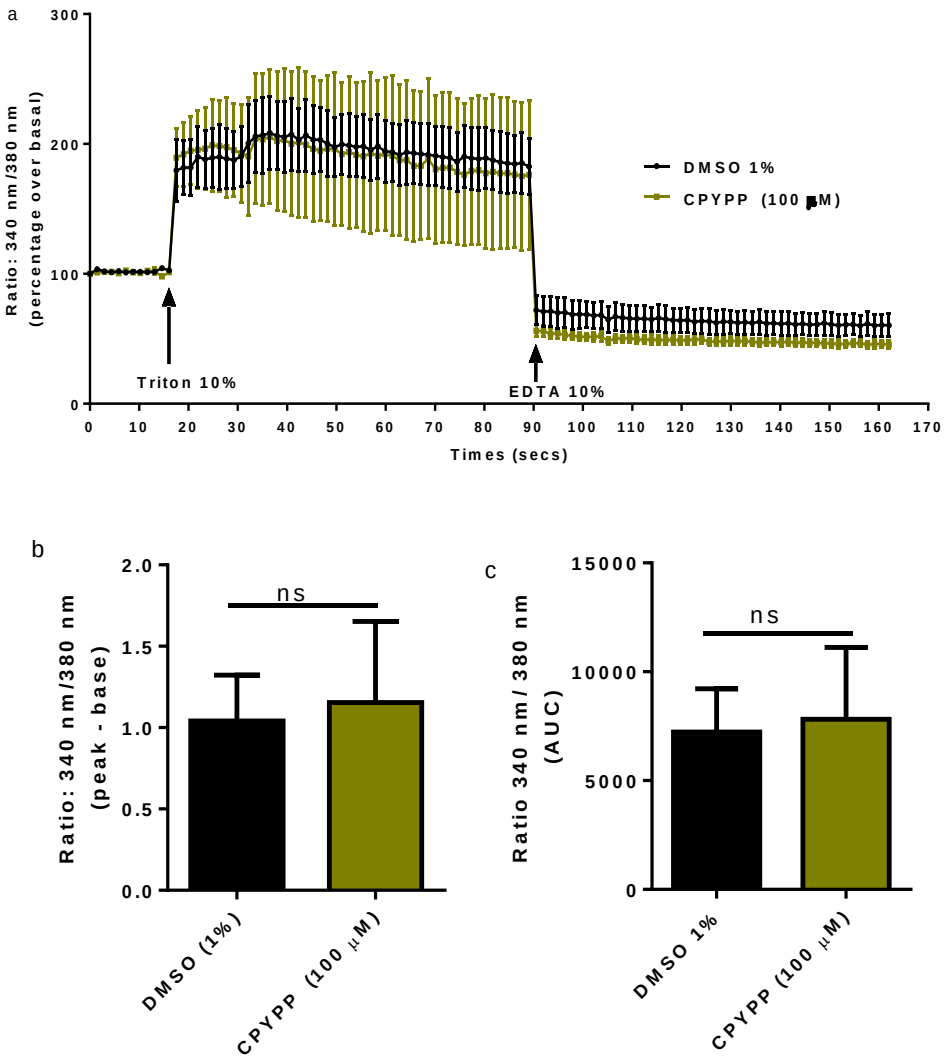

Figure 5.6. CPYPP (100 µM) does not quench Fura-2 AM fluorescence in THP-1 cells. (a) Representation of a calcium measurement trace following Triton x-100 (10%) and EDTA (10%) injection in THP-1 cells pretreated with CPYPP (30 mins) after 160 secs. Calcium levels were determined by measuring the difference between the peak and base readings (b) or the AUC (c). Results represents the mean ± S.E.M data in three independent experiments. (Student's t-test, ns = p≥0.05 of no significance).

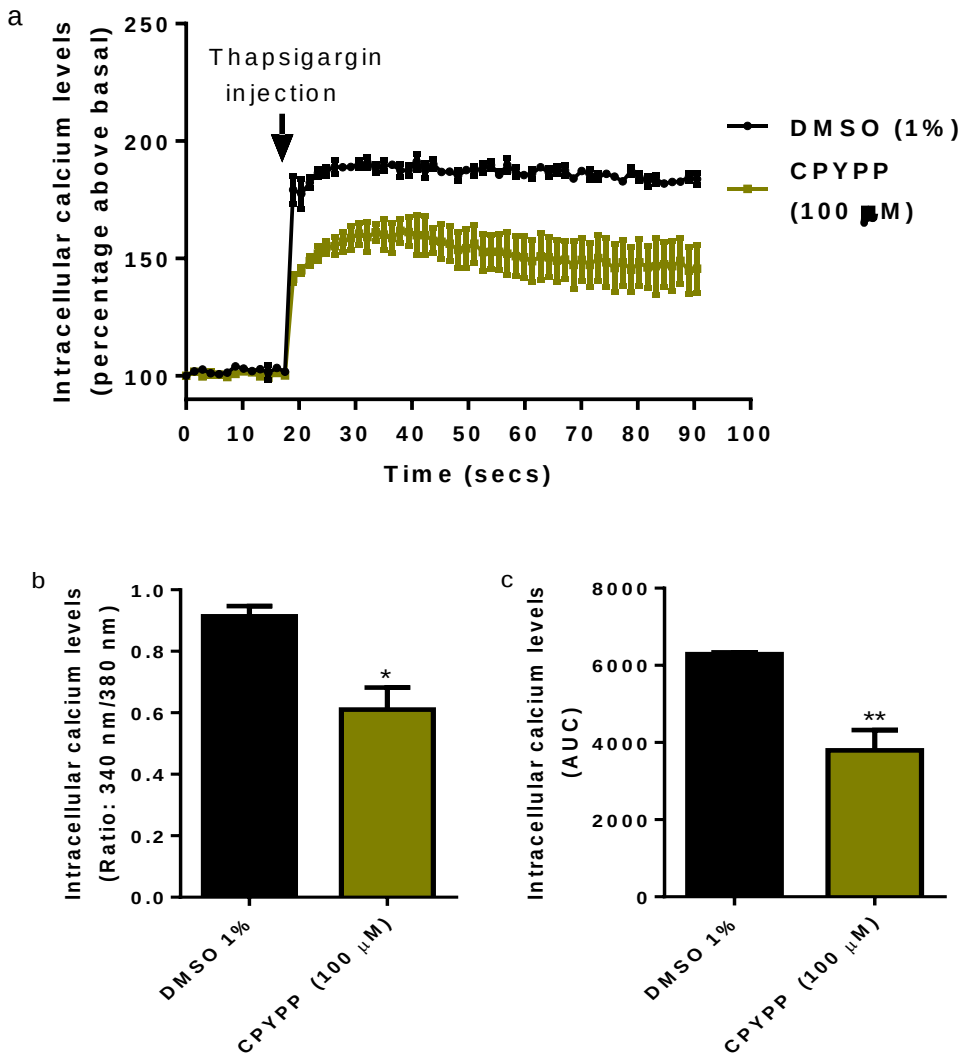

Figure 5.7. CPYPP (100 µM) depletes the intracellular calcium stores in THP-1 cells. (a) Representation of an intracellular calcium measurement trace following Thapsigargin (1%) injection in THP-1 cells pretreated with CPYPP (30 mins) after 90 secs. Increases in intracellular calcium was determined by either measuring the difference between the peak and base readings (b) or the AUC (c). ER Ca^{2+} ATPase inhibitor: Thapsigargin. Results represent the mean ± S.E.M data in three independent experiments. (Student's t-test, ** = p≤0.01, * = p≤0.05).

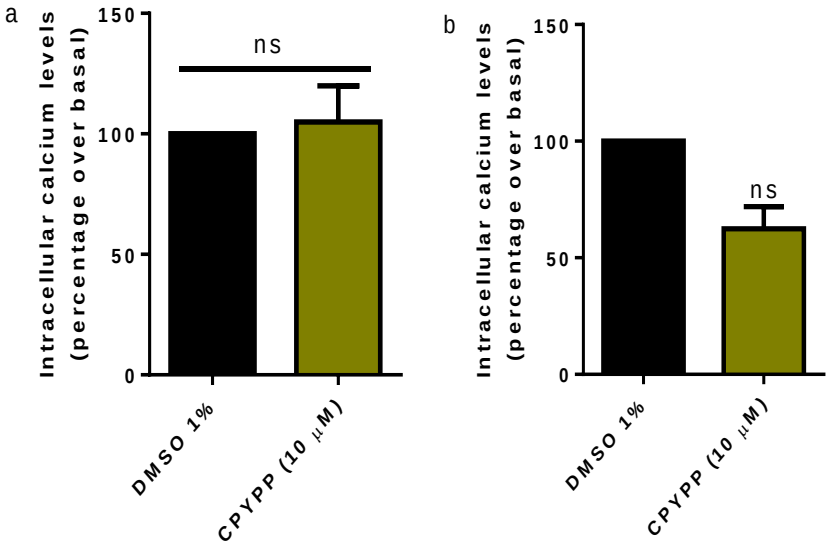

Figure 5.8. CPYPP (10 μM) does not deplete the intracellular calcium stores of THP-1 cells. (a) THP-1 cells were pretreated with CPYPP (30 mins) prior to Thapsigargin injection with the increases in intracellular calcium determined by measuring the difference between the peak and base readings (n=4). (b) THP-1 cells were pretreated with CPYPP (30 mins) prior to CCL3 (200 nM) stimulation, with the increases in intracellular calcium determined by measuring the difference between the peak and base readings (n=3). ER Ca^{2+} ATPase inhibitor: Thapsigargin. DOCK1/2/5 inhibitor: CPYPP. All results were normalised to the control (DMSO 1%) and represent the mean ± S.E.M data in at least three independent experiments. (Wilcoxon Signed Rank Test, ns = p≥0.05 of no significance).

When using Triton x-100 (10%) to increase the levels of calcium bound Fura-2 AM, pretreatment with CPYPP (100 μM) showed no effect on the fluorescence levels in THP-1 cells (figure 5.6). The calcium chelating agent EDTA (10%) confirmed the increase in calcium bound Fura-2 AM by decreasing the levels of fluorescence (figure 5.6a). This experiment demonstrates that CPYPP does not quench Fura-2 AM fluorescence.

When assessing for the depletion of calcium from the intracellular stores. CPYPP (100 μM) showed significant inhibition of Thapsigargin (1%) increases in intracellular calcium (mean difference between peak and base readings = 0.3033 ± 0.07965 ($p \leq 0.05$)) (figure 5.7). This indicates that pretreatment with CPYPP (100 μM) for 30 mins is able to deplete some calcium from the intracellular stores of THP-1 cells.

In response to these findings the concentration of CPYPP was reduced to 10 μM and its effects on increases in intracellular calcium was reassessed within THP-1 cells treated with either Thapsigargin or CCL3 (200 nM). In these two experiments CPYPP (10 μM) showed no significant inhibition on either Thapsigargin or CCL3 increases in intracellular calcium (figure 5.8a). However some blocking of CCL3 intracellular calcium signalling was still observed with CPYPP (10 μM) (figure 5.8b).

Overall these experiments would suggests that CPYPPs (100 μM) inhibition on chemokine intracellular calcium signalling can be partly attributed to some depletion of the intracellular calcium stores with the remaining inhibitory effect likely to be associated with DOCK1/2/5 blockade.

5.7 CPYPP inhibits CXCL12 chemotaxis of Jurkat cells in a concentration dependent manner

As discussed in the introduction cytoskeletal arrangement is crucial for cellular migration. Previous chemotaxis studies with CPYPP have shown that it can significantly block the migration of both neutrophils [548] and lymphocytes [408]. Whilst studies using CK666 and Arp2/3 knockouts did not show any effect on the chemotaxis of dendritic cells [549] or macrophages [550] in response to CCL21 or CXC3CL1 respectively. For Taxol its effect on chemokine induced migration is unknown. Therefore to see how the results from the intracellular calcium measurement experiments would compare in a more functional context such as cellular migration the roles of Arp2/3, DOCK1/2/5 and microtubule stabilisation were explored within a disease state using Jurkat and THP-1 cells to model CXCL12 cancer cell migration.

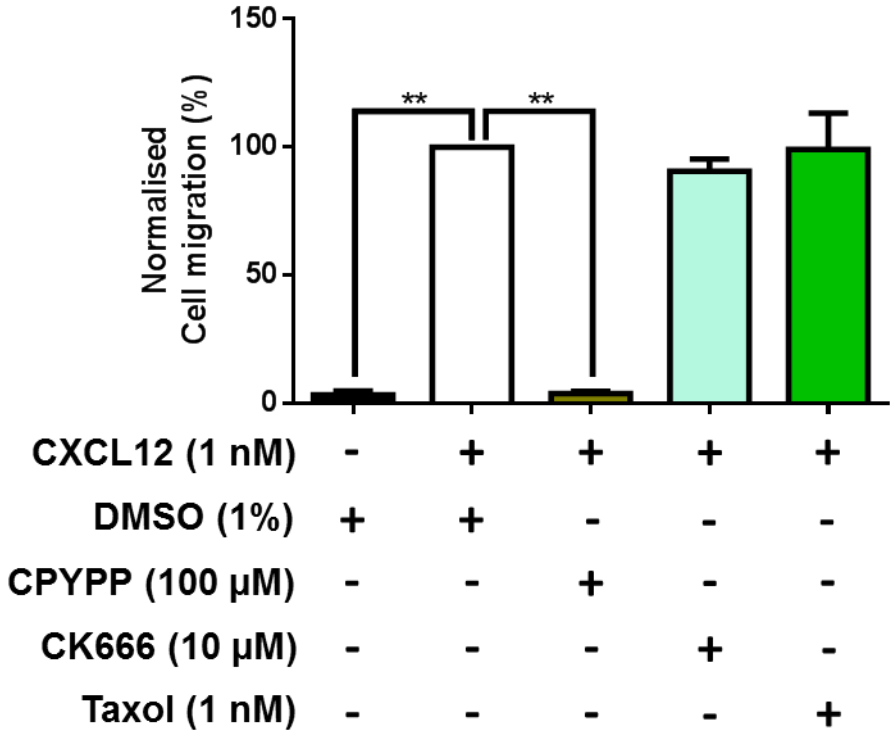

Figure 5.9. CPYPP (100 µM) inhibition of DOCK1/2/5 blocks CXCL12 (1 nM) chemotaxis of Jurkat cells after 4 hrs. DOCK1/2/5 inhibitor: CPYPP. Arp2/3 inhibitor: CK666. Microtubule stabiliser: Taxol. Results were normalised to DMSO (1 %) with CXCL12 (1 nM) and represent the mean ± S.E.M data in four independent experiments. (Kruskal-Wallis test, Dunn's multiple comparisons test, ** = p≤0.01).

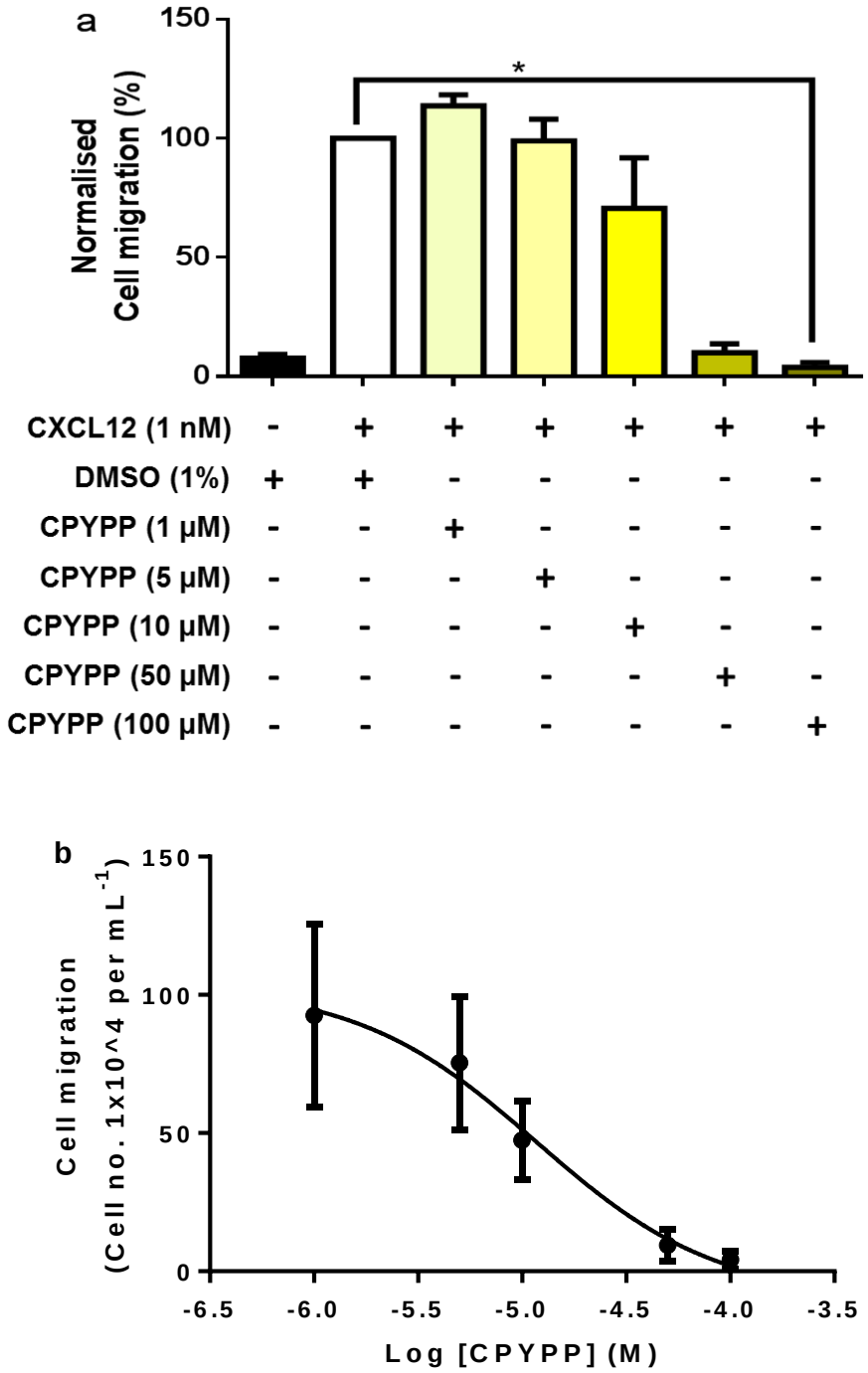

Figure 5.10. Concentration response of CPYPP against CXCL12 (1 nM) chemotaxis of Jurkat cells after 4 hrs. (a) CPYPP blocks CXCL12 chemotaxis in a concentration dependent manner. (b) Concentration curve of CPYPP against CXCL12 (1 nM) chemotaxis of Jurkat cells. DOCK1/2/5 inhibitor: CPYPP. Results represent the mean ± S.E.M data in four independent experiments. (Kruskal-Wallis test, Dunn's multiple comparisons test, * = p≤0.05).

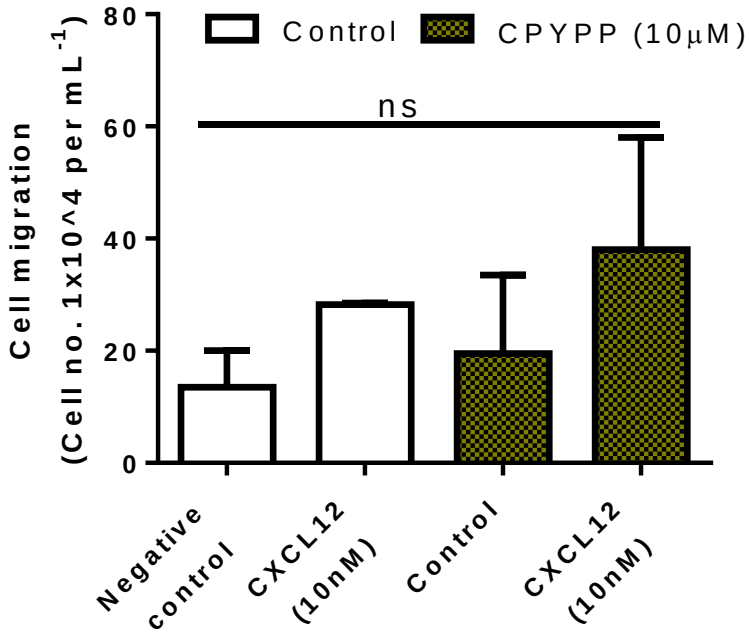

Figure 5.11. CPYPP (10 μM) inhibition of DOCK1/2/5 has no effect on CXCL12 (10 nM) chemotaxis in THP-1 cells after 4 hrs. (Data from Wing Yee Lai, Georgia Eagleton and Veronica Youssef). DOCK1/2/5 inhibitor: CPYPP. Results represent the mean ± S.E.M data in two independent experiments. (One-way ANOVA, Tukey's test, ns = p value≥0.05 of no significance).

The results from the chemotaxis assay in Jurkat cells identified that CPYPP (100 μM) was able to significantly block CXCL12 (1 nM) chemotaxis (p≤0.0001) (figure 5.9). Neither Taxol (1 nM) nor CK666 (10 μM) showed any inhibition on the chemotaxis of Jurkat cells towards CXCL12.

As the chemotaxis experiment with the Jurkat cells used CPYPP at a high concentration (100 μM), the specificity of CPYPPs inhibition on CXCL12 chemotaxis in Jurkat cells was established by titrating various concentrations of CPYPP against CXCL12 (1 nM) stimulated Jurkat cells. Data from the concentration response experiment showed a concentration dependent blocking of Jurkat cell migration by CPYPP (figure 5.10a). From this

concentration response curve the IC_{50} of CPYPP was calculated as 11.72 μM (figure 5.10b).

Furthermore the effects of CPYPP (10 μM) on CXCL12 (10 nM) chemotaxis in THP-1 cells was also assessed with the preliminary data showing treatment with CPYPP had no effect on CXCL12 chemotaxis (figure 5.11).

Overall these experiments suggest that DOCK1/2/5 is important for CXCL12 induced chemotaxis in Jurkat but not THP-1 cells.

5.8 CPYPP, U73122, EHT 1864 and Bosutinib do not block CXCL12 chemotaxis in Jurkat cells.

Published studies from the Mueller group using the small molecule inhibitors EHT 1864 and Bosutinib have shown that CXCL12 relies on Rac and Src activation respectively to promote Jurkat chemotaxis [340, 346]. In the canonical downstream signalling pathway, DOCK2 acts downstream of members of the Src family to promote Rac activity and cell migration [551]. Based on these findings the positioning of DOCK1/2/5 in the downstream signalling pathway of CXCL12 chemotaxis in Jurkat cells was explored.

To map this signalling pathway both EHT 1864 (100 nM) and Bosutinib (25 and 250 nM) were used together with CPYPP (10 μM) to establish the presence or absence of an additive effect on the inhibition of Jurkat chemotaxis in response to CXCL12. Src and PLC are considered to be involved in two independent G-protein signalling pathways: $G\alpha_i$ and Gβγ respectively. As such the Jurkat cells were also incubated with U73122 (100 nM) together with CPYPP to identify whether DOCK1/2/5 could be acting downstream of Gβγ-PLC signalling.

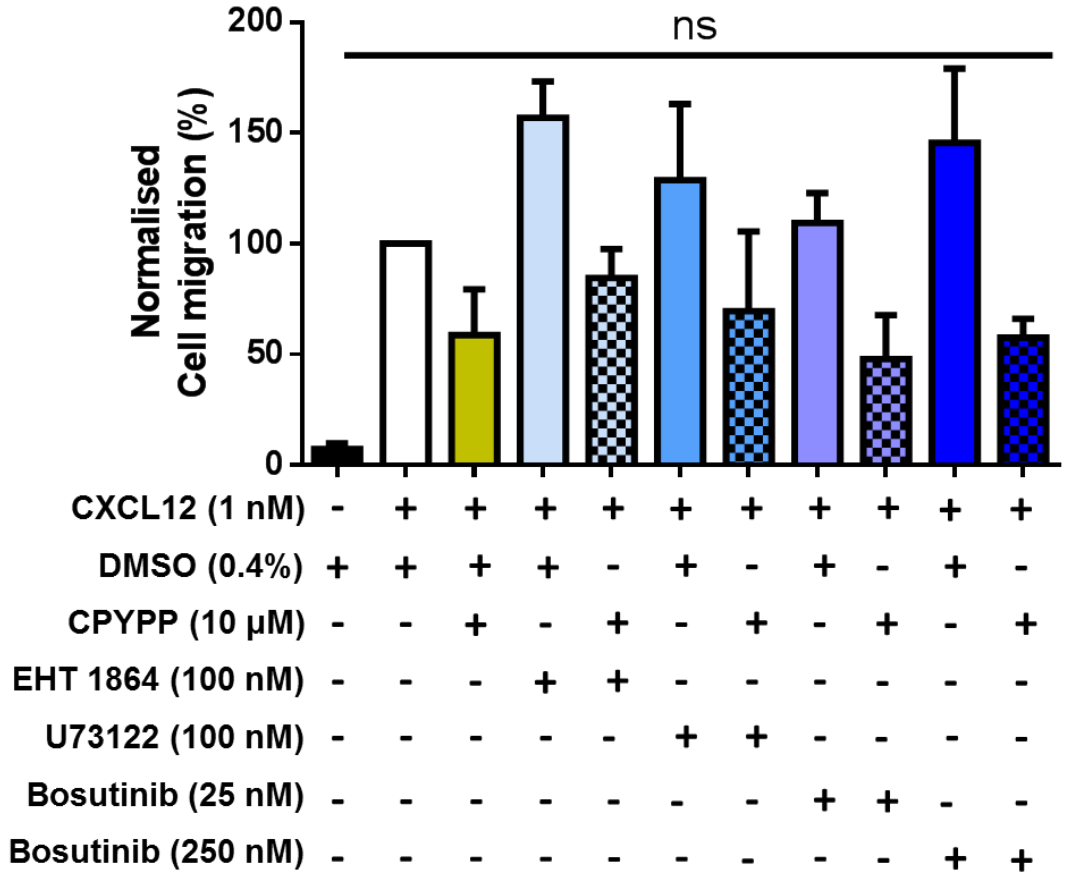

Figure 5.12. CPYPP (10 µM) showed no additive effect on CXCL12 (1 nM) chemotaxis of Jurkat cells after 4 hrs. PLC inhibitor: U73122. DOCK1/2/5 inhibitor: CPYPP. Src inhibitor: Bosutinib. Rac inhibitor: EHT 1864. Results were normalised to DMSO (0.4%) and CXCL12 (1 nM) and represent the mean ± S.E.M data in at least two independent experiments. (Kruskal-Wallis test, Dunn's multiple comparisons test, ns = p≥0.05 of no significance).

Incubating Jurkat cells with CPYPP (10 µM) alone, or together with either EHT 1864 (100 nM), U73122 (100 nM) or Bosutinib (25 nM and 250 nM) showed no significant inhibition on CXCL12 chemotaxis after 4 hrs. Nonetheless, Jurkat cells treated with CPYPP did have a tendency to display lower levels of migration towards CXCL12 (figure 5.12). Overall there was no additive effect when using EHT 1864, U73122 or Bosutinib together with CPYPP.

5.9 CPYPP and CK666 do not inhibit PC-3 cell velocity

Chemokine receptor activation can increase the migratory speed of cells [552, 553] which may contribute to their chemotactic effect. Preliminary experiments from the Mueller lab have shown that PC-3 cells stimulated with CXCL12 (10 nM) display a faster cellular velocity after 10 hrs when compared against the basal migration.

To explore whether CPYPP could also affect cellular velocity a separate cancer model, the PC-3 cells were used to measure the speed of cellular migration over 10 hrs in response to CXCL12. The PC-3 cells were chosen instead of the MCF-7 cells as PC-3 cells have a much higher migratory speed. For this experiment the PC-3 cells were stimulated with CXCL12 (10 nM) in both the presence and absence of CPYPP (100 μM) and CK666 (10 μM) to establish if DOCK1/2/5 and Arp2/3 respectively promoted PC-3 cell migration in response to CXCL12.

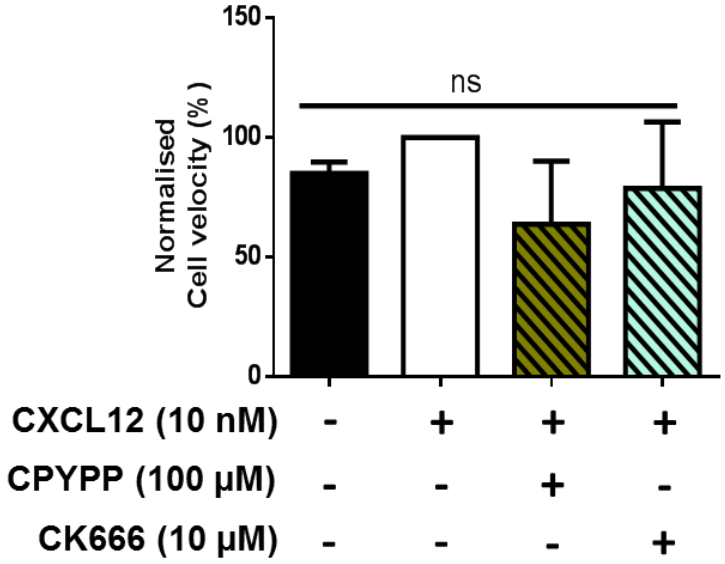

Figure 5.13. CPYPP (100 μM) and CK666 (10 μM) inhibition of DOCK1/2/5 and CK666 respectively does not block CXCL12 (10 nM) induced velocity of PC-3 cells after 10 hrs. Results were normalised to CXCL12 (10 nM) and represent the mean ± S.E.M data in three independent experiments. (Data produced by Isabel Hamshaw). (Kruskal-Wallis test, Dunn's multiple comparisons test, ns = p≥0.05 of no significance).

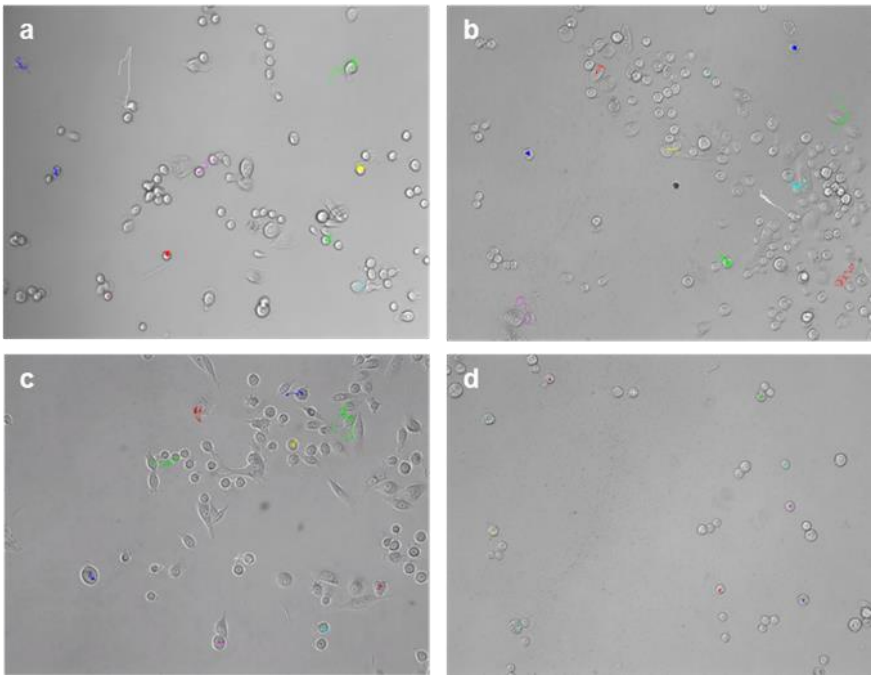

Figure 5.14. Endpoint images from time-lapse tracking of PC-3 cell after 10 hrs. (a) Control. (b) CXCL12 (10 nM). (c) CXCL12 (10 nM) & CK666 (10 µM). (d) CXCL12 (10 nM) & CPYPP (100 µM). Images are a representation of the cell population and were taken at 10x objective with a Zeiss Axiovert 200M microscope and using AxioVision Rel 4.8 software.

Treating PC-3 cells with and without CXCL12 (10 nM) and in the presence of either CPYPP (100 µM) or CK666 (10 µM), had no significant effect on PC-3 cell velocity after 10 hrs (figure 5.13). Though PC-3 cells treated with CPYPP did display lower levels of cellular velocity compared to both the basal and CXCL12 alone. This was also observed in two of the time lapse videos. Whereby PC-3 cells incubated with CPYPP showed limited cellular movement and protrusions and retained a circular morphology throughout the 10 hrs. Also in the presence of CPYPP there were less cells present and higher levels of detachment compared to the other conditions: indicating cytotoxicity (figure 5.14d). Overall CXCL12 treatment only displayed a modest upward trend in cell velocity compared to the basal. Whilst there was no clear evidence of DOCK1/2/5 and Arp2/3 being important for the migration speed of PC-3 cells.

5.10 EHT 1864 and Y27632 have no significant effect on the actin cytoskeleton of CHO-CCR5 and PC-3 cells

Actin staining of CHO-CCR5 cells with phalloidin showed that CCL3 increases cellular elongation after 24 hrs (figure 3.27). Previous investigation of this downstream signalling pathway suggested that neither PI3K nor FAK were important for inducing cellular elongation caused by CCL3 stimulation (figure 4.22).

Changes to the cellular shape is known to be driven by cytoskeleton remodelling. Therefore the roles of Rac and ROCK, a serine/threonine kinase regulated by RhoA [554] were investigated to determine whether they were acting downstream of CCL3 signalling to facilitate CHO-CCR5 cellular elongation.

To inhibit Rac and ROCK, CHO-CCR5 cells were treated with EHT 1864 and Y27632 respectively for 24 hrs, before being fixed and stained with Phalloidin CruzFluor TM^{594}. Y27632 is an orthosteric ROCK inhibitor which disrupts ATP binding and therefore inhibits ROCK's kinase activity. Y27632 has been proven to interfere with actin stress fiber formation [184].

PC-3 cells were also used as a secondary model for actin staining. As although CXCL12 had no definite effect on the F-actin or cell shape, the PC-3 cells could serve as an additional control for any non-specific effects caused by EHT 1864 or Y27632.

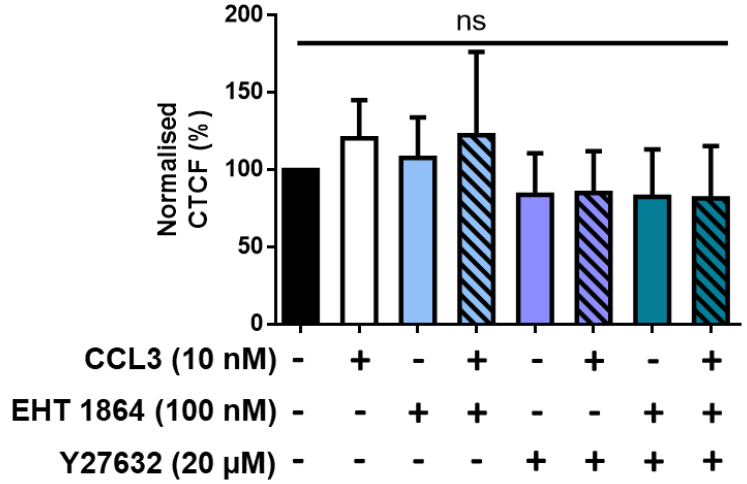

Figure 5.15. EHT 1864 (100 nM) and Y27632 (20 µM) inhibition of Rac and ROCK respectively did not affect the corrected total cellular fluorescence (CTCF) of CHO-CCR5 cells in the absence or presence of CCL3 (10 nM) after 24 hrs. ImageJ 1.48v was used to calculate the CTCF for all images of phalloidin staining before being normalised to the control (CCL3 absent). Results represent the mean ± SEM of at least two independent experiments. (Kruskal-Wallis test, Dunn's multiple comparisons test, ns = p value≥0.05 of no significance).

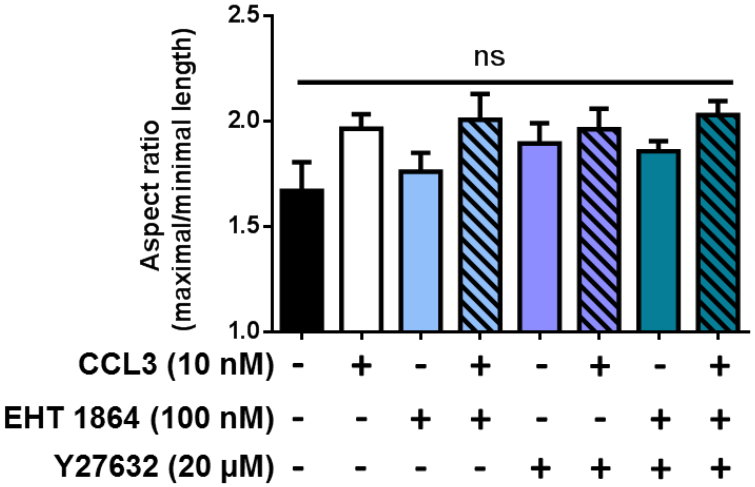

Figure 5.16. EHT 1864 (100 nM) and Y27632 (20 µM) inhibition of Rac and ROCK respectively did not affect the aspect ratio of CHO-CCR5 cells in the absence or presence of CCL3 (10 nM) after 24 hrs. Results represent the mean ± SEM of at least two independent experiments. (One-way ANOVA, Tukey's test, ns = p value≥0.05 of no significance).

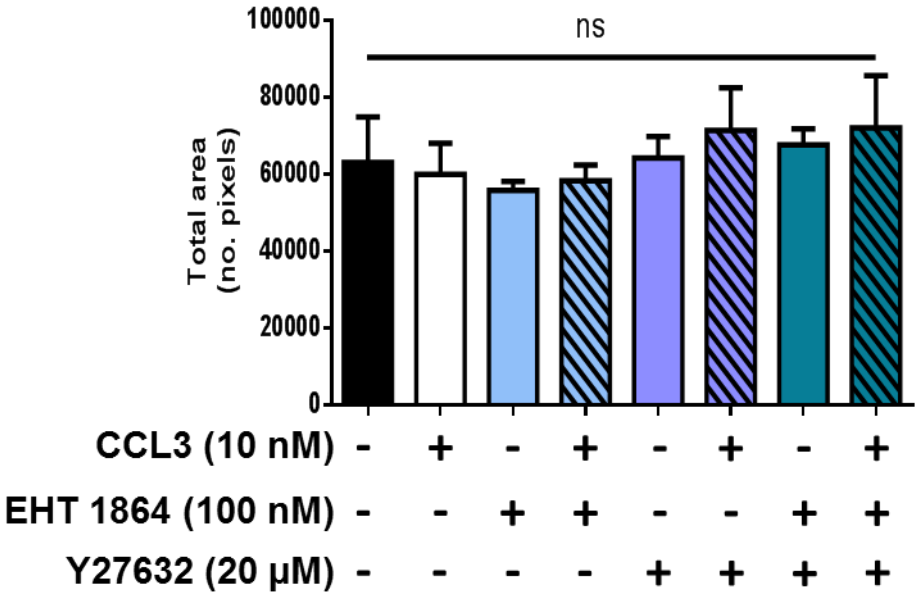

Figure 5.17. EHT 1864 (100 nM) and Y27632 (20 µM) inhibition of Rac and ROCK respectively did not affect the total area of CHO-CCR5 cells in the absence or presence of CCL3 (10 nM) after 24 hrs. Results represent the mean ± SEM of at least two independent experiments. (One-way ANOVA, Tukey's test, ns = p value≥0.05 of no significance).

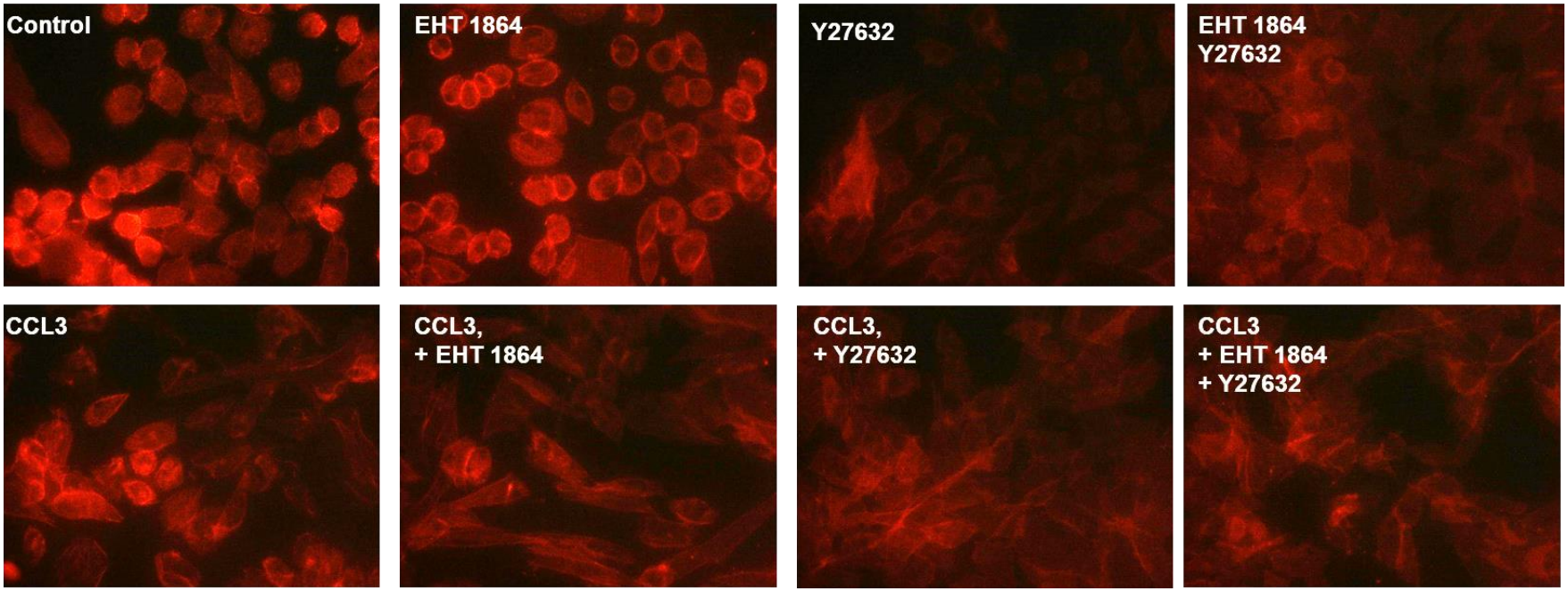

Figure 5.18. Phalloidin actin staining of CHO-CCR5 cells in the presence and absence of CCL3 (10 nM) with EHT 1864 (100 nM) and Y27632 (20 μM) inhibitors after 24 hrs. Rac inhibitor: EHT 1864. ROCK inhibitor: Y27632. CHO-CCR5 cells were fixed and stained with Phalloidin CruzFluor TM^{594} conjugate (red) for imaging the F-actin cytoskeleton. Images are a representation of the cell population and were taken at 63x objective with a Leica DMI6000 inverted microscope and using Leica imaging suite.

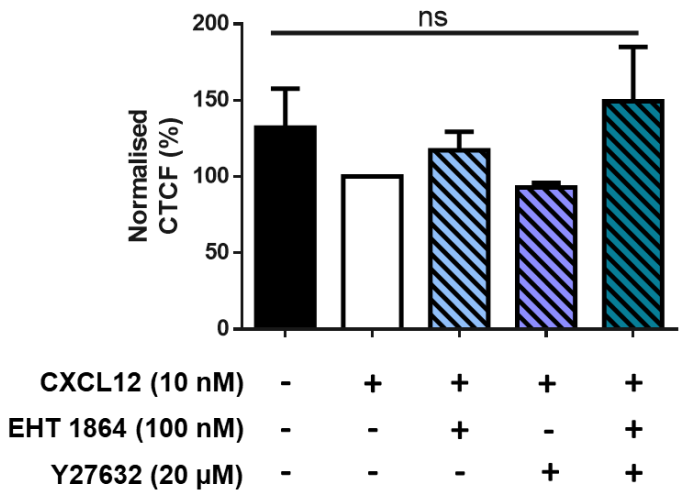

Figure 5.19. EHT 1864 (100 nM) and Y27632 (20 µM) inhibition of Rac and ROCK respectively did not affect the CTCF of PC-3 cells stimulated with CXCL12 (10 nM) after 24 hrs. ImageJ 1.48v was used to calculate the CTCF for all images from the phalloidin stain before being normalised to CXCL12 (alone). Results represent the mean ± SEM of three independent experiments. (Kruskal-Wallis test, Dunn's multiple comparisons test, ns = p value≥0.05 of no significance).

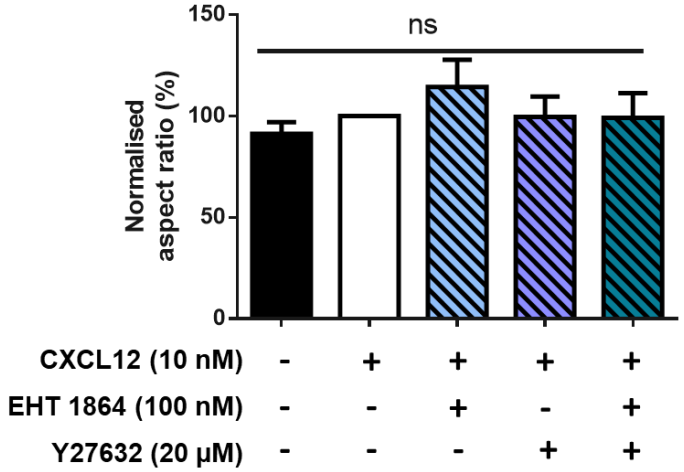

Figure 5.20. EHT 1864 (100 nM) and Y27632 (20 µM) inhibition of Rac and ROCK respectively did not affect the aspect ratio of PC-3 cells stimulated with CXCL12 (10 nM) after 24 hrs. Results were normalised to CXCL12 (alone) and represent the mean ± SEM of three independent experiments. (Kruskal-Wallis test, Dunn's multiple comparisons test, ns = p value≥0.05 of no significance).

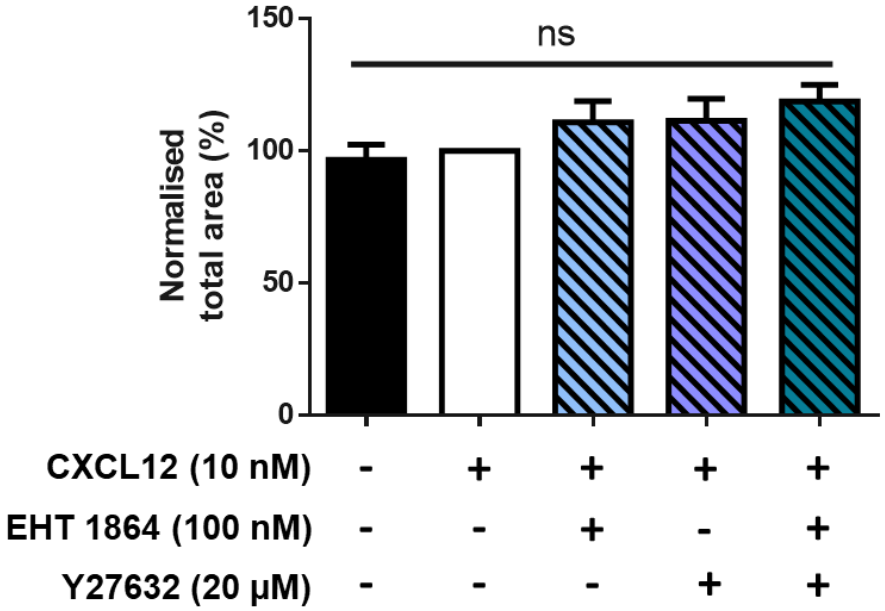

Figure 5.21. EHT 1864 (100 nM) and Y27632 (20 µM) inhibition of Rac and ROCK respectively did not affect the total area of PC-3 cells stimulated with CXCL12 (10 nM) after 24 hrs. Results were normalised to CXCL12 (alone) and represent the mean ± SEM of three independent experiments. (Kruskal-Wallis test, Dunn's multiple comparisons test, ns = p value≥0.05 of no significance).

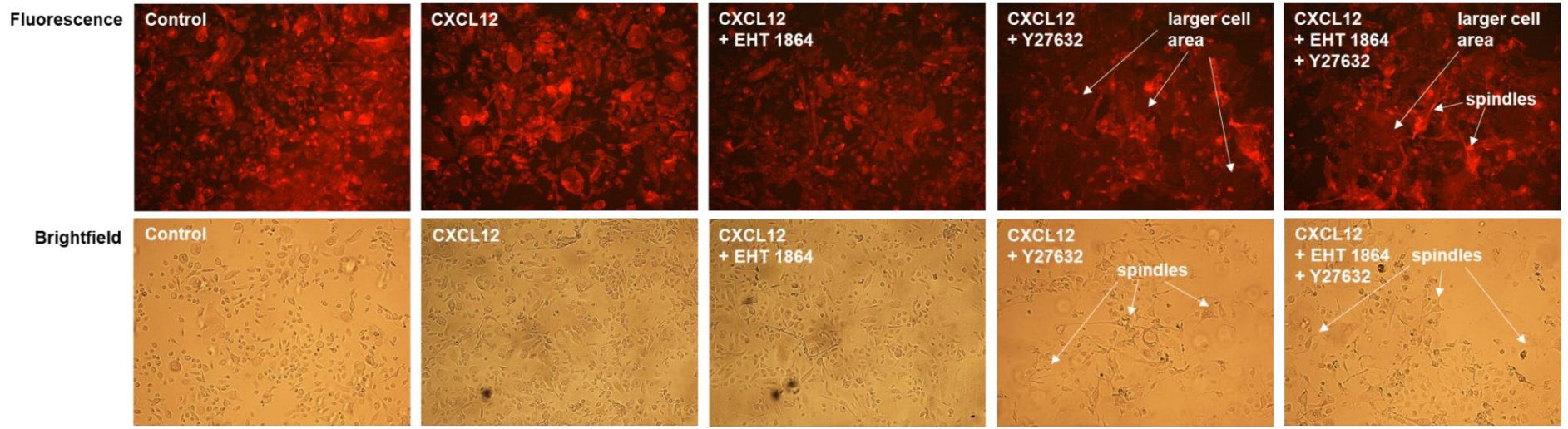

Figure 5.22. Fluorescent and brightfield images of PC-3 cell staining with phalloidin in the presence of CXCL12 (10 nM), EHT 1864 (100 nM) and Y27632 (20 μM) inhibitors after 24 hrs. Rac inhibitor: EHT 1864. ROCK inhibitor: Y27632. PC-3 cells were fixed and stained with Phalloidin CruzFluor TM^{594} conjugate (red) for imaging the F-actin cytoskeleton. Images represent a population of cells and were taken at 10x objective with a Leica DMI6000 inverted microscope and using Leica imaging suite.

Blockade of Rac and ROCK using EHT 1864 (100 nM) and Y27632 (20 μM) respectively, showed no significant effect on the fluorescence levels (CTCF), cellular elongation (aspect ratio) and cell size (total area in no. pixels) in either PC-3 and CHO-CCR5 cells after 24 hrs (figures 5.15-5.22)

There were however some identifiable trends from both the data analysis and images. Treatment with Y27632 displayed lower levels of fluorescence (CTCF) compared to the control in PC-3 cells (figure 5.19) as well as for CCL3 in CHO-CCR5 cells (figure 5.15). This was clearly shown from the images of both PC-3 (figure 5.20) and CHO-CCR5 (figure 5.15) actin staining.

In one of the PC-3 experiments treatment with Y27632 showed a larger cell size and exhibited a spindly morphology as clearly evidenced from the images (figure 5.22). However the data analysis of PC-3 cell size only showed a modest increase in total area when treated with Y27632 (figure 5.21).

In summary Rac and ROCK have no significant measureable effect on cell shape or F-actin formation in both PC-3 and CHO-CCR5 cells. However there did appear to be a visible and mostly likely non chemokine specific effect of ROCK blockade on PC-3 cell morphology.

5.11 EHT 1864 and Y27632 are not cytotoxic in CHO-CCR5 cells

From the phalloidin staining a tendency of the Y27632 (20 μM) to display lower levels of fluorescence in both the absence and presence of CCL3 in CHO-CCR5 cells was observed. To establish any possibility of cytotoxicity with EHT 1864 (100 μM) and Y27632 (20 μM) in CHO-CCR5 cells, the effect of both these compounds on cellular proliferation after 24 hrs was assessed using an MTS assay.

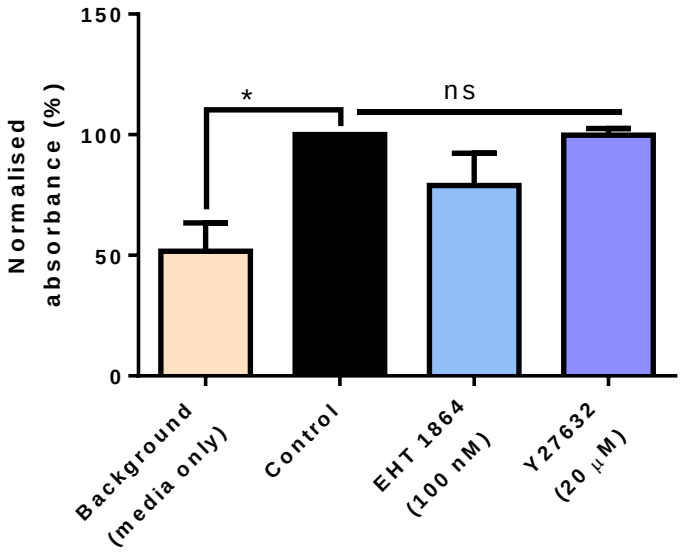

Figure 5.23. Cell proliferation assay of CHO-CCR5 cells after 24 hrs incubation and 1 hrs MTS metabolisation. Rac inhibitor: EHT 1864. ROCK inhibitor: Y27632. Results were normalised to the control and represent the mean ± SEM of at least three independent experiments (Data from Wing Yee Lai). (Kruskal-Wallis test, Dunn's multiple comparisons test, * = p≤0.05, ns = p value≥0.05 of no significance).

The data from the MTS assay showed that neither EHT1864 nor Y27326 were cytotoxic at 100 nM and 20 µM in CHO-CCR5 cells after 25 hrs incubation respectively (figure 5.23). Therefore both inhibitors were at suitable concentrations to avoid cytotoxicity in CHO-CCR5 cells for phalloidin staining.

5.12 Discussion

Remodelling of the cellular cytoskeleton is crucial for the migration of both adherent and suspension cells and as such chemokine signalling activates various modulators for F-actin assembly at the cells leading edge to facilitate chemotaxis [555]. Aberrations within this signalling pathway is associated with cancer metastasis and therefore many of its downstream effectors like Rac, RhoA and WAVE2 are considered potential therapeutic targets for cancer treatment [536, 537]. However these downstream signalling pathways are not always uniform and can vary substantially according to the cell type and chemokine involved which limits the development of targeted treatments.

The aim of this chapter was to delineate the molecular mechanisms which influence cytoskeletal remodelling in CCL3 and CXCL12 signalling in two leukemic and carcinoma cell lines: THP-1 and MCF-7 cells respectively. The CHO-CCR5 cell line was used to additionally characterise the CCL3-CCR5 signalling axis.

This chapter began by exploring the role of two known regulators of F-actin remodelling Arp2/3 and DOCK1/2/5 (using CK666 and CPYPP respectively) as well as microtubule stabilisation (Taxol) in the increase of intracellular calcium downstream of CXCR4 and CCR1/5 activation. From the findings relating to F-actin remodelling, DOCK1/2/5 was identified as being involved in the intracellular calcium signalling of CCL3 and CXCL12 in both THP-1 and MCF-7 cells, whilst Arp2/3 was more important for chemokine intracellular calcium signalling in MCF-7 rather than THP-1 cells (figures 5.1 and 5.2).

DOCK1/2/5 and Arp2/3 belong to the same signalling axis: DOCK1/2/5-Rac-WAVE2-Arp2/3 and neither have been directly implicated in intracellular calcium signalling before. Research from the Mueller lab has shown that Rac is not essential for CCL3 and CXCL12 increases in intracellular calcium in THP-1 cells [346]. For MCF-7 cells the role of Rac in chemokine intracellular calcium signalling has not yet been defined. As such it is possible that MCF-7 cells utilize the DOCK1/2/5-Rac-WAVE2-Arp2/3 signalling axis for CCL3 and CXCL12 increases in intracellular calcium. Whereas for THP-1 cells the data would suggest that DOCK1/2/5 activates an alternative pathway independent

of Rac and Arp2/3 for intracellular calcium signalling (figure 5.24). Rac is currently the only known effector downstream of DOCK1/2/5 activity and as such an alternative pathway is completely unknown.

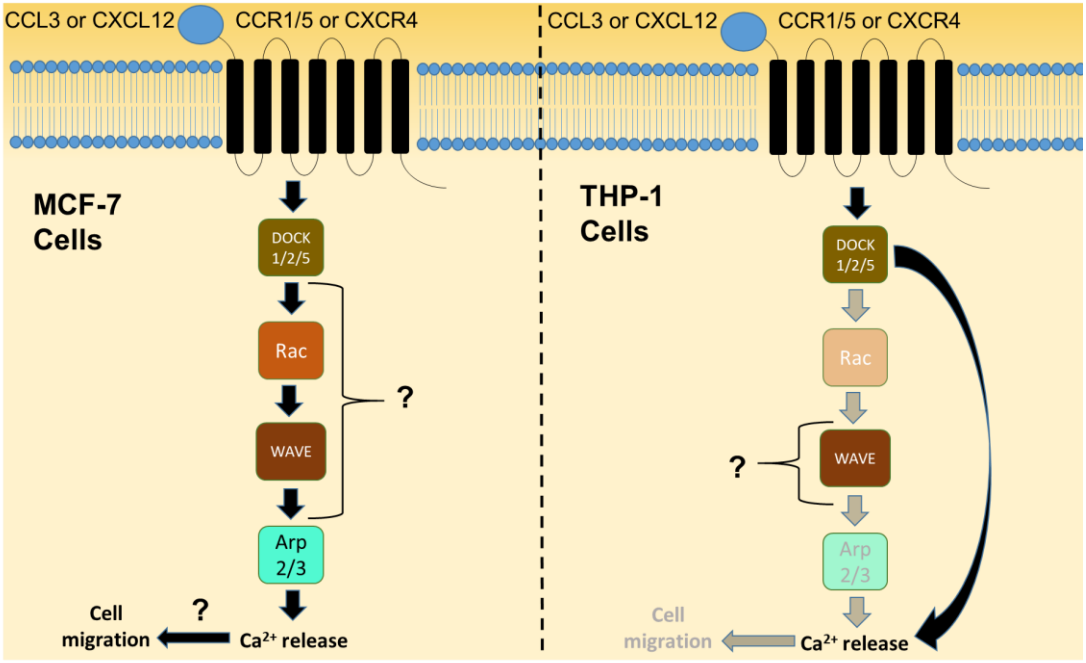

Figure 5.24. Current model of the DOCK1/2/5-Rac-WAVE-Arp2/3 pathway in the intracellular calcium signalling of CCL3 and CXCL12 in MCF-7 and THP-1 cells. DOCK1/2/5 is important for chemokine intracellular calcium signalling in both THP-1 and MCF-7 cells. Whereas Arp2/3s role in chemokine intracellular calcium signalling was important for MCF-7 cells only. Neither Rac nor Arp2/3 are important for chemokine induced increases in intracellular calcium in THP-1 cells. In THP-1 cells neither CCL3 nor CXCL12 appear to rely on intracellular calcium signalling for cell migration. WAVEs role in the intracellular calcium signalling of chemokines in MCF-7 and THP-1 cells is unknown. Whilst the importance of Rac in chemokine intracellular calcium signalling and the role of this calcium signalling for MCF-7 cell migration has not been determined. Faded arrows and objects indicate that they are not important for the signalling pathway.

DOCK1/2/5 and Arp2/3 both regulate F-actin formation, therefore it is possible that changes in the F-actin cytoskeleton could contribute to intracellular

calcium signalling. Several studies have identified the involvement of F-actin in the increase of intracellular calcium in neurons [556], T-cells [557] and platelets [558]. Furthermore, upstream modulators of F-actin assembly such as WAVE2 and DOCK7 (a member of the related DOCK subfamily C and regulator of both Cdc42 and Rac) have also been implicated in increases in intracellular calcium [559, 560]. However the exact mechanisms behind F-actin mediated increase in intracellular calcium remains unclear.

One proposed model is that the actin cytoskeleton is involved in the direct coupling of the ER membrane to the calcium channels present on the plasma membrane to induce an influx of calcium into the cell [558]. As the intracellular calcium measurement experiments were performed in the presence of $CaCl_2$, the possibility of extracellular calcium as a source of, or some of the intracellular calcium flux observed cannot be excluded. Alternatively, F-actin is also associated with the recycling of chemokine receptors following activation [561]. Therefore F-actin perturbation could lead to less receptor recycling and thus a lower cell surface expression thereby reducing the levels of intracellular calcium signalling. Due to the fast kinetics of intracellular calcium signalling (70 secs) it is more likely that the down regulation of the chemokine receptor would have occurred during the 30 mins pretreatment time with either CK666 or CPYPP. Although this would need to be confirmed using flow cytometry.

In CHO-CCR5 cells, CK666 treatment showed a trend towards enhancing CCL3 intracellular calcium signalling, which although not significant with Dunnett's multiple comparisons test did show a significance with the Fischer's LSD Test (figure 5.3). Previous studies in CHO-CCR5 cells have shown showed that F-actin destruction using Cytochalasin D blocked CCR5 internalisation [184] and enhanced β-arrestin clustering [562] following CCL3 and CCL5 stimulation respectively. However, treatment with Cytochalasin D on CHO-CCR5 cells had no effect on CCL3 intracellular calcium signalling [184] nor β-arrestin recruitment [562], suggesting that the actin cytoskeleton is not essential for receptor desensitization. Whether this is also the case for Arp2/3 remains to be determined but it could be possible that Arp2/3 blockade does not completely disturb the actin cytoskeleton in a similar fashion to Cytochalasin D.

Besides the actin cytoskeleton, the role of the microtubules in chemokine signalling was also explored. Using Taxol, microtubule stabilisation was shown to attenuate CXCL12 increases in intracellular calcium in MCF-7 cells (figure 5.1 c and d). Whereas using nocodazole to disrupt microtubule polymerisation had no such effect on CXCL12 intracellular calcium signalling in MCF-7 cells (figure 5.4). Together these results would imply that microtubule stabilisation specifically effects the increase in intracellular calcium of CXCL12 in MCF-7 cells. However to truly determine the involvement of microtubule turnover for chemokine intracellular calcium signalling, a microtubule stain of MCF-7 cells would need to be performed to confirm the microtubule depolymerisation and stabilisation activities of nocodazole and Taxol respectively.

To further explore the functionality of DOCK1/2/5, Arp2/3 and microtubule stabilisation on cell migration the effects of CPYPP, CK666 and Taxol were assessed on the chemotaxis of Jurkat cells towards CXCL12, as well as in THP-1 cells with CPYPP. From these experiments DOCK1/2/5 was shown to be essential for CXCL12 chemotaxis in Jurkat cells but not in THP-1 cells (figures 5.9-5.11). For Jurkat chemotaxis CPYPP had an IC_{50} of 11.72 μM, which was comparable to the IC_{50} of 22.8 ± 2.4 μM for the inhibition of DOCK2 guanine nucleotide exchange activity by CPYPP within a cell-free assay [408].

As DOCK1/2/5 was shown to be important for CXCL12 intracellular calcium signalling but most likely not for THP-1 chemotaxis. This suggests that THP-1 chemotaxis may not be reliant on intracellular calcium signalling, which has been similarly reported for the chemotaxis of THP-1 cells towards CCL3 [480]. Whether intracellular calcium signalling is important for Jurkat chemotaxis to CXCL12 is unclear due to the difficulties in reliably measuring intracellular calcium levels. However one way this could be investigated is by using Xestospongin C to block IP_3 activation during chemokine stimulated chemotaxis. Additionally, intracellular calcium imaging of individual Jurkat cells could also be performed to accurately model intracellular calcium signalling as demonstrated in Tomilin VN *et al.* (2016) [563].

To further elucidate the signalling axis involved in CXCL12 chemotaxis of Jurkat cells, Rac, Src and PLC and were targeted alongside DOCK1/2/5 to see

if any of the compounds had a synergistic inhibition on cell migration. Unfortunately, besides CPYPP none of the compounds showed any sign of inhibition and thus these results provided no further insight into the downstream signalling pathway (figure 5.12). The likely explanation for this outcome was that the concentrations used for Bosutinib (Src inhibitor) and U73122 (PLC inhibitor) were too low to block any cell migration.

In Mills S.C *et al*. (2018), EHT 1864 (100 nM) was able to inhibit around 50% of CXCL12 chemotaxis in Jurkat cells [346]. This may suggest that only a subpopulation of Jurkat cells use Rac for CXCL12 induced migration. From the results presented in this chapter the Jurkats had a chemotactic response of 33.2 $x10^4$ per mL^{-1} towards CXCL12 compared to 80 $x10^4$ per mL^{-1} for Mills S.C *et al*. (2018). Therefore perhaps a greater window of difference in the cell migration between CXCL12 treatment and the basal was required to detect EHT1864 (100 nM) inhibition.

Based on emerging evidence from both Mills S.C *et al*. (2018) and the results from the chemotaxis assays performed in this chapter, a hypothetical model of the DOCK1/2/5-Rac-WAVE-Arp2/3 signalling axis in Jurkat and THP-1 chemotaxis towards CXCL12 has been proposed (see figure 5.25).

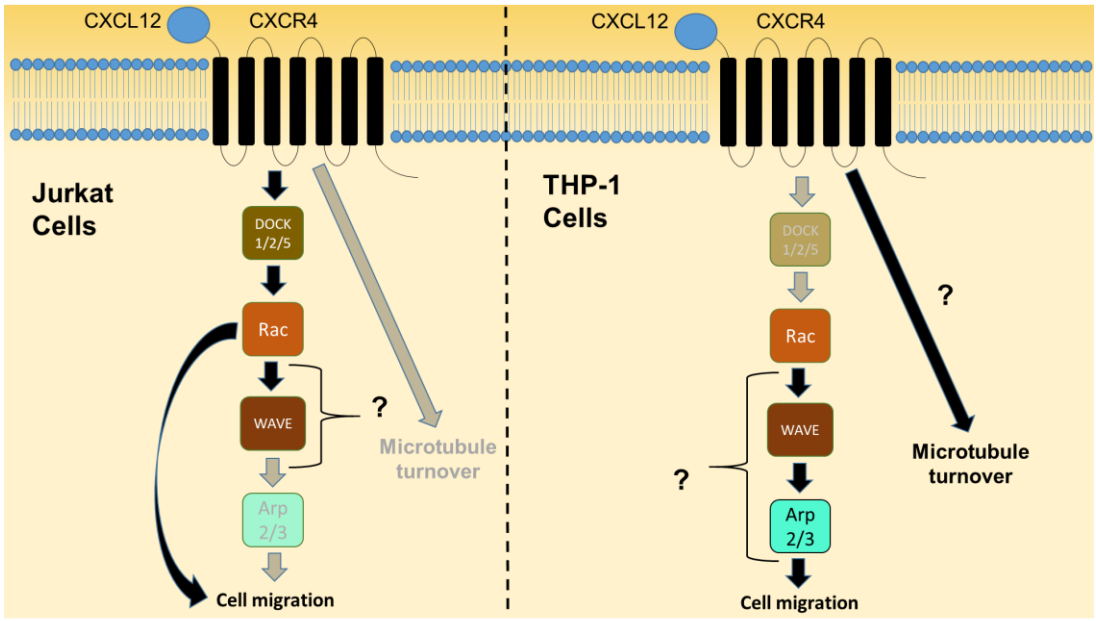

Figure 5.25. Current model of CXCL12 chemotaxis in Jurkat and THP-1 cells. In Jurkat cells CXCL12 activates DOCK1/2/5 and Rac but not Arp2/3 or microtubule turnover for chemotaxis. In THP-1 cells CXCL12 activates only Rac for chemotaxis. The role of WAVE in CXCL12 chemotaxis is currently unknown whilst the importance of Arp2/3 and microtubule turnover for CXCL12 chemotaxis in THP-1 cells was not established. Faded arrows and objects indicate that they are not important for the signalling pathway.

PC-3 cells are known to express DOCK2, however, DOCK2 was shown not to be important for CXCL13-CXCR5 cell invasion [564]. Whether this is also true for CXCL12-CXCR4 signalling or DOCK1/5 is not known. Therefore the effects of CPYPP and CK666 on PC-3 cell velocity in response to CXCL12 was assessed. From this time lapse experiment no clear role for DOCK1/2/5 or Arp2/3 on PC-3 cellular velocity was identified, with CPYPP displaying evidence of cytotoxicity. Furthermore treatment with CXCL12 showed no significant increase in PC-3 cellular speed over 10 hrs. This suggests that CXCL12-CXCR4 signalling does not influence PC-3 cellular speed.

Finally, to further probe the molecular mechanisms involved in CCL3 elongation of CHO-CCR5 cells, known F-actin regulators Rac and ROCK were blocked with EHT-1684 and Y27362 respectively. Neither inhibitor showed any

significant effect on cell morphology indicating that CCL3 elongation of CHO-CCR5 cells was not dependent on either Rac or ROCK activation (figures 5.16 and 5.18). As a control both compounds were tested on PC-3 cells stimulated with CXCL12 with the results showing no significant effect on cellular morphology (figures 5.19-5.21). However, PC-3 cells treated with Y27632 exhibited a more spindly morphology (figure 5.22) which has also been observed by another study on melanoma cells [565]. This observation in PC-3 cells indicates that the Y27632 is active and identifies an importance of ROCK for cellular shape.

5.13 Conclusion

The main findings from this chapter were also follows:

- DOCK 1/2/5 is important for the downstream signalling of CCL3 and CXCL12 in both THP-1 and MCF-7 cells and furthermore cell specific for CXCL12 chemotaxis in Jurkat cells.

- Arp2/3 is involved in the downstream signalling of CCL3 and CXCL12 in MCF-7 cells.

- Microtubule stabilisation blocks CXCL12 intracellular calcium signalling in MCF-7 cells.

Chapter 6 Final Discussion

The overall aim of this thesis was to identify alternative and viable therapeutic targets to block chemokine associated cancer progression. Consequently in this chapter the identification of suitable chemokine signalling axis for blocking carcinoma metastasis will be discussed first before proceeding to highlight potential therapeutic targets downstream of chemokine G-protein signalling and upstream of cytoskeleton remodelling. Furthermore the impact of biased signalling on the therapeutic targeting of the chemokine signalling network will be discussed, before concluding with future work.

6.1 Chapter 3. Chemokine signalling pathways involved in carcinoma metastasis

To identify the involvement of different chemokines signalling axis in carcinoma metastasis a screen comprised of seven different chemokines CCL23, CCL2, CCL3, CCL4, CCL8, CXCL9 and CXCL12 was devised. The effects of these chemokines were assessed in the wound healing assay of breast (MCF-7 and MDA-MB-231), pancreatic (MIA PaCa-2) and prostate cancer (PC-3) cell types as a model for cancer metastasis. From the screen, two chemokines CCL3 and CCL2 were implicated in the migration of MCF-7 and PC-3 cells respectively. As both chemokines had been previously identified as promoters of cellular migration in their respective cell type [278, 346, 437, 441] neither can be considered a novel target.

6.1.1 CCL2-CCR2 signalling axis

The CCL2-CCR2 signalling axis is one of the better studied chemokine signalling pathways in cancer and is particularly well known for its association with prostate cancer [278, 279, 287]. Due to preclinical success in targeting the CCL2-CCR2 signalling axis, two antibodies carlumab and MLN1202 were developed and underwent clinical trials to target CCL2 and CCR2 respectively [307, 308]. Carlumab has been involved in three clinical trials, one in combination with docetaxel to treat patients with prostate metastasis and two for advanced solid tumours. Unfortunately carlumab demonstrated no significant anti-tumour efficacy in both trials perhaps in part due to a lack of robust reduction in the CCL2 levels in patients [307, 308, 310]. MLN1202 on the other hand showed potentially promising results with 14% of patients displaying lower levels of the bone metastasis marker N-telopeptide however its efficacy has not been disclosed (Trial registration ID: NCT01015560) [262].

There is a wealth of preclinical evidence and clear interest in targeting CCL2-CCR2 signalling especially for prostate cancer. However current approaches have not been proven to be beneficial in the clinic [310]. The identification of CCL2s role in PC-3 scratch closure could offer the opportunity to interrogate the downstream pathway further to discover alternative therapeutic candidates. Nonetheless due to the unreliability and variability with the wound healing assay this approach could not be used for compound screening with the PC-3 cells. Also the lack of detectable chemotaxis and increases in intracellular calcium of PC-3 cells in response to CCL2 stimulation prevented the use of the transwell migration and intracellular calcium flux assays as alternative methods for characterising the downstream signalling pathway. Therefore there is still a need for robust and sensitive methods to detect chemokine induced migration. Recently implemented cell migration assays within the Mueller lab such as the time-lapse, Boyden chamber and Oris™ assays have shown some encouraging results with PC-3 cells for detecting CXCL8 and CXCL12 induced migration. Therefore these assays could also be applied to CCL2 for mapping the downstream signalling pathway.

6.1.2 CCL3-CCR1/5 signalling axis

CCL3 was also identified from the screen as a promoter of MCF-7 scratch closure. At least two other cell migration studies have also shown that CCL3 can induce migration in MCF-7 cells [346, 437]. Besides these studies CCL3s role in breast cancer has not been heavily explored although some clinical data from breast cancer patients has shown that breast cancers display elevated levels of CCL3 mRNA [566, 567] and that these levels correlated with the infiltration of pre-metastatic mononuclear inflammatory cells to the primary tumour site [568]. Also in a murine triple negative breast cancer model, CCL3 was shown to be upregulated in the more invasive cells leading the authors to propose a role for CCL3 in breast cancer cell migration [569]. Most of these studies have only demonstrated an association between CCL3 and breast cancer progression rather than a direct role. Hence CCL3 is a poorly validated target for treating breast cancer [566-569].

To further probe the molecular mechanism of CCL3 in MCF-7 scratch closure two of its known cognate receptors CCR1 and CCR5 were targeted using J113863 and maraviroc respectively. From this experiment the results showed that CCL3 activates both CCR1 and CCR5 to promote MCF-7 scratch closure. This provides direct evidence of the involvement of receptor redundancy in chemokine induced cancer cell migration and further supports the idea that chemokine signalling redundancy is an obstacle for blocking cancer metastasis [320].

Maraviroc has been widely used to establish CCR5s involvement in breast cancer metastasis. In these studies mararviroc was shown to successfully block MDA-MB-231 bone [570], lung [338, 571], lymph node [571] and thoracic [572] metastasis *in vivo*, with the latter enhanced when combined with an IL-6 neutralising antibody. Two studies also observed a reduction in MCF-7 and MDA-MB-231 cell migration with maraviroc *in vitro*, although this was in the absence of CCL5 [338, 570]. This suggests that maraviroc could have an off-target or non-specific inhibitory effect on cell migration, although this was not observed in the wound healing assay experiments presented in this thesis. Interestingly in MDA-MB-231 cells only maraviroc was able to block CCL5 induced migration whilst the CCR1 and CCR3 antagonists BX513 and

SB328437 respectively had no effect [571]. This would imply that there is no functional redundancy amongst CCR1, CCR3 and CCR5 in the migration of MDA-MB-231 cells in response to CCL5. Which is a contrast to what was observed in MCF-7 cells where CCL3 was able to signal via both CCR1 and CCR5 to promote scratch closure. This suggests that the importance of a chemokine receptor could be dependent on either the chemokine and/or cell type and therefore highlights a need for appropriate target selection to successfully block chemokine signalling.

In instances of chemokine receptor redundancy dual inhibitors remain a possible option such as Repaxirin, which is a small molecule inhibitor for both CXCR1 and CXCR2 and is currently in clinical trial in combination with Taxol for treating triple negative breast cancer (Trial registration ID: NCT02370238). Nonetheless whether this approach is effective at a clinical level remains to be determined. However due to the structural homology of the CCR1 and CCR5 transmembrane domain (79%) dual inhibition remains a viable option. Although it is important to note that CCR1 and CCR5 are also structurally similar to CCR3 (85%) and CCR2 (91%) according to their respective pairwise sequence alignments [573]. Thus a dual inhibitor for CCR1 and CCR5 would also likely target CCR2 and CCR3 which may reduce its *in vivo* efficacy and/or possibly lead to unwanted side effects.

Consequently the downstream molecular mechanisms of CCL3 signalling in MCF-7 cells was investigated by using the wound healing and intracellular calcium flux assays as both showed evidence of reproducibility from chapter 3.

6.2 Identifying novel CCL3 and CXCL12 downstream targets in cancer

As previously mentioned, the downstream signalling pathway could serve as an alternative strategy to target the chemokine receptor as many proteins downstream of receptor activation are frequently dysregulated in a variety of different cancers [224-226, 352].

To delineate the chemokine and cell specific molecular pathways a pharmacological based approach was used to assess the particular importance of FAK, PLC, PI3K, c-Raf, Src/Syk, DOCK1/2/5, Arp2/3 and microtubule turnover in both cellular signalling and migration. This broad spectrum of proteins allows the possibility to build a detailed map of the downstream signalling pathway which can then be compared with previous research findings. This then enables the development of more accurate hypothetical models of the cellular signalling pathway.

6.2.1 Chapter 4. Targeting downstream effectors of G-protein signalling

6.2.1.1 FAK

Amongst the downstream effectors of G-protein signalling FAK was the most comprehensively characterised through the use of three separate inhibitors FAK14, PF562271 and Masitinib. Using these inhibitors FAK was only shown to be important for CXCL12 intracellular calcium signalling and not chemotaxis in THP-1 cells. Similarly neither CCL3 nor CXCL12 induced chemotaxis of THP-1 or Jurkat cells relied on FAK for migration respectively. This indicates that under these conditions FAK is not an appropriate target for leukemic cell invasion.

FAK is better known for its involvement in carcinoma metastasis than leukemogenesis, nevertheless its overexpression has been observed in AML (42% of cases) [574] as well as for B-cell but not T-cell leukaemia [575]. In THP-1 cells one study showed that FAK was expressed at a low basal level but that it was constitutively activated [576]. For chemokine driven

leukemogenesis extremely little is known about FAKs role, however an siRNA knockdown of FAK was shown to abolish CXCL12 chemotaxis in the B-cell leukaemia cell line Reh [498]. Based on this and evidence from this thesis, it is perhaps likely that FAKs role in CXCL12 chemotaxis is specific for B-cell but not T-cell leukaemia.

Although FAK was not important for THP-1 chemotaxis, FAK was shown to be critical for the mobilisation of calcium from the intracellular stores in response to CXCL12. As only cell migration was investigated, FAKs involvement in intracellular calcium signalling may indicate that FAK could be important for other cell responses e.g. cell survival or adhesion instead. Therefore FAK could still present itself as a therapeutic target for CXCL12 signalling in AML but just not within the context of cell migration.

6.2.1.2 PI3K

Besides FAK, a pharmacological blockade of PI3K using both LY294002 and AS6052425 was also performed on the intracellular calcium flux assays of CCL3 and CXCL12 in PC-3, MCF-7 and THP-1 cells, with no evidence of PI3K being important for intracellular calcium signalling. Furthermore, investigations into CCL3 and CXCL12 induced migration of MCF-7 and Jurkat cells respectively also suggested that PI3Ks role was dispensable. Similar results to these have also been reported for CCL3 and CXCL12 induced migration of THP-1 and MCF-7 cells respectively [340, 347]. However for the chemotaxis of THP-1 cells towards CXCL12, PI3K was shown to play a role [577]. In contrast to this thesis, results from Mills S.C *et al*. (2016) did observe a moderate reduction in Jurkat chemotaxis towards CXCL12 using either LY294002 or PI3K siRNA [340]. Based on the findings from this thesis and those from other studies it appears that PI3K is not an ideal target for blocking CCL3 or CXCL12 induced migration of MCF-7 cells, as well as, for CCL3 and CXCL12 chemotaxis in THP-1 and Jurkat cells respectively.

6.2.1.3 c-Raf and Src/Syk

Both c-Raf and Src/Syk were discovered to be specific for the downstream release of calcium from the intracellular stores of MCF-7 cells in response to CXCL12. As no effect on CXCL12 intracellular calcium signalling was observed in the presence of PLC and Gβγ inhibitors, this implies that the $G\alpha_i$-Syk/Src-c-Raf pathway could be utilised by CXCL12 instead of Gβγ-PLC to increase intracellular calcium. Unfortunately due to no reliable model for detecting CXCL12 induced migration of MCF-7 cells being available at the time the involvement of Src/Syk and c-Raf in MCF-7 cell migration was not investigated. Nonetheless previous research has implicated both Src and Raf in CXCL12 scratch closure of MCF-7 cells using bosutinib and L779450 respectively [340]. Due to the concentration used for MNS (10 μM) it is highly likely that inhibition observed on CXCL12 intracellular calcium signalling could be attributed to Syk (IC_{50} = 2.5 μM) rather than Src (IC_{50} = 29.3 μM).

MCF-7 cells are known to express Syk, with Syk considered as a negative regulator of MCF-7 basal migration by phosphorylating PI3K which disrupts PI3K-IκBα binding and subsequently the secretion of urokinase-type plasminogen activator [578]. In Jurkat cells neither c-Raf nor Src/Syk were shown to be essential for CXCL12 chemotaxis. From the wider literature Syk's role in chemokine migration is unknown, although one study confirmed the activation of Syk for CCL4 signalling in 'normal' T-cells however no functionality was established [579]. Whether Syk would also play a tumour suppressive role in CXCL12 driven migration in MCF-7 cells remains to be established although it is involved in the downstream signalling. Evidence already suggests that Raf is involved in CXCL12 induced migration of MCF-7 cells and thus establishing whether this role would be specific to c-Raf would be worthwhile studying.

6.2.1.4 PLC

In THP-1 cells PLC was shown to be pivotal for chemokine intracellular calcium signalling, as well as specific to CCL3 increases in intracellular calcium in MCF-7 cells. This suggests that PLC could be of critical importance for regulating chemokine related cellular responses in THP-1 cells, as well as, for CCL3 in MCF-7 cells. However establishing any meaningful functionality of PLC in any of these cancer cells using U73122 is impossible due to its high level of cellular cytotoxicity. As such other approaches are needed to better understand PLCs role, however, there is a current lack of specific PLC inhibitors available on the market. One alternative is edelfosine, which has been shown to block PLC activity in Swiss 3T3 fibroblasts and BG1 ovarian adenocarcinoma cells [580], although it is also an agonist for platelet-activating factor receptor and therefore cannot be used in cells expressing this receptor [581, 582]. Hence there is a great need to develop suitable inhibitors not only for investigating PLCs role in both *in vitro* and *in vivo* disease models, but also for potential drug development as PLC overexpression has been identified in breast and colorectal cancers [350, 351].

6.2.2 Chapter 5. Targeting downstream modulators of the cellular cytoskeleton

6.2.2.1 Arp2/3

Using the small molecule inhibitor CK666, a significant role for Arp2/3 in CCL3 and CXCL12 intracellular calcium signalling was identified for MCF-7 but not THP-1 cells. This indicates that Arp2/3s role in chemokine intracellular calcium signalling is specific to MCF-7 cells. In Jurkat and PC-3 cells, CXCL12 induced chemotaxis and cellular velocity was independent of Arp2/3 activity. Consequently for Jurkat cells, Arp2/3 is not a suitable target for blocking migration. However for PC-3 cells only the cellular speed and not chemotaxis was assessed, therefore Arp2/3 could still be important for migration. Nonetheless, Arp2/3 overexpression has not yet been established in prostate cancer, whilst another Arp2/3 inhibitor CK-0944636 was shown to actually

enhance PC-3 basal migration [583]. This is therefore an area of cancer research that still requires further investigation.

In breast cancer, coexpression of Arp2/3 and WAVE2 is associated with a poorer prognosis in breast cancer patients [540]. Which based on the intracellular calcium measurement experiments in MCF-7 cells suggests that Arp2/3 merits further validation as a therapeutic target against chemokine induced migration of breast cancer cells.

6.2.2.2 DOCK A subfamily

Using CPYPP to target the downstream signalling of CCL3 and CXCL12, the results showed that members of the DOCK A subfamily: DOCK1, DOCK2 and DOCK5 were important for the intracellular calcium signalling of both chemokines in THP-1 and MCF-7 cells. Furthermore for the CXCL12 chemotaxis of Jurkat cells the pharmacological blockade of DOCK1/2/5 completely abolished migration and thus could serve as a therapeutic target for T-cell leukaemia. Preliminary experiments with THP-1 cells did not show a similar effect suggesting that DOCK1/2/5s role in intracellular calcium signalling could involve other cellular responses aside from chemotaxis. In Jurkat cells CXCL12 driven chemotaxis is known to utilise Rac [346] and therefore to confirm DOCK1/2/5s involvement in CXCL12 chemotaxis the inhibition of Rac activation in the presence of CPYPP would need to be confirmed.

DOCK1/2/5 has already been shown to be important for the chemotaxis of neutrophils [548] and normal T-cells and B-cells [408]. Indicating that DOCK1/2/5 has a general importance for the immune system function. As such its pharmacological blockade would most likely impair normal leukocyte migration and thus would need to be taken into consideration if used as a form of cancer treatment especially for solid tumours.

In PC-3 cells no significant inhibition on cellular speed in the presence of CXCL12 was detected following DOCK1/2/5 blockade. Although evidence of cellular cytotoxicity was observed instead which may limit the use of CPYPP

as a research tool in PC-3 cells. DOCK2 overexpression has been identified in PC-3 cells suggesting it may have a functional importance although this was not shown to be the case for CXCL13-CXCR5 migration [512]. Therefore the importance of DOCK1/2/5 in prostate cancer progression is still not clear.

In breast cancer DOCK1 mRNA expression was associated with a poor prognosis for both the HER-2 and basal subtypes but not for the luminal oestrogen positive subtype [584]. In the triple negative breast cancer model, MDA-MB-231 cells, DOCK5 expression was shown to be associated with lung metastasis [585] whilst a regulator of DOCK1 activity, ELMO, was implicated in CXCL12 induced breast cancer cell migration with the same study confirming ELMO-DOCK1 binding [344]. Consequently the DOCK A subfamily are an emerging therapeutic candidate for breast cancer. Hence the role of DOCK1/2/5 in both CCL3 and CXCL12 intracellular calcium signalling in MCF-7 cells supports the need for further research in this area.

6.2.2.3 Microtubule turnover

The effects of microtubule stabilisation on cancer cellular proliferation using Taxol is widely known [586, 587]. However with regards to cell migration, in particular chemokine facilitated migration the role of the microtubules is less clear. To look further into this the effects of Taxol on CXCL12 chemotaxis in Jurkat cells was studied though no inhibition was shown. For intracellular calcium signalling Taxols effects were shown to be both chemokine and cell specific. For MCF-7 cells Taxol blocked CXCL12 intracellular calcium signalling. The mechanism behind Taxols effect on intracellular calcium signalling are unclear but the use of nocodazole suggested that it was specific to microtubule stabilisation. The functional significance of Taxol on CXCL12 signalling pathway in MCF-7 cells was not established.

Taxol is widely used for cancer treatment and hence improved understanding of its impact on cancer cell behaviour would help better tailor its use in cancer patients to either enhance its therapeutic benefit or minimize any deleterious effects.

6.3 Biased signalling in chemokine mediate cancer progression

As part of the research of this thesis a large range of chemokine ligands and cell types were used. This provided the opportunity to identify any signalling biases involved within the chemokine signalling network. For cancer cell migration there appeared to a potential ligand bias towards CCL3 in MCF-7 cells and CCL2 in PC-3 cells. Also CCL3 indicated a cell specific bias for MCF-7 over PC-3 cells in the wound healing assay. When assessing for chemokine receptor activation by measuring increases in intracellular calcium, chemokine efficacy levels showed no particular correlation to scratch closure. Suggesting that differing efficacy levels between the chemokines may not be the only contributing factor towards variations in the migratory response. When investigating the downstream signalling pathway ligand biases were observed within the MCF-7 cells regarding the importance of PLC for CCL3 but not CCL5 or CCL23 intracellular calcium signalling despite sharing the same receptors.

This research highlights that although the CCR1/5 receptors exhibit some functional redundancy in MCF-7 cell migration there appears to be a potential bias towards CCL3 agonism. Interestingly this is somewhat reflected in the downstream signalling with CCL3-CCR1/5 signalling relying on PLC activation for intracellular calcium signalling and therefore could be important for cell migration. In both THP-1 and MCF- cells CCL3-CCR1/5 intracellular calcium signalling involved PLC and DOCK1/2/5 whereas Arp2/3 was important in MCF-7 cells only. Furthermore in PC-3 cells CCL3 intracellular calcium signalling did not rely on PLC. Therefore despite some overlapping molecular mechanisms the downstream signalling pathway of CCL3-CCR1/5 is cell type dependent (figure 6.1).

Besides the CCR1/5 receptors the downstream signalling events of CXCL12-CXCR4 were also investigated in different cell types. As CXCR4 has one known cognate ligand (CXCL12) no ligand bias could be explored. Similar to CCL3 signalling, CXCL12 also utilised DOCK1/2/5 for mediating increases in intracellular calcium in both MCF-7 and THP-1 cells as well as having a specific bias towards Arp2/3 in MCF-7 cells and an absence of PLC importance for PC-3 intracellular calcium signalling. Furthermore there were substantial

differences between CXCL12-CXCR4 downstream signalling in MCF-7 and THP-1 cells. Whilst MCF-7 cells utilised Src/Syk, c-Raf and the microtubules to increase intracellular calcium, the THP-1 cells relied on FAK and PLC instead. DOCK1/2/5 also appeared to be cell specific for Jurkat CXCL12 chemotaxis .This indicates that there is a significant level of diversity within CXCL12-CXCR4 downstream signalling in different cell types (figure 6.1).

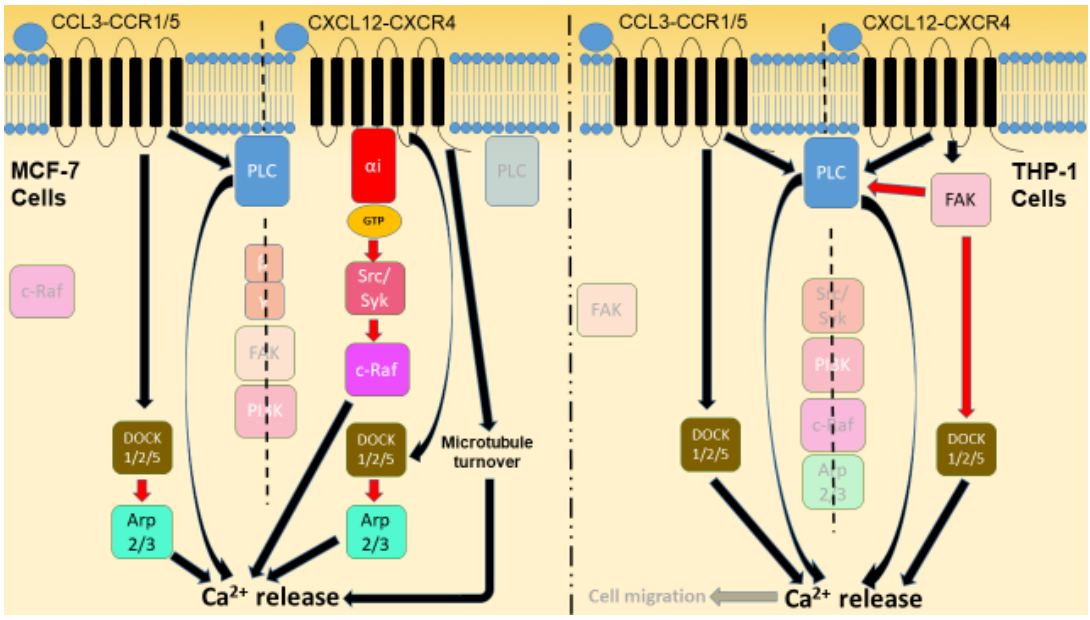

Figure 6.1. Overview and hypothetical model of the main cellular signalling pathways investigated in this thesis: CXCL12-CXCR4 and CCL3-CCR1/5 in MCF-7 and THP-1 cells. Black arrows corresponds to signal transduction whilst red arrow corresponds to hypothetical signalling pathways. Dotted lines divide both the THP-1 and MCF-7 cellular models, as well as, the CXCL12-CXCR4 and CCL3-CCR1/5 signalling axis. All proteins with faded lettering and colour were identified as not important for the respective signalling pathways studied in this thesis.

In conclusion although chemokines can be promiscuous in their receptor binding, their downstream cellular responses can vary substantially depending on the chemokine ligand and cell type. Identifying key cell and chemokine specific molecular mechanisms which are important for the progression of

cancer would allow the opportunity to develop and tailor more targeted treatments for patients diagnosed with higher stage tumours (such as stages II and III) to either prevent or slow down metastasis.

6.4 Future work

One of the biggest drawbacks with the research output from this thesis was the lack of characterisation of the downstream signalling pathway for carcinoma cell migration. Therefore future work would be to use alternative cell migration assays such as Oris^{TM}, Boyden chamber and possibly time lapse to establish the functional importance of microtubule stabilisation, Arp2/3, DOCK1/2/5 and FAK on the migration of MCF-7, PC-3 and MDA-MB-231 cells in response to CCL3, CCL2 and CXCL12.

Although the effects of CK666 and Taxol were assessed on CCL3 and CXCL12 intracellular calcium signalling in THP-1 cells their impact on chemotaxis was not established. In THP-1 cells, intracellular calcium signalling appears not be essential for chemotaxis and as such the roles of Arp2/3 and the microtubules may still be important for CCL3 and CXCL12 migration.

DOCK1/2/5 is a potential therapeutic target for the chemotaxis of T-cell leukaemia towards CXCL12. Therefore further target validation of this pathway would be worthwhile. One of the most important controls would be to confirm that the blockade of DOCK1/2/5 with CPYPP inhibits Rac activation. Following this experiment it would be interesting to further interrogate the importance of the different DOCK A subfamily members using siRNA, peptides or more specific DOCK1 and DOCK5 small molecule inhibitors such as TBOPP [588] and C21 [589, 590] respectively. This would allow the elucidation of more subtle differences in the downstream signalling pathway and increase the reliability of the findings presented in this thesis, particularly as CPYPP has been shown to inhibit another GEF, TRIO [589]. Finally, DOCK1/2/5 are known to be regulated by ELMO and Crk [591, 592], thus exploring the upstream molecular mechanisms could identify additional therapeutic targets which could be beneficial should resistance to DOCK1/2/5 blockade arise.

Abbreviations

7TM	Seven transmembrane α-helical domain
AC	Adenylate cyclase
ACKR	Atypical chemokine receptor
AML	Acute myeloid leukaemia
ANOVA	Analysis of variance
Arp2/3	Actin-related protein 2/3
AS	Agarose spot assay
ATP	Adenosine triphosphate
BSA	Bovine serum albumin
cAMP	Cyclic adenosine monophosphate
CCL	CC motif chemokine ligand
CCR	CC motif chemokine receptor
CD8 T	CD8 T-cells
CHO	Chinese hamster ovaries
CTCF	Corrected total cellular fluorescence
CTX	Chemotaxis assay
CXCL	CXC motif chemokine ligand
CXCR	CXC motif chemokine receptor
DAG	Diacyl-glycerol
DMEM	Dulbecco's Modified Eagle's Medium
DMSO	Dimethyl sulfoxide
DOCK	Dedicator of cytokinesis
EC_{50}	Concentration of agonist which produces 50% of the maximal biological response
ECM	Extracellular matrix
EDTA	Ethylenediaminetetraacetic acid
ELMO	Engulfment and Cell Motility
ENA/VASP	Enabled/Vasodilator-stimulated phosphoprotein

ER	Endoplasmic reticulum
ERK	Extracellular signal-regulated kinase
ETOH	Ethanol
FA	Focal adhesion
FAK	Focal adhesion kinase
FAT	Focal adhesion targeting
F-actin	Actin filaments
FCS	Foetal calf serum
FDA	Food and Drug Administration
FERM	Four-point-one, Ezrin, Radixin, Moesin
GAG	Glycosaminoglycans
GAP	GTPase activating protein
GDP	Guanosine diphosphate
GTP	Guanosine triphosphate
GEF	Guanine nucleotide exchange factors
GFP	Green fluorescent protein
GPCR	G-protein coupled receptor
Grb	Growth factor receptor-bound protein 2
Grk	G-protein receptor kinase
GTP	Guanosine triphosphate
G-actin	Globular actin
G-protein	Guanine nucleotide-binding protein
HEK	Human embryonic kidney
HTLA	HEK293 cell line stably expressing a tTA-dependent luciferase reporter and a β-arrestin2-TEV fusion gene
IC_{50}	Inhibitor concentration which inhibits 50% of the maximal biological response
IP_3	Inositol 1,4,5-triphosphate
IRSp53	Insulin receptor tyrosine kinase substrate p53
JAK-STAT	Janus-family tyrosine kinase-Signal transducer and activator of transcription
JNK	Jun N-terminal kinase

K_d	Concentration of ligand which occupies 50% of the total binding sites at equilibrium
K_i	Inhibitor constant
Lyn	Lck/Yes novel tyrosine kinase
MAPK	Mitogen activated protein kinases
MCF-7	Michigan Cancer Foundation-7
MDSC	Myeloid derived suppressor cells
MEK	MAPK ERK kinase
MLCK	Myosin light chain kinase
MM	Multiple myeloma
NK	Natural killer cells
PBS	Phosphate buffered saline
PC-3	Prostate cancer-3
PH	Pleckstrin Homology
PI3K	Phosphoinositide 3-kinases
PIP_2	Phosphatidylinositol 4,5-biphosphate
PIP_3	Phosphatidylinositol (3,4,5)-trisphosphate
PKC	Protein kinase C
PLC	Phospholipase C
PLC2	Phospholipase Cβ2
PTEN	Phosphatase and tensin homolog
PTX	Pertussis toxin
Raf	Rapidly Accelerated Fibrosarcoma
ROCK	Rho-associated protein kinase
RPM	revolutions per minute
RPMI	Roswell Park Memorial Institute
SH2	Src-homology-2
SH3	Src-homology-3
SRC	Sarcoma non-receptor tyrosine kinase
SYK	Spleen tyrosine kinase
TAM	Tumour associated macrophages

Th1	Type 1 helper T-cells
Treg	Regulatory T-cells
WASP	Wiskott–Aldrich Syndrome protein
WAVE	WASP-family verprolin-homologous
WH	Wound healing assay

References

1. Radák, Z., *The Physiology of Physical Training*. 2018: Academic Press.
2. Berg, J., J. Tymoczko, and L. Stryer, *Cells can respond to changes in their environments*. 2002, New York: WH Freeman.
3. Alberts, B., et al., *General principles of cell communication*, in *Molecular Biology of the Cell. 4th edition*. 2002, Garland Science.
4. Hancock, J.T., *Cell signalling*. 2017: Oxford University Press.
5. Bradshaw, R.A. and E.A. Dennis, *Handbook of cell signaling*. 2009: Academic press.
6. Newton, A.C., M.D. Bootman, and J.D. Scott, *Second messengers.* Cold Spring Harbor perspectives in biology, 2016. **8**(8): p. a005926.
7. Lohrmann, J. and K. Harter, *Plant two-component signaling systems and the role of response regulators.* Plant physiology, 2002. **128**(2): p. 363-369.
8. Pohorille, A., K. Schweighofer, and M.A. Wilson, *The origin and early evolution of membrane channels.* Astrobiology, 2005. **5**(1): p. 1-17.
9. Blackstone, N.W., *Evolution and cell physiology. 2. The evolution of cell signaling: from mitochondria to Metazoa.* American Journal of Physiology-Cell Physiology, 2013.
10. Morrison, D.K., *MAP kinase pathways.* Cold Spring Harbor perspectives in biology, 2012. **4**(11): p. a011254.
11. Cooper, G.M. and S. MA, *Functions of Cell Surface Receptors*, in *The cell: a molecular approach*. 2000, ASM press Washington, DC.
12. Zhang, W. and H.T. Liu, *MAPK signal pathways in the regulation of cell proliferation in mammalian cells.* Cell research, 2002. **12**(1): p. 9.
13. De Mendoza, A., A. Sebé-Pedrós, and I. Ruiz-Trillo, *The evolution of the GPCR signaling system in eukaryotes: modularity, conservation, and the transition to metazoan multicellularity.* Genome biology and evolution, 2014. **6**(3): p. 606-619.

14. Alberts. B, J.A., Lewis. J, Raff. M, Roberts. K, and Walter. P, *Molecular Biology of the Cell*. 2002, Garland Science.
15. Stevens, R.C., et al., *The GPCR Network: a large-scale collaboration to determine human GPCR structure and function.* Nature reviews Drug discovery, 2013. **12**(1): p. 25.
16. Palczewski, K., et al., *Crystal structure of rhodopsin: AG protein-coupled receptor.* science, 2000. **289**(5480): p. 739-745.
17. Clark, T., *G-Protein coupled receptors: answers from simulations.* Beilstein journal of organic chemistry, 2017. **13**(1): p. 1071-1078.
18. Venkatakrishnan, A., et al., *Molecular signatures of G-protein-coupled receptors.* Nature, 2013. **494**(7436): p. 185.
19. Peeters, M., et al., *Importance of the extracellular loops in G protein-coupled receptors for ligand recognition and receptor activation.* Trends in pharmacological sciences, 2011. **32**(1): p. 35-42.
20. Rovati, G.E., V. Capra, and R.R. Neubig, *The highly conserved DRY motif of class AG protein-coupled receptors: beyond the ground state.* Molecular pharmacology, 2007. **71**(4): p. 959-964.
21. Rasmussen, S.G., et al., *Crystal structure of the β 2 adrenergic receptor–Gs protein complex.* Nature, 2011. **477**(7366): p. 549.
22. Calebiro, D. and A. Godbole, *Internalization of GPCRs: implication in receptor function, physiology and diseases.* Best Practice & Research Clinical Endocrinology & Metabolism, 2018.
23. Hu, G.-M., T.-L. Mai, and C.-M. Chen, *Visualizing the GPCR Network: Classification and Evolution.* Scientific reports, 2017. **7**(1): p. 15495.
24. Fritze, O., et al., *Role of the conserved NPxxY (x) 5, 6F motif in the rhodopsin ground state and during activation.* Proceedings of the National Academy of Sciences, 2003. **100**(5): p. 2290-2295.
25. Ha, C.-E. and N. Bhagavan, *Essentials of medical biochemistry: with clinical cases*. 2011: Academic Press.
26. Milligan, G. and E. Kostenis, *Heterotrimeric G-proteins: a short history.* British journal of pharmacology, 2006. **147**(S1): p. S46-S55.
27. Woehler, A. and E.G. Ponimaskin, *G protein-mediated signaling: same receptor, multiple effectors.* Current molecular pharmacology, 2009. **2**(3): p. 237-248.

28. Wettschureck, N. and S. Offermanns, *Mammalian G proteins and their cell type specific functions.* Physiological reviews, 2005. **85**(4): p. 1159-1204.
29. Smrcka, A., *G protein βγ subunits: central mediators of G protein-coupled receptor signaling.* Cellular and molecular life sciences, 2008. **65**(14): p. 2191-2214.
30. Hilger, D., M. Masureel, and B.K. Kobilka, *Structure and dynamics of GPCR signaling complexes.* Nature structural & molecular biology, 2018. **25**(1): p. 4.
31. Stateczny, D., J. Oppenheimer, and P. Bommert, *G protein signaling in plants: minus times minus equals plus.* Current opinion in plant biology, 2016. **34**: p. 127-135.
32. Lynch, J. and J. Wang, *G protein-coupled receptor signaling in stem cells and cancer.* International journal of molecular sciences, 2016. **17**(5): p. 707.
33. Tan, Q., et al., *Structure of the CCR5 chemokine receptor–HIV entry inhibitor maraviroc complex.* Science, 2013. **341**(6152): p. 1387-1390.
34. Murphy, P.M., *Chemokines and Chemokine Receptors*, in *Clinical Immunology: Principles and Practice*. 2019, Elsevier. p. 157-170.
35. Ulvmar, M.H., E. Hub, and A. Rot, *Atypical chemokine receptors.* Experimental cell research, 2011. **317**(5): p. 556-568.
36. Phillips, R. and A. Ager, *Activation of pertussis toxin-sensitive CXCL12 (SDF-1) receptors mediates transendothelial migration of T lymphocytes across lymph node high endothelial cells.* European journal of immunology, 2002. **32**(3): p. 837-847.
37. Dwinell, M.B., et al., *SDF-1/CXCL12 regulates cAMP production and ion transport in intestinal epithelial cells via CXCR4.* American Journal of Physiology-Gastrointestinal and Liver Physiology, 2004. **286**(5): p. G844-G850.
38. Martin, D., R. Galisteo, and J.S. Gutkind, *CXCL8/IL8 stimulates vascular endothelial growth factor (VEGF) expression and the autocrine activation of VEGFR2 in endothelial cells by activating NFκB through the CBM (Carma3/Bcl10/Malt1) complex.* Journal of Biological Chemistry, 2009. **284**(10): p. 6038-6042.

39. Lagane, B., et al., *Mutation of the DRY motif reveals different structural requirements for the CC chemokine receptor 5-mediated signaling and receptor endocytosis.* Molecular pharmacology, 2005. **67**(6): p. 1966-1976.
40. Mangmool, S. and H. Kurose, *Gi/o protein-dependent and-independent actions of pertussis toxin (PTX).* Toxins, 2011. **3**(7): p. 884-899.
41. Al-Aoukaty, A., et al., *MIP-3 alpha, MIP-3 beta and fractalkine induce the locomotion and the mobilization of intracellular calcium, and activate the heterotrimeric G proteins in human natural killer cells (vol 95, pg 618, 1998).* IMMUNOLOGY, 1999. **96**(3): p. 505-505.
42. Arai, H. and I.F. Charo, *Differential regulation of G-protein-mediated signaling by chemokine receptors.* Journal of Biological Chemistry, 1996. **271**(36): p. 21814-21819.
43. Turner, M.D., et al., *Cytokines and chemokines: at the crossroads of cell signalling and inflammatory disease.* Biochimica et Biophysica Acta (BBA)-Molecular Cell Research, 2014. **1843**(11): p. 2563-2582.
44. Walz, A., et al., *Purification and amino acid sequencing of NAF, a novel neutrophil-activating factor produced by monocytes.* Biochemical and biophysical research communications, 1987. **149**(2): p. 755-761.
45. Yoshimura, T., et al., *Purification of a human monocyte-derived neutrophil chemotactic factor that has peptide sequence similarity to other host defense cytokines.* Proceedings of the National Academy of Sciences, 1987. **84**(24): p. 9233-9237.
46. Griffith, J.W., C.L. Sokol, and A.D. Luster, *Chemokines and chemokine receptors: positioning cells for host defense and immunity.* Annual review of immunology, 2014. **32**: p. 659-702.
47. Mantovani, A., *The chemokine system: redundancy for robust outputs.* Immunology today, 1999. **20**(6): p. 254-257.
48. Balkwill, F.R., *The chemokine system and cancer.* The Journal of pathology, 2012. **226**(2): p. 148-157.
49. Murphy, P.M., et al., *International union of pharmacology. XXII. Nomenclature for chemokine receptors.* Pharmacological reviews, 2000. **52**(1): p. 145-176.

50. Miller, M. and K. Mayo, *Chemokines from a structural perspective.* International journal of molecular sciences, 2017. **18**(10): p. 2088.
51. Baggiolini, M., *Chemokines in pathology and medicine.* Journal of internal medicine, 2001. **250**(2): p. 91-104.
52. Sahingur, S.E. and W.A. Yeudall, *Chemokine function in periodontal disease and oral cavity cancer.* Frontiers in immunology, 2015. **6**: p. 214.
53. Rajagopalan, L. and K. Rajarathnam, *Structural basis of chemokine receptor function—a model for binding affinity and ligand selectivity.* Bioscience reports, 2006. **26**(5): p. 325-339.
54. Crump, M.P., et al., *Solution structure and basis for functional activity of stromal cell-derived factor-1; dissociation of CXCR4 activation from binding and inhibition of HIV-1.* The EMBO journal, 1997. **16**(23): p. 6996-7007.
55. Nguyen, L.T. and H. Vogel, *Structural perspectives on antimicrobial chemokines.* Frontiers in immunology, 2012. **3**: p. 384.
56. Kleist, A.B., et al., *New paradigms in chemokine receptor signal transduction: Moving beyond the two-site model.* Biochemical pharmacology, 2016. **114**: p. 53-68.
57. Scholten, D., et al., *Pharmacological modulation of chemokine receptor function.* British journal of pharmacology, 2012. **165**(6): p. 1617-1643.
58. Allen, S.J., S.E. Crown, and T.M. Handel, *Chemokine: receptor structure, interactions, and antagonism.* Annu. Rev. Immunol., 2007. **25**: p. 787-820.
59. Laurence, J.S., et al., *Importance of basic residues and quaternary structure in the function of MIP-1β: CCR5 binding and cell surface sugar interactions.* Biochemistry, 2001. **40**(16): p. 4990-4999.
60. Ma, Y.-C., et al., *Src tyrosine kinase is a novel direct effector of G proteins.* Cell, 2000. **102**(5): p. 635-646.
61. Xing, Z., et al., *Direct interaction of v-Src with the focal adhesion kinase mediated by the Src SH2 domain.* Molecular biology of the cell, 1994. **5**(4): p. 413-421.

62. Westhoff, M., et al., *SRC-mediated phosphorylation of focal adhesion kinase couples actin and adhesion dynamics to survival signaling.* Molecular and cellular biology, 2004. **24**(18): p. 8113-8133.
63. Zou, J.X., et al., *Activated SRC oncogene phosphorylates R-ras and suppresses integrin activity.* Journal of Biological Chemistry, 2002. **277**(3): p. 1824-1827.
64. Tran, N.H. and J.A. Frost, *Phosphorylation of Raf-1 by p21-activated kinase 1 and Src regulates Raf-1 autoinhibition.* Journal of Biological Chemistry, 2003. **278**(13): p. 11221-11226.
65. Rexer, B., et al., *Intracellular Src Family Kinases Mediate PI3K-Akt Pathway Activation and Resistance to Lapatinib in HER2-Overexpressing Human Breast Cancer Cells*. 2009, AACR.
66. Riggins, R.B., et al., *Src-Dependent Association of Cas and p85 Phosphatidylinositol 3'-Kinase in v-crk-Transformed Cells1 1 Thomas F. Jeffress and Kate Miller Jeffress Memorial Trust (J-556) and the National Science Foundation (MCB-9723820 and MCB-0078022) to AHB Note: RBR and RMD contributed equally to this work.* Molecular cancer research, 2003. **1**(6): p. 428-437.
67. Yang, W.-R., et al., *PI3K/Akt activated by GPR30 and Src regulates 17β-estradiol-induced cultured immature boar Sertoli cells proliferation.* Reproductive Sciences, 2017. **24**(1): p. 57-66.
68. Zhao, X. and J.-L. Guan, *Focal adhesion kinase and its signaling pathways in cell migration and angiogenesis.* Advanced drug delivery reviews, 2011. **63**(8): p. 610-615.
69. Chang, F., et al., *Involvement of PI3K/Akt pathway in cell cycle progression, apoptosis, and neoplastic transformation: a target for cancer chemotherapy.* Leukemia, 2003. **17**(3): p. 590.
70. Reif, S., et al., *The role of focal adhesion kinase-phosphatidylinositol 3-kinase-akt signaling in hepatic stellate cell proliferation and type I collagen expression.* Journal of Biological Chemistry, 2003. **278**(10): p. 8083-8090.
71. Chen, H.-C., et al., *Phosphorylation of tyrosine 397 in focal adhesion kinase is required for binding phosphatidylinositol 3-kinase.* Journal of Biological Chemistry, 1996. **271**(42): p. 26329-26334.

72. Reiske, H.R., et al., *Requirement of phosphatidylinositol 3-kinase in focal adhesion kinase-promoted cell migration.* Journal of Biological Chemistry, 1999. **274**(18): p. 12361-12366.
73. Igishi, T., et al., *Divergent signaling pathways link focal adhesion kinase to mitogen-activated protein kinase cascades evidence for a role of paxillin in C-jun NH2-terminal kinase activation.* Journal of Biological Chemistry, 1999. **274**(43): p. 30738-30746.
74. Wu, D., G.J. LaRosa, and M.I. Simon, *G protein-coupled signal transduction pathways for interleukin-8.* Science, 1993. **261**(5117): p. 101-103.
75. Wu, D., A. Katz, and M.I. Simon, *Activation of phospholipase C beta 2 by the alpha and beta gamma subunits of trimeric GTP-binding protein.* Proceedings of the National Academy of Sciences, 1993. **90**(11): p. 5297-5301.
76. Johnson, J.E., J. Giorgione, and A.C. Newton, *The C1 and C2 domains of protein kinase C are independent membrane targeting modules, with specificity for phosphatidylserine conferred by the C1 domain.* Biochemistry, 2000. **39**(37): p. 11360-11369.
77. Ueda, Y., et al., *Protein kinase C δ activates the MEK-ERK pathway in a manner independent of Ras and dependent on Raf.* Journal of Biological Chemistry, 1996. **271**(38): p. 23512-23519.
78. Kolch, W., et al., *Protein kinase Cα activates RAF-1 by direct phosphorylation.* Nature, 1993. **364**(6434): p. 249.
79. Monick, M.M., et al., *Protein kinase C ζ plays a central role in activation of the p42/44 mitogen-activated protein kinase by endotoxin in alveolar macrophages.* The Journal of Immunology, 2000. **165**(8): p. 4632-4639.
80. Lee, J.Y., et al., *Inhibition of PI3K binding to activators by serine phosphorylation of PI3K regulatory subunit p85α Src homology-2 domains.* Proceedings of the National Academy of Sciences, 2011. **108**(34): p. 14157-14162.
81. Hsu, A.H., et al., *Crosstalk between PKCα and PI3K/AKT Signaling Is Tumor Suppressive in the Endometrium.* Cell reports, 2018. **24**(3): p. 655-669.

82. Lorenzen, E., et al., *G protein subtype–specific signaling bias in a series of CCR5 chemokine analogs.* Sci. Signal., 2018. **11**(552): p. eaao6152.
83. Leopoldt, D., et al., *Gβγ stimulates phosphoinositide 3-kinase-γ by direct interaction with two domains of the catalytic p110 subunit.* Journal of Biological Chemistry, 1998. **273**(12): p. 7024-7029.
84. Fogh, B.S., H.A. Multhaupt, and J.R. Couchman, *Protein kinase C, focal adhesions and the regulation of cell migration.* Journal of Histochemistry & Cytochemistry, 2014. **62**(3): p. 172-184.
85. O'Neill, A.K., et al., *Protein kinase Cα promotes cell migration through a PDZ-dependent interaction with its novel substrate discs large homolog 1 (DLG1).* Journal of Biological Chemistry, 2011. **286**(50): p. 43559-43568.
86. Harrington, E.O., et al., *Enhancement of migration by protein kinase Cα and inhibition of proliferation and cell cycle progression by protein kinase Cδ in capillary endothelial cells.* Journal of Biological Chemistry, 1997. **272**(11): p. 7390-7397.
87. Li, Z., et al., *Roles of PLC-β2 and-β3 and PI3Kγ in chemoattractant-mediated signal transduction.* Science, 2000. **287**(5455): p. 1046-1049.
88. Soldevila, G. and E.A. García-Zepeda, *The role of the Jak-Stat pathway in chemokine-mediated signaling in T lymphocytes.* Signal Transduction, 2007. **7**(5-6): p. 427-438.
89. Soriano, S.F., et al., *Chemokines integrate JAK/STAT and G-protein pathways during chemotaxis and calcium flux responses.* European journal of immunology, 2003. **33**(5): p. 1328-1333.
90. Marrero, M.B., et al., *Direct stimulation of Jak/STAT pathway by the angiotensin II AT1 receptor.* Nature, 1995. **375**(6528): p. 247.
91. Sasaguri, T., et al., *Linkage between α1 adrenergic receptor and the Jak/STAT signaling pathway in vascular smooth muscle cells.* Biochemical and biophysical research communications, 2000. **268**(1): p. 25-30.
92. DeFea, K., et al., *β-Arrestin–dependent endocytosis of proteinase-activated receptor 2 is required for intracellular targeting of activated ERK1/2.* The Journal of cell biology, 2000. **148**(6): p. 1267-1282.

93. McDonald, P.H., et al., *β-Arrestin 2: a receptor-regulated MAPK scaffold for the activation of JNK3.* Science, 2000. **290**(5496): p. 1574-1577.
94. Jørgensen, A.S., M.M. Rosenkilde, and G.M. Hjortø, *Biased signaling of G protein-coupled receptors–From a chemokine receptor CCR7 perspective.* General and comparative endocrinology, 2018. **258**: p. 4-14.
95. Bologna, Z., et al., *Biased G protein-coupled receptor signaling: new player in modulating physiology and pathology.* Biomolecules & therapeutics, 2017. **25**(1): p. 12.
96. Corbisier, J., et al., *Biased signaling at chemokine receptors.* Journal of Biological Chemistry, 2015: p. jbc. M114. 596098.
97. Zweemer, A.J., et al., *Bias in chemokine receptor signalling.* Trends in immunology, 2014. **35**(6): p. 243-252.
98. Zidar, D.A., et al., *Selective engagement of G protein coupled receptor kinases (GRKs) encodes distinct functions of biased ligands.* Proceedings of the National Academy of Sciences, 2009. **106**(24): p. 9649-9654.
99. Nandagopal, S., D. Wu, and F. Lin, *Combinatorial guidance by CCR7 ligands for T lymphocytes migration in co-existing chemokine fields.* PloS one, 2011. **6**(3): p. e18183.
100. Ricart, B.G., et al., *Dendritic cells distinguish individual chemokine signals through CCR7 and CXCR4.* The Journal of Immunology, 2010: p. 1002358.
101. Cheng, Z.-J., et al., *β-arrestin differentially regulates the chemokine receptor CXCR4-mediated signaling and receptor internalization, and this implicates multiple interaction sites between β-arrestin and CXCR4.* Journal of Biological Chemistry, 2000. **275**(4): p. 2479-2485.
102. Rajagopal, S., et al., *β-arrestin-but not G protein-mediated signaling by the "decoy" receptor CXCR7.* Proceedings of the National Academy of Sciences, 2010. **107**(2): p. 628-632.
103. Smith, J.S., R.J. Lefkowitz, and S. Rajagopal, *Biased signalling: from simple switches to allosteric microprocessors.* Nature Reviews Drug Discovery, 2018. **17**(4): p. 243.

104. Drury, L.J., et al., *Monomeric and dimeric CXCL12 inhibit metastasis through distinct CXCR4 interactions and signaling pathways.* Proceedings of the National Academy of Sciences, 2011. **108**(43): p. 17655-17660.
105. Stephens, B. and T.M. Handel, *Chemokine receptor oligomerization and allostery*, in *Progress in molecular biology and translational science*. 2013, Elsevier. p. 375-420.
106. Sierro, F., et al., *Disrupted cardiac development but normal hematopoiesis in mice deficient in the second CXCL12/SDF-1 receptor, CXCR7.* Proceedings of the National Academy of Sciences, 2007. **104**(37): p. 14759-14764.
107. Le, Y., et al., *Chemokines and chemokine receptors: their manifold roles in homeostasis and disease.* Cell Mol Immunol, 2004. **1**(2): p. 95-104.
108. Sokol, C.L. and A.D. Luster, *The chemokine system in innate immunity.* Cold Spring Harbor perspectives in biology, 2015. **7**(5): p. a016303.
109. Esche, C., C. Stellato, and L.A. Beck, *Chemokines: key players in innate and adaptive immunity.* Journal of Investigative Dermatology, 2005. **125**(4): p. 615-628.
110. Salazar-Mather, T. and K. Hokeness, *Cytokine and chemokine networks: pathways to antiviral defense*, in *Chemokines and viral infection*. 2006, Springer. p. 29-46.
111. Proudfoot, A.E., et al., *Glycosaminoglycan binding and oligomerization are essential for the in vivo activity of certain chemokines.* Proceedings of the National Academy of Sciences, 2003. **100**(4): p. 1885-1890.
112. Murphy, P.M., *Viral exploitation and subversion of the immune system through chemokine mimicry.* Nature immunology, 2001. **2**(2): p. 116.
113. White, G.E., A.J. Iqbal, and D.R. Greaves, *CC chemokine receptors and chronic inflammation—therapeutic opportunities and pharmacological challenges.* Pharmacological reviews, 2013. **65**(1): p. 47-89.
114. Charo, I.F. and R.M. Ransohoff, *The many roles of chemokines and chemokine receptors in inflammation.* New England Journal of Medicine, 2006. **354**(6): p. 610-621.

115. Zlotnik, A., A.M. Burkhardt, and B. Homey, *Homeostatic chemokine receptors and organ-specific metastasis.* Nature reviews Immunology, 2011. **11**(9): p. 597-606.
116. Williams, J.L., D.W. Holman, and R.S. Klein, *Chemokines in the balance: maintenance of homeostasis and protection at CNS barriers.* Frontiers in cellular neuroscience, 2014. **8**: p. 154.
117. Anders, H.-J., P. Romagnani, and A. Mantovani, *Pathomechanisms: homeostatic chemokines in health, tissue regeneration, and progressive diseases.* Trends in molecular medicine, 2014. **20**(3): p. 154-165.
118. Sugiyama, T., et al., *Maintenance of the hematopoietic stem cell pool by CXCL12-CXCR4 chemokine signaling in bone marrow stromal cell niches.* Immunity, 2006. **25**(6): p. 977-988.
119. Schilling, M., et al., *Turn-over of meningeal and perivascular macrophages in the brain of MCP-1-, CCR-2-or double knockout mice.* Experimental neurology, 2009. **219**(2): p. 583-585.
120. López-Pacheco, C., et al., *CCR9 is a key regulator of early phases of allergic airway inflammation.* Mediators of inflammation, 2016. **2016**.
121. Grayson, M.H. and M.J. Holtzman, *Chemokine signaling regulates apoptosis as well as immune cell traffic in host defense.* Cell Cycle, 2006. **5**(4): p. 380-383.
122. Mantovani, A., et al., *The chemokine system in diverse forms of macrophage activation and polarization.* Trends in immunology, 2004. **25**(12): p. 677-686.
123. Strieter, R.M., et al., *The functional role of the ELR motif in CXC chemokine-mediated angiogenesis.* Journal of Biological Chemistry, 1995. **270**(45): p. 27348-27357.
124. Sarmiento, J., et al., *Diverging mechanisms of activation of chemokine receptors revealed by novel chemokine agonists.* PloS one, 2011. **6**(12): p. e27967.
125. Tachibana, K., et al., *The chemokine receptor CXCR4 is essential for vascularization of the gastrointestinal tract.* Nature, 1998. **393**(6685): p. 591.

126. Gupta, S.K., et al., *Chemokine receptors in human endothelial cells functional expression of cxcr4 and its transcriptional regulation by inflammatory cytokines.* Journal of Biological Chemistry, 1998. **273**(7): p. 4282-4287.
127. Godessart, N. and S.L. Kunkel, *Chemokines in autoimmune disease.* Current opinion in immunology, 2001. **13**(6): p. 670-675.
128. Zernecke, A. and C. Weber, *Chemokines in atherosclerosis: proceedings resumed.* Arteriosclerosis, thrombosis, and vascular biology, 2014. **34**(4): p. 742-750.
129. Kryczek, I., et al., *Stromal derived factor (SDF-1/CXCL12) and human tumor pathogenesis.* American Journal of Physiology-Cell Physiology, 2007.
130. Müller, A., et al., *Involvement of chemokine receptors in breast cancer metastasis.* nature, 2001. **410**(6824): p. 50-56.
131. Chow, M.T. and A.D. Luster, *Chemokines in cancer.* Cancer immunology research, 2014. **2**(12): p. 1125-1131.
132. Allegretti, M., et al., *Current status of chemokine receptor inhibitors in development.* Immunology letters, 2012. **145**(1): p. 68-78.
133. Schall, T.J. and A.E. Proudfoot, *Overcoming hurdles in developing successful drugs targeting chemokine receptors.* Nature Reviews Immunology, 2011. **11**(5): p. 355.
134. Aman, A. and T. Piotrowski, *Cell migration during morphogenesis.* Developmental biology, 2010. **341**(1): p. 20-33.
135. Gonzalez, A.C.d.O., et al., *Wound healing-A literature review.* Anais brasileiros de dermatologia, 2016. **91**(5): p. 614-620.
136. Madri, J.A. and D. Graesser, *Cell migration in the immune system: the evolving inter-related roles of adhesion molecules and proteinases.* Journal of Immunology Research, 2000. **7**(2-4): p. 103-116.
137. Kriegstein, A.R., *Constructing circuits: neurogenesis and migration in the developing neocortex.* Epilepsia, 2005. **46**: p. 15-21.
138. Friedl, P. and K. Wolf, *Plasticity of cell migration: a multiscale tuning model.* The Journal of cell biology, 2010. **188**(1): p. 11-19.

139. Titus, M.A. and H.V. Goodson, *An evolutionary perspective on cell migration: Digging for the roots of amoeboid motility.* J Cell Biol, 2017. **216**(6): p. 1509-1511.
140. Paňková, K., et al., *The molecular mechanisms of transition between mesenchymal and amoeboid invasiveness in tumor cells.* Cellular and molecular life sciences, 2010. **67**(1): p. 63-71.
141. Clark, A.G. and D.M. Vignjevic, *Modes of cancer cell invasion and the role of the microenvironment.* Current opinion in cell biology, 2015. **36**: p. 13-22.
142. Bear, J.E. and J.M. Haugh, *Directed migration of mesenchymal cells: where signaling and the cytoskeleton meet.* Current opinion in cell biology, 2014. **30**: p. 74-82.
143. Lodish. H., B.A., Zipursky L.S., Matsudaira. P., Baltimore. D. and Darnell. J., *Molecular Cell Biology*. 4th edition ed. 2000: New York: W. H. Freeman.
144. Pollard, T.D. and G.G. Borisy, *Cellular motility driven by assembly and disassembly of actin filaments.* Cell, 2003. **112**(4): p. 453-465.
145. Ireton, K., *Molecular mechanisms of cell–cell spread of intracellular bacterial pathogens.* Open biology, 2013. **3**(7): p. 130079.
146. Mechanobiology Institute, N.U.o.S. *How do actin filaments grow?* 2018 [cited 2019; Available from: https://www.mechanobio.info/cytoskeleton-dynamics/what-is-the-cytoskeleton/what-are-actin-filaments/how-do-actin-filaments-grow.
147. Pollard, T.D., et al., *Section IX: Cytoskeleton and Cellular Motility*, in *Cell Biology International Edition*. 2016, Elsevier Health Sciences. p. 575-591.
148. Dominguez, R. and K.C. Holmes, *Actin structure and function.* 2011.
149. Shekhar, S., J. Pernier, and M.-F. Carlier, *Regulators of actin filament barbed ends at a glance.* J Cell Sci, 2016. **129**(6): p. 1085-1091.
150. Pollard, T.D., *Regulation of actin filament assembly by Arp2/3 complex and formins.* Annu. Rev. Biophys. Biomol. Struct., 2007. **36**: p. 451-477.
151. Lämmermann, T. and M. Sixt, *Mechanical modes of 'amoeboid'cell migration.* Current opinion in cell biology, 2009. **21**(5): p. 636-644.

152. Shankar, J., et al., *Pseudopodial actin dynamics control epithelial-mesenchymal transition in metastatic cancer cells.* Cancer research, 2010. **70**(9): p. 3780-3790.
153. Mattila, P.K. and P. Lappalainen, *Filopodia: molecular architecture and cellular functions.* Nature reviews Molecular cell biology, 2008. **9**(6): p. 446.
154. Mogilner, A. and B. Rubinstein, *The physics of filopodial protrusion.* Biophysical journal, 2005. **89**(2): p. 782-795.
155. Krause, M. and A. Gautreau, *Steering cell migration: lamellipodium dynamics and the regulation of directional persistence.* Nature reviews Molecular cell biology, 2014. **15**(9): p. 577.
156. Oikawa, T., et al., *PtdIns (3, 4, 5) P 3 binding is necessary for WAVE2-induced formation of lamellipodia.* Nature cell biology, 2004. **6**(5): p. 420.
157. Arjonen, A., R. Kaukonen, and J. Ivaska, *Filopodia and adhesion in cancer cell motility.* Cell adhesion & migration, 2011. **5**(5): p. 421-430.
158. Faix, J., et al., *Filopodia: Complex models for simple rods.* The international journal of biochemistry & cell biology, 2009. **41**(8-9): p. 1656-1664.
159. Miki, H., et al., *IRSp53 is an essential intermediate between Rac and WAVE in the regulation of membrane ruffling.* Nature, 2000. **408**(6813): p. 732.
160. Huttenlocher, A., *Cell polarization mechanisms during directed cell migration.* Nature cell biology, 2005. **7**(4): p. 336.
161. Tsai, F., Kuo, GH., Chang, SW, and Tsai PJ, *Ca2+ Signaling in Cytoskeletal Reorganization, Cell Migration, and Cancer Metastasis.* BioMed Research International, 2015. **2015**: p. 13.
162. Merlot, S. and R.A. Firtel, *Leading the way: directional sensing through phosphatidylinositol 3-kinase and other signaling pathways.* Journal of cell science, 2003. **116**(17): p. 3471-3478.
163. Haugh, J.M., et al., *Spatial sensing in fibroblasts mediated by 3′ phosphoinositides.* The Journal of cell biology, 2000. **151**(6): p. 1269-1280.

164. Servant, G., et al., *Polarization of chemoattractant receptor signaling during neutrophil chemotaxis.* Science, 2000. **287**(5455): p. 1037-1040.
165. Meili, R., et al., *Chemoattractant-mediated transient activation and membrane localization of Akt/PKB is required for efficient chemotaxis to cAMP in Dictyostelium.* The EMBO journal, 1999. **18**(8): p. 2092-2105.
166. Martin, K.J., et al., *The role of phosphoinositide 3-kinases in neutrophil migration in 3D collagen gels.* PloS one, 2015. **10**(2): p. e0116250.
167. Funamoto, S., et al., *Role of Phosphatidylinositol 3' Kinase and a Downstream Pleckstrin Homology Domain–Containing Protein in Controlling Chemotaxis inDictyostelium.* The Journal of cell biology, 2001. **153**(4): p. 795-810.
168. Insall, R.H. and O.D. Weiner, *PIP3, PIP2, and cell movement—similar messages, different meanings?* Developmental cell, 2001. **1**(6): p. 743-747.
169. Krishnan, K. and P.D. Moens, *Structure and functions of profilins.* Biophysical reviews, 2009. **1**(2): p. 71-81.
170. Hoeller, O. and R.R. Kay, *Chemotaxis in the absence of PIP3 gradients.* Current Biology, 2007. **17**(9): p. 813-817.
171. Wang, Y., C.L. Chen, and M. Iijima, *Signaling mechanisms for chemotaxis.* Development, growth & differentiation, 2011. **53**(4): p. 495-502.
172. Wei, C., et al., *Calcium gradients underlying cell migration.* Current opinion in cell biology, 2012. **24**(2): p. 254-261.
173. Holinstat, M., et al., *Protein kinase Cα-induced p115RhoGEF phosphorylation signals endothelial cytoskeletal rearrangement.* Journal of Biological Chemistry, 2003. **278**(31): p. 28793-28798.
174. Komatsu, S. and M. Ikebe, *The Phosphorylation of Myosin II at the Ser1 and Ser2 Is Critical for Normal Platelet-derived Growth Factor–induced Reorganization of Myosin Filaments.* Molecular biology of the cell, 2007. **18**(12): p. 5081-5090.
175. Anilkumar, N., et al., *Interaction of fascin and protein kinase Cα: a novel intersection in cell adhesion and motility.* The EMBO journal, 2003. **22**(20): p. 5390-5402.

176. Mechanobiology Institute, N.U.o.S. *What is the role of Rho GTPases in the regulation of focal adhesion assembly?*. 2018 [cited 2019; Available from: https://www.mechanobio.info/what-is-mechanosignaling/what-is-the-extracellular-matrix-and-the-basal-lamina/what-are-focal-adhesions/what-is-the-role-of-rho-gtpases-in-the-regulation-of-focal-adhesion-assembly/.
177. Barry, D.M., et al., *Cdc42 is required for cytoskeletal support of endothelial cell adhesion during blood vessel formation in mice.* Development, 2015. **142**(17): p. 3058-3070.
178. Guo, F., et al., *Genetic deletion of Rac1 GTPase reveals its critical role in actin stress fiber formation and focal adhesion complex assembly.* Journal of Biological Chemistry, 2006. **281**(27): p. 18652-18659.
179. Tojkander, S., G. Gateva, and P. Lappalainen, *Actin stress fibers–assembly, dynamics and biological roles.* J Cell Sci, 2012. **125**(8): p. 1855-1864.
180. Pellegrin, S. and H. Mellor, *Actin stress fibres.* Journal of cell science, 2007. **120**(20): p. 3491-3499.
181. Schwarz, U.S. and M.L. Gardel, *United we stand–integrating the actin cytoskeleton and cell–matrix adhesions in cellular mechanotransduction.* J Cell Sci, 2012. **125**(13): p. 3051-3060.
182. Gardel, M.L., et al., *Mechanical integration of actin and adhesion dynamics in cell migration.* Annual review of cell and developmental biology, 2010. **26**: p. 315-333.
183. McLeod, S.J., et al., *The Rap GTPases regulate integrin-mediated adhesion, cell spreading, actin polymerization, and Pyk2 tyrosine phosphorylation in B lymphocytes.* Journal of Biological Chemistry, 2004. **279**(13): p. 12009-12019.
184. Mueller, A. and P.G. Strange, *Mechanisms of internalization and recycling of the chemokine receptor, CCR5.* European journal of biochemistry, 2004. **271**(2): p. 243-252.
185. McEver, R.P., *Immunobiology: Dampening neutrophil integrins.* Blood, 2016. **128**(4): p. 467.
186. Burbach, B.J., et al., *T-cell receptor signaling to integrins.* Immunological reviews, 2007. **218**(1): p. 65-81.

187. Campbell, I.D. and M.J. Humphries, *Integrin structure, activation, and interactions.* Cold Spring Harbor perspectives in biology, 2011. **3**(3): p. a004994.
188. Huttenlocher, A. and A.R. Horwitz, *Integrins in cell migration.* Cold Spring Harbor perspectives in biology, 2011. **3**(9): p. a005074.
189. Truong, H. and E.H. Danen, *Integrin switching modulates adhesion dynamics and cell migration.* Cell adhesion & migration, 2009. **3**(2): p. 179-181.
190. Jacquemet, G., M.J. Humphries, and P.T. Caswell, *Role of adhesion receptor trafficking in 3D cell migration.* Current opinion in cell biology, 2013. **25**(5): p. 627-632.
191. Wang, J.-h., *Pull and push: talin activation for integrin signaling.* Cell research, 2012. **22**(11): p. 1512.
192. Lawson, C., et al., *FAK promotes recruitment of talin to nascent adhesions to control cell motility.* J Cell Biol, 2012. **196**(2): p. 223-232.
193. Serrels, B. and M.C. Frame, *FAK and talin: who is taking whom to the integrin engagement party?* J Cell Biol, 2012. **196**(2): p. 185-187.
194. Mitra, S.K., D.A. Hanson, and D.D. Schlaepfer, *Focal adhesion kinase: in command and control of cell motility.* Nature reviews Molecular cell biology, 2005. **6**(1): p. 56.
195. Frame, M.C., et al., *The FERM domain: organizing the structure and function of FAK.* Nature reviews Molecular cell biology, 2010. **11**(11): p. 802.
196. Zhou, J., et al., *Allosteric regulation of focal adhesion kinase by PIP2 and ATP.* Biophysical journal, 2015. **108**(3): p. 698-705.
197. Lawson, C. and D. Schlaepfer, *Integrin adhesions: Who's on first? What's on second?* Cell adhesion & migration, 2012. **6**(4): p. 302-306.
198. Schaller, M.D., et al., *Autophosphorylation of the focal adhesion kinase, pp125FAK, directs SH2-dependent binding of pp60src.* Molecular and cellular biology, 1994. **14**(3): p. 1680-1688.
199. Calalb, M.B., T.R. Polte, and S.K. Hanks, *Tyrosine phosphorylation of focal adhesion kinase at sites in the catalytic domain regulates kinase activity: a role for Src family kinases.* Molecular and cellular biology, 1995. **15**(2): p. 954-963.

200. López-Colomé, A.M., et al., *Paxillin: a crossroad in pathological cell migration.* Journal of hematology & oncology, 2017. **10**(1): p. 50.
201. Cho, S.Y. and R.L. Klemke, *Extracellular-regulated kinase activation and CAS/Crk coupling regulate cell migration and suppress apoptosis during invasion of the extracellular matrix.* The Journal of cell biology, 2000. **149**(1): p. 223-236.
202. Cheresh, D.A., J. Leng, and R.L. Klemke, *Regulation of cell contraction and membrane ruffling by distinct signals in migratory cells.* The Journal of cell biology, 1999. **146**(5): p. 1107-1116.
203. Vallés, A.M., M. Beuvin, and B. Boyer, *Activation of Rac1 by paxillin-Crk-DOCK180 signaling complex is antagonized by Rap1 in migrating NBT-II cells.* Journal of Biological Chemistry, 2004. **279**(43): p. 44490-44496.
204. Wu, X., et al., *Focal adhesion kinase regulation of N-WASP subcellular localization and function.* Journal of Biological Chemistry, 2004. **279**(10): p. 9565-9576.
205. Beningo, K.A., et al., *Nascent focal adhesions are responsible for the generation of strong propulsive forces in migrating fibroblasts.* The Journal of cell biology, 2001. **153**(4): p. 881-888.
206. Tan, J.L., et al., *Cells lying on a bed of microneedles: an approach to isolate mechanical force.* Proceedings of the National Academy of Sciences, 2003. **100**(4): p. 1484-1489.
207. Pankov, R., et al., *Integrin dynamics and matrix assembly.* The Journal of cell biology, 2000. **148**(5): p. 1075-1090.
208. Parsons, J.T., A.R. Horwitz, and M.A. Schwartz, *Cell adhesion: integrating cytoskeletal dynamics and cellular tension.* Nature reviews Molecular cell biology, 2010. **11**(9): p. 633.
209. Hamadi, A., et al., *Regulation of focal adhesion dynamics and disassembly by phosphorylation of FAK at tyrosine 397.* Journal of cell science, 2005. **118**(19): p. 4415-4425.
210. Webb, D.J., et al., *FAK–Src signalling through paxillin, ERK and MLCK regulates adhesion disassembly.* Nature cell biology, 2004. **6**(2): p. 154.

211. Schober, M., et al., *Focal adhesion kinase modulates tension signaling to control actin and focal adhesion dynamics.* The Journal of cell biology, 2007. **176**(5): p. 667-680.
212. del Pozo, M.A., et al., *Phospho-caveolin-1 mediates integrin-regulated membrane domain internalization.* Nature cell biology, 2005. **7**(9): p. 901.
213. Ezratty, E.J., M.A. Partridge, and G.G. Gundersen, *Microtubule-induced focal adhesion disassembly is mediated by dynamin and focal adhesion kinase.* Nature cell biology, 2005. **7**(6): p. 581.
214. Wang, Y., et al., *A direct interaction between the large GTPase dynamin-2 and FAK regulates focal adhesion dynamics in response to active Src.* Molecular biology of the cell, 2011. **22**(9): p. 1529-1538.
215. Lawson, M.A. and F.R. Maxfield, *Ca2+-and calcineurin-dependent recycling of an integrin to the front of migrating neutrophils.* Nature, 1995. **377**(6544): p. 75.
216. Franco, S.J. and A. Huttenlocher, *Regulating cell migration: calpains make the cut.* Journal of cell science, 2005. **118**(17): p. 3829-3838.
217. Chan, K.T., D.A. Bennin, and A. Huttenlocher, *Regulation of adhesion dynamics by calpain-mediated proteolysis of focal adhesion kinase (FAK).* Journal of Biological Chemistry, 2010: p. jbc. M109. 090746.
218. Cortesio, C.L., et al., *Calpain-mediated proteolysis of paxillin negatively regulates focal adhesion dynamics and cell migration.* Journal of Biological Chemistry, 2011: p. jbc. M110. 187294.
219. Giannone, G., et al., *Calcium rises locally trigger focal adhesion disassembly and enhance residency of focal adhesion kinase at focal adhesions.* Journal of Biological Chemistry, 2004. **279**(27): p. 28715-28723.
220. Carragher, N.O., et al., *A novel role for FAK as a protease-targeting adaptor protein: regulation by p42 ERK and Src.* Current Biology, 2003. **13**(16): p. 1442-1450.
221. Paul, N.R., G. Jacquemet, and P.T. Caswell, *Endocytic trafficking of integrins in cell migration.* Current Biology, 2015. **25**(22): p. R1092-R1105.

222. Desgrosellier, J.S. and D.A. Cheresh, *Integrins in cancer: biological implications and therapeutic opportunities.* Nature Reviews Cancer, 2010. **10**(1): p. 9.
223. Shin, S., L. Wolgamott, and S.-O. Yoon, *Integrin trafficking and tumor progression.* International journal of cell biology, 2012. **2012**.
224. Mitra, S.K. and D.D. Schlaepfer, *Integrin-regulated FAK–Src signaling in normal and cancer cells.* Current opinion in cell biology, 2006. **18**(5): p. 516-523.
225. Bolós, V., et al., *The dual kinase complex FAK-Src as a promising therapeutic target in cancer.* OncoTargets and therapy, 2010. **3**: p. 83.
226. Irby, R.B. and T.J. Yeatman, *Role of Src expression and activation in human cancer.* Oncogene, 2000. **19**(49): p. 5636.
227. Cooper, G.M., R.E. Hausman, and R.E. Hausman, *The Development and Causes of Cancer*, in *The cell: a molecular approach*. 2000, ASM press Washington, DC.
228. Wirtz, D., K. Konstantopoulos, and P.C. Searson, *The physics of cancer: the role of physical interactions and mechanical forces in metastasis.* Nature Reviews Cancer, 2011. **11**(7): p. 512-522.
229. Chaffer, C.L. and R.A. Weinberg, *A perspective on cancer cell metastasis.* science, 2011. **331**(6024): p. 1559-1564.
230. UK, C.R. *Former Anglia Cancer Network, 2002-2006*. 2016 [cited 2019; Available from: https://www.cancerresearchuk.org/health-professional/cancer-statistics-for-the-uk.
231. Institute, N.C. *Metastatic Cancer*. 2017 [cited 2019; Available from: https://www.cancer.gov/types/metastatic-cancer.
232. UK, C.R. *Pancreatic cancer survival statistics*. 2014 [cited 2019; Available from: https://www.cancerresearchuk.org/health-professional/cancer-statistics/statistics-by-cancer-type/pancreatic-cancer/survival#ref-0.
233. Mansoori, B., et al., *The different mechanisms of cancer drug resistance: a brief review.* Advanced pharmaceutical bulletin, 2017. **7**(3): p. 339.
234. Wang, W., et al., *Chromosomal instability and acquired drug resistance in multiple myeloma.* Oncotarget, 2017. **8**(44): p. 78234.

235. Friedman, R., *Drug resistance in cancer: molecular evolution and compensatory proliferation.* Oncotarget, 2016. **7**(11): p. 11746.
236. Vargas-Rondón, N., V. Villegas, and M. Rondón-Lagos, *The role of chromosomal instability in cancer and therapeutic responses.* Cancers, 2017. **10**(1): p. 4.
237. Comaills, V., et al., *Genomic instability is induced by persistent proliferation of cells undergoing epithelial-to-mesenchymal transition.* Cell reports, 2016. **17**(10): p. 2632-2647.
238. Bolognese, A. and L. Izzo, *Surgery in Multimodal Management of Solid Tumors*. 2009: Springer.
239. DeSantis, C.E., et al., *Cancer treatment and survivorship statistics, 2014.* CA: a cancer journal for clinicians, 2014. **64**(4): p. 252-271.
240. Uramoto, H. and F. Tanaka, *Recurrence after surgery in patients with NSCLC.* Translational lung cancer research, 2014. **3**(4): p. 242.
241. Herfarth.Ch, L.W., *Resection of recurrent liver cancer*, in *Surgical treatment: evidence-based and problem-oriented*, R.G. Holzheimer and J.A. Mannick, Editors. 2001, Zuckschwerdt.
242. Hidalgo, M., et al., *Addressing the challenges of pancreatic cancer: future directions for improving outcomes.* Pancreatology, 2015. **15**(1): p. 8-18.
243. Lee, S.B., et al., *A retrospective prognostic evaluation analysis using the 8th edition of the American Joint Committee on Cancer staging system for breast cancer.* Breast cancer research and treatment, 2018. **169**(2): p. 257-266.
244. Hess, K.R., et al., *Metastatic patterns in adenocarcinoma.* Cancer, 2006. **106**(7): p. 1624-1633.
245. Mierke, F., et al., *Impact of portal vein involvement from pancreatic cancer on metastatic pattern after surgical resection.* Annals of surgical oncology, 2016. **23**(5): p. 730-736.
246. Bissolati, M., et al., *Portal vein-circulating tumor cells predict liver metastases in patients with resectable pancreatic cancer.* Tumor Biology, 2015. **36**(2): p. 991-996.

247. Ribatti, D., G. Mangialardi, and A. Vacca, *Stephen Paget and the 'seed and soil'theory of metastatic dissemination.* Clinical and experimental medicine, 2006. **6**(4): p. 145-149.
248. Paget, S., *The distribution of secondary growths in cancer of the breast.* The Lancet, 1889. **133**(3421): p. 571-573.
249. Psaila, B. and D. Lyden, *The metastatic niche: adapting the foreign soil.* Nature Reviews Cancer, 2009. **9**(4): p. 285.
250. Coussens, L.M. and Z. Werb, *Inflammation and cancer.* Nature, 2002. **420**(6917): p. 860.
251. Dep Prete, A., et al., *Molecular pathways in cancer-related inflammation.* Biochemia medica: Biochemia medica, 2011. **21**(3): p. 264-275.
252. Allavena, P., et al., *Pathways connecting inflammation and cancer.* Current opinion in genetics & development, 2008. **18**(1): p. 3-10.
253. Helbig, G., et al., *NF-κ B promotes breast cancer cell migration and metastasis by inducing the expression of the chemokine receptor CXCR4.* Journal of biological chemistry, 2003. **278**(24): p. 21631-21638.
254. Kukreja, P., et al., *Up-regulation of CXCR4 expression in PC-3 cells by stromal-derived factor-1α (CXCL12) increases endothelial adhesion and transendothelial migration: role of MEK/ERK signaling pathway–dependent NF-κB activation.* Cancer research, 2005. **65**(21): p. 9891-9898.
255. Bai, W., et al., *Hypoxia-increased RAGE expression regulates chemotaxis and pro-inflammatory cytokines release through nuclear translocation of NF-κ B and HIF1α in THP-1 cells.* Biochemical and biophysical research communications, 2018. **495**(3): p. 2282-2288.
256. Richmond, A., *NF-κB, chemokine gene transcription and tumour growth.* Nature Reviews Immunology, 2002. **2**(9): p. 664.
257. Singha, B., H. Gatla, and I. Vancurova, *Transcriptional regulation of chemokine expression in ovarian cancer.* Biomolecules, 2015. **5**(1): p. 223-243.

258. Xiao, L.-J., et al., *Hypoxia increases CX3CR1 expression via HIF-1 and NF‐κB in androgen-independent prostate cancer cells.* International journal of oncology, 2012. **41**(5): p. 1827-1836.
259. Lin, S., et al., *Chemokine C-C motif receptor 5 and C-C motif ligand 5 promote cancer cell migration under hypoxia.* Cancer Science, 2012. **103**(5): p. 904-912.
260. Fei, M., et al., *Hypoxia promotes the migration and invasion of human hepatocarcinoma cells through the HIF-1α–IL-8–Akt axis.* Cellular & Molecular Biology Letters, 2018. **23**(1): p. 46.
261. Chatterjee, S., B.B. Azad, and S. Nimmagadda, *The intricate role of CXCR4 in cancer*, in *Advances in cancer research*. 2014, Elsevier. p. 31-82.
262. Lim, S.Y., et al., *Targeting the CCL2-CCR2 signaling axis in cancer metastasis.* Oncotarget, 2016. **7**(19): p. 28697.
263. Aldinucci, D. and A. Colombatti, *The inflammatory chemokine CCL5 and cancer progression.* Mediators of inflammation, 2014. **2014**.
264. Legler, D.F., E. Uetz-von Allmen, and M.A. Hauser, *CCR7: roles in cancer cell dissemination, migration and metastasis formation.* The international journal of biochemistry & cell biology, 2014. **54**: p. 78-82.
265. Ma, B., A. Khazali, and A. Wells, *CXCR3 in carcinoma progression.* Histology and histopathology, 2015. **30**(7): p. 781.
266. Ha, H., B. Debnath, and N. Neamati, *Role of the CXCL8-CXCR1/2 axis in cancer and inflammatory diseases.* Theranostics, 2017. **7**(6): p. 1543.
267. Nagarsheth, N., M.S. Wicha, and W. Zou, *Chemokines in the cancer microenvironment and their relevance in cancer immunotherapy.* Nature Reviews Immunology, 2017. **17**(9): p. 559.
268. Karin, N., *Chemokines and cancer: new immune checkpoints for cancer therapy.* Current opinion in immunology, 2018. **51**: p. 140-145.
269. Keeley, E.C., B. Mehrad, and R.M. Strieter, *CXC chemokines in cancer angiogenesis and metastases*, in *Advances in cancer research*. 2010, Elsevier. p. 91-111.
270. Sarvaiya, P.J., et al., *Chemokines in tumor progression and metastasis.* Oncotarget, 2013. **4**(12): p. 2171.

271. Han, T.-T., et al., *Role of chemokines and their receptors in chronic lymphocytic leukemia: function in microenvironment and targeted therapy.* Cancer biology & therapy, 2014. **15**(1): p. 3-9.
272. Till, K.J., et al., *The chemokine receptor CCR7 and α4 integrin are important for migration of chronic lymphocytic leukemia cells into lymph nodes.* Blood, 2002. **99**(8): p. 2977-2984.
273. Cho, B.-S., H.-J. Kim, and M. Konopleva, *Targeting the CXCL12/CXCR4 axis in acute myeloid leukemia: from bench to bedside.* The Korean journal of internal medicine, 2017. **32**(2): p. 248.
274. Meng, W., S. Xue, and Y. Chen, *The role of CXCL12 in tumor microenvironment.* Gene, 2018. **641**: p. 105-110.
275. Ping, Y.-f., et al., *The anti-cancer compound Nordy inhibits CXCR4-mediated production of IL-8 and VEGF by malignant human glioma cells.* Journal of Neuro-oncology, 2007. **84**(1): p. 21-29.
276. Fang, W.B., et al., *CCL2/CCR2 chemokine signaling coordinates survival and motility of breast cancer cells through Smad3 protein-and p42/44 mitogen-activated protein kinase (MAPK)-dependent mechanisms.* Journal of Biological Chemistry, 2012. **287**(43): p. 36593-36608.
277. Billadeau, D.D., et al., *Characterization of the CXCR4 signaling in pancreatic cancer cells.* Journal of Gastrointestinal Cancer, 2006. **37**(4): p. 110-119.
278. Loberg, R.D., et al., *CCL2 is a potent regulator of prostate cancer cell migration and proliferation.* Neoplasia, 2006. **8**(7): p. 578-586.
279. Roca, H., Z. Varsos, and K.J. Pienta, *CCL2 protects prostate cancer PC3 cells from autophagic death via phosphatidylinositol 3-kinase/AKT-dependent survivin up-regulation.* Journal of Biological Chemistry, 2008. **283**(36): p. 25057-25073.
280. Wang, J., C. Gareri, and H.A. Rockman, *G-Protein–Coupled Receptors in Heart Disease.* Circulation Research, 2018. **123**(6): p. 716-735.
281. Heng, B.C., D. Aubel, and M. Fussenegger, *An overview of the diverse roles of G-protein coupled receptors (GPCRs) in the pathophysiology of various human diseases.* Biotechnology advances, 2013. **31**(8): p. 1676-1694.

282. Hauser, A.S., et al., *Trends in GPCR drug discovery: new agents, targets and indications.* Nature Reviews Drug Discovery, 2017. **16**(12): p. 829.
283. Walser, T.C., et al., *Antagonism of CXCR3 inhibits lung metastasis in a murine model of metastatic breast cancer.* Cancer research, 2006. **66**(15): p. 7701-7707.
284. Xiang, J., et al., *CXCR4 Protein Epitope Mimetic Antagonist, POL5551, Disrupts Metastasis and Enhances Chemotherapy Effect in Triple Negative Breast Cancer.* Molecular cancer therapeutics, 2015: p. molcanther. 0252.2015.
285. Peng, S.-B., et al., *Identification of LY2510924, a novel cyclic peptide CXCR4 antagonist that exhibits antitumor activities in solid tumor and breast cancer metastatic models.* Molecular cancer therapeutics, 2015. **14**(2): p. 480-490.
286. Huang, E.H., et al., *A cxcr4 antagonist ctce-9908 inhibits primary tumor growth and metastasis of breast cancer1.* Journal of Surgical Research, 2009. **155**(2): p. 231-236.
287. Loberg, R.D., et al., *Targeting CCL2 with systemic delivery of neutralizing antibodies induces prostate cancer tumor regression in vivo.* Cancer research, 2007. **67**(19): p. 9417-9424.
288. Wilson, C., et al., *Constitutive and treatment-induced CXCL8-signalling selectively modulates the efficacy of anti-metabolite therapeutics in metastatic prostate cancer.* PLoS One, 2012. **7**(5): p. e36545.
289. Habringer, S., et al., *Dual targeting of acute leukemia and supporting niche by CXCR4-directed theranostics.* Theranostics, 2018. **8**(2): p. 369.
290. Tavor, S., et al., *CXCR4 regulates migration and development of human acute myelogenous leukemia stem cells in transplanted NOD/SCID mice.* Cancer research, 2004. **64**(8): p. 2817-2824.
291. Jacquelot, N., et al., *Targeting chemokines and chemokine receptors in melanoma and other cancers.* Frontiers in immunology, 2018. **9**: p. 2480.

292. Lazennec, G. and A. Richmond, *Chemokines and chemokine receptors: new insights into cancer-related inflammation.* Trends in molecular medicine, 2010. **16**(3): p. 133-144.
293. De Clercq, E., *Mozobil®(Plerixafor, AMD3100), 10 years after its approval by the US Food and Drug Administration.* Antiviral Chemistry and Chemotherapy, 2019. **27**: p. 2040206619829382.
294. DiPersio, J.F., et al., *Phase III prospective randomized double-blind placebo-controlled trial of plerixafor plus granulocyte colony-stimulating factor compared with placebo plus granulocyte colony-stimulating factor for autologous stem-cell mobilization and transplantation for patients with non-Hodgkin's lymphoma.* Journal of Clinical Oncology, 2009. **27**(28): p. 4767-4773.
295. Uy, G.L., et al., *A phase I/II study of chemosensitization with the CXCR4 antagonist plerixafor in relapsed or refractory acute myeloid leukemia.* Blood, 2012: p. blood-2011-10-383406.
296. Karpova, D., et al., *Potent Stem Cell Mobilization with the Novel CXCR4 Antagonist POL6326-Results of a Phase IIa Dose Escalation Study in Comparison to G-CSF*. 2015, Am Soc Hematology.
297. Setia, G., et al., *A Phase II, Open-Label Pilot Study to Evaluate the Hematopoietic Stem Cell Mobilization of TG-0054 Combined with G-CSF in 12 Patients with Multiple Myeloma, Non-Hodgkin Lymphoma or Hodgkin Lymphoma-an Interim Analysis*. 2015, Am Soc Hematology.
298. Salgia, R., et al., *A randomized phase II study of LY2510924 and carboplatin/etoposide versus carboplatin/etoposide in extensive-disease small cell lung cancer.* Lung Cancer, 2017. **105**: p. 7-13.
299. Hainsworth, J.D., et al., *A randomized, open-label phase 2 study of the CXCR4 inhibitor LY2510924 in combination with sunitinib versus sunitinib alone in patients with metastatic renal cell carcinoma (RCC).* Targeted oncology, 2016. **11**(5): p. 643-653.
300. Schott, A.F., et al., *Phase Ib pilot study to evaluate reparixin in combination with weekly paclitaxel in patients with HER-2–negative metastatic breast cancer.* Clinical Cancer Research, 2017.
301. Yoshie, O. and K. Matsushima, *CCR4 and its ligands: from bench to bedside.* International immunology, 2014. **27**(1): p. 11-20.

302. Administration, U.S.F.a.D. *FDA approves treatment for two rare types of non-Hodgkin lymphoma*. 2018 [cited 2019; Available from: https://www.fda.gov/NewsEvents/Newsroom/PressAnnouncements/ucm616176.htm.
303. Agency, E.M., *EU/3/16/1756*. 2018.
304. Vela, M., et al., *Chemokine receptor-specific antibodies in cancer immunotherapy: achievements and challenges.* Frontiers in immunology, 2015. **6**.
305. Loberg, R.D., et al., *CCL2 as an important mediator of prostate cancer growth in vivo through the regulation of macrophage infiltration.* Neoplasia, 2007. **9**(7): p. 556-562.
306. Fujimoto, H., et al., *Stromal MCP-1 in mammary tumors induces tumor-associated macrophage infiltration and contributes to tumor progression.* International journal of cancer, 2009. **125**(6): p. 1276-1284.
307. Pienta, K.J., et al., *Phase 2 study of carlumab (CNTO 888), a human monoclonal antibody against CC-chemokine ligand 2 (CCL2), in metastatic castration-resistant prostate cancer.* Investigational new drugs, 2013. **31**(3): p. 760-768.
308. Sandhu, S.K., et al., *A first-in-human, first-in-class, phase I study of carlumab (CNTO 888), a human monoclonal antibody against CC-chemokine ligand 2 in patients with solid tumors.* Cancer chemotherapy and pharmacology, 2013. **71**(4): p. 1041-1050.
309. Brana, I., et al., *Carlumab, an anti-CC chemokine ligand 2 monoclonal antibody, in combination with four chemotherapy regimens for the treatment of patients with solid tumors: an open-label, multicenter phase 1b study.* Targeted oncology, 2015. **10**(1): p. 111-123.
310. Lim, S.Y., et al., *Targeting the CCL2-CCR2 signaling axis in cancer metastasis.* Oncotarget, 2016. **5**.
311. Bannas, P., J. Hambach, and F. Koch-Nolte, *Nanobodies and nanobody-based human heavy chain antibodies as antitumor therapeutics.* Frontiers in immunology, 2017. **8**: p. 1603.

312. Hotte, S., et al., *Phase I/II study of CTCE-9908, a novel anticancer agent that inhibits CXCR4, in patients with advanced solid cancers*. 2007, AACR.
313. Lee, H.H., V. Bellat, and B. Law, *Chemotherapy induces adaptive drug resistance and metastatic potentials via phenotypic CXCR4-expressing cell state transition in ovarian cancer.* PloS one, 2017. **12**(2): p. e0171044.
314. Gravina, G.L., et al., *CXCR4 pharmacogical inhibition reduces bone and soft tissue metastatic burden by affecting tumor growth and tumorigenic potential in prostate cancer preclinical models.* The Prostate, 2015. **75**(12): p. 1227-1246.
315. Drenckhan, A., et al., *Effective inhibition of metastases and primary tumor growth with CTCE-9908 in esophageal cancer.* journal of surgical research, 2013. **182**(2): p. 250-256.
316. Kazmierski W. W., G.K.S.a.P.S.C., *Small Molecule CCR5 and CXCR4 Based Viral Entry Inhibitors for anti-HIV therapy currently in development*, in *Annual Reports in Medicinal Chemistry*, J. Macor, Editor. 2007. p. 312.
317. Klarenbeek, A., et al., *Targeting chemokines and chemokine receptors with antibodies.* Drug Discovery Today: Technologies, 2012. **9**(4): p. e237-e244.
318. Allegretti, M., et al., *Current status of chemokine receptor inhibitors in development.* Immunology letters, 2012. **145**(1-2): p. 68-78.
319. Horuk, R., *Chemokine receptor antagonists: overcoming developmental hurdles.* Nature reviews Drug discovery, 2009. **8**(1): p. 23.
320. Nasser, M.W., et al., *Conditioning solid tumor microenvironment through inflammatory chemokines and S100 family proteins.* Cancer letters, 2015. **365**(1): p. 11-22.
321. Moser, B. and K. Willimann, *Chemokines: role in inflammation and immune surveillance.* Annals of the rheumatic diseases, 2004. **63**(suppl 2): p. ii84-ii89.

322. Al-haidari, A.A., et al., *CCR4 mediates CCL17 (TARC)-induced migration of human colon cancer cells via RhoA/Rho-kinase signaling.* International journal of colorectal disease, 2013. **28**(11): p. 1479-1487.
323. Laurent, V., et al., *Periprostatic adipocytes act as a driving force for prostate cancer progression in obesity.* Nature communications, 2016. **7**: p. 10230.
324. D'Agostino, G., V. Cecchinato, and M. Uguccioni, *Chemokine Heterocomplexes and Cancer: A Novel Chapter to Be Written in Tumor Immunity.* Frontiers in immunology, 2018. **9**: p. 2185.
325. Idorn, M., et al., *Improved migration of tumor ascites lymphocytes to ovarian cancer microenvironment by CXCR2 transduction.* Oncoimmunology, 2018. **7**(4): p. e1412029.
326. Panse, J., et al., *Chemokine CXCL13 is overexpressed in the tumour tissue and in the peripheral blood of breast cancer patients.* British journal of cancer, 2008. **99**(6): p. 930.
327. Tu, Z., et al., *CCR9 in cancer: oncogenic role and therapeutic targeting.* Journal of hematology & oncology, 2016. **9**(1): p. 10.
328. Lee, B., et al., *Quantification of CD4, CCR5, and CXCR4 levels on lymphocyte subsets, dendritic cells, and differentially conditioned monocyte-derived macrophages.* Proceedings of the National Academy of Sciences, 1999. **96**(9): p. 5215-5220.
329. Saban, D.R., *The chemokine receptor CCR7 expressed by dendritic cells: a key player in corneal and ocular surface inflammation.* The ocular surface, 2014. **12**(2): p. 87-99.
330. Campbell, J.J., et al., *CCR7 expression and memory T cell diversity in humans.* The Journal of Immunology, 2001. **166**(2): p. 877-884.
331. Zhang, L., et al., *Intratumoral T cells, recurrence, and survival in epithelial ovarian cancer.* New England journal of medicine, 2003. **348**(3): p. 203-213.
332. Yang, Q., et al., *Antitumor activity of NK cells.* Immunologic research, 2006. **36**(1-3): p. 13.
333. Shapouri-Moghaddam, A., et al., *Macrophage plasticity, polarization, and function in health and disease.* Journal of cellular physiology, 2018. **233**(9): p. 6425-6440.

334. Bao, L., et al., *CXCR4 is a good survival prognostic indicator in multiple myeloma patients.* Leukemia research, 2013. **37**(9): p. 1083-1088.
335. Hu, M., et al., *Overexpression of the chemokine receptor CXCR3 and its correlation with favorable prognosis in gastric cancer.* Human pathology, 2015. **46**(12): p. 1872-1880.
336. Klatte, T., et al., *The chemokine receptor CXCR3 is an independent prognostic factor in patients with localized clear cell renal cell carcinoma.* The Journal of urology, 2008. **179**(1): p. 61-66.
337. Baumhoer, D., et al., *Strong expression of CXCL12 is associated with a favorable outcome in osteosarcoma.* Modern Pathology, 2012. **25**(4): p. 522.
338. Velasco-Velázquez, M., et al., *CCR5 antagonist blocks metastasis of basal breast cancer cells.* Cancer research, 2012. **72**(15): p. 3839-3850.
339. Cabioglu, N., et al., *CXCL-12/stromal cell–derived factor-1α transactivates HER2-neu in breast cancer cells by a novel pathway involving Src kinase activation.* Cancer research, 2005. **65**(15): p. 6493-6497.
340. Mills, S.C., et al., *Cell migration towards CXCL12 in leukemic cells compared to breast cancer cells.* Cellular signalling, 2016. **28**(4): p. 316-324.
341. Xie, Y., et al., *Identification of upregulated phosphoinositide 3-kinase γ as a target to suppress breast cancer cell migration and invasion.* Biochemical pharmacology, 2013. **85**(10): p. 1454-1462.
342. Fernandis, A.Z., et al., *Regulation of CXCR4-mediated chemotaxis and chemoinvasion of breast cancer cells.* Oncogene, 2004. **23**(1): p. 157.
343. Lee, B.-C., et al., *Involvement of the Chemokine Receptor CXCR4 and Its Ligand Stromal Cell-Derived Factor 1α in Breast Cancer Cell Migration Through Human Brain Microvascular Endothelial Cells11NIH grant NS39558 (S. Avraham), the Susan G. Komen Fellowship (S. Avraham), the Milheim Foundation (S. Avraham), CA97153 (H. Avraham), and K18 PAR-02-069 (H. Avraham). Note: This work was done during the term of an established investigatorship from the American Heart Association (H. Avraham). This article is dedicated to*

Charlene Engelhard for her continuing friendship and support for our research program. Molecular Cancer Research, 2004. **2**(6): p. 327-338.

344. Li, H., et al., *Association between Gαi2 and ELMO1/Dock180 connects chemokine signalling with Rac activation and metastasis.* Nature communications, 2013. **4**: p. 1706.
345. Alsayed, Y., et al., *Mechanisms of regulation of CXCR4/SDF-1 (CXCL12)–dependent migration and homing in multiple myeloma.* Blood, 2007. **109**(7): p. 2708-2717.
346. Mills, S.C., et al., *Rac1 plays a role in CXCL12 but not CCL3-induced chemotaxis and Rac1 GEF inhibitor NSC23766 has off target effects on CXCR4.* Cellular signalling, 2018. **42**: p. 88-96.
347. Kerr, J.S., et al., *Differential regulation of chemotaxis: Role of Gβγ in chemokine receptor-induced cell migration.* Cellular signalling, 2013. **25**(4): p. 729-735.
348. Koizumi, K., et al., *Chemokine receptors in cancer metastasis and cancer cell-derived chemokines in host immune response.* Cancer science, 2007. **98**(11): p. 1652-1658.
349. Dillenburg-Pilla, P., et al., *SDF-1/CXCL12 induces directional cell migration and spontaneous metastasis via a CXCR4/G α i/mTORC1 axis.* The FASEB Journal, 2014. **29**(3): p. 1056-1068.
350. Bertagnolo, V., et al., *PLC-β2 is highly expressed in breast cancer and is associated with a poor outcome: a study on tissue microarrays.* International journal of oncology, 2006. **28**(4): p. 863-872.
351. Lee, S.-J., et al., *Overexpression of phospholipase C-γ1 in colorectal carcinomas is associated with overexpression of factors that bind its promoter.* Journal of Biological Chemistry, 1995. **270**(27): p. 16378-16384.
352. Fruman, D.A. and C. Rommel, *PI3K and cancer: lessons, challenges and opportunities.* Nature reviews Drug discovery, 2014. **13**(2): p. 140.
353. Olson, M.F. and E. Sahai, *The actin cytoskeleton in cancer cell motility.* Clinical & experimental metastasis, 2009. **26**(4): p. 273.
354. Yamaguchi, H. and J. Condeelis, *Regulation of the actin cytoskeleton in cancer cell migration and invasion.* Biochimica et Biophysica Acta (BBA)-Molecular Cell Research, 2007. **1773**(5): p. 642-652.

355. Mueller, A., et al., *Pharmacological characterization of the chemokine receptor, CCR5.* British journal of pharmacology, 2002. **135**(4): p. 1033-1043.
356. ATCC, *MCF7 (ATCC® HTB-22™)* 2016.
357. Subik, K., et al., *The expression patterns of ER, PR, HER2, CK5/6, EGFR, Ki-67 and AR by immunohistochemical analysis in breast cancer cell lines.* Breast cancer: basic and clinical research, 2010. **4**: p. 117822341000400004.
358. Hevir, N., et al., *Expression of estrogen and progesterone receptors and estrogen metabolizing enzymes in different breast cancer cell lines.* Chemico-biological interactions, 2011. **191**(1-3): p. 206-216.
359. Neve, R.M., et al., *A collection of breast cancer cell lines for the study of functionally distinct cancer subtypes.* Cancer cell, 2006. **10**(6): p. 515-527.
360. ATCC, *MDA-MB-231 (ATCC® HTB-26™)* 2016.
361. Leung, E., et al., *Evidence for the existence of triple-negative variants in the MCF-7 breast cancer cell population.* BioMed research international, 2014. **2014**.
362. ATCC, *MIA PaCa-2 (ATCC® CRL-1420™)* 2016.
363. ATCC, *PC-3 (ATCC® CRL-1435™)* 2016.
364. Bennett, N.C., et al., *Expression profiles and functional associations of endogenous androgen receptor and caveolin-1 in prostate cancer cell lines.* The Prostate, 2014. **74**(5): p. 478-487.
365. Alimirah, F., et al., *DU-145 and PC-3 human prostate cancer cell lines express androgen receptor: Implications for the androgen receptor functions and regulation.* FEBS letters, 2006. **580**(9): p. 2294-2300.
366. Resources, C.C.L.G.I.a. *CHO Transfection Protocols, Kits, Methods*. 2019 [cited 2019; Available from: http://www.cho-cell-transfection.com/transfection-information/.
367. ATCC, *THP-1 (ATCC® TIB-202™)* 2016.
368. ATCC, *Jurkat, Clone E6-1 (ATCC® TIB-152™)* 2016.
369. Czaplewski, L.G., et al., *Identification of Amino Acid Residues Critical for Aggregation of Human CC Chemokines Macrophage Inflammatory Protein (MIP)-1α, MIP-1β, and RANTES CHARACTERIZATION OF*

ACTIVE DISAGGREGATED CHEMOKINE VARIANTS. Journal of Biological Chemistry, 1999. **274**(23): p. 16077-16084.

370. Haasen, D., et al., *Pharmacological Profiling of Chemokine Receptor–Directed Compounds Using High-Content Screening.* Journal of biomolecular screening, 2008. **13**(1): p. 40-53.
371. Lüttichau, H.R., et al., *A highly selective CCR2 chemokine agonist encoded by human herpesvirus 6.* Journal of Biological Chemistry, 2003. **278**(13): p. 10928-10933.
372. Sayyed, S.G., et al., *An orally active chemokine receptor CCR2 antagonist prevents glomerulosclerosis and renal failure in type 2 diabetes.* Kidney international, 2011. **80**(1): p. 68-78.
373. Poon, K., et al., *Stimulatory role of the chemokine CCL2 in the migration and peptide expression of embryonic hypothalamic neurons.* Journal of neurochemistry, 2014. **131**(4): p. 509-520.
374. Gong, X., et al., *Monocyte chemotactic protein-2 (MCP-2) uses CCR1 and CCR2B as its functional receptors.* Journal of Biological Chemistry, 1997. **272**(18): p. 11682-11685.
375. Chou, C.C., et al., *Pharmacological characterization of the chemokine receptor, hCCR1 in a stable transfectant and differentiated HL-60 cells: antagonism of hCCR1 activation by MIP-1β.* British journal of pharmacology, 2002. **137**(5): p. 663-675.
376. Ben-Baruch, A., et al., *Monocyte Chemotactic Protein-3 (MCP3) Interacts with Multiple Leukocyte Receptors CC CKR1, a receptor for macrophage inflammatory protein-1α/RANTES, is also a functional receptor for MCP3.* Journal of Biological Chemistry, 1995. **270**(38): p. 22123-22128.
377. Camps, M., et al., *Blockade of PI3Kγ suppresses joint inflammation and damage in mouse models of rheumatoid arthritis.* Nature medicine, 2005. **11**(9): p. 936.
378. Proudfoot, A.E., et al., *Characterisation of the RANTES/MIP-1α receptor (CC CKR-1) stably transfected in HEK 293 cells and the recombinant ligands.* FEBS letters, 1995. **376**(1-2): p. 19-23.

379. Daugherty, B.L., et al., *Cloning, expression, and characterization of the human eosinophil eotaxin receptor.* Journal of Experimental Medicine, 1996. **183**(5): p. 2349-2354.
380. Jin, J., et al., *Targeting Spare CCR5 as a Principle to Inhibit HIV-1 Entry.* Journal of Biological Chemistry, 2014: p. jbc. M114. 559831.
381. Gong, W., et al., *Monocyte chemotactic protein-2 activates CCR5 and blocks CD4/CCR5-mediated HIV-1 entry/replication.* Journal of Biological Chemistry, 1998. **273**(8): p. 4289-4292.
382. Joseph, P.R.B., et al., *Probing the role of CXC motif in chemokine CXCL8 for high affinity binding and activation of CXCR1 and CXCR2 receptors.* Journal of Biological Chemistry, 2010: p. jbc. M110. 146555.
383. Nasser, M.W., et al., *CXCR1 and CXCR2 Activation and Regulation ROLE OF ASPARTATE 199 OF THE SECOND EXTRACELLULAR LOOP OF CXCR2 IN CXCL8-MEDIATED RAPID RECEPTOR INTERNALIZATION.* Journal of Biological Chemistry, 2007. **282**(9): p. 6906-6915.
384. Richardson, R.M., et al., *Role of the cytoplasmic tails of CXCR1 and CXCR2 in mediating leukocyte migration, activation, and regulation.* The Journal of Immunology, 2003. **170**(6): p. 2904-2911.
385. Nasser, M.W., et al., *Differential activation and regulation of CXCR1 and CXCR2 by CXCL8 monomer and dimer.* The Journal of Immunology, 2009: p. jimmunol. 0900305.
386. Tanino, Y., et al., *Kinetics of chemokine–glycosaminoglycan interactions control neutrophil migration into the airspaces of the lungs.* The Journal of Immunology, 2010: p. ji_0903274.
387. Heise, C.E., et al., *Pharmacological characterization of CXC chemokine receptor 3 ligands and a small molecule antagonist.* Journal of Pharmacology and Experimental Therapeutics, 2005. **313**(3): p. 1263-1271.
388. Costa, C., et al., *Enhanced monocyte migration to CXCR3 and CCR5 chemokines in COPD.* European Respiratory Journal, 2016: p. ERJ-01642-2015.

389. Van Hout, A., et al., *Comparison of cell-based assays for the identification and evaluation of competitive CXCR4 inhibitors.* PloS one, 2017. **12**(4): p. e0176057.
390. Otte, M., et al., *CXCL14 is no direct modulator of CXCR4.* FEBS letters, 2014. **588**(24): p. 4769-4775.
391. Murphy, J.W., et al., *Structural and functional basis of CXCL12 (stromal cell-derived factor-1α) binding to heparin.* Journal of Biological Chemistry, 2007. **282**(13): p. 10018-10027.
392. Luan, S., et al., *A microfabricated 96-well wound-healing assay.* Cytometry Part A, 2017. **91**(12): p. 1192-1199.
393. Eby, J.M., et al., *Functional and structural consequences of chemokine (C-X-C motif) receptor 4 activation with cognate and non-cognate agonists.* Molecular and Cellular Biochemistry, 2017. **434**(1): p. 143-151.
394. Gravel, S., et al., *The peptidomimetic CXCR4 antagonist TC14012 recruits β-arrestin to CXCR7 roles of receptor domains.* Journal of Biological Chemistry, 2010: p. jbc. C110. 147470.
395. Balabanian, K., et al., *The chemokine SDF-1/CXCL12 binds to and signals through the orphan receptor RDC1 in T lymphocytes.* Journal of Biological Chemistry, 2005.
396. Zabel, B.A., et al., *Elucidation of CXCR7-mediated signaling events and inhibition of CXCR4-mediated tumor cell transendothelial migration by CXCR7 ligands.* The Journal of Immunology, 2009: p. jimmunol. 0900269.
397. Naya, A., et al., *Design, synthesis, and discovery of a novel CCR1 antagonist.* Journal of medicinal chemistry, 2001. **44**(9): p. 1429-1435.
398. Dorr, P., et al., *Maraviroc (UK-427,857), a potent, orally bioavailable, and selective small-molecule inhibitor of chemokine receptor CCR5 with broad-spectrum anti-human immunodeficiency virus type 1 activity.* Antimicrobial agents and chemotherapy, 2005. **49**(11): p. 4721-4732.
399. Golubovskaya, V.M., et al., *A small molecule inhibitor, 1, 2, 4, 5-benzenetetraamine tetrahydrochloride, targeting the y397 site of focal adhesion kinase decreases tumor growth.* Journal of medicinal chemistry, 2008. **51**(23): p. 7405-7416.

400. Roberts, W.G., et al., *Antitumor activity and pharmacology of a selective focal adhesion kinase inhibitor, PF-562,271.* Cancer research, 2008. **68**(6): p. 1935-1944.
401. Dubreuil, P., et al., *Masitinib (AB1010), a potent and selective tyrosine kinase inhibitor targeting KIT.* PloS one, 2009. **4**(9): p. e7258.
402. Boschelli, D.H., et al., *Optimization of 4-phenylamino-3-quinolinecarbonitriles as potent inhibitors of Src kinase activity.* Journal of medicinal chemistry, 2001. **44**(23): p. 3965-3977.
403. Wang, W.-Y., Y.-C. Wu, and C.-C. Wu, *Prevention of platelet glycoprotein IIb/IIIa activation by 3, 4-methylenedioxy-β-nitrostyrene, a novel tyrosine kinase inhibitor.* Molecular pharmacology, 2006. **70**(4): p. 1380-1389.
404. Ishizaki, T., et al., *Pharmacological properties of Y-27632, a specific inhibitor of rho-associated kinases.* Molecular pharmacology, 2000. **57**(5): p. 976-983.
405. Hall-Jackson, C.A., et al., *Paradoxical activation of Raf by a novel Raf inhibitor.* Chemistry & biology, 1999. **6**(8): p. 559-568.
406. Bleasdale, J.E., et al., *Selective inhibition of receptor-coupled phospholipase C-dependent processes in human platelets and polymorphonuclear neutrophils.* Journal of Pharmacology and Experimental Therapeutics, 1990. **255**(2): p. 756-768.
407. Thastrup, O., et al., *Thapsigargin, a tumor promoter, discharges intracellular Ca2+ stores by specific inhibition of the endoplasmic reticulum Ca2 (+)-ATPase.* Proceedings of the National Academy of Sciences, 1990. **87**(7): p. 2466-2470.
408. Nishikimi, A., et al., *Blockade of inflammatory responses by a small-molecule inhibitor of the Rac activator DOCK2.* Chemistry & biology, 2012. **19**(4): p. 488-497.
409. Vlahos, C.J., et al., *A specific inhibitor of phosphatidylinositol 3-kinase, 2-(4-morpholinyl)-8-phenyl-4H-1-benzopyran-4-one (LY294002).* Journal of Biological Chemistry, 1994. **269**(7): p. 5241-5248.
410. Lehmann, D.M., P. Seneviratne, and A.V. Smrcka, *Small molecule disruption of G protein βγ subunit signaling inhibits neutrophil chemotaxis and inflammation.* Molecular pharmacology, 2007.

411. Liang, B.T. and J.B. Galper, *Differential sensitivity of αo and αi to ADP-ribosylation by pertussis toxin in the intact cultured embryonic chick ventricular myocyte: Relationship to the role of g proteins in the coupling of muscarinic cholinergic receptors to inhibition of adenylate cyclase activity.* Biochemical pharmacology, 1988. **37**(23): p. 4549-4555.
412. Shutes, A., et al., *Specificity and mechanism of action of EHT 1864, a novel small molecule inhibitor of Rac family small GTPases.* Journal of Biological Chemistry, 2007.
413. Nolen, B., et al., *Characterization of two classes of small molecule inhibitors of Arp2/3 complex.* Nature, 2009. **460**(7258): p. 1031.
414. Xu, K., P.M. Schwarz, and R.F. Ludueña, *Interaction of nocodazole with tubulin isotypes.* Drug development research, 2002. **55**(2): p. 91-96.
415. Wang, J., et al., *Paclitaxel at ultra low concentrations inhibits angiogenesis without affecting cellular microtubule assembly.* Anti-cancer drugs, 2003. **14**(1): p. 13-19.
416. Thompson, S., et al., *Regulation of chemokine function: the roles of GAG-binding and post-translational nitration.* International journal of molecular sciences, 2017. **18**(8): p. 1692.
417. Dyer, D.P., et al., *The dependence of chemokine–glycosaminoglycan interactions on chemokine oligomerization.* Glycobiology, 2015. **26**(3): p. 312-326.
418. Müller, A., et al., *Involvement of chemokine receptors in breast cancer metastasis.* nature, 2001. **410**(6824): p. 50.
419. Andre, F., et al., *Expression of chemokine receptors predicts the site of metastatic relapse in patients with axillary node positive primary breast cancer.* Annals of Oncology, 2006. **17**(6): p. 945-951.
420. Singh, S.K., et al., *CCR5/CCL5 axis interaction promotes migratory and invasiveness of pancreatic cancer cells.* Scientific reports, 2018. **8**(1): p. 1323.
421. Salazar, N., et al., *Chemokines and chemokine receptors as promoters of prostate cancer growth and progression.* Critical Reviews™ in Eukaryotic Gene Expression, 2013. **23**(1).

422. Ogilvie, P., et al., *Unusual chemokine receptor antagonism involving a mitogen-activated protein kinase pathway.* The Journal of Immunology, 2004. **172**(11): p. 6715-6722.
423. Jones, S.A., et al., *Different functions for the interleukin 8 receptors (IL-8R) of human neutrophil leukocytes: NADPH oxidase and phospholipase D are activated through IL-8R1 but not IL-8R2.* Proceedings of the National Academy of Sciences, 1996. **93**(13): p. 6682-6686.
424. Steen, A., et al., *Biased and g protein-independent signaling of chemokine receptors.* Frontiers in immunology, 2014. **5**: p. 277.
425. Palacios-Arreola, M.I., et al., *The role of chemokines in breast cancer pathology and its possible use as therapeutic targets.* Journal of immunology research, 2014. **2014**.
426. Ali, S. and G. Lazennec, *Chemokines: novel targets for breast cancer metastasis.* Cancer and Metastasis Reviews, 2007. **26**(3-4): p. 401-420.
427. Borsig, L., et al., *Inflammatory chemokines and metastasis—tracing the accessory.* Oncogene, 2014. **33**(25): p. 3217.
428. Sleightholm, R.L., et al., *Emerging roles of the CXCL12/CXCR4 axis in pancreatic cancer progression and therapy.* Pharmacology & therapeutics, 2017.
429. Sperveslage, J., et al., *Lack of CCR7 expression is rate limiting for lymphatic spread of pancreatic ductal adenocarcinoma.* International journal of cancer, 2012. **131**(4): p. E371-E381.
430. Mo, M., et al., *CCL21/CCR7 enhances the proliferation, migration, and invasion of human bladder cancer T24 cells.* PloS one, 2015. **10**(3): p. e0119506.
431. Bonecchi, R. and G.J. Graham, *Atypical chemokine receptors and their roles in the resolution of the inflammatory response.* Frontiers in immunology, 2016. **7**: p. 224.
432. Nimmagadda, S., *Differential expression of chemokine receptors and their roles in cancer imaging.* Frontiers in oncology, 2012. **2**: p. 46.
433. Vaday, G.G., et al., *Expression of CCL5 (RANTES) and CCR5 in prostate cancer.* The Prostate, 2006. **66**(2): p. 124-134.

434. Murooka, T.T., R. Rahbar, and E.N. Fish, *CCL5 promotes proliferation of MCF-7 cells through mTOR-dependent mRNA translation.* Biochemical and biophysical research communications, 2009. **387**(2): p. 381-386.
435. Sun, Y., et al., *CXCL12-CXCR4 axis promotes the natural selection of breast cancer cell metastasis.* Tumor Biology, 2014. **35**(8): p. 7765-7773.
436. Liu, X., et al., *Activation of STAT3 is involved in malignancy mediated by CXCL12-CXCR4 signaling in human breast cancer.* Oncology reports, 2014. **32**(6): p. 2760-2768.
437. Youngs, S.J., et al., *Chemokines induce migrational responses in human breast carcinoma cell lines.* International journal of cancer, 1997. **71**(2): p. 257-266.
438. Rohena-Rivera, K., et al., *CCL-4 enhances prostate cancer migration and invasion by modulating integrin expression.* Int J Clin Exp Med, 2016. **9**(3): p. 5426-5438.
439. Fang, W.B., et al., *CCL2/CCR2 chemokine signaling coordinates survival and motility of breast cancer cells through Smad3 and p42/44MAPK dependent mechanisms.* Journal of Biological Chemistry, 2012: p. jbc. M112. 365999.
440. Nam, J.-S., et al., *Chemokine (CC motif) ligand 2 mediates the prometastatic effect of dysadherin in human breast cancer cells.* Cancer research, 2006. **66**(14): p. 7176-7184.
441. He, S., et al., *The chemokine (CCL2-CCR2) signaling axis mediates perineural invasion.* Molecular Cancer Research, 2014: p. molcanres. 0303.2014.
442. Vinader, V., et al., *An agarose spot chemotaxis assay for chemokine receptor antagonists.* Journal of pharmacological and toxicological methods, 2011. **64**(3): p. 213-216.
443. Kang, H., et al., *Stromal cell derived factor-1: its influence on invasiveness and migration of breast cancer cells in vitro, and its association with prognosis and survival in human breast cancer.* Breast Cancer Research, 2005. **7**(4): p. R402.

444. Roy, I., et al., *CXCL12 chemokine expression suppresses human pancreatic cancer growth and metastasis.* PloS one, 2014. **9**(3): p. e90400.
445. Shen, B., et al., *CXCL12-CXCR4 promotes proliferation and invasion of pancreatic cancer cells.* Asian Pacific Journal of Cancer Prevention, 2013. **14**(9): p. 5403-5408.
446. Morimoto, M., et al., *Enhancement of the CXCL12/CXCR4 axis due to acquisition of gemcitabine resistance in pancreatic cancer: effect of CXCR4 antagonists.* Bmc Cancer, 2016. **16**(1): p. 305.
447. Roy, I., et al., *Pancreatic cancer cell migration and metastasis is regulated by chemokine-biased agonism and bioenergetic signaling.* Cancer research, 2015. **75**(17): p. 3529-3542.
448. Ahmed, M., et al., *Agarose spot as a comparative method for in situ analysis of simultaneous chemotactic responses to multiple chemokines.* Scientific Reports, 2017. **7**(1): p. 1075.
449. Reinke, J. and H. Sorg, *Wound repair and regeneration.* European Surgical Research, 2012. **49**(1): p. 35-43.
450. Rees, P.A., et al., *Chemokines in wound healing and as potential therapeutic targets for reducing cutaneous scarring.* Advances in wound care, 2015. **4**(11): p. 687-703.
451. Lowe, J.S., P.G. Anderson, and S.I. Anderson, *Stevens & Lowe's Human Histology*. 2019: Elsevier Health Sciences.
452. Lintz, M., A. Muñoz, and C.A. Reinhart-King, *The mechanics of single cell and collective migration of tumor cells.* Journal of biomechanical engineering, 2017. **139**(2): p. 021005.
453. Zhang, Y., et al., *Role of CCL5 in invasion, proliferation and proportion of CD44+/CD24− phenotype of MCF-7 cells and correlation of CCL5 and CCR5 expression with breast cancer progression.* Oncology reports, 2009. **21**(4): p. 1113-1121.
454. Ray, N., *Maraviroc in the treatment of HIV infection.* Drug design, development and therapy, 2008. **2**: p. 151.
455. Garcia-Perez, J., et al., *New insights into the mechanisms whereby low molecular weight CCR5 ligands inhibit HIV-1 infection.* Journal of Biological Chemistry, 2011. **286**(7): p. 4978-4990.

456. Corbisier, J., et al., *Partial agonist and biased signaling properties of the synthetic enantiomers J113863/UCB35625 at chemokine receptors CCR2 and CCR5.* Journal of Biological Chemistry, 2017. **292**(2): p. 575-584.
457. Cardaba, C.M., J.S. Kerr, and A. Mueller, *CCR5 internalisation and signalling have different dependence on membrane lipid raft integrity.* Cellular signalling, 2008. **20**(9): p. 1687-1694.
458. Werry, T.D., et al., *Ca2+ signalling by recombinant human CXCR2 chemokine receptors is potentiated by P2Y nucleotide receptors in HEK cells.* British journal of pharmacology, 2002. **135**(5): p. 1199-1208.
459. Kong, S. and C. Lee, *The use of fura 2 for measurement of free calcium concentration.* Biochemical Education, 1995. **23**(2): p. 97-98.
460. Jacques, R., *Pharmacological insights into C-C motif chemokine receptor 5 mediated chemotaxis*, in *School of Pharmacy*. 2013, University of East Anglia: Norwich, England.
461. Zimerman, B., T. Volberg, and B. Geiger, *Early molecular events in the assembly of the focal adhesion-stress fiber complex during fibroblast spreading.* Cell motility and the cytoskeleton, 2004. **58**(3): p. 143-159.
462. Baxendale, S. and T. Whitfield, *Methods to study the development, anatomy, and function of the zebrafish inner ear across the life course*, in *Methods in cell biology*. 2016, Elsevier. p. 165-209.
463. Di Marzio, P., et al., *Role of Rho family GTPases in CCR1-and CCR5-induced actin reorganization in macrophages.* Biochemical and biophysical research communications, 2005. **331**(4): p. 909-916.
464. Akashi, T., et al., *Androgen receptor negatively influences the expression of chemokine receptors (CXCR4, CCR1) and ligand-mediated migration in prostate cancer DU-145.* Oncology reports, 2006. **16**(4): p. 831-836.
465. He, S., et al., *The Chemokine (CCL2–CCR2) Signaling Axis Mediates Perineural Invasion.* Molecular Cancer Research, 2015. **13**(2): p. 380-390.
466. Riedl, A., et al., *Comparison of cancer cells in 2D vs 3D culture reveals differences in AKT–mTOR–S6K signaling and drug responses.* J Cell Sci, 2017. **130**(1): p. 203-218.

467. Petrie, R.J., et al., *Nonpolarized signaling reveals two distinct modes of 3D cell migration.* J Cell Biol, 2012. **197**(3): p. 439-455.
468. Liu, C., et al., *Hybrid collagen alginate hydrogel as a platform for 3D tumor spheroid invasion.* Acta biomaterialia, 2018. **75**: p. 213-225.
469. Rappel, W.-J. and L. Edelstein-Keshet, *Mechanisms of cell polarization.* Current opinion in systems biology, 2017. **3**: p. 43-53.
470. Siegel, G.J., *Basic neurochemistry: molecular, cellular and medical aspects*. 1999.
471. Golubovskaya, V.M., *Targeting FAK in human cancer: from finding to first clinical trials.* Frontiers in bioscience (Landmark edition), 2014. **19**: p. 687.
472. Samuels, Y. and K. Ericson, *Oncogenic PI3K and its role in cancer.* Current opinion in oncology, 2006. **18**(1): p. 77-82.
473. Fernández-Medarde, A. and E. Santos, *Ras in cancer and developmental diseases.* Genes & cancer, 2011. **2**(3): p. 344-358.
474. Koivunen, J., V. Aaltonen, and J. Peltonen, *Protein kinase C (PKC) family in cancer progression.* Cancer letters, 2006. **235**(1): p. 1-10.
475. Cai, S., et al., *Expression of phospholipase C isozymes in human breast cancer and their clinical significance.* Oncology reports, 2017. **37**(3): p. 1707-1715.
476. Noh, D.Y., et al., *Elevated content of phospholipase C-γ1 in colorectal cancer tissues.* Cancer, 1994. **73**(1): p. 36-41.
477. Dubrovska, A., et al., *CXCR4 expression in prostate cancer progenitor cells.* PloS one, 2012. **7**(2): p. e31226.
478. Lodge, R., et al., *Regulation of CD4 Receptor and HIV-1 Entry by MicroRNAs-221 and-222 during Differentiation of THP-1 Cells.* Viruses, 2018. **10**(1): p. 13.
479. Sánchez-Martín, L., et al., *The chemokine CXCL12 regulates monocyte-macrophage differentiation and RUNX3 expression.* Blood, 2011. **117**(1): p. 88-97.
480. Cardaba, C.M., et al., *CCL3 induced migration occurs independently of intracellular calcium release.* Biochemical and biophysical research communications, 2012. **418**(1): p. 17-21.

481. Jin, W., et al., *U73122 inhibits phospholipase C-dependent calcium mobilization in neuronal cells.* Brain research, 1994. **642**(1-2): p. 237-243.
482. Kim, T.-J., et al., *Prolonged mechanical stretch initiates intracellular calcium oscillations in human mesenchymal stem cells.* PLoS One, 2014. **9**(10): p. e109378.
483. Digby, G.C., et al., *Phospholipase C, calcium and calmodulin are critical for alpha4beta1integrin affinity up-regulation and monocyte arrest triggered by chemoattractants.* Blood, 2007. **109**(1): p.176-84
484. Pulcinelli, F.M., et al., *Evidence for separate effects of U73122 on phospholipase C and calcium channels in human platelets.* Biochemical pharmacology, 1998. **56**(11): p. 1481-1484.
485. Macmillan, D. and J. McCarron, *The phospholipase C inhibitor U-73122 inhibits Ca2+ release from the intracellular sarcoplasmic reticulum Ca2+ store by inhibiting Ca2+ pumps in smooth muscle.* British journal of pharmacology, 2010. **160**(6): p. 1295-1301.
486. Klein, R.R., et al., *Direct activation of human phospholipase C by its well known inhibitor u73122.* Journal of Biological Chemistry, 2011. **286**(14): p. 12407-12416.
487. Smrcka, A.V., *Molecular targeting of Gα and Gβγ subunits: a potential approach for cancer therapeutics.* Trends in pharmacological sciences, 2013. **34**(5): p. 290-298.
488. Lehmann, D.M., A. Seneviratne, and A.V. Smrcka, *Small molecule disruption of G protein βγ subunit signaling inhibits neutrophil chemotaxis and inflammation.* Molecular pharmacology, 2008. **73**(2): p. 410-418.
489. Kim, Y.S., et al., *Histamine 1 receptor-G βγ-cAMP/PKA-CFTR pathway mediates the histamine-induced resetting of the suprachiasmatic circadian clock.* Molecular brain, 2016. **9**(1): p. 49.
490. Schwetz, T.A., A. Ustione, and D.W. Piston, *Neuropeptide Y and somatostatin inhibit insulin secretion through different mechanisms.* American Journal of Physiology-Endocrinology and Metabolism, 2012. **304**(2): p. E211-E221.

491. Jason.S, K., *Heterotrimeric G-protein Interactions and Activation in Chemokine Receptor 5 Signalling*, in *School of Pharmacy*. 2010, University of East Anglia: Norwich p. 204.
492. Leelawat, K., et al., *Roles of the MEK1/2 and AKT pathways in CXCL12/CXCR4 induced cholangiocarcinoma cell invasion.* World journal of gastroenterology: WJG, 2007. **13**(10): p. 1561.
493. Ma, J., et al., *CXCL12 gene silencing down-regulates metastatic potential via blockage of MAPK/PI3K/AP-1 signaling pathway in colon cancer.* Clinical and Translational Oncology, 2018: p. 1-11.
494. Monterrubio, M., et al., *PI3Kγ activation by CXCL12 regulates tumor cell adhesion and invasion.* Biochemical and biophysical research communications, 2009. **388**(2): p. 199-204.
495. Wang, S., et al., *CXCL12-induced upregulation of FOXM1 expression promotes human glioblastoma cell invasion.* Biochemical and biophysical research communications, 2014. **447**(1): p. 1-6.
496. Azab, A.K., et al., *RhoA and Rac1 GTPases play major and differential roles in stromal cell–derived factor-1–induced cell adhesion and chemotaxis in multiple myeloma.* Blood, 2009. **114**(3): p. 619-629.
497. Zagzag, D., et al., *Hypoxia-and vascular endothelial growth factor-induced stromal cell-derived factor-1α/CXCR4 expression in glioblastomas: one plausible explanation of Scherer's structures.* The American journal of pathology, 2008. **173**(2): p. 545-560.
498. Glodek, A., et al., *Focal adhesion kinase is required for CXCL12-induced chemotactic and pro-adhesive responses in hematopoietic precursor cells.* Leukemia, 2007. **21**(8): p. 1723.
499. Yang, Q., et al., *Antitumour activity of the recombination polypeptide GST-NT21MP is mediated by inhibition of CXCR4 pathway in breast cancer.* British journal of cancer, 2014. **110**(5): p. 1288.
500. Zhang, H., et al., *Paracrine SDF-1α signaling mediates the effects of PSCs on GEM chemoresistance through an IL-6 autocrine loop in pancreatic cancer cells.* Oncotarget, 2015. **6**(5): p. 3085.
501. Wen, W.-w., et al., *Oligomannurarate sulfate inhibits CXCL12/SDF-1-mediated proliferation and invasion of human tumor cells in vitro.* Acta Pharmacologica Sinica, 2013. **34**(12): p. 1554.

502. Lee, H.W., et al., *Tpl2 induces castration resistant prostate cancer progression and metastasis.* International journal of cancer, 2015. **136**(9): p. 2065-2077.
503. Izumi, D., et al., *CXCL12/CXCR4 activation by cancer-associated fibroblasts promotes integrin β1 clustering and invasiveness in gastric cancer.* International journal of cancer, 2016. **138**(5): p. 1207-1219.
504. Marech, I., et al., *Masitinib (AB1010), from canine tumor model to human clinical development: where we are?* Critical Reviews in Oncology/Hematology, 2014. **91**(1): p. 98-111.
505. Stokoe, D. and F. McCormick, *Activation of c-Raf-1 by Ras and Src through different mechanisms: activation in vivo and in vitro.* The EMBO journal, 1997. **16**(9): p. 2384-2396.
506. Mebratu, Y. and Y. Tesfaigzi, *How ERK1/2 activation controls cell proliferation and cell death: Is subcellular localization the answer?* Cell cycle, 2009. **8**(8): p. 1168-1175.
507. Parsons, J.T., et al., *Focal adhesion kinase: targeting adhesion signaling pathways for therapeutic intervention.* Clinical Cancer Research, 2008. **14**(3): p. 627-632.
508. Cain, R.J. and A.J. Ridley, *Phosphoinositide 3-kinases in cell migration.* Biology of the Cell, 2009. **101**(1): p. 13-29.
509. Wang, L., et al., *CXCL5 regulation of proliferation and migration in human non-small cell lung cancer cells.* Journal of physiology and biochemistry, 2018. **74**(2): p. 313-324.
510. Zhou, H., et al., *CXCL10/CXCR3 axis promotes the invasion of gastric cancer via PI3K/AKT pathway-dependent MMPs production.* Biomedicine & Pharmacotherapy, 2016. **82**: p. 479-488.
511. Wang, B., et al., *Production of CCL 20 from lung cancer cells induces the cell migration and proliferation through PI 3K pathway.* Journal of cellular and molecular medicine, 2016. **20**(5): p. 920-929.
512. Zhu, Z., et al., *CXCL13-CXCR5 axis promotes the growth and invasion of colon cancer cells via PI3K/AKT pathway.* Molecular and cellular biochemistry, 2015. **400**(1-2): p. 287-295.

513. Liu, P., et al., *CX3CL1/fractalkine enhances prostate cancer spinal metastasis by activating the Src/FAK pathway.* International journal of oncology, 2018. **53**(4): p. 1544-1556.
514. Kalluri, R. and R.A. Weinberg, *The basics of epithelial-mesenchymal transition.* The Journal of Clinical Investigation, 2009. **119**(6): p. 1420-1428.
515. Panetti, T.S., *Tyrosine phosphorylation of paxillin, FAK, and p130CAS: effects on cell spreading and migration.* Front Biosci, 2002. **7**(January): p. d143-d150.
516. Hadad, I., et al., *Stroma cell-derived factor-1α signaling enhances calcium transients and beating frequency in rat neonatal cardiomyocytes.* PloS one, 2013. **8**(2): p. e56007.
517. Cardaba, C.M. and A. Mueller, *Distinct modes of molecular regulation of CCL3 induced calcium flux in monocytic cells.* Biochemical pharmacology, 2009. **78**(8): p. 974-982.
518. Boddeke, E.W., et al., *Cultured rat microglia express functional β-chemokine receptors.* Journal of neuroimmunology, 1999. **98**(2): p. 176-184.
519. Inngjerdingen, M., et al., *Differential utilization of cyclic ADP-ribose pathway by chemokines to induce the mobilization of intracellular calcium in NK cells.* Biochemical and biophysical research communications, 1999. **262**(2): p. 467-472.
520. Doijen, J., et al., *Signaling properties of the human chemokine receptors CXCR4 and CXCR7 by cellular electric impedance measurements.* PloS one, 2017. **12**(9): p. e0185354.
521. Bonacci, T.M., et al., *Differential targeting of Gßγ-subunit signaling with small molecules.* Science, 2006. **312**(5772): p. 443-446.
522. Mathews, J.L., A.V. Smrcka, and J.M. Bidlack, *A novel Gβγ-subunit inhibitor selectively modulates μ-opioid-dependent antinociception and attenuates acute morphine-induced antinociceptive tolerance and dependence.* Journal of Neuroscience, 2008. **28**(47): p. 12183-12189.
523. Jones, M.L., et al., *Characterization of a novel focal adhesion kinase inhibitor in human platelets.* Biochemical and biophysical research communications, 2009. **389**(1): p. 198-203.

524. Leung, C.S., et al., *Calcium-dependent FAK/CREB/TNNC1 signalling mediates the effect of stromal MFAP5 on ovarian cancer metastatic potential.* Nature communications, 2014. **5**: p. 5092.
525. Zhang, X., et al., *Focal adhesion kinase promotes phospholipase C-γ1 activity.* Proceedings of the National Academy of Sciences, 1999. **96**(16): p. 9021-9026.
526. Kawakami, Y., et al., *A Ras activation pathway dependent on Syk phosphorylation of protein kinase C.* Proceedings of the National Academy of Sciences, 2003. **100**(16): p. 9470-9475.
527. Butanda-Ochoa, A., et al., *Recognition and activation of ryanodine receptors by purines.* Current medicinal chemistry, 2006. **13**(6): p. 647-657.
528. Vyklicka, L., et al., *The human transient receptor potential vanilloid 3 channel is sensitized via the ERK pathway.* Journal of Biological Chemistry, 2017. **292**(51): p. 21083-21091.
529. Martin, S., et al., *Phosphorylation sites on calcium channel α1 and β subunits regulate ERK-dependent modulation of neuronal N-type calcium channels.* Cell calcium, 2006. **39**(3): p. 275-292.
530. Kansra, V., et al., *Phosphatidylinositol 3-kinase-dependent extracellular calcium influx is essential for CX3CR1-mediated activation of the mitogen-activated protein kinase cascade.* Journal of Biological Chemistry, 2001.
531. Chen, S., et al., *RACK1 regulates directional cell migration by acting on Gβγ at the interface with its effectors PLCβ and PI3Kγ.* Molecular biology of the cell, 2008. **19**(9): p. 3909-3922.
532. Alon, R. and Z. Shulman, *Chemokine triggered integrin activation and actin remodeling events guiding lymphocyte migration across vascular barriers.* Experimental cell research, 2011. **317**(5): p. 632-641.
533. Forth, S. and T.M. Kapoor, *The mechanics of microtubule networks in cell division.* J Cell Biol, 2017. **216**(6): p. 1525-1531.
534. Fletcher, D.A. and R.D. Mullins, *Cell mechanics and the cytoskeleton.* Nature, 2010. **463**(7280): p. 485.
535. Etienne-Manneville, S., *Microtubules in cell migration.* Annual review of cell and developmental biology, 2013. **29**: p. 471-499.

536. Porter, A.P., A. Papaioannou, and A. Malliri, *Deregulation of Rho GTPases in cancer.* Small GTPases, 2016. **7**(3): p. 123-138.
537. Fernando, H.S., H.G. Kynaston, and W.G. Jiang, *WASP and WAVE proteins: vital intrinsic regulators of cell motility and their role in cancer.* International journal of molecular medicine, 2009. **23**(2): p. 141-148.
538. Molinie, N. and A. Gautreau, *The Arp2/3 regulatory system and its deregulation in cancer.* Physiological reviews, 2017. **98**(1): p. 215-238.
539. Iwaya, K., et al., *Correlation between liver metastasis of the colocalization of actin-related protein 2 and 3 complex and WAVE2 in colorectal carcinoma.* Cancer science, 2007. **98**(7): p. 992-999.
540. Iwaya, K., K. Norio, and K. Mukai, *Coexpression of Arp2 and WAVE2 predicts poor outcome in invasive breast carcinoma.* Modern pathology, 2007. **20**(3): p. 339.
541. Semba, S., et al., *Coexpression of actin-related protein 2 and Wiskott-Aldrich syndrome family verproline-homologous protein 2 in adenocarcinoma of the lung.* Clinical cancer research, 2006. **12**(8): p. 2449-2454.
542. Cardama, G., et al., *Rho GTPases as therapeutic targets in cancer.* International journal of oncology, 2017. **51**(4): p. 1025-1034.
543. Xu, Z., et al., *Chemokine receptor 7 promotes tumor migration and invasiveness via the RhoA/ROCK pathway in metastatic squamous cell carcinoma of the head and neck.* Oncology reports, 2015. **33**(2): p. 849-855.
544. Zhang, L., et al., *Role of Rho-ROCK signaling in MOLT4 cells metastasis induced by CCL25.* Leukemia research, 2011. **35**(1): p. 103-109.
545. Mao, T., K. Fan, and C. Liu, *Targeting the CXCR4/CXCL12 axis in treating epithelial ovarian cancer.* Gene therapy, 2017. **24**(10): p. 621.
546. Hetrick, B., et al., *Small molecules CK-666 and CK-869 inhibit actin-related protein 2/3 complex by blocking an activating conformational change.* Chemistry & biology, 2013. **20**(5): p. 701-712.
547. Xiao, H., et al., *Insights into the mechanism of microtubule stabilization by Taxol.* Proceedings of the National Academy of Sciences, 2006. **103**(27): p. 10166-10173.

548. Watanabe, M., et al., *DOCK2 and DOCK5 act additively in neutrophils to regulate chemotaxis, superoxide production, and extracellular trap formation.* The Journal of Immunology, 2014: p. 1400885.
549. Vargas, P., et al., *Innate control of actin nucleation determines two distinct migration behaviours in dendritic cells.* Nature cell biology, 2016. **18**(1): p. 43.
550. Rotty, J.D., et al., *Arp2/3 complex is required for macrophage integrin functions but is dispensable for FcR phagocytosis and in vivo motility.* Developmental cell, 2017. **42**(5): p. 498-513. e6.
551. Sai, J., et al., *Parallel PI3K-dependent and Src-dependent pathways lead to CXCL8-mediated Rac2 activation and chemotaxis.* Journal of Biological Chemistry, 2008.
552. Schwarz, J., et al., *Dendritic cells interpret haptotactic chemokine gradients in a manner governed by signal-to-noise ratio and dependent on GRK6.* Current Biology, 2017. **27**(9): p. 1314-1325.
553. Coelho, F.M., et al., *Naïve B cell trafficking is shaped by local chemokine availability and LFA-1-independent stromal interactions.* Blood, 2013: p. blood-2012-10-465336.
554. Amano, M., M. Nakayama, and K. Kaibuchi, *Rho-kinase/ROCK: a key regulator of the cytoskeleton and cell polarity.* Cytoskeleton, 2010. **67**(9): p. 545-554.
555. Matsushima, K., et al., *Chemokines in inflammatory and immune diseases.* Inflammation and Regeneration, 2011. **31**(1): p. 11-22.
556. Wang, Y., M.P. Mattson, and K. Furukawa, *Endoplasmic reticulum calcium release is modulated by actin polymerization.* Journal of neurochemistry, 2002. **82**(4): p. 945-952.
557. Valitutti, S., et al., *Sustained signaling leading to T cell activation results from prolonged T cell receptor occupancy. Role of T cell actin cytoskeleton.* Journal of Experimental Medicine, 1995. **181**(2): p. 577-584.
558. Rosado, J.A., S. Jenner, and S.O. Sage, *A role for the actin cytoskeleton in the initiation and maintenance of store-mediated calcium entry in human platelets Evidence for conformational coupling.* Journal of Biological Chemistry, 2000. **275**(11): p. 7527-7533.

559. Wilkes, M.M., et al., *Activation of Cdc42 is necessary for sustained oscillations of Ca2+ and PIP2 stimulated by antigen in RBL mast cells.* Biology open, 2014: p. BIO20148862.
560. Nolz, J.C., et al., *The WAVE2 complex regulates actin cytoskeletal reorganization and CRAC-mediated calcium entry during T cell activation.* Current biology, 2006. **16**(1): p. 24-34.
561. Zaslaver, A., R. Feniger-Barish, and A. Ben-Baruch, *Actin filaments are involved in the regulation of trafficking of two closely related chemokine receptors, CXCR1 and CXCR2.* The Journal of Immunology, 2001. **166**(2): p. 1272-1284.
562. Truan, Z., et al., *Quantitative morphological analysis of arrestin2 clustering upon G protein-coupled receptor stimulation by super-resolution microscopy.* Journal of structural biology, 2013. **184**(2): p. 329-334.
563. Tomilin, V.N., et al., *TRPV5/V6 channels mediate Ca2+ influx in jurkat T cells under the control of extracellular pH.* Journal of cellular biochemistry, 2016. **117**(1): p. 197-206.
564. El-Haibi, C., et al., *CXCL13 mediates prostate cancer cell proliferation through JNK signalling and invasion through ERK activation.* Cell proliferation, 2011. **44**(4): p. 311-319.
565. Routhier, A., et al., *Pharmacological inhibition of Rho-kinase signaling with Y-27632 blocks melanoma tumor growth.* Oncology reports, 2010. **23**(3): p. 861-867.
566. Wolf, M., et al., *Cathepsin D specifically cleaves the chemokines macrophage inflammatory protein-1α, macrophage inflammatory protein-1β, and SLC that are expressed in human breast cancer.* The American journal of pathology, 2003. **162**(4): p. 1183-1190.
567. Bièche, I., et al., *Molecular profiling of inflammatory breast cancer identification of a poor-prognosis gene expression signature.* Clinical cancer research, 2004. **10**(20): p. 6789-6795.
568. Eiró, N., et al., *Relationship between the inflammatory molecular profile of breast carcinomas and distant metastasis development.* PLoS One, 2012. **7**(11): p. e49047.

569. Roberti, M.P., et al., *Protein expression changes during human triple negative breast cancer cell line progression to lymph node metastasis in a xenografted model in nude mice.* Cancer biology & therapy, 2012. **13**(11): p. 1123-1140.
570. Pervaiz, A., et al., *CCR5 blockage by maraviroc: a potential therapeutic option for metastatic breast cancer.* Cellular Oncology, 2018: p. 1-14.
571. Lee, E., et al., *Breast cancer cells condition lymphatic endothelial cells within pre-metastatic niches to promote metastasis.* Nature communications, 2014. **5**: p. 4715.
572. Jin, K., N.B. Pandey, and A.S. Popel, *Simultaneous blockade of IL-6 and CCL5 signaling for synergistic inhibition of triple-negative breast cancer growth and metastasis.* Breast Cancer Research, 2018. **20**(1): p. 54.
573. Arimont, M., et al., *Structural analysis of chemokine receptor–ligand interactions.* Journal of medicinal chemistry, 2017. **60**(12): p. 4735-4779.
574. Recher, C., et al., *Expression of focal adhesion kinase in acute myeloid leukemia is associated with enhanced blast migration, increased cellularity, and poor prognosis.* Cancer research, 2004. **64**(9): p. 3191-3197.
575. Ozkal, S., et al., *Focal adhesion kinase (FAK) expression in normal and neoplastic lymphoid tissues.* Pathology-Research and Practice, 2009. **205**(11): p. 781-788.
576. Shiratsuchi, H. and M.D. Basson, *Extracellular pressure stimulates macrophage phagocytosis by inhibiting a pathway involving FAK and ERK.* American Journal of Physiology-Cell Physiology, 2004. **286**(6): p. C1358-C1366.
577. Tripathi, A., et al., *CXC chemokine receptor 4 signaling upon co-activation with stromal cell-derived factor-1α and ubiquitin.* Cytokine, 2014. **65**(2): p. 121-125.
578. Mahabeleshwar, G.H. and G.C. Kundu, *Syk, a protein-tyrosine kinase, suppresses the cell motility and nuclear factor κB-mediated secretion of urokinase type plasminogen activator by inhibiting the*

phosphatidylinositol 3'-kinase activity in breast cancer cells. Journal of Biological Chemistry, 2003. **278**(8): p. 6209-6221.

579. Ganju, R.K., et al., *β-Chemokine receptor CCR5 signals through SHP1, SHP2, and Syk.* Journal of Biological Chemistry, 2000. **275**(23): p. 17263-17268.
580. Powis, G., et al., *Selective inhibition of phosphatidylinositol phospholipase C by cytotoxic ether lipid analogues.* Cancer research, 1992. **52**(10): p. 2835-2840.
581. Semini, G., et al., *The novel synthetic ether lipid inositol-C2-PAF inhibits phosphorylation of the tyrosine kinases Src and FAK independent of integrin activation in transformed skin cells.* Biochemical pharmacology, 2011. **81**(8): p. 985-995.
582. Flasiński, M., et al., *Influence of platelet-activating factor, lyso-platelet-activating factor and edelfosine on Langmuir monolayers imitating plasma membranes of cell lines differing in susceptibility to anti-cancer treatment: the effect of plasmalogen level.* Journal of The Royal Society Interface, 2014. **11**(95): p. 20131103.
583. Weeks, H.P., et al., *The Association Between WAVE1 and-3 and the ARP2/3 Complex in PC 3 Cells.* Anticancer research, 2016. **36**(3): p. 1135-1142.
584. Laurin, M., et al., *Rac-specific guanine nucleotide exchange factor DOCK1 is a critical regulator of HER2-mediated breast cancer metastasis.* Proceedings of the National Academy of Sciences, 2013: p. 201213050.
585. Frank, S.R., et al., *The focal adhesion-associated proteins DOCK5 and GIT2 comprise a rheostat in control of epithelial invasion.* Oncogene, 2017. **36**(13): p. 1816.
586. Mitchison, T.J., *The proliferation rate paradox in antimitotic chemotherapy.* Molecular biology of the cell, 2012. **23**(1): p. 1-6.
587. Weaver, B.A., *How Taxol/paclitaxel kills cancer cells.* Molecular biology of the cell, 2014. **25**(18): p. 2677-2681.
588. Tajiri, H., et al., *Targeting Ras-driven cancer cell survival and invasion through selective inhibition of DOCK1.* Cell reports, 2017. **19**(5): p. 969-980.

589. Ferrandez, Y., et al., *Allosteric inhibition of the guanine nucleotide exchange factor DOCK5 by a small molecule.* Scientific reports, 2017. **7**(1): p. 14409.
590. Vives, V., et al., *The Rac1 exchange factor Dock5 is essential for bone resorption by osteoclasts.* Journal of Bone and Mineral Research, 2011. **26**(5): p. 1099-1110.
591. Laurin, M. and J.-F. Côté, *Insights into the biological functions of Dock family guanine nucleotide exchange factors.* Genes & development, 2014. **28**(6): p. 533-547.
592. Hasegawa, H., et al., *DOCK180, a major CRK-binding protein, alters cell morphology upon translocation to the cell membrane.* Molecular and cellular biology, 1996. **16**(4): p. 1770-1776.